horticulturae

Postharvest Handling of Horticultural Crops

Edited by

Maria Dulce Carlos Antunes,
Custódia Maria Luís Gago and Adriana Guerreiro

Printed Edition of the Special Issue Published in *Horticulturae*

www.mdpi.com/journal/horticulturae

MDPI

Postharvest Handling of Horticultural Crops

Postharvest Handling of Horticultural Crops

Editors

Maria Dulce Carlos Antunes
Custódia Maria Luís Gago
Adriana Guerreiro

MDPI

Editors

Maria Dulce Carlos Antunes
University of Algarve
Portugal

Custódia Maria Luís Gago
University of Algarve
Portugal

Adriana Guerreiro
Campus deGambelas
Portugal

This is a reprint of articles from the Special Issue published online in the open access journal *Horticulturae* (ISSN 2311-7524) (available at: https://www.mdpi.com/journal/horticulturae/ special_issues/Postharvest_Handling).

For citation purposes, cite each article independently as indicated on the article page online and as indicated below:

LastName, A.A.; LastName, B.B.; LastName, C.C. Article Title. *Journal Name* **Year**, *Volume Number*, Page Range.

Cover image courtesy of Adriana Guerreiro

Contents

About the Editors

Maria Dulce Carlos Antunes

Maria Dulce Carlos Antunes graduated in Agricultural Engineering and has a Master's degree in Protected Crop Cultivation and a PhD in Horticultural Production-Agricultural Sciences from the University of Algarve. Her domain of specialisation is the postharvest physiology and technology of horticultural products, with present research interests in the development of postharvest technologies to improve the storage life of horticultural commodities, which retain quality and food safety and minimize the environmental impact and the physiology and biotechnology of the metabolic processes that occur during the ripening and senescence of horticultural commodities. She has published more than 100 papers in scientific journals and international conferences. She is a faculty member in the Department of Biological Sciences and Bio-engineering at the Faculty of Science and Technology in the Algarve University and an integrated member in the Mediterranean Institute for Agriculture, Environment and Development. Presently, she is the head of the Post-harvest Laboratory, coordinating research projects on Postharvest science and technology for horticultural crops.

Custódia Maria Luís Gago

Custódia Maria Luís Gago graduated in Agronomic Engineering and has a Master's degree in Horticulture and a PhD in Agrarian Sciences. She is an integrated member in the Mediterranean Institute for Agriculture, Environment and Development (MED) and is a researcher hired by the University of Algarve (UAlg). She has worked on research projects in postharvest science and technology of horticultural products. Currently, her research is focused on the utilization of edible nano-coatings to delay ripening and prevent chilling injuries in susceptible fruits. The coating's formulations include essential oils with antimicrobial and antioxidant properties. She has published at least 50 papers in scientific journals and international conferences.

Adriana Guerreiro

Adriana Guerreiro (PhD) graduated in Agronomic Engineering since 2009, with a Master's degree in Horticulture (2012). She completed her PhD in Agrarian sciences at the University of Algarve, Portugal in 2016. Her work is related to the research she has been conducting since her graduation. She has demonstrated skills in reading, analysis, research, critical thinking, and writing, resulting in the publication of over 40 articles in specialized journals and books. She participates in several research projects. In her professional activities, she has interacted with 85 collaborators in terms of the co-authorship of scientific papers. She works in the areas of agricultural sciences, on postharvest, agriculture, horticulture, food biotechnology, in exact sciences with respect to physics, and in biological sciences with respect to microbiology.

Editorial

Postharvest Handling of Horticultural Products

Maria Dulce Antunes [1,*], Custódia Gago [1] and Adriana Guerreiro [2]

1   MED—Mediterranean Institute for Agriculture, Environment and Development & CHANGE—Global Change and Sustainability Institute, FCT, Universidade do Algarve, edf. 8, Campus de Gambelas, 8005-139 Faro, Portugal
2   CEOT—Centre for Electronics, Optoelectronics and Telecommunications, FCT, Universidade do Algarve, edf. 8, Campus de Gambelas, 8005-139 Faro, Portugal
*   Correspondence: mantunes@ualg.pt

Fruit and vegetables are in a live state after harvest. Continued respiration results in carbon dioxide production, moisture, and heat, which influence the storage environment, packaging, and refrigeration requirements. A current knowledge of good practices for the harvest and postharvest handling of fresh horticultural products is fundamental due to their high perishability [1,2]. It is estimated that 30% of produced horticultural commodities are lost in the process between harvest and consumption [3]. The reduction in these losses is imperative nowadays, because it will impact back the amount of produced food, with benefits on agricultural inputs, water and land use, contributing to the sustainability of agriculture and the planet.

Over time, postharvest researchers have looked for the best ways and technologies that allow us to reduce quality loss after harvest and increase the storage capacity of horticultural products with the aim of reducing their losses.

In this "Special Issue" of the *Horticulturae* MDPI journal we intended to collect a series of research recently conducted on the subject. This Special Issue contains 13 scientific papers covering different areas of the postharvest handling of horticultural products. The subjects covered report on the knowledge of the physiology and biochemistry of the horticultural commodities and the study of technologies that can improve product quality and storage, reducing postharvest loss.

Raspberries are of the most perishable fresh fruit. Although classified as non-climacteric fruit, several studies have reported that fruit ripening and abscission are regulated by ethylene production from the receptacle [4–6]. To understand the relationship between ethylene production and fruit quality at the beginning of the ripening process, ref. [7] reported ethylene and ripening parameter changes in fruit at 0 and 10 °C. They conclude that ethylene production is negatively correlated to firmness through ripening, but not with SSC or titratable acidity. Moreover, the positive correlation between firmness and CO_2 production in the whole fruit suggests a ripening behavior for 'Heritage' raspberry, raising the importance of further studies on the physiology of non-climacteric fruit ripening.

Physiological disorders in long-term cold storage are a key issue concerning postharvest losses in susceptible horticultural commodities. The physiology of the disorder and pre- and postharvest technologies that reduce those physiological disorders have a major impact in the postharvest industry. In the present "Special Issue", four papers report on apple, pear, and peach. For apple, the effects of 1-MCP and $CaCl_2$ on fatty acid composition and their relationship with storage physiological disorders were studied [8]. A new method to induce superficial scald in stored pear was developed by [9] in order to better study the mechanisms of physiological disorder developments. The postharvest treatment with calcium and ascorbic acid was reported to reduce symptoms of chilling injury in peaches storage [10].

In banana, the enzymes involved in the browning of the cut-end surface were studied; it was found that postharvest treatments with oxalic acid could significantly reduce browning, improving fruit quality [11].

Tomato is a very important crop worldwide. In this Special Issue, three studies of this fruit are presented. The maintenance of tomato quality was improved over its shelf-life using calcium chloride, hydrogen peroxide, chitosan, and ozonated water postharvest fruit treatment [12]. Different packaging materials and storage temperatures were studied to reduce okra pod decay through storage and marketing [13].

A kinetic model for the effect of the vibrations of fruit after harvest on their quality during storage was presented [14]. Another paper reports the effect of transport temperature and vibration on final tomato fruit quality [15]. Additionally, the bruising impact drop in guava fruit was modulated by using image processing and response surface methodology, with the objective to reduce the impact bruising incidence of guava throughout its supply chain [16].

Another study provides a scientific basis for investigating the molecular mechanisms of pepper storage tolerance via transcriptomics and metabolomics [17].

One paper also presents the importance of ethephon treatment, a commercial product releasing ethylene, on the abscission of palm fruit, which are grown for seed oil production [18].

Vase life is one of the most important factors that determines the marketability of cut flowers. A study on hydrangea flowers reports the importance of preservative solutions in order to improve the water balance for each distribution stage in its supply chain [19].

This Special Issue provides a valuable contribution for the understanding of the horticultural products' postharvest physiology and implementation of technologies to reduce quality loss during the supply chain. In this way, this Special Issue contributes to reductions in food loss, promoting the sustainability of agriculture.

Conflicts of Interest: The authors declare no conflict of interest.

References

1. Antunes, M.D.C.; Cavaco, A.M. The use of essential oils for postharvest decay control. *Flavour Fragr. J.* **2010**, *25*, 351–366. [CrossRef]
2. Antunes, M.D.; Miguel, M.G.; Neves, A. Neves. Sustainable Postharvest Handling of Horticultural Products. *WSEAS Trans. Environ. Dev.* **2007**, *3*, 111–116.
3. FAO. Available online: https://www.fao.org/in-action/seeking-end-to-loss-and-waste-of-food-along-production-chain/en/ (accessed on 20 July 2022).
4. Iannetta, P.P.M.; Wyman, M.; Neelam, A.; Jones, C.; Davies, H.V.; Sexton, R. A causal role for ethylene and endo-b-1,4-glucanase in the abscission of red-raspberry (*Rubus idaeus* L.) drupelets. *Physiol. Plant.* **2000**, *110*, 535–543. [CrossRef]
5. Fuentes, L.; Monsalve, L.; Morales-Quintana, L.; Valdenegro, M.; Martínez, J.P.; Defilippi, B.G.; González-Agüero, M. Differential expression of ethylene biosynthesis genes in drupelets and receptacle of raspberry (*Rubus idaeus*). *J. Plant Physiol.* **2015**, *179*, 100–105. [CrossRef] [PubMed]
6. Fuentes, L.; Figueroa, C.R.; Valdenegro, M. Recent advances in hormonal regulation and Cross-Talk during non-climacteric fruit development and ripening. *Horticulturae* **2019**, *5*, 45. [CrossRef]
7. Monsalve, L.; Bernales, M.; Ayala-Raso, A.; Álvarez, F.; Valdenegro, M.; Alvaro, J.E.; Figueroa, C.R.; Defilippi, B.G.; Fuentes, L. Relationship between Endogenous Ethylene Production and Firmness during the Ripening and Cold Storage of Raspberry (*Rubus idaeus* 'Heritage') Fruit. *Horticulturae* **2022**, *8*, 262. [CrossRef]
8. Antunes, M.D.; Guimarães, A.C.; Gago, C.; Guerreiro, A.; Panagopoulos, J.; Vilas Boas, E.; Miguel, M.G. Membrane Fatty Acids and Physiological Disorders in Cold-Stored 'Golden Delicious' Apples Treated with 1-MCP and Calcium Chloride. *Horticulturae* **2022**, *8*, 162. [CrossRef]
9. Dias, C.; Amaro, A.; Fonseca, A.; Ferrante, A.; Silvestre, A.; Rocha, S.M.; Isidoro, N.; Pintado, M. ß-Farnesene Exogenous Application as a Novel Damage Induction Model to Fast Explore the Effectiveness of Postharvest Strategies: The Case Study of the 'Rocha' Pear DOP. *Horticulturae* **2022**, *8*, 93. [CrossRef]
10. Lo'ay, A.A.; Ismail, H.; Kassem, H.S. Postharvest Treatment of 'Florida Prince' Peaches with a Calcium Nanoparticle–Ascorbic Acid Mixture during Cold Storage and Its Effect on Antioxidant Enzyme Activities. *Horticulturae* **2021**, *7*, 499.
11. Kaewjumpol, G.; Srisamlee, S.; Beckles, D.M.; Kietsuda Luengwilai, K. Enzymatic Browning in Banana Blossoms and Techniques for Its Reduction. *Horticulturae* **2021**, *7*, 373. [CrossRef]

12. Shehata, S.A.; Abdelrahman, S.Z.; Megahed, M.M.A.; Abdeldaym, E.A.; Mohamed, M.; El-Mogy, M.M.; Abdelgawad, K.F. Extending Shelf Life and Maintaining Quality of Tomato Fruit by Calcium Chloride, Hydrogen Peroxide, Chitosan, and Ozonated Water. *Horticulturae* **2021**, *7*, 309. [CrossRef]

13. Rattanakaran, J.; Saengrayap, R.; Prahsarn, C.; Kitazawa, H.; Chaiwong, S. Application of Room Cooling and Thermal Insulation Materials to Maintain Quality of Okra during Storage and Transportation. *Horticulturae* **2021**, *7*, 188. [CrossRef]

14. Pathare, P.B.; Al-Dairi, M. Effect of Simulated Vibration and Storage on Quality of Tomato. *Horticulturae* **2021**, *7*, 417. [CrossRef]

15. Al-Dairi, M.; Pathare, P.B.; Al-Yahyai, R. Effect of Postharvest Transport and Storage on Color and Firmness Quality of Tomato. *Horticulturae* **2021**, *7*, 163. [CrossRef]

16. Htike, T.; Saengrayap, R.; Aunsri, N.; Tontiwattanakul, K.; Chaiwong, S. Investigation and Evaluation of Impact Bruising in Guava Using Image Processing and Response Surface Methodology. *Horticulturae* **2021**, *7*, 411. [CrossRef]

17. Sun, H.; Li, Q.; Mao, L.-Z.; Yuan, Q.-L.; Huang, Y.; Chen, M.; Fu, C.-F.; Zhao, X.-H.; Li, Z.-Y.; Dai, Y.-H.; et al. Investigating the Molecular Mechanisms of Pepper Fruit Tolerance to Storage via Transcriptomics and Metabolomics. *Horticulturae* **2021**, *7*, 242. [CrossRef]

18. Low, J.Y.-S.; Fong, P.-Y.; Teh, C.-K.; Ong, A.-L.; Lim, C.-M.; Appleton, D.R. Ethephon-Induced Abscission of Oil Palm Fruits at Optimal Bunch Ripeness and Retting Period to Improve Commercial Seed Production. *Horticulturae* **2021**, *7*, 380. [CrossRef]

19. Yang, H.; Lim, S.; Lee, J.-H.; Choi, J.-W.; Shin, I.-S. Influence of Solution Combination for Postharvest Treatment Stage on Vase Life of Cut Hydrangea Flowers (*Hydrangea macrophylla* cv. 'Verena'). *Horticulturae* **2021**, *7*, 406. [CrossRef]

Article

Relationship between Endogenous Ethylene Production and Firmness during the Ripening and Cold Storage of Raspberry (*Rubus idaeus* 'Heritage') Fruit

Liliam Monsalve [1], Maricarmen Bernales [1], Aníbal Ayala-Raso [2], Fernanda Álvarez [1], Mónika Valdenegro [3], Juan-Eugenio Alvaro [3], Carlos Rodrigo Figueroa [4,5], Bruno Giorgio Defilippi [6] and Lida Fuentes [1,*]

1   Centro Regional de Estudios en Alimentos Saludables (CREAS), CONICYT-Regional GORE Valparaíso Proyecto R17A10001, Avenida Universidad 330, Placilla, Curauma, Valparaíso 2362696, Chile; liliam.monsalve.v@gmail.com (L.M.); maricarmen.bernales.p@mail.pucv.cl (M.B.); falvarez@creas.cl (F.Á.)
2   Instituto de Estadística, Facultad de Ciencias, Universidad de Valparaíso, Valparaíso 2360102, Chile; anibal.ayala@postgrado.uv.cl
3   Escuela de Agronomía, Facultad de Ciencias Agronómicas y de los Alimentos, Pontificia Universidad Católica de Valparaíso, Casilla 4-D, Quillota 2260000, Chile; monika.valdenegro@pucv.cl (M.V.); juan-eugenio.alvaro@pucv.cl (J.-E.A.)
4   Millennium Nucleus for the Development of Super Adaptable Plants (MN-SAP), Santiago 8340755, Chile; cfigueroa@utalca.cl
5   Laboratory of Plant Molecular Physiology, Institute of Biological Sciences, Universidad de Talca, Talca 3465548, Chile
6   Unidad de Postcosecha, INIA La Platina, Santa Rosa, Santiago 8820000, Chile; bdefilip@inia.cl
*   Correspondence: lfuentes@creas.cl; Tel.: +56-322372868

Abstract: The raspberry (*Rubus idaeus*) is an important fruit crop; however, its accelerated softening is a critical postharvest problem, even at low temperatures. Its softening has been partially associated with the endogenous production of ethylene from the receptacle during ripening. To understand the relationship between ethylene production and fruit quality at the beginning of the ripening process, the physiological and quality parameters were evaluated during the ripening of the 'Heritage' cultivar. Two storage assays, at 0 °C and 10 °C, were carried out with independent groups of fruits attached to their receptacle at the white stage of fruit development. The treatments included fruit treated with ethylene (1000 ppb) and ethylene perception inhibitor 1-methyl cyclopropene (1-MCP, 1600 ppb) and a control treatment. During ripening, the endogenous production of ethylene in whole fruit was negatively correlated with the loss of firmness. During storage at 0 °C, firmness and ethylene production only decreased by the effect of storage time, with a firmness near 1.5 Newtons at 16 days. On the other hand, the storage at 10 °C showed a delay in the firmness loss and lower ethylene production of the fruit treated with 1-MCP, compared to the control and ethylene-treated fruit. In addition, these two last assays showed a firmness close to 1 Newton at 5 days. No significant differences were observed in the total soluble solids content and titratable acidity between the three treatments at the two storage temperatures. The results during ripening and storage at 10 °C indicate that the loss of the fruit's firmness is positively related to the endogenous ethylene production of the whole fruit from 1 to 5 days of storage. Future assays should be performed to determine the role of ethylene in raspberry ripening.

Keywords: receptacle; drupelets; 1-methylcyclopropene; firmness; postharvest

1. Introduction

Raspberry (*Rubus idaeus* L.) is a fruit with an extremely short shelf life (1–2 days) due to rapid softening; therefore, it is highly susceptible to damage during harvesting and postharvest operations [1–3]. Although the raspberry has been classified as a non-climacteric fruit, several studies have reported that fruit ripening and abscission are regulated by ethylene

production from the receptacle [1,3–6]. Furthermore, ethylene production is known to increase in raspberry fruit as ripening progresses, leading to a sharp decrease in fruit firmness and shelf life towards maturity [1,3,5–11]. Raspberry fruit development has generally been classified into seven developmental stages, as follows: small green (SG), medium green (MG), large green (LG), white (W), pink (P), red or ripe stage (R), and overripe (OR) fruit [1,3,5,9,11].

The onset of raspberry fruit ripening is at the W stage. In this stage, the red color starts to appear, the titratable acidity decreases, and conversely, the soluble solids content begins to increase [5,7–9]. Additionally, some changes associated with phytohormone metabolism can be observed, such as increases in the production of ethylene from the receptacle, which is associated with the expression of their biosynthetic genes [5,7], and the expression of the genes encoding for the enzyme that conjugate indole acetic acid (IAA) into amino acids [9].

The respiration rate values limit the storage life of the raspberry fruit [12,13]. Therefore, the physiological stage governs the main difference in storage life. It has been reported that the pink stage of different cultivars, such as 'Heritage', 'Santa Catalina', 'Santa Clara' and 'Santa Teresa', allows a longer storage life with differences in the loss-of-firmness rate between temperatures [12]. 'Heritage' has been described as a cultivar with a dramatic decrease in firmness as the fruit ripens, compared to 28 cultivars [14].

The application of the competitive inhibitor of ethylene, 1-methyl cyclopropene (1-MCP), to green fruit suggests that endogenous ethylene from the receptacle accelerates raspberry abscission and increases both the expression and activity of 1,4-endoglucanase (EGase) in receptacle tissue [3]. Nevertheless, the relationship of endogenous ethylene with the loss of firmness has still been scarcely studied. Thus, with the aim of determining the potential role of ethylene on the changes of fruit quality during 'Heritage' raspberry ripening, a cultivar with a high softening rate, the endogenous production of ethylene, and the production of CO_2 and fruit quality parameters (i.e., total soluble solids, titratable acidity, firmness) were evaluated during ripening and under ethylene and 1-MCP application during two storage assays at 0 °C and 10 °C.

2. Materials and Methods

2.1. Plant Material and Treatments

Raspberry (*Rubus idaeus* L.) 'Heritage' fruit was collected from commercial orchards located in Chimbarongo (34°41′45.54 S; 71°10′01.71 W; 333 masl), O'Higgins Region, Chile. The details of the growing conditions have been described previously in Bernales et al., 2019 [9]. Fruit bound to the receptacle and with peduncle were harvested and sorted by size and color [3,5,7–9,11] as follows: large green (LG), white (W), pink (P), red (R) and overripe (OR) fruit (Figure 1). Immediately after harvest, the collected fruits were used to determine the quality and physiological parameters (100 fruits of each stage) under the respective treatments.

| LG | W | P | R | OR |

Developmental stages of raspberry Heritage

Figure 1. Developmental stages of raspberry (*Rubus idaeus* 'Heritage') fruit. The fruit was harvested and sorted by size and color as follows: large green (LG), white (W), pink (P), red (R) and overripe (OR) fruit.

Treatments to determine the role of ethylene were performed using the W-stage fruit (1350 fruits) according to the method of Li et al., 2015 [15]. Briefly, the fruit was put in a clamshell (containing ten whole fruit) and five clamshells were kept in sealed chambers (50 L) for each treatment. The first group was the control group without treatment, the second group was treated by injection with ethylene at 1000 ppb (1 μL L^{-1} in the chamber), and a third group was treated with 1-methyl cyclopropane (1-MCP; SmartFresh, Rohm and Haas, Vicenza, Italy) by placing tablets of 1-MCP in 20 mL of activator solution to provide a concentration of 1.6 μL L^{-1} in the chamber [15]. First, all fruit was treated in a camera at 20 °C for 16 h. Then, half of the fruit was immediately kept in a growth chamber at 10 °C and the other group was kept in a growth chamber at 0 °C throughout the experiment. The assay was carried out until firmness nearly reached 1 N, and the sample days were 0, 1, 2, 5 days for 10 °C and 0, 1, 2, 5, 9 and 16 days for 0 °C assays. Day 0 was considered as starting after the samples underwent treatments and from 3 h in cold storage. Five independent experimental units (each containing ten whole fruits with an average weight of 2.4 g per fruit) were analyzed for firmness, total soluble solids, titratable acidity, CO_2, and ethylene production from each sampling date.

2.2. Physiological and Quality Assessments during Ripening

During ripening, the CO_2 and ethylene production were determined in whole fruits (five experimental units of ten intact fruits binding to the receptacle), drupelets (five experimental units of ten fruits without a receptacle) and receptacles (five experimental units of ten receptacles) of the developmental stages. The drupelets and the receptacle of the LG stage could not be separate, and the CO_2 and ethylene production were determined only in whole fruit. For this same reason and for the low ethylene production, the SG and MG states were not analyzed in the present study.

The samples of each independent unit for each assay were introduced into close tight chambers (500 mL) and were incubated at 20 °C for 1 h. Furthermore, 1 mL of the gas sample was quantified for ethylene in a gas chromatograph (Shimadzu 8A, Tokyo, Japan) equipped with a flame ionization detector [16]. The results are expressed as microliters of ethylene per kilogram per hour. For CO_2 determination, the needle of a CO_2 detector (MAP Headspace gas analyzer, Bridge Analyzers, Bedford Heights, Ohio, USA) was introduced into the same chambers, and the CO_2 concentrations were recorded. The results are expressed as milligrams of CO_2 per kilogram per hour.

The firmness of each fruit of the experimental units was measured using FirmTech 2 equipment (BioWorks Inc., Wamego, KS, USA). The firmness was determined as the grams necessary to compress the fruit to 1 mm with a 2.5-cm diameter plunger. Firmness was determined in g/mm and expressed as Newton (N) [16–18]. A total of 8 g of fruit tissue (drupelets) from each experimental unit was homogenized in a mortar. The juice was analyzed for total soluble solids (TSS) using a refractometer (ATAGO, Tokyo, Japan), expressed as the °Brix (percentage of sugar per 100 g of the fresh weight (FW) of fruit). The titratable acidity (TA) is expressed as the percentage (v/v) of citric acid.

2.3. Statistical Analysis

Five independent units (ten fruits) for each sample were used during the development and storage assay (fruit storage in clamshells). The data were analyzed using R statistical software [19]. All results were expressed as the mean ± standard deviation (S.D.). The variance in data was analyzed by one-way ANOVA when normality was proved; otherwise, non-parametric techniques were used (Wilcoxon test). Additionally, a principal component analysis (PCA) and correlation matrix (Kendall method) were performed for data. The mean significance differences were determined at $p \leq 0.05$ (*), $p \leq 0.01$ (**), $p \leq 0.001$ (***) and $p \leq 0.0001$ (****).

3. Results

3.1. Physiological and Quality Parameters during the Development of Raspberry Fruit

First, the ripening stages (Figure 1) were characterized by the evolution of ethylene and CO_2 contents. The ethylene production was found to be very low in the whole fruit at the LG stage (1.0 μL kg^{-1} h^{-1}) but increased ten times at the OR stage (10.0 μL kg^{-1} h^{-1}) (Figure 2A). Variable ethylene production was observed in drupelets (Figure 2B). A continuous increase in ethylene production was observed in the receptacle from W (32.7 μL kg^{-1} h^{-1}) to OR (42.8 μL kg^{-1} h^{-1}) stages (Figure 2C), being seven times higher than ethylene produced by drupelets. A constant decrease in CO_2 production was observed for all tissues analyzed, showing the receptacle values to be ten times higher than whole fruit for all stages (Figure 2D–F).
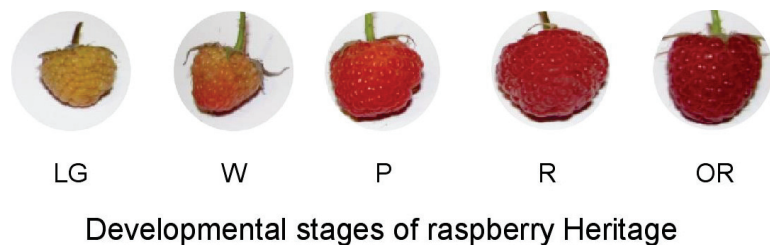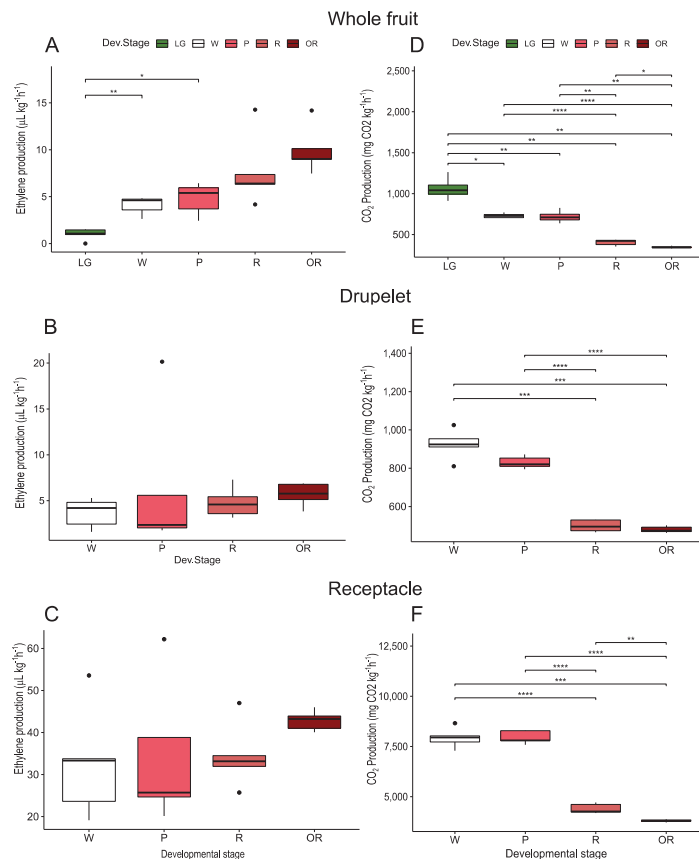

Figure 2. Physiological parameters during the development of raspberry (*Rubus idaeus* 'Heritage') fruit. The fruit was harvested and sorted by size and color as follows: large green (LG), white (W), pink (P), red (R) and overripe (OR) fruit. Ethylene production (μL kg^{-1} h^{-1}) and CO_2 production (mg CO_2 kg^{-1} h^{-1}) were determined in whole fruit (**A,D**), drupelets (**B,E**) and receptacles (**C,F**) from each stage. The drupelets and the receptacle of the green stage cannot be separated, and the CO_2 and ethylene production were non-determined (n.d) in the drupelets and receptacle. Data represent the means ± S.D. from five sample units (each containing ten fruits) by the development stage. Asterisks indicate significant differences between all developmental stages, $p \leq 0.05$ (*), $p \leq 0.01$ (**), $p \leq 0.001$ (***) and $p \leq 0.0001$ (****). Boxplots show each group's distribution (developmental stages), and the black line (central value in the box) signs the median value. Points out of the boxplots show outlier values.

On the other hand, a drastic firmness reduction was observed in the W stage compared to LG (28%) and in the P stage compared to W (34%) (Figure 3A). Moreover, a constant decrease in titratable acidity (TA) and an increase in total soluble solids (TSS) from the LG to OR stages were observed (Figure 3B,C).
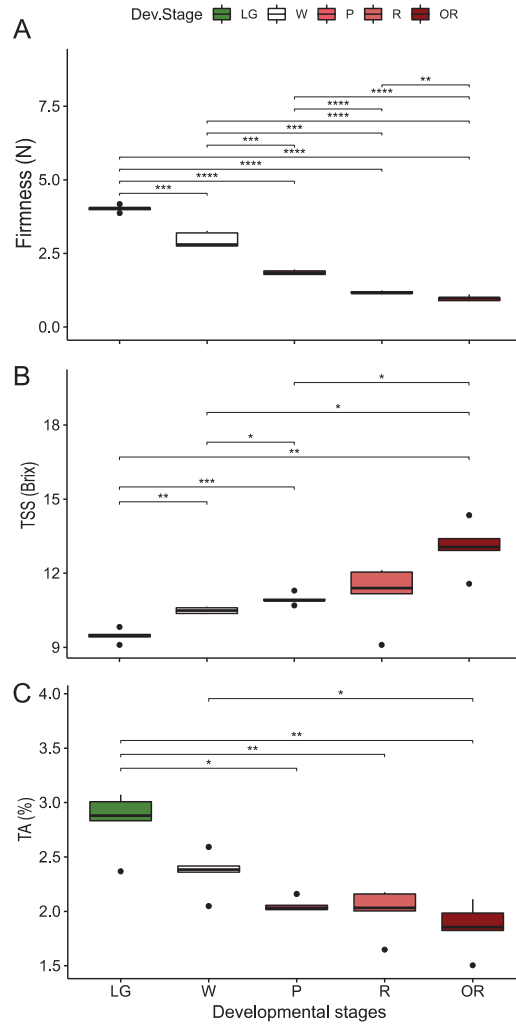
Figure 3. Quality parameters during raspberry (*Rubus idaeus* 'Heritage') fruit development. Firmness (N) (**A**) was determined in whole fruit, total soluble solids content (TSS, °Brix) (**B**) and titratable acidity (TA, %) (**C**) were determined in drupelets. The fruit was harvested and sorted by size and color as follows: large green (LG), white (W), pink (P), red (R) and overripe (OR) fruit. Data represent the means ± S.D. from five sample units (each containing ten fruits) by the development stage. Asterisks indicate significant differences between all developmental stages, $p \leq 0.05$ (*), $p \leq 0.01$ (**), $p \leq 0.001$ (***) and $p \leq 0.0001$ (****). Boxplots show each group's distribution (developmental stages), and the black line (central value in the box) signs the median value. Points out of the boxplots show outlier values.

The principal component analysis (PCA) showed that the first two components (PC1 and PC2) explained 64.5% and 14.2%, respectively, of the total variability of the physiological and quality parameters determined during development (Figure 4). In addition, standardized components described a positive correlation between variables, i.e., firmness and CO_2 production in whole fruit (0.81) and the firmness and CO_2 production of drupelets (0.84), and a negative correlation between firmness and ethylene production of whole fruit (−0.73) (Figure 5).
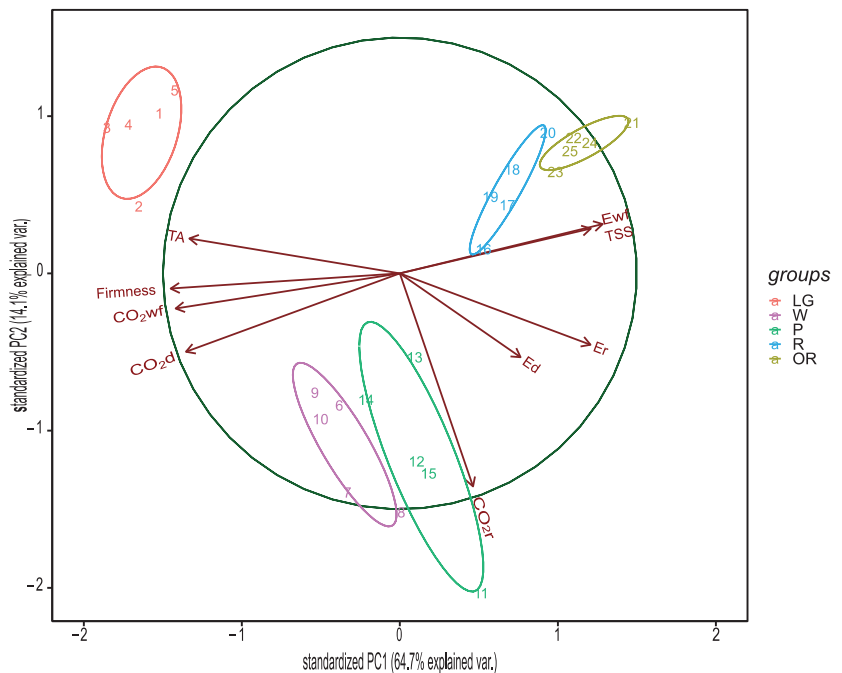
Figure 4. The principal component analysis (PCA) biplot for physiological and quality indices of raspberry (*Rubus idaeus* 'Heritage') fruit during development. The fruit was harvested and sorted by size and color as follows: large green (LG), white (W), pink (P), red (R) and overripe (OR) fruit. Ewf: ethylene production in whole fruit; Ed: ethylene production in drupelets; Er: ethylene production in the receptacle; CO_2wf: ethylene production in whole fruit; CO_2d: ethylene production in drupelets; CO_2r: ethylene production in the receptacle; TSS: total soluble solids content; and TA: titratable acidity.

These results indicate that fruit ripening beginning from the W stage gives way to ethylene production in the whole fruit, drupe, and mainly from the receptacle, and quality modifications such as the decrease in fruit firmness and acidity and an increase in TSS. Therefore, the W stage (i.e., transition stage) was chosen to evaluate the effects through the storage assay at different temperatures (0 and 10 °C) of ethylene and 1-MCP application.

3.2. Change in Physiological and Quality Parameters during Treatments
3.2.1. Physiological Changes during Treatments

During the assay at 10 °C, significant differences in ethylene production were observed between 1-MCP and the control and ethylene treatments from 1 to 5 d of cold storage (Figure 6A). At 5 days, the fruit reached ethylene production values of 7.66 μL kg^{-1} h^{-1} for ethylene treatment, 7.76 μL kg^{-1} h^{-1} for control fruit, and 3.86 μL kg^{-1} h^{-1} for 1-MCP treatment. Therefore, the 1-MCP treatment decreased the endogenous ethylene production

at half that observed in the control and ethylene-treated fruit at five days of storage at 10 °C. On the other hand, the exogenous ethylene did not increase ethylene production compared to the control fruit.
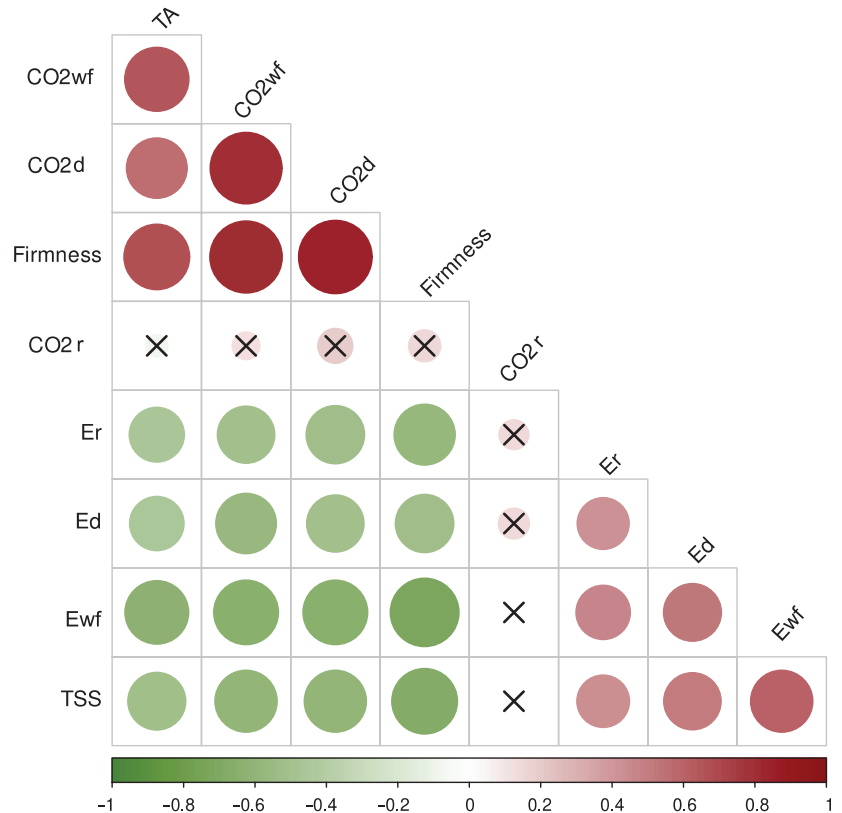
Figure 5. Correlation matrix of variables during raspberry (Rubus idaeus 'Heritage') fruit development. The correlation was carried out by Kendall's method and on non-grouped data. Ewf: ethylene production in whole fruit; Ed: ethylene production in drupelets; Er: ethylene production in the receptacle; CO_2wf: ethylene production in whole fruit; CO_2d: ethylene production in drupelets; CO_2r: ethylene production in the receptacle; TSS: total soluble solids content; and TA: titratable acidity.

During treatment at 0 °C, ethylene production was kept similar to the harvest (4.1 μL kg^{-1} h^{-1}) up to 5 d, showing significant differences between treatments only at 16 d (Figure 6), observing an ethylene production in the 1-MCP-treated fruit of 37 μL kg^{-1} h^{-1}, which was 2.5 times higher than the control fruit. At this temperature, endogenous ethylene production was not associated with the inhibition treatment by 1-MCP.

Concerning CO_2 production, the assay at 10 °C showed a similar trend for all treatments, with a significant increase in CO_2 production immediately after treatment application (after harvest at the W stage); with a CO_2 production of 2016, 2056, and 1800 mg kg^{-1} h^{-1} for ethylene, control, and 1-MCP treatments, respectively (Figure 7A). In the assay at 0 °C, no significant differences were observed between treatments and a decreasing trend was observed after treatment application up to 2 d. A peak in the CO_2 production was observed at 5 d, and then a decrease was observed at 9 d, maintaining similar values (near 400 mg kg^{-1} h^{-1}) until 16 d (Figure 7B).

Figure 6. Ethylene production of raspberry (*Rubus idaeus* 'Heritage') fruit during treatment with ethylene and 1-methyl cyclopropane (1-MCP). The storage assay was performed at the W stage of raspberry and stored for 5 and 16 days at 10 °C (**A**) and 0 °C (**B**), respectively. Ethylene production (μL kg^{-1} h^{-1}) was determined for ethylene and 1-MCP-treated fruits and controls. Data represent the means $\pm$ S.D. from five sample units (each containing ten fruits). Asterisks indicate significant differences between treatments at the same storage time ($p \leq 0.05$). Boxplots show each group's distribution (treatment) and the black line (central value in the box) signs the median value. Points out of the boxplots show outlier values.
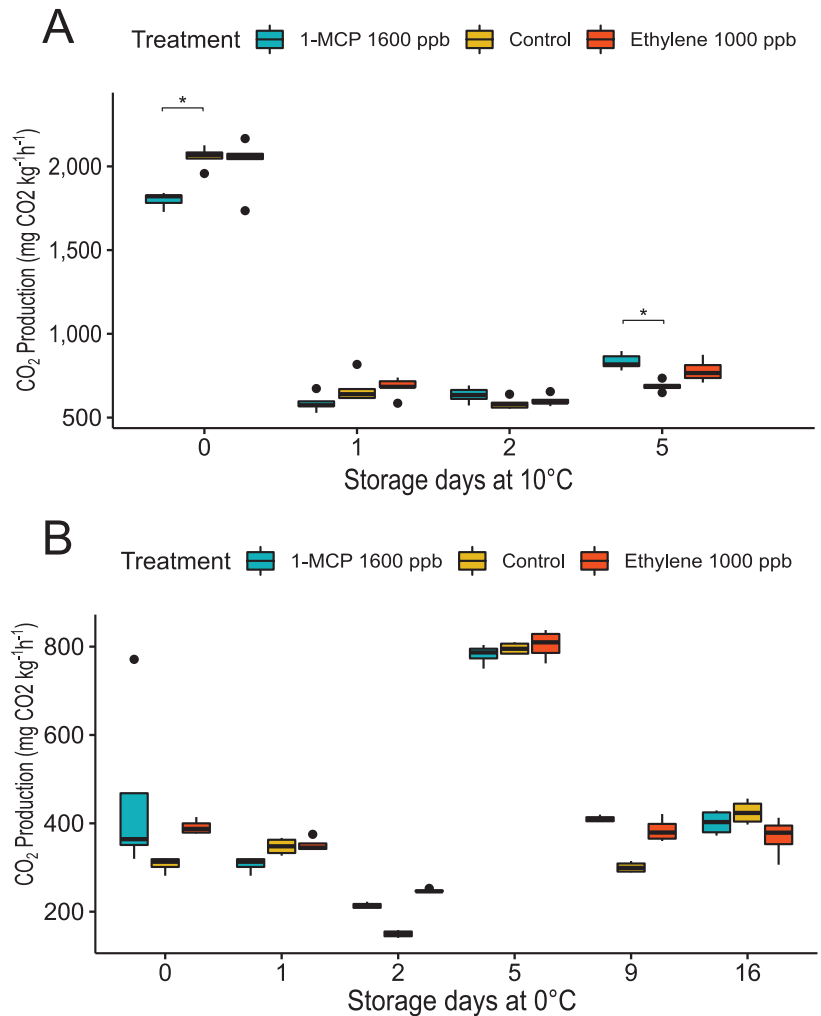
Figure 7. CO_2 production of raspberry (*Rubus idaeus* 'Heritage') fruit during treatment with ethylene and 1-methyl cyclopropane (1-MCP). The storage assay was performed at the W stage of raspberry and stored for 5 and 16 days at 10 °C (**A**) and 0 °C (**B**), respectively. CO_2 production (mg CO_2 kg^{-1} h^{-1}) was determined for ethylene and 1-MCP-treated fruits and controls. Data represent the means $\pm$ S.D. from five sample units (each containing ten fruits). Asterisks indicate significant differences between treatments at the same storage time ($p \leq 0.05$). Boxplots show each group's distribution (treatment) and the black line (central value in the box) signs the median value. Points out of the boxplots show outlier values.

3.2.2. Firmness Changes during Treatments

During the assay at 10 °C, significant firmness differences were observed between 1-MCP compared to control and ethylene treatments during each time evaluated at this cold storage temperature, except for day 1, where there were no significant differences between 1-MCP and ethylene-treated fruit due to an outlier point. At 5 days under this storage temperature, the fruit reached firmness values of 0.97, 1.07, and 1.59 N for ethylene, control, and 1-MCP treatments, respectively. Therefore, the ethylene receptor inhibition allowed

for maintaining 55% of the firmness determined at the harvest, suggesting a relation of endogenous ethylene production with the firmness (Figure 8A). Nevertheless, 1-MCP treatment did not preserve the firmness above 2 N even on the first day of storage and failed to prolong the storage of the fruit for more than 5 days, with temperature being a key factor for the preservation of fruit firmness.
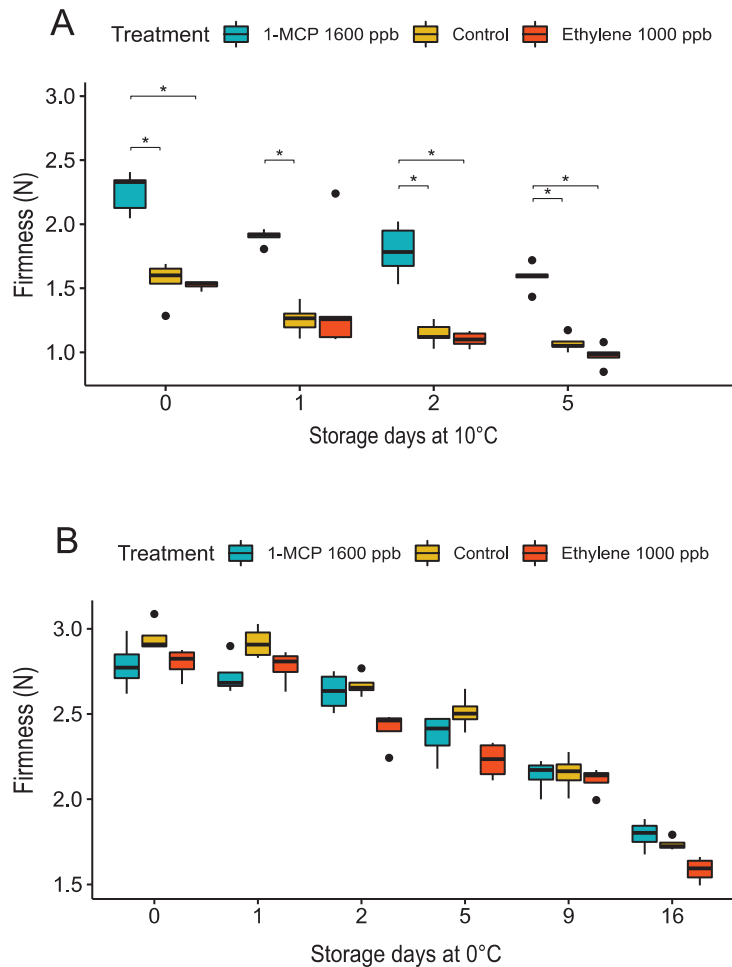
Figure 8. The firmness of raspberry (*Rubus idaeus* 'Heritage') fruit during treatment with ethylene and 1-methyl cyclopropane (1-MCP). The storage assay was performed at the W stage of raspberry fruit and stored for 5 and 16 days at 10 °C (**A**) and 0 °C (**B**), respectively. Firmness (N) was determined for ethylene and 1-MCP-treated fruits and controls. Data represent the means ± S.D. from five sample units (each containing ten fruits). Asterisks indicate significant differences between treatments at the same storage time ($p \leq 0.05$). Boxplots show each group's distribution (treatment) and the black line (central value in the box) signs the median value. Points out of the boxplots show outlier values.

During treatment at 0 °C, the fruit showed a firmness over 2 N for up to 9 days. No significant differences were observed between 1-MCP treatment, control and exogenous ethylene-treated fruit at this cold storage temperature (Figure 8B). At this temperature, no effect on fruit firmness was observed by inhibiting the ethylene receptor.

The principal component analysis (PCA) was conducted for each day to better visualize variable behavior by day. The PCA showed that the first two components (PC1 and PC2) explained more than 60% and more than 20%, respectively, of the variability, i.e., ethylene production, CO_2 production and firmness determined between treatments at 10 °C storage temperature (Figure 9). At this temperature, the 1-MCP treatment behaved independently of the control and ethylene-treated fruit groups during all sampling days' analyses. At 10 °C, standardized components described a low negative correlation between firmness and CO_2 production at 0 days (0.43) and a low positive correlation at 5 days (0.24). At this temperature, there was a low negative correlation between firmness and ethylene production at 0 days (-0.24), increasing partially at 5 days (-0.54) (Figure 10). These results suggest that although the 1-MCP group had an independent behavior from the other treatments, the firmness relationship with the production of whole fruit ethylene during this assay was partial.
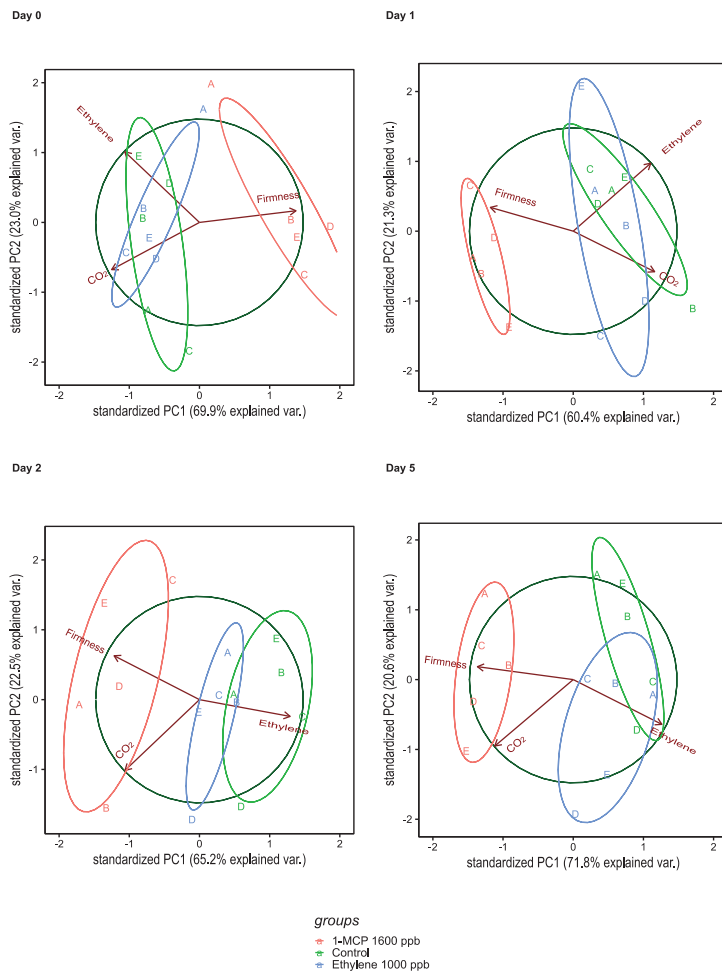
Figure 9. PCA biplot for ethylene, CO_2 and firmness indices of raspberry (*Rubus idaeus* 'Heritage') fruit during treatment with ethylene and 1-methyl cyclopropane (1-MCP) at 10 °C. The storage assay was performed at the W stage of the raspberries and stored for 5 days and at 10 °C. The PCA analysis was conducted on each sampling day.
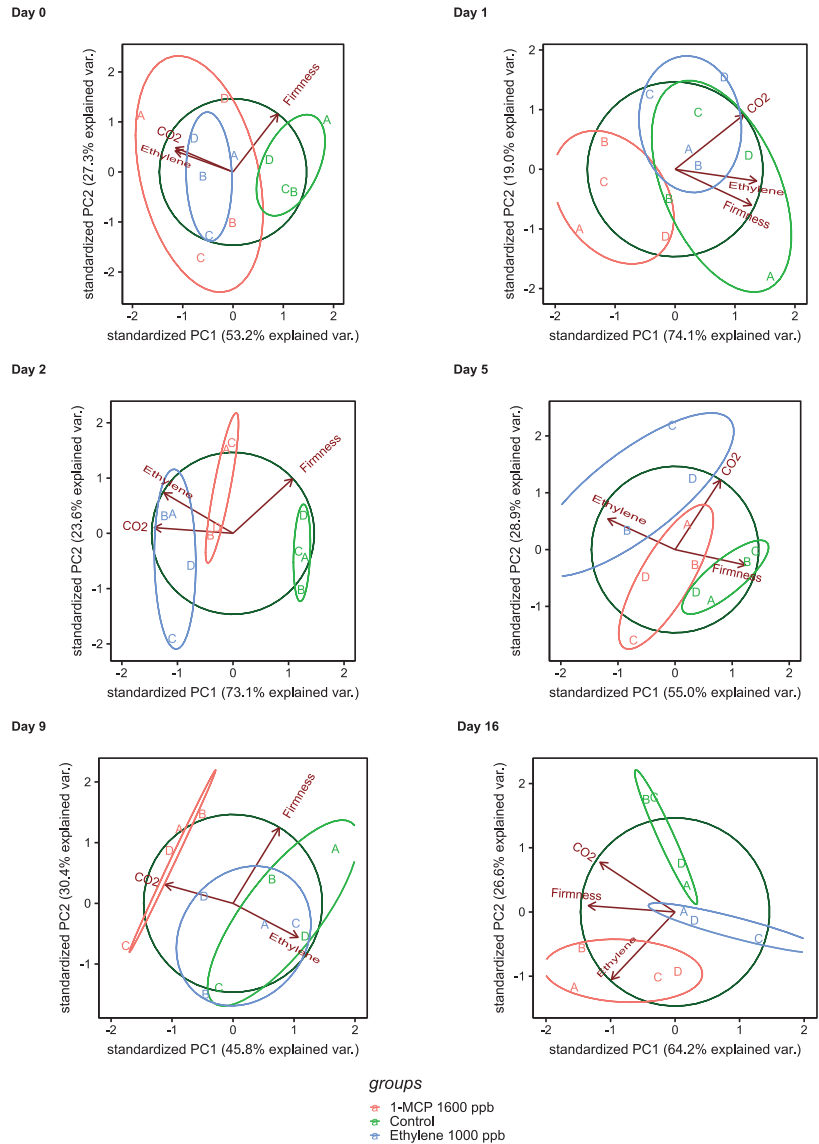
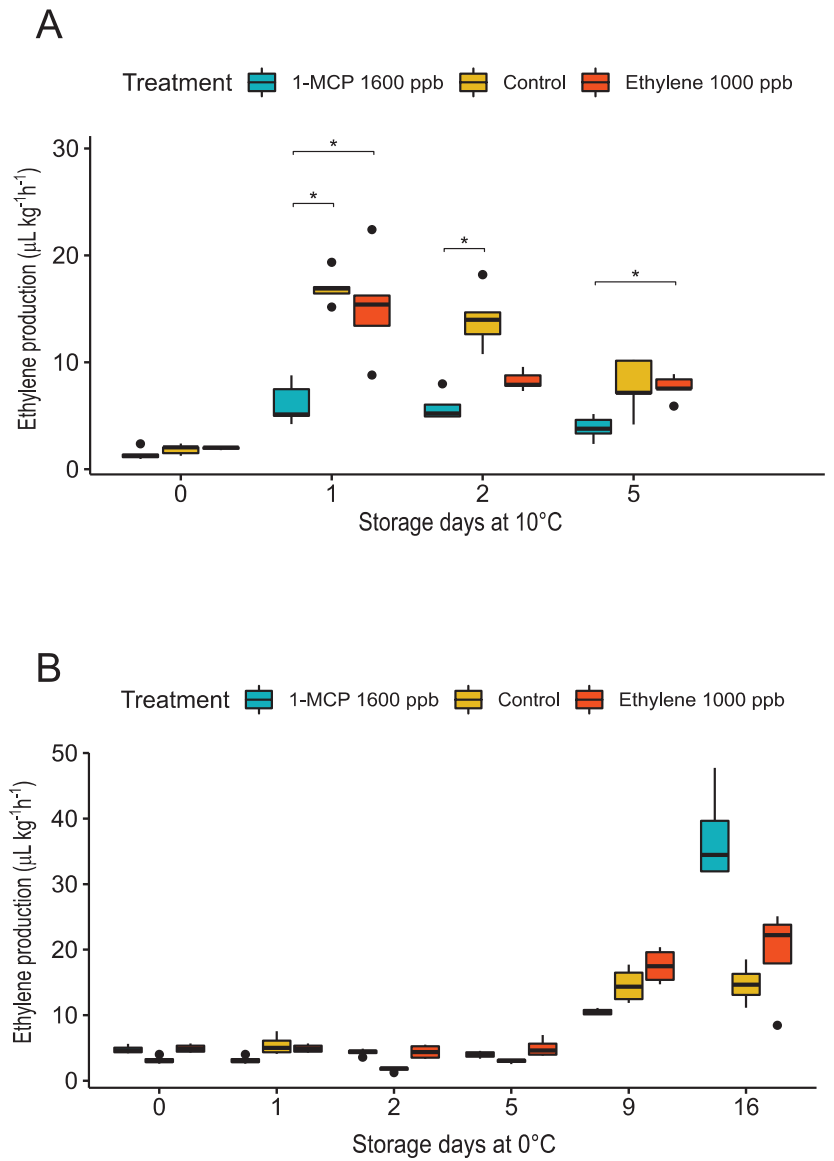**Figure 10.** PCA biplot for ethylene, CO_2 and firmness indices of raspberry (*Rubus idaeus* 'Heritage') fruit during treatment with ethylene and 1-methyl cyclopropane (1-MCP) at 0 °C. The storage assay was performed at the W stage of the raspberry fruit and stored for 16 days and at 0 °C. The PCA analysis was carried out on each sampling day.

The principal component analysis showed that the first two components (PC1 and PC2) explained more than 45% and more than 19%, respectively, of the variability in ethylene production, CO_2 production and firmness, determined between treatments at a storage temperature of 0 °C (Figure 10). At this temperature, the 1-MCP-treated fruit was independent of the control and the ethylene-treated fruit was only at 9 and 6 days of storage (Figure 10), confirming that the treatment with 1-MCP was ineffective at 0 °C.

3.2.3. Total Soluble Solids (TSS) and Titratable Acidity (TA) Changes during Treatments

During the cold storage assay, no significant differences in TSS were observed between treatments independent of the temperature of the assay (Figure 11). During the assay at 10 °C (Figure 11A), the fruit reached values of 12.6 °Brix at 5 days of storage, whereas the fruit under 0 °C reached similar TSS values after 16 days of storage, independent of the treatment (Figure 11B). Therefore, the TSS increased 1.2 times to harvest value after 5 days of storage at 10 °C and after 16 days at 0 °C. The TA values (average 2.5%) during the different treatments and cold storage temperature (Figure 11) remained similar to those obtained in the harvest (2.4%).
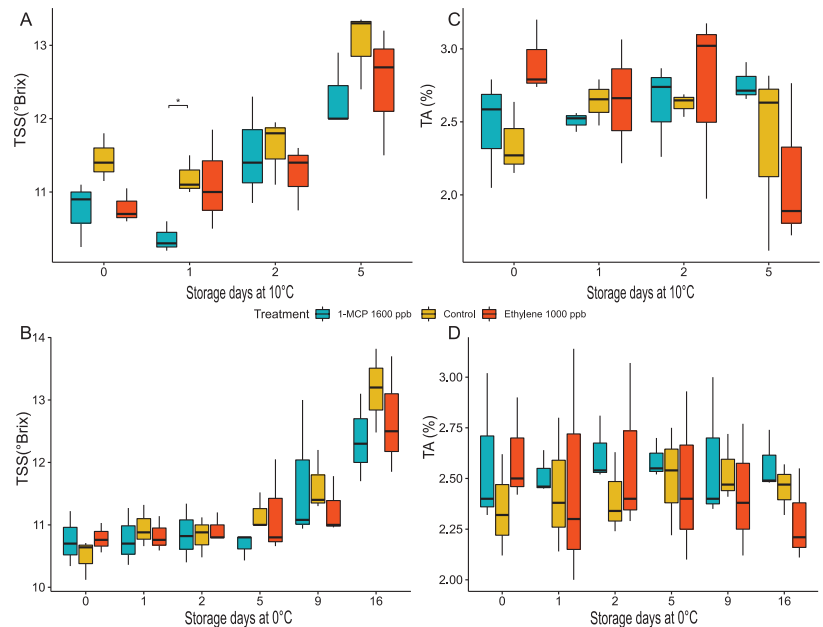
Figure 11. The total soluble solids and titratable acidity of raspberry (*Rubus idaeus* 'Heritage') fruit during treatment with ethylene and 1-methyl cyclopropane (1-MCP). The storage assay was performed at the W stage of the raspberry fruit and stored for 5 and 16 days at 10 °C (**A,C**) and 0 °C (**B,D**), respectively. Total soluble solids (TSS, °Brix) (**A,B**) and titratable acidity (TA, %) (**C,D**) were determined for ethylene and 1-MCP-treated fruits and controls. Data represent the means ± S.D. from five sample units (each containing ten fruits). Asterisks indicate significant differences between treatments at the same storage time ($p \leq 0.05$). Boxplots show each group's distribution (treatment), and the black line (central value in the box) signs the median value. Points out of the boxplots show outlier values.

4. Discussion

In this study, the physiological and quality parameters of 'Heritage' raspberry fruit were evaluated during its development, showing a continuous increase in ethylene production in the receptacle, at least sevenfold higher than that produced by drupelets at R and OR stages. Conversely, a constant decrease in CO_2 production was observed for all tissues analyzed from LG to OR stages, ten times higher in the receptacle than whole fruit for all stages. This ethylene production pattern with different respiratory rates can be observed in raspberries ('Heritage') grown in the same location during three seasons [5,9]. Furthermore, a negative correlation between ethylene and fruit firmness has been described during the ripening of the whole fruit of this cultivar [7], as observed in the present analysis of PCA and the correlation matrix (Figures 4 and 5) for the whole fruit. In the present and previous

studies [5,9], the continuous ethylene production observed in raspberry fruit is not similar to other non-climacteric species. For example, in strawberry, the ethylene production was higher only in the green fruit stage, decreasing in white (W) stage fruit, and then showed an increasing trend towards the red stage, concomitant with an enhanced respiration rate [20].

Previous studies have indicated the W stage of fruit development as the onset of 'Heritage' raspberry ripening [5–9]. Moreover, the W stage has been described as the first stage of ripening in the three new Chilean raspberry cultivars: 'Santa Catalina', 'Santa Clara' and 'Santa Teresa' [12]. It has been described that 'Heritage' showed a sharp decline in fruit firmness throughout the developmental stages compared to 'Santa Catalina', 'Santa Clara' and 'Santa Teresa' cultivars [12]. In these four cultivars, the ethylene production rate measured one day after harvest was always the highest at the dark red stage and lowest in the less mature fruit at the pink stage [12]. Therefore, the drastic decline in firmness and increase in ethylene production observed at the W stage (Figures 2 and 3) led us to analyze the relationship between this fruit quality parameter and the hormone.

In the present study, the 1-MCP reduced the ethylene production compared to control and ethylene treatments only at 10 °C. At 0 °C, ethylene production was kept similar to the harvest for a duration of five days, independent of treatment (Figure 6), suggesting that 'Heritage' maintains a metabolic rate at 10 °C, where the response to ethylene is clearly perceived compared to the fruit stored at 0 °C. Furthermore, our results obtained for 1-MCP-treated 'Heritage' fruit stored at 10 °C are consistent with the decreased ethylene production reported in strawberry following 1 μL L^{-1} 1-MCP exposure and stored at 5 °C [21].

The increase in ethylene and decrease in CO_2 production during the ripening and the reduction in ethylene production by 1-MCP application, with a non-effect in CO_2 production at 10 °C, indicate both a climacteric behavior of ethylene production, similar to tomato [22], and a non-climacteric production of CO_2. The decreasing trend of CO_2 of raspberry fruit coincides with the non-climacteric fruit behavior and previous studies of different raspberry cultivars, including 'Heritage' [8,12]. On the other hand, the constant increase in ethylene in whole fruit during ripening is very different from that in other non-climacteric fruit, such as grape [23,24] and strawberry fruits [20], with ethylene peaks during early development, a typical pattern in non-climacteric fruit. However, some outlier points in the determination of ethylene production during development (Figure 2) make it necessary to deepen the understanding of ethylene production during raspberry ('Heritage') fruit development, for example, using chambers for ethylene determination of fruit in planta. It has been reported that an anti-sense suppression of the gene encoding for *Malus domestica*, 1-amino-cyclopropane-carboxylase oxidase (MdACO1), resulted in fruit with early ripening events (conversion of starch to sugars), showing a low dependency for ethylene, but a high sensitivity to low concentrations of ethylene (0.01 μL L^{-1}). By contrast, late ripening events (flesh softening) showed a high dependency for ethylene but were less sensitive to low concentrations (needing 0.1 μL L^{-1} for a response) [25].

The extremely short shelf-life of raspberry fruit (1–2 days) is one of the most critical limitations during harvest and postharvest operations [1,3,26]. In strawberry fruit (*F.* × *ananassa* 'Oso Grande'), it has been reported that 1-MCP delayed the softening of the fruit, since fruit treated with 100 nL L^{-1} 1-MCP showed greater firmness and a minor percentage of pectin solubilization during storage at room temperature [27]. In *F.* × *ananassa* 'Toyonoka', the application of ethylene (2 mmol L^{-1} ethephon) did not modify the activity of cell wall hydrolases related to softening (e.g., polygalacturonase), whereas treatment with 1 μL L^{-1} 1-MCP clearly did [28]. In the present study, the ethylene receptor inhibition by 1-MCP treatment during storage at 10 °C allowed for maintaining 55% of the firmness determined at the harvest, suggesting a relation of endogenous ethylene production with the firmness at this temperature (Figure 8A). Nevertheless, this treatment does not preserve the firmness observed at harvest and fails to prolong the storage of the fruit for more than 5 days. Under 0 °C, the fruit showed a firmness (over to 2 N) for up to 9 days. No significant differences were observed for 1-MCP treatment compared to the control and

ethylene-treated fruit at this cold storage temperature (Figure 8B). At this temperature, it is likely that the low metabolic rate allows a lower response to ethylene and, therefore, a lower effect of the ethylene receptor inhibitor. In 'Selva' strawberry, Ku et al., 1999 [29] describe that the 1-MCP treatment at a lower concentration (5 to 15 nL·L^{-1}) extended its postharvest life (i.e., freshness or gloss, firmness and mold absence) by 35% and 150% at 20 °C and at 5 °C, respectively. On the other hand, the same authors [29] indicated that higher 1-MCP concentrations (500 nL·L^{-1}) accelerated the loss of quality (60%) of four strawberry cultivars at 5 °C. Therefore, the partial effect of 1-MCP on the maintenance of raspberry fruit's firmness may be due to the 1-MCP concentration.

Other key phytohormones probably regulate raspberry firmness that is associated with ethylene. In non-climacteric fruit, abscisic acid (ABA) has been described as the main hormone that regulates the ripening process [6]. Early in the 1980s, ABA was reported to be involved in strawberry ripening [30] and has been defined as the main regulator of the onset of grape berry ripening [31], regulating the softening, coloration and sugar accumulation [31–34]. On the other hand, it has been suggested that ethylene plays a secondary role in strawberry ripening compared to abscisic acid. Therefore, ethylene can regulate specific events related to the ripening process in strawberries and grapes, such as coloration. In grape (*Vitis vinifera* 'Cabernet Sauvignon'), it has been described that ethylene increases anthocyanin content [35]. The ethylene effect depends on the developmental stage and species evaluated in strawberries. It has been reported that unripe fruit of *Fragaria chiloensis* (large green stage) treated with ethephon showed a lower anthocyanin content but a higher lignin content compared to the control at 48 and 216 h after treatment [36]. These findings contrast with the results observed in *F.* × *ananassa* fruit ('Toyonoka' and 'Camarosa'), where ethylene treatment at the white developmental stage promoted the accumulation of anthocyanins [28,37], and the application of 1-MCP [28] decreased that process. To date, no changes in ABA levels have been described during ripening, but it is certainly a possible candidate to regulate raspberry ripening.

The bright red stage of the 'Heritage' raspberry has been described with a low sugar/acid ratio (3.8) [12,38]. However, in the present study, fruit at the red stage shows an average total soluble solids (TSS) content (11.2 °Brix) (Figure 3B) higher than previously described by Contreras et al., 2021 [12] for 'Heritage' (8.2 °Brix) harvested in winter in Santo Domingo (33°38′09″ S, 71°37′41″ W), Valparaíso Region, Chile. Our result related to the TSS value was similar to that described for 'Santa Catalina' raspberry fruit (10.6 °Brix) [12]. These differences may be due to the month of harvest and localities, where the summer–autumn season favors the accumulation of soluble solids content. A constant decrease in titratable acidity (TA), and an increase in TSS content were observed during development (Figure 3B,C). In fact, TSS (0.60) and TA (−0.63) did not show a high correlation, positive or negative, with the ethylene production from whole fruit during development (Figure 5). On the other hand, a TSS content increase was observed only in the final days of each assay, without marked differences between treatments at both temperatures (Figure 11). Conversely, TA remained similar to those obtained in the harvest during all storage times, and no significant differences were observed between treatments, independent of storage temperature (Figure 11). These findings are similar to those described by Perkins-Veazie and Nonnecke (1992) [8], with a TSS content and TA independent of ethylene levels in 'Heritage' raspberry. In the present study, no correlation was observed between TSS and TA with ethylene production from whole fruit during development (Figure 5). Therefore, TSS and TA changes can be regulated by an independent ethylene mechanism. Similarly, in *F.* × *ananassa* 'Pajaro', ethylene (100 µL L^{-1}) treatment showed no changes in soluble solids content [39].

In 'Pajaro' strawberry fruit, ethylene treatment showed that fruit softening and color development were slightly accelerated by ethylene (100 µL L^{-1}) treatment, stimulating the respiration in early-harvested strawberry fruit within 2 days. The 1-MCP affected the respiratory rise induced by exogenous ethylene dependent on fruit maturity [39]. In the present study, the fruit treated with 1-MCP and stored at 10 °C presented a lower loss of

firmness associated with lower ethylene production during the days of storage, compared to the control fruit and ethylene-treated fruit. The results indicate that the firmness of the fruit stored at 10 °C partially depends on the endogenous production of ethylene, but does not respond to exogenous ethylene application. The PCA showed that the 1-MCP treatment behaved as an independent group to the control and ethylene-treated fruit at that temperature, but with a low negative correlation between firmness and ethylene production. These results suggest a partial effect of the endogenous ethylene from the receptacle on the firmness loss of the whole fruit.

5. Conclusions

In the present study, a decrease in firmness and titratable acidity (TA) with increased total soluble solids (TSS) was observed through ripening. The increase in ethylene production with a negative correlation with a decrease in the firmness of whole fruit (–0.73) during ripening and the effect of 1-MCP application suggests an effect of endogenous ethylene mainly over firmness. Moreover, the positive correlation between firmness and CO_2 production in the whole fruit (0.81) suggests a ripening behavior for 'Heritage' raspberry fruit that could be placed between climacteric and non-climacteric behavior. On the other hand, the lack of correlation, positive or negative, between TSS and TA with ethylene production from whole fruit during development, and the lack of effect of 1-MCP treatment on TSS and TA, suggest an ethylene-independent regulation mechanism of sugars and organic acid accumulation. Therefore, even though endogenous ethylene could partially regulate the firmness of 'Heritage' raspberry fruit detached from plants, more information must be gathered from field assays to determine the regulatory role of ethylene on the loss of firmness during ripening, along with its crosstalk with other hormones and the impact of these applications during storage.

References

1. Iannetta, P.P.M.; van den Berg, J.; Wheatley, R.E.; McNicol, R.J.; Davies, H.V. The role of ethylene and cell wall modifying enzymes in raspberry (*Rubus idaeus*) fruit ripening. *Physiol. Plant.* **1999**, *105*, 338–347. [CrossRef]
2. Zheng, D.; Hrazdina, G. Cloning and characterization of an expansin gene, RiEXP1, and a 1-aminocyclopropane-1-carboxylic acid synthase gene, RiACS1 in ripening fruit of raspberry (*Rubus idaeus* L.). *Plant Sci.* **2010**, *179*, 133–139. [CrossRef]
3. Iannetta, P.P.M.; Wyman, M.; Neelam, A.; Jones, C.; Davies, H.V.; Sexton, R. A causal role for ethylene and endo-b-1,4-glucanase in the abscission of red-raspberry (*Rubus idaeus* L.) drupelets. *Physiol. Plant.* **2000**, *110*, 535–543. [CrossRef]
4. Sexton, R.; Palmer, J.M.; Whyte, N.; Littlejohns, S. Cellulase, fruit softening and abscission in red raspberry *Rubus idaeus* L. cv Glen Clova. *Ann. Bot.* **1997**, *80*, 371–376. [CrossRef]
5. Fuentes, L.; Monsalve, L.; Morales-Quintana, L.; Valdenegro, M.; Martínez, J.P.; Defilippi, B.G.; González-Agüero, M. Differential expression of ethylene biosynthesis genes in drupelets and receptacle of raspberry (*Rubus idaeus*). *J. Plant Physiol.* **2015**, *179*, 100–105. [CrossRef]

6.   Fuentes, L.; Figueroa, C.R.; Valdenegro, M. Recent Advances in Hormonal Regulation and Cross-Talk during Non-Climacteric Fruit Development and Ripening. *Horticulturae* **2019**, *5*, 45. [CrossRef]
7.   Monsalve, L.; Ayala-Raso, A.; Bernales, M.; Valdenegro, M.; Defilippi, B.; González-Agüero, M.; Cherian, S.; Fuentes, L. Dataset on quality and physiological changes of raspberry fruit during their development and under auxin in-vitro assay. *Data Brief* **2018**, *21*, 1521–1525. [CrossRef]
8.   Perkins-Veazie, P.M.; Nonnecke, G. Physiological changes during ripening of raspberry fruit. *J. Hortic. Sci.* **1992**, *27*, 331–333. [CrossRef]
9.   Bernales, M.; Monsalve, L.; Ayala-Raso, A.; Valdenegro, M.; Martínez, J.P.; Travisany, D.; Defilippi, B.; González-Agüero, M.; Cherian, S.; Fuentes, L. Expression of two indole-3-acetic acid (IAA)-amido synthetases (GH3) genes during fruit development and ripening of raspberry (*Rubus idaeus* Heritage). *Sci. Hortic.* **2019**, *246*, 168–175. [CrossRef]
10.   Stewart, D.; Iannetta, P.P.; Davies, H.V. Ripening-related changes in raspberry cell wall composition and structure. *Phytochemistry* **2001**, *56*, 423–428. [CrossRef]
11.   El-Kayal, W.E.; Paliyath, G.; Sullivan, J.A.; Subramanian, J. Phospholipase D inhibition by hexanal is associated with calcium signal transduction events in raspberry. *Hortic. Res.* **2017**, *4*, 17042. [CrossRef] [PubMed]
12.   Contreras, C.; Hermosilla, A.; Contreras, E.; Naranjo, P.; Zoffoli, J.P.; Gambardella, M. Postharvest physiology and storage potential of new Chilean raspberry cultivars. *Chil. J. Agric. Res.* **2021**, *81*, 161–171. [CrossRef]
13.   Giovanelli, G.; Limbo, S.; Buratti, S. Effects of new packaging solutions on physico-chemical, nutritional and aromatic characteristics of red raspberries (*Rubus idaeus* L.) in postharvest storage. *Postharvest Biol. Technol.* **2014**, *98*, 72–81. [CrossRef]
14.   Giongo, L.; Ajelli, M.; Poncetta, P.; Ramos-García, M.; Sambo, P.; Farneti, B. Raspberry texture mechanical profiling during fruit ripening and storage. *Postharvest Biol. Technol.* **2019**, *149*, 177–186. [CrossRef]
15.   Li, L.; Kaplunov, T.; Zutahy, Y.; Daus, A.; Porat, R.; Lichter, A. The effects of 1-methylcyclopropane and ethylene on postharvest rachis browning in table grapes. *Postharvest Biol. Technol.* **2015**, *107*, 16–22. [CrossRef]
16.   Muñoz-Robredo, P.; Gudenschwager, O.; Chervin, C.; Campos-Vargas, R.; González-Agüero, M.; Defilippi, B. Study on differential expression of 1-aminocyclopropane-1-carboxylic acid oxidase genes in table grape cv. Thompson Seedless. *Postharvest Biol. Technol.* **2013**, *76*, 163–169. [CrossRef]
17.   Correa, J.; Mamani, M.; Muñoz, C.; González, M.; Defilippi, B.; Campos, R.; Pinto, M.; Hinrichsen, P. New Stable QTLs for Berry Firmness in Table Grapes. *Am. J. Enol. Vitic.* **2016**, *67*, 212–217. [CrossRef]
18.   Lurie, S.; Ovadia, R.; Nissim-Levi, A.; Oren-Shamir, M.; Kaplunov, T.; Zutahy, Y.; Weksler, H.; Lichter, A. Abscisic acid improves colour development in 'Crimson Seedless' grapes in the vineyard and on detached berries. *J. Hortic. Sci.* **2009**, *84*, 639–644. [CrossRef]
19.   R Core Team. *R: A Language and Environment for Statistical Computing*; R Foundation for Statistical Computing: Vienna, Austria, 2021. Available online: https://www.R-project.org/ (accessed on 23 February 2022).
20.   Iannetta, P.P.M.; Laarhovenb, L.J.; Medina-Escobar, N.; James, E.K.; McManus, M.T.; Davies, H.V.; Harren, F.J.M. Ethylene and carbon dioxide production by developing strawberries show a correlative pattern that is indicative of ripening climacteric fruit. *Physiol. Plant.* **2006**, *127*, 247–259. [CrossRef]
21.   Bower, J.H.; Biasi, W.V.; Mitcham, E.J. Effects of ethylene and 1-MCP on the quality and storage life of strawberries. *Postharvest Biol. Technol.* **2003**, *28*, 417–423. [CrossRef]
22.   Cara, B.; Giovannoni, J. Molecular biology of ethylene during tomato fruit development and maturation. *Plant Sci.* **2008**, *175*, 106–113. [CrossRef]
23.   Chervin, C.; El-Kereamy, A.; Roustan, J.-P.; Latché, A.; Lamon, J.; Bouzayen, M. Ethylene seems required for the berry development and ripening in grape, a non-climacteric fruit. *Plant Sci.* **2004**, *167*, 1301–1305. [CrossRef]
24.   Sun, L.; Zhang, M.; Ren, J.; Qi, J.; Zhang, G.; Leng, P. Reciprocity between abscisic acid and ethylene at the onset of berry ripening and after harvest. *BMC Plant Biol.* **2010**, *10*, 257–267. [CrossRef] [PubMed]
25.   Johnston, J.W.; Gunaseelan, K.; Pidakala, P.; Wang, M.; Schaffer, R.J. Co-ordination of early and late ripening events in apples is regulated through differential sensitivities to ethylene. *J. Exp. Bot.* **2009**, *60*, 2689–2699. [CrossRef]
26.   Sjulin, T.M.; Robbins, J. Effects of maturity, harvest date and storage time on postharvest quality of red raspberry fruit. *J. Am. Soc. Hortic. Sci.* **1987**, *112*, 481–487.
27.   Silva, P.A.; de Abreu, C.M.P.; de Queiroz, E.R.; Corrêa, A.D.; Santos, C.D. Storage of Strawberries (*Fragaria ananassa* L.) Cv. 'Oso Grande', Subjected to 1-MCP. *Acta Sci. Technol.* **2012**, *34*, 353–358. [CrossRef]
28.   Villarreal, N.M.; Bustamante, C.A.; Civello, P.M.; Martínez, G.A. Effect of ethylene and 1-MCP treatments on strawberry fruit ripening. *J. Sci. Food Agric.* **2010**, *90*, 683–689. [CrossRef]
29.   Ku, V.V.V.; Wills, R.B.H.; Ben-Yehoshua, S. 1-Methylcyclopropene can differentially affect the postharvest life of strawberries exposed to ethylene. *HortScience* **1999**, *34*, 119–120. [CrossRef]
30.   Kano, Y.; Asahira, T. Roles of cytokinin and abscisic acid in the maturing of strawberry fruits. *J. JPN Soc. Hortic. Sci.* **1981**, *50*, 31–36. [CrossRef]
31.   Pilati, S.; Bagagli, G.; Sonego, P.; Moretto, M.; Brazzale, D.; Castorina, G.; Simoni, L.; Tonelli, C.; Guella, G.; Engelen, K.; et al. Abscisic acid is a major regulator of grape berry ripening onset: New insights into ABA signaling network. *Front. Plant Sci.* **2017**, *8*, 1093. [CrossRef]

32. Gagné, S.; Cluzet, S.; Mérillon, J.M.; Gény, L. ABA initiates anthocyanin production in grape cell cultures. *J. Plant Growth Regul.* **2011**, *30*, 1–10. [CrossRef]
33. Lecourieux, F.; Kappel, C.; Lecourieux, D.; Serrano, A.; Torres, E.; Arce-Johnson, P.; Delrot, S. An update on sugar transport and signalling in grapevine. *J. Exp. Bot.* **2013**, *65*, 821–832. [CrossRef]
34. Kühn, N.; Guan, L.; Dai, Z.W.; Wu, B.H.; Lauvergeat, V.; Gomès, E.; Li, S.H.; Godoy, F.; Arce-Johnson, P.; Delrot, S. Berry ripening: Recently heard through the grapevine. *J. Exp. Bot.* **2014**, *65*, 4543–4559. [CrossRef] [PubMed]
35. El-Kereamy, A.; Chervin, C.; Roustan, J.P.; Cheynier, V.; Souquet, J.M.; Moutounet, M.; Raynal, J.; Ford, C.; Latch'e, A.; Pech, J.C.; et al. Exogenous ethylene stimulates the longterm expression of genes related to anthocyanin biosynthesis in grape berries. *Physiol. Plant.* **2003**, *119*, 175–182. [CrossRef]
36. Figueroa, N.E.; Gatica-Meléndez, C.; Figueroa, C.R. Ethylene application at the immature stage of Fragaria chiloensis fruit represses the anthocyanin biosynthesis with a concomitant accumulation of lignin. *Food Chem.* **2021**, *358*, 129913. [CrossRef] [PubMed]
37. Sun, J.-H.; Luo, J.-J.; Tian, L.; Li, C.-L.; Xing, Y.; Shen, Y.-Y. New evidence for the role of ethylene in strawberry fruit ripening. *J. Plant Growth Regul.* **2013**, *32*, 461–470. [CrossRef]
38. Yang, J.; Cui, J.; Chen, J.; Yao, J.; Hao, Y.; Fan, Y.; Liu, Y. Evaluation of physicochemical properties in three raspberries (*Rubus idaeus*) at five ripening stages in northern China. *Sci. Hortic.* **2020**, *263*, 109–146. [CrossRef]
39. Tian, M.; Prakash, S.; Elgar, H.; Young, H.; Burmeister, D.M.; Ross, G.S. Responses of strawberry fruit to 1-Methylcyclopropene (1-MCP) and ethylene. *Plant Growth Regul.* **2000**, *32*, 83–90. [CrossRef]

Membrane Fatty Acids and Physiological Disorders in Cold-Stored 'Golden Delicious' Apples Treated with 1-MCP and Calcium Chloride

Maria Dulce Antunes [1,*], **Ana Clara Guimarães** [2], **Custódia Gago** [1], **Adriana Guerreiro** [3], **Jorge Panagopoulos** [1,4], **Eduardo Vilas Boas** [5] **and Maria Graça Miguel** [1]

[1] MED, Faculdade de Ciências e Tecnologia, Universidade do Algarve, Edf. 8, Campus de Gambelas, 8005-139 Faro, Portugal; cgago@ualg.pt (C.G.); jorantpan@gmail.com (J.P.); mgmiguel@ualg.pt (M.G.M.)

[2] Centro Universitário de Patos de Minas—UNIPAM, Rua Major Gote, 808-Bairro Caiçaras, Patos de Minas 38700-207, MG, Brazil; anaclaragg.nutricionista@gmail.com

[3] CEOT, Faculdade de Ciências e Tecnologia, Edf. 8, Campus de Gambelas, 8005-139 Faro, Portugal; acguerreiro@ualg.pt

[4] C-MAST, Department of Aerospace Sciences, Faculty of Engineering, Universidade da Beira Interior, 62001-001 Covilhã, Portugal

[5] Department of Food Science, Federal University of Lavras, P.O. Box 3037, Lavras 37200-900, MG, Brazil; evbvboas@ufla.br

* Correspondence: mantunes@ualg.pt; Tel.: +351-289-800-900

Abstract: The present research intents to study skin fatty acids and physiological disorders developed during cold storage in 'Golden Delicious' apples treated with 1-MCP and calcium. Harvested fruits were treated with calcium chloride (Ca), 1-MCP (MCP), Ca + MCP or no treatment (control) and then subjected to cold storage at 0.5 °C for 6 months. Fatty acids' composition, malondialdehyde (MDA) and the physiological disorders bitter pit (BP), superficial scald and diffuse skin browning (DSB) were measured at harvest and after storage plus 7 days of shelf-life at room temperature ≈22 °C. Palmitic acid decreased and linoleic acid increased over time, while oleic and stearic acids had few changes. Generally, unsaturated/saturated fatty acids and MDA increased over the storage period. Treatment with Ca showed that, at the end of the experiment, the lowest MDA values and the highest unsaturated/saturated fatty acids ratio were mainly due to higher linoleic and lower palmitic acids concentrations, which are coincident with less severe BP. There was no clear correlation between the measured fatty acids (palmitic, linoleic, oleic and stearic), unsaturated-to-saturated fatty acids ratio or MDA with chilling skin physiological disorders. Further research is needed to clarify the changes in membrane properties and the effect of some treatments in response to chilling injury during storage.

Keywords: quality; MDA; bitter pit; superficial scald; chilling

1. Introduction

To increase the postharvest life of fresh fruits, cold storage is the first aspect that needs to be considered, combined or not with other postharvest technologies. During storage, postharvest losses occur due to mechanical damage, diseases and physiological disorders [1,2]. Fresh apple marketing is an important subject worldwide. Apples (*Malus domestica* Borkh) can develop many physiological disorders during cold storage at 0 °C, one of the most prominent of which is bitter pit (BP) together with superficial scald, causing significant losses to apple growers worldwide [3,4]. BP occurs mainly during the period of cold storage and is characterized by black spots in the pulp, which dehydrate with time and form depressions in the skin of the fruit, reducing the marketability and quality of apple [5].

Calcium, in low concentrations in fruits, favors the formation of injuries that progress to the death of the tissues, leading to BP. This is because Ca has a role in the selective

permeability, the structure and functionality of the cell membranes by monogalactosyl diacylglycerols and phospholipids connections on the membrane surface [6]. Thus, the positive effects of Ca in preserving postharvest quality have been attributed to the fact that it is associated with the pectic substances of the middle lamella and cell membranes, stiffening tissues and preserving the characteristics of selective permeability in the cell membrane system [5,7].

Scald is also a physiological disorder appearing in the skin after long-term cold storage in apples and pears, which is related to the synthesis of α-farnesene and the accumulation of its conjugated trienols in the fruit epidermis and hypodermis. This event causes the rupture of the cell membranes, leading to polyphenoloxidase-mediated browning of the fruit peel [2,3,8,9].

Fatty acids and lipids are important structural and metabolic constituents of plant/fruit cells. Disturbances in membrane lipid composition often have severe consequences on the ability of the cell to adapt to extreme temperatures and other stress conditions, which, in fruit, may led to various storage physiological disorders [10,11].

Oxidative damage is the initial response of tissues to chilling. The production and accumulation of reactive oxygen species (ROS) are responsible for lipid oxidation. The end product of poly-unsaturated fatty acid oxidation is the toxic product malondialdehyde (MDA) [12]. Cheng et al. [13] reported a higher ratio of unsaturated/saturated fatty acids and lower levels of MDA in a pear treated with 1-MCP than in the control, explaining the lower CI in the first fruit. Additionally, cell membranes are considered to be the primary sites for the development of CI. A higher ratio of unsaturated/saturated fatty acids has been shown to improve tolerance to low-temperature storage in some fruits such as loquats [14], bananas [15] and mangoes [16].

Ethylene, known as the ripening hormone, triggers a series of biochemical changes that culminate in the ripening and senescence of fruits. The volatile compound 1-methylcyclopropene (1-MCP) binds permanently to ethylene receptors in fruit tissue [1,17] and prevents their action [18]. Thus, the postharvest application of 1-MCP can maintain the quality of apples, inhibit the growth of certain physiological disorders during storage such as superficial scald and demonstrate a positive effect on fruit quality preservation, leading to a delay in ripening and improved firmness retention [4,19].

However, 1-MCP treatment may also cause disorders such as bitter pit (BP) [2,20,21], which can be reduced by adding Ca to the 1-MCP treatment [4]. Larrigaudière et al. [22] and Gamrasni et al. [23] also reported a disorder known as diffuse skin browning (DSB) in 1-MCP-treated fruit, which can be misguidedly interpreted as superficial scald, with the appearance of diffuse browning of the skin; but in this case, the skin becomes very rough. Interestingly, this disorder appears only in countries that have very hot summers and little rainfall. Further, it was found that by progressive cooling and delaying the time after harvest to 1-MCP, application may prevent this disorder [22,23]. No induction [2] or a minor induction [4] of DSB by 1-MCP was found when the application was delayed 3 days after cooling the fruit.

The objective of this work was to investigate the effect of Smart fresh TM (625 nL/L^{-1} 1-MCP) and calcium chloride (1.5%) on the skin membrane fatty acids and their relation with the development of physiological disorders during cold storage (0.5 °C in normal atmosphere for 6 months) and subsequent shelf life (7 days) at room temperature ≈22 °C in 'Golden Delicious' apples.

2. Material and Methods

2.1. Plant Material and Treatments

Apples of the cultivar Golden Delicious were harvested from 10 orchards located in the west-center region of Portugal with ≈15% soluble solid content (°Brix), ≈15N firmness and 6–7 starch index. All the orchards were under commercial management conditions.

Half of the fruits from each producer (4 crates) were immersed for 2 min in a solution containing 1.5% CaCl$_2$ (calcium chloride anhydrous 95% PANREAC) and TECTO 500SC

(thiabendazole 42.9% p/p–200 mL/100 L water). The other half of the fruits were immersed for 2 min in a solution only with TECTO 500SC (thiabendazole 42.9% p/p –200 mL/100 L water). After, all fruits (not treated or treated with CaCl$_2$) were stored in a cold room at 0.5 °C, and after 3 days of storage, half of the fruits treated with CaCl$_2$ and half of the fruits without calcium treatment were treated with 625 nL/L 1-MCP using Smartfresh^{TM} (AgroFresh, Spain) for 20 h at 0.5 °C. Treatments were as follows: control (no treatment), Ca (treated with CaCl$_2$), MCP (treated with 1-MCP) and Ca + MCP (treated with CaCl$_2$ and 1-MCP). All fruits were stored at 0.5 °C in normal atmosphere and 90–95% relative humidity for 6 months. Four replications were carried out for each treatment.

Sampling dates were at harvest (0 d) and 7 days of shelf-life at ≈22 °C and after 6 months storage at 0.5 °C (0 d poststorage) and 7 more days of shelf-life (7d poststorage) at room temperature (≈22 °C). On these dates, fatty acid identification and quantification as well as MDA content were carried out, and the incidence of superficial scald, DSB and BP on the apple exocarp were also observed and registered.

2.2. Fatty Acid Identification and Quantification

Fatty acids derived from the same exocarp tissue sample were extracted according to Meyer and Terry [24]. Briefly, 3 g of ground lyophilized exocarp tissue was homogenized with hexane and filtered under vacuum through a Fisherbrand QL 100 filter paper (Fisher Scientific, Leicester, UK). The solvent from the lipid-containing filtrate was evaporated under vacuum.

Fatty acid methyl esters (FAMEs) were produced according to the method prescribed by the International Olive Oil Council (IOOC) with modifications. Briefly, 0.2 mL of methanolic KOH (2 N) was added to 0.1 g of apple oil extract in 2 mL of hexane. Hexane was chosen as the preferred solvent due to improved peak resolution. The mixture was shaken vigorously for 30 s and left to stratify until the upper layer became clear. The hexane layer containing the methyl esters was decanted and kept for no more than 12 h at 5 °C until needed. This solution was diluted 1:100 (*v/v*) with fresh hexane immediately before injection into a Trace 1300 GC (Thermo Scientific, San Jose, CA, USA) equipped with a G1540N flame ionization detector (FID) and a 7683B autosampler. The identification and quantification of selected compounds were performed using two capillary columns: TG-17MS capillary column (30 m × 0.25 mm i.d., 0.25 μm film thickness; Thermo Scientific, San Jose, CA, USA) and TG-1MS (30 m × 0.25 mm i.d., 0.25 μm film thickness; Thermo Scientific, San Jose, CA, USA). Column temperature was programmed at 55 °C for 3 min and then raised to 175 °C at 13 °C min^{-1} intervals, followed by an isothermal period of 1 min, and increased again to a final temperature of 220 °C at 8 °C min^{-1}. The carrier gas was He at a constant flow rate of 1.6 mL min^{-1}. The injector and detector temperatures were set at 220 and 250 °C, respectively. The presence and abundance of fatty acids were calculated by comparison of peak area as a percentage.

Fatty acid identification was carried out by comparison of the retention times of each peak with retention times of standards of oleic acid, linoleic acid, stearic acid and palmitic acid from Sigma-Aldrich, which were injected using the same conditions. The unsaturated/saturated fatty acid ratio was calculated by the formula: (18:1 + 18:2)/(16:0 + 18:0) where: 16:0 = palmitic acid; 18:0 = stearic acid; 18:1 = oleic acid; and 18:2 = linoleic acid.

2.3. Malondialdehyde (MDA) Content

Lipid peroxidation was determined by measuring the MDA content of frozen ground tissue according to the method of Hodges et al. [25] and Lee et al. [26]. Frozen ground apple skin tissues (1.0 g) were homogenized in 8 mL of 80% (*v/v*) ice-cold ethanol and 5% (*w/v*) insoluble polyvinylpolypyrrolidone (PVPP) with an Ultra-Turax then centrifuged at 3000× *g* at 4 °C for 10 min in Microfuge$^{®}$ 18 Centrifuge (Beckman Coulter, Brea, CA, USA). One aliquot (0.6 mL) was mixed with 0.6 mL of a solution without thiobarbituric acid (−TBA), which consisted of 20% trichloroacetic acid (TCA) and 0.01% butylated hydroxyltoluene (BHT), while the other aliquot was mixed with 0.6 mL of TBA solution

(+TBA), which was composed of the above with 0.65% TBA. After vigorous mixing, the sample was incubated at 95 °C for 25 min, cooled down quickly on ice and then centrifuged at 3000× *g* at 4 °C for 10 min.

The absorbance of the sample was recorded at 440, 532 and 600 nm using a spectrophotometer. MDA equivalents were calculated in the following manner:

(1) $[(Abs\ 532_{+TBA}) - (Abs\ 600_{+TBA}) - (Abs\ 532_{-TBA} - Abs600_{-TBA})] = A;$
(2) $[(Abs\ 440_{+TBA} - Abs\ 600_{+TBA}) \times 0.0571] = B;$
(3)   MDA equivalent (nmol g^{-1} FW) = $[(A - B/157,000) \times 10^6 \times (\text{adjusted sample FW}) \times (\text{buffer volume})].$

2.4. Physiological Disorders and Rots

The presence of diffuse skin browning (DSB), superficial scald, bitter pit (BP) and rot was visually evaluated for 100 fruits per orchard per treatment after 6 months of cold storage and 7 d of shelf-life. The incidence of each disorder or rot was calculated as the percentage of affected fruits compared to the total number of fruits per replicate [2].

2.5. Statistical Analysis

The experimental was conducted with a complete randomized block design. Statistical analysis was carried out with SPSS 16.0 software (SPSS Inc., Chicago, IL, USA). Two-way analysis of variance (ANOVA) was performed using treatments and storage time as factors. Duncan's multiple-range tests ($p < 0.05$) for means comparison were conducted.

3. Results and Discussion

3.1. Changes in Fatty Acids Composition

Four main fatty acids were identified in the apple peel: palmitic (16:0), stearic (18:0), oleic (18:1) and linoleic (18:2) acids (Figures 1 and 2). Palmitic acid, a saturated fatty acid (SFA), was found in the highest percentage in the fruits at the harvest stage; nevertheless, after 7 days of shelf-life, there was a significant reduction in its percentage (Figure 1A). After 6 months of cold storage, palmitic acid was reduced and was similar for all treatments, maintaining these values during posterior shelf-life, except for Ca-treated fruits, which had significantly lower values. Stearic acid, another SFA, was significantly reduced during shelf-life after harvest but did not change throughout the cold storage period except for showing a significant decrease in Ca + MCP-treated fruits, nevertheless increasing again after 7 days of shelf-life poststorage (Figure 1B).

The percentage of oleic acid, an important mono-unsaturated fatty acid, increased significantly during the shelf-life after harvest, but it is important to notice that after cold storage, there was a reduction in Ca + MCP-treated fruits, which recovered during the posterior shelf-life as stearic acid did (Figure 2A). The linoleic acid content, an essential poly-unsaturated fatty acid (PUFA), increased after 7 days of shelf-life after harvest (Figure 2B). After cold storage, the content of linoleic acid continued to increase; the Ca + MCP-treated fruits had higher values than the other treatments. After the shelf-life poststorage, the percentage of linoleic acid continued to increase except for Ca + MCP.

Studies by Wu et al. [27] found that palmitic acid and linoleic acid were the dominant fatty acids in eight commercially harvested apple cultivars, constituting 70–80% of the total fatty acids in the fruits. Similar results were obtained in the present work for 'Golden Delicious' apples, which had at harvest nearly 50% palmitic acid and 27% linoleic acid; nevertheless, after shelf-life and after storage, there was an increase in the percentage of linoleic acid and a decrease in the percentage of palmitic acid. As far as essential fatty acids are concerned, this is of nutritional interest, since diets rich in unsaturated fatty acids are healthier.
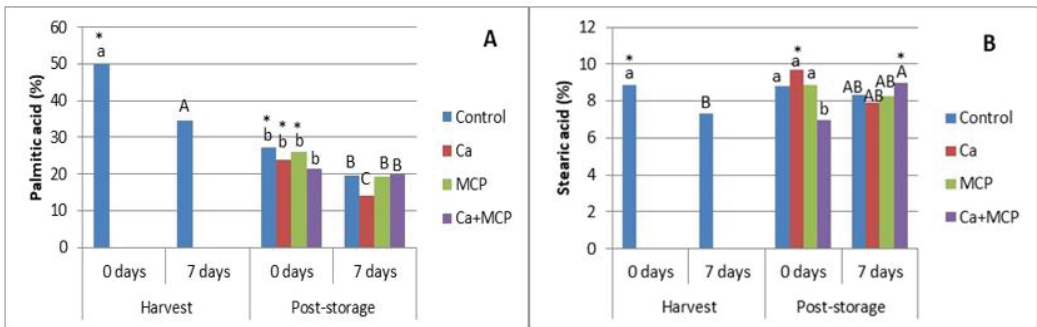
Figure 1. Changes in the saturated fatty acids, palmitic (**A**) and stearic (**B**), at harvest and after 6 months of storage at 0.5 °C and their respective shelf-life (7 days at ≈22 °C), in 'Golden Delicious' apples subjected to postharvest treatments with calcium chloride (Ca), 1-MCP (MCP), calcium chloride plus 1-MCP (Ca + MCP) and control. Lower-case letters compare treatments at harvest and after 6 months, and upper-case letters compare treatments after shelf-life. Columns with the same lower- or upper-case letter are not significantly different as determined by Duncan's multiple range test at $p < 0.05$. * represents significant differences between harvest and shelf-life or between poststorage and shelf-life for each treatment, at $p < 0.05$.
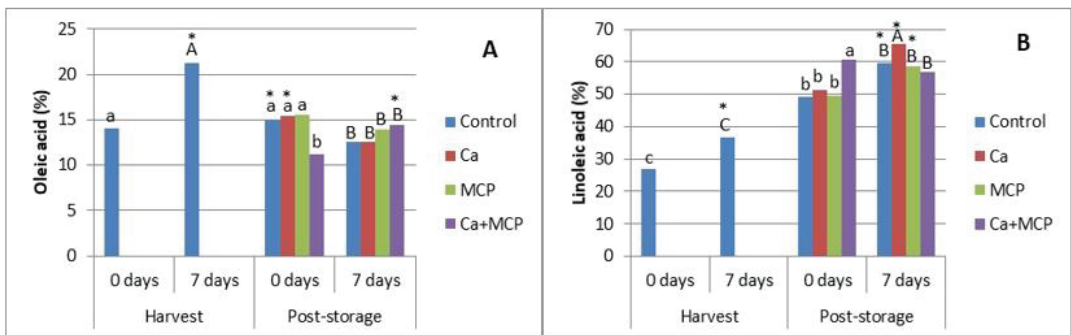
Figure 2. Changes in the unsaturated fatty acids, oleic (**A**) and linoleic (**B**), at harvest and after 6 months of storage at 0.5 °C and their respective shelf-life (7 days at ≈22 °C), in 'Golden Delicious' apples subjected to postharvest treatments with calcium chloride (Ca), 1-MCP (MCP), calcium chloride plus 1-MCP (Ca + MCP) and control. Lower-case letters compare treatments at harvest and after 6 months, and upper-cases letters compare treatments after shelf-life. Columns with the same lower- or upper-case letters are not significantly different as determined by Duncan's multiple range test at $p < 0.05$. * represents significant differences between harvest and shelf-life or between poststorage and shelf-life for each treatment, at $p < 0.05$.

3.2. Changes in the Ratio of Unsaturated/Saturated Fatty Acids

The ratio of unsaturated/saturated fatty acids in our experiment increased over time in both storage and shelf-life conditions (Figure 3A). This is mainly due to the decrease in the saturated palmitic acid and the increase in the PUFA linoleic acid (Figures 1A and 2B). According to our experiments, it appears that Ca treatment had a positive effect on the ratio of unsaturated/saturated fatty acids, since after 6 months of cold storage Ca + MCP-treated apples showed significantly higher values, and after 7 more days, the same happened in Ca-treated apples (Figure 3A).
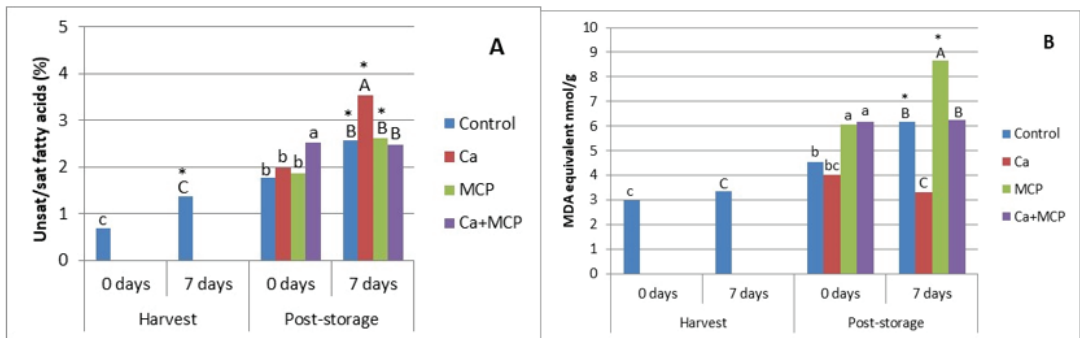
Figure 3. Changes in the unsaturated/saturated fatty acids ratio (**A**) and MDA equivalent (**B**) at harvest and after 6 months of storage at 0.5 °C and their respective shelf-life (7 days at ≈22 °C), in 'Golden Delicious' apples subjected to postharvest treatments with calcium chloride (Ca), 1-MCP (MCP), calcium chloride plus 1-MCP (Ca + MCP) and control. Lower-case letters compare treatments at harvest and after 6 months, and upper-cases letters compare treatments after shelf-life. Columns with the same lower- or upper-case letters are not significantly different as determined by Duncan's multiple range test at $p < 0.05$. * represents significant differences between harvest and shelf-life or between poststorage and shelf-life for each treatment, at $p < 0.05$.

Phospholipids and fatty acids are metabolic constituents of plant/fruit cells, and disturbances in membrane lipid composition frequently have severe consequences on the ability of the cell to adapt to extreme temperatures and other stress conditions, leading to several storage-induced physiological disorders [10,11]. Ge at al. [28] and Antunes and Sfakiotakis [29] found an increase in unsaturated/saturated fatty acids in kiwifruits and bell peppers, respectively, after cold storage. However, in peppers, the increase only lasted until 15 days storage at 4 °C, while chilling injury started to develop after 5 days; nevertheless, unsaturated/saturated fatty acids decreased thereafter, although chilling injury continued. Gao et al. [30] reported decreased unsaturated/saturated fatty acids as peaches developed chilling injury, while there were no reported unsaturated/saturated fatty acid ratio changes in pineapples developing chilling injury [31]. It is noteworthy that the fatty acids used in the formulas to calculate the unsaturated/saturated ratio were not always the same in all mentioned studies.

3.3. Changes in Malondialdehyde (MDA)

The content of MDA is often used as an indicator of lipid peroxidation stress and cell damage [32,33]. At 7 days of shelf-life after harvest, apples had a similar MDA content to that found at harvest, but it increased in storage, except for the Ca-treated apples (Figure 3B).

After 6 months of cold storage, MCP- and MCP+Ca-treated apples showed a higher MDA content than the other treatments. Interestingly, after 7 more days of shelf-life, the control and MCP treatments continued to increase, resulting in MCP-treated apples having the highest values and the Ca-treated apples having the lowest. After shelf-life post storage, it seems that in fruits treated with 1-MCP (MCP) or not (control), when calcium was added (Ca) or (Ca + MCP) there was an effect of reducing MDA. Additionally, as observed after the 6 months of cold storage, it seems that when MCP treatment was included (MCP and Ca + MCP), MDA increased, suggesting a temperature-dependent effect. Further research is needed to understand this point. Moreover, lower temperatures promote lipid oxidation, affecting the structural integrity of the plant membrane cells [12]. Interestingly, the higher value of unsaturated/saturated fatty acids obtained after storage plus shelf-life in Ca-treated apples was coincident with the lowest MDA value (Figure 3B), which may reveal a positive effect of Ca on reducing lipid peroxidation.

As in our case, 'Golden Delicious' and 'Fuji' apples in cold storage had increased concentrations of peroxides and MDA [34,35]. However, the last study reported a reduced MDA content in apples treated with MCP. Nevertheless, those authors reported MDA content on flesh. Our results are based on apple peels, and the higher MDA values found at the end of storage plus shelf-life could be related to the higher BP damage present in fruits treated with MCP (Figure 3B and Table 1).

Table 1. Physiological disorders and rot in 'Golden Delicious' apples stored for 6 months at 0.5 °C plus 7 days at ≈22 °C, as a percentage of total fruit subjected to postharvest treatments with calcium chloride (Ca), 1-MCP (MCP), calcium chloride plus 1-MCP (Ca + MCP) and control.

Disorder	Control	Ca	MCP	Ca + MCP
BP (%)	18.61 [b]	13.95 [b]	27.21 [a]	17.74 [b]
Scald (%)	3.53 [a]	1.99 [a]	0.10 [a]	3.73 [a]
DSB (%)	2.50 [b]	5.02 [a]	0.62 [b]	1.82 [b]
Rot (%)	5.56 [a]	1.15 [b]	2.56 [b]	0.80 [b]

Rows with the same case are not significantly different as determined by Duncan's Multiple Range Test at $p < 0.05$.

3.4. Physiological Disorders

Table 1 depicts the effect of the postharvest treatments on the peels' physiological disorders after 6 months of storage at 0.5 °C plus 7 days of shelf-life in 'Golden Delicious' apples.

As previously observed, 1-MCP treatment significantly increased the percentage of fruit with BP as compared with the other treatments or control [2,4]. Nevertheless, 1-MCP has been applied to apples to increase their storage life and reduce superficial scald, as has been previously reported [2,19]. In fact, MCP showed lower superficial scald in our apples as compared to the other treatments, although in this experiment superficial scald was not a big problem (Table 1).

The degree of inhibition of scald produced by 1-MCP is cultivar-dependent. Inhibition is almost complete for 'Granny Smith' [36,37]. However, scald inhibition is less consistent for many other cultivars, being affected by factors such as the type of storage (air versus controlled atmosphere) and storage length [19,38,39].

Studies by Miqueloto et al. [40] in apples 'Catherine' and 'Fuji' showed that the fruits with BP had lower Ca in the tissues of the skin. Similar results were found in 'Golden Delicious' apples [2,4]. When Ca was added to MCP, BP was reduced to a value similar to that of the control (Table 1). The treatments where calcium was added showed a positive effect on reducing BP induced by 1-MCP [2,4]. Calcium chloride was already considered as having a positive effect on ROS homeostasis in loquat fruit (*Eribotrya japonica*). The authors suggested that $CaCl_2$ treatment alleviated chilling injury through rising antioxidant enzyme activities and the ascorbate–glutathione (AsA-GSH) cycle system to scavenge ROS [41], which could, therefore, prevent the lipid peroxidation.

Interestingly, DSB, which has been reported in countries with warm summers and low rainfall, in fruits treated with 1-MCP [22,23], had higher development in fruit treated only with Ca (Table 1). The same authors reported that by gradually decreasing the storage temperature and delaying 1-MCP application, this disorder can be avoided. In our experiment, fruits were put in the cold rooms, and 1-MCP treatment occurred only after 3 days, which was proved to be effective to reduce DSB development.

3.5. Correlations among Fatty Acids, MDA and Physiological Disorders

There was no found correlation between palmitic, linoleic, oleic, stearic, unsaturated/saturated fatty acids ratio or MDA and any of the peel chilling physiological disorders studied in this experiment (Table 2). Previous authors also found no correlation between that ratio and chilling in apples [31]. There was a negative correlation

between palmitic acid and MDA and a positive correlation between linoleic or unsaturated/saturated fatty acids ratio and MDA, as was expected and explained above (Table 2).

Table 2. Pearson's correlations among the different fatty acids, unsat/sat ratio, MDA and chilling physiological disorders.

Parameters	Palmitic	Linoleic	Oleic	Stearic	Unsat/sat	MDA
Palmitic acid	1	−0.930 **	0.106	−0.026	−0.957 **	−0.554 *
Linoleic acid	−0.930 **	1	−0.440	−0.108	0.944 **	0.577 *
Oleic acid	0.106	−0.440	1	0.239	−0.189	−0.183
Stearic acid	−0.026	−0.108	0.239	1	0.014	0.135
Unsaturated/saturated	−0.957 **	0.944 **	−0.189	0.014	1	0.639 **
MDA	−0.554 *	0.577 *	−0.183	0.135	0.639 **	1
BP	0.151	−0.074	−0.166	0.032	−0.199	0.139
Scald	−0.151	0.076	0.168	−0.028	0.203	−0.135
DSB	−0.056	0.057	0.091	0.079	0.148	0.035
Rot	−0.083	0.068	0.118	0.066	0.178	0.004

*. Significance level $p < 0.05$ (2-tailed). **. Significance level $p < 0.01$ (2-tailed).

With the results of this work, it can be concluded that there is no clear correlation between the measured fatty acids (palmitic, linoleic, oleic or stearic fatty acids), unsaturated/saturated fatty acids ratio and MDA with chilling skin physiological disorders BP, scald and DSB in 'Golden Delicious' apples. However, after 6 months of storage at 0.5 °C plus 7 days of shelf-life, the treatment with Ca showed the lowest MDA values and the highest unsaturated/saturated fatty acids ratio, mainly due to higher linoleic acid and lower palmitic acid concentrations, which was coincident with lower BP occurrence. More research is needed to clarify the properties of the membranes' effect on physiological disorders, namely the identification and quantification of other membrane fatty acids' evolution during storage.

Author Contributions: M.D.A., A.C.G. and C.G. conceptualized the study and designed the experiments; A.C.G. and C.G. performed the experiments; A.G. and M.G.M. assisted in laboratory analysis and results interpretation; J.P. assisted in the statistics and laboratory analyses; E.V.B. assisted in the revision of the research; M.D.A. wrote the article, with the contribution of all authors. All authors have read and agreed to the published version of the manuscript.

Conflicts of Interest: The authors declare no conflict of interest.

References

1. Brackmann, A.; Schorr, M.R.W.; Pinto, J.A.V.; Venturi, T.L. Pre-harvest applications of calcium in post-harvest quality of 'Fuji' apples. *Cienc. Rural* **2010**, *40*, 1435–1438. [CrossRef]
2. Gago, C.M.L.; Guerreiro, A.C.; Miguel, G.; Panagopoulos, T.; Sánchez, C.; Antunes, M.D.C. Effect of harvest date and 1-MCP (SmartfreshTM) treatment on 'Golden Delicious' apple cold storage physiological disorders. *Postharvest Biol. Technol.* **2015**, *110*, 77–85. [CrossRef]
3. Pesis, E.; Ibanez, A.M.; Phu, M.L.; Mitcham, E.J.; Susan, E.; Ebeler, S.E.; Dandekar, A.M. Superficial scald and bitter pit development in cold-stored transgenic apples suppressed for ethylene biosynthesis. *J. Agric. Food Chem.* **2009**, *57*, 2786–2792. [CrossRef] [PubMed]
4. Gago, C.M.L.; Guerreiro, A.C.; Miguel, G.; Panagopoulos, T.; Silva, M.M.; Antunes, M.D.C. Effect of calcium chloride and 1-MCP (SmartfreshTM) postharvest treatment on 'Golden Delicious' apple cold storage physiological disorders. *Sci. Hortic.* **2016**, *211*, 440–448. [CrossRef]

5. Ferguson, I.B.; Watkins, C.B. Bitter-pit in apple fruit. *Hortic. Rev.* **1989**, *11*, 289–355.
6. Freitas, S.T.; Amarante, C.V.T.; Labavitch, J.M.; Mitcham, E.J. Cellular approach to understand bitter pit development in apple fruit. *Postharvest Biol. Technol.* **2010**, *57*, 6–13. [CrossRef]
7. Poovaiah, B.W.; Glenn, G.M.; Reddy, A.S.N. Calcium and fruit softening: Physiology and biochemistry. *Hortic. Rev.* **1988**, *10*, 107–152.
8. Lurie, S.; Watkins, C.B. Superficial scald, its etiology and control. *Postharvest Biol. Technol.* **2012**, *65*, 44–60. [CrossRef]
9. Gago, C.; Antão, R.; Dores, C.; Guerreiro, A.; Miguel, M.G.; Faleiro, M.L.; Figueiredo, A.C.; Antunes, M.D. The effect of nanocoatings enriched with essential oils on 'Rocha' pear long storage. *Foods* **2020**, *9*, 240. [CrossRef]
10. Marangoni, A.G.; Palma, T.; Stanley, D.W. Membrane effects in postharvest physiology. *Postharvest Biol. Technol.* **1996**, *7*, 193–217. [CrossRef]
11. Saquet, A.A.; Streif, J.; Bangerth, F. Changes in ATP, ADP and pyridine nucleotide levels related to the incidence of physiological disorders in 'Conference' pears and 'Jonagold' apples during controlled atmosphere storage. *J. Hortic. Sci. Biotechnol.* **2000**, *75*, 243–249. [CrossRef]
12. Imahori, Y.; Takemura, M.; Bai, J. Chilling-induced oxidative stress and antioxidant responses in mume (Prunus mume) fruit during low temperature storage. *Postharvest Biol. Technol.* **2008**, *49*, 54–60. [CrossRef]
13. Cheng, S.; Wei, B.; Zhou, Q.; Tan, D.; Ji, S. 1-Methylcyclopropene alleviates chilling injury by regulating energy metabolism and fatty acid content in 'Nanguo' pears. *Postharvest Biol. Technol.* **2015**, *109*, 130–136. [CrossRef]
14. Cao, S.; Zheng, Y.; Wang, K.; Jin, P.; Rui, H. Methyl jasmonate reduces chilling injury and enhances antioxidant enzyme activity in postharvest loquat fruit. *Food Chem.* **2009**, *115*, 1458–1463. [CrossRef]
15. Jiang, Y.; Joyce, D.C.; Jiang, W.; Lu, W. Effects of chilling temperatures on ethylene binding by banana fruit. *Plant Growth Regul.* **2004**, *43*, 109–115. [CrossRef]
16. Li, P.; Zheng, X.; Liu, Y.; Zhu, Y. Pre-storage application of oxalic acid alleviates chilling injury in mango fruit by modulating proline metabolism and energy status under chilling stress. *Food Chem.* **2014**, *142*, 72–78. [CrossRef] [PubMed]
17. Hall, A.E.; Findell, J.L.; Schaller, G.E.; Sisler, E.C.; Bleecker, A.B. Ethylene perception by the ERS1 protein in Arabidopsis. *Plant Physiol.* **2000**, *123*, 1449–1457. [CrossRef]
18. Ambaw, A.; Beaudry, R.; Bulens, I.; Delele, M.A.; Ho, Q.T.; Schenk, A.; Nicolaï, B.M.; Verboven, P. Modeling the diffusion–adsorption kinetics of 1-methylcyclopropene (1-MCP) in apple fruit and non-target materials in storage rooms. *J. Food Eng.* **2011**, *102*, 257–265. [CrossRef]
19. Rupasinghe, H.P.V.; Murr, D.P.; Paliyath, G.; Skog, L. Inhibitory effect of 1-MCP on ripening and superficial scald development in 'McIntosh' and 'Delicious' apples. *J. Hort. Sci. Biotechnol.* **2000**, *75*, 271–276. [CrossRef]
20. Calvo, G.; Candan, A.P. 1-Methylcyclopropene (1-MCP) affects physiological disorders in 'Granny Smith' apples depending on maturity stage. *Acta Hort.* **2010**, *857*, 63–69. [CrossRef]
21. Larrigaudière, C.; Ubach, D.; Soria, Y.; Recaenses, I. Biochemical changes in 1-MCP treated skin tissue during cold storage and their relationship with physiological disorders. *Acta Hort.* **2008**, *796*, 119–123. [CrossRef]
22. Larrigaudière, C.; Vilaplana, R.; Recasens, I.; Soria, Y.; Dupille, E. 'Diffuse skin browning' in 1-MCP-treated apples: Etiology and systems of control. *J. Sci. Food Agric.* **2010**, *90*, 2379–2385. [CrossRef] [PubMed]
23. Gamrasni, D.; Nerya, O.; Tsvilling, A.; Gizis, A.; Maoz-Katz, M.; Ben-Arie, R. The complexity of preventing diffuse skin browning (DSB) on 1-MCP (Smartfresh) -treated 'GoldenDelicious' apples. *Acta Hort.* **2010**, *877*, 507–511. [CrossRef]
24. Meyer, M.D.; Terry, L.A. Development of a rapid method for the sequential extraction and subsequent quantification of fatty acids and sugars from avocado mesocarp tissue. *J. Agric. Food Chem.* **2008**, *56*, 7439–7445. [CrossRef] [PubMed]
25. Hodges, D.M.; DeLong, J.M.; Forney, C.F.; Prange, R.K. Improving the thiobarbituric acid-reactive-substances assay for estimating lipid peroxidation in plant tissues containing anthocyanin and other interfering compounds. *Planta* **1999**, *207*, 604–611. [CrossRef]
26. Lee, J.; Cheng, L.; Rudell, D.R.; Watkins, C.B. Antioxidant metabolism of 1-methylcyclopropene (1-MCP) treated 'Empire' apples during controlled atmosphere storage. *Postharvest Biol. Technol.* **2012**, *65*, 79–91. [CrossRef]
27. Wu, J.; Gao, H.; Zhao, L.; Liao, X.; Chen, F.; Wang, Z.; Hu, X. Chemical compositional characterization of some apple cultivars. *Food Chem.* **2007**, *103*, 88–93. [CrossRef]
28. Ge, W.; Kong, X.; Zhao, Y.; Wei, B.; Zhou, Q.; Ji, S. Insights into the metabolism of membrane lipid fatty acids associated with chilling injury in post-harvest bell peppers. *Food Chem.* **2019**, *295*, 26–35. [CrossRef] [PubMed]
29. Antunes, M.D.C.; Sfakiotakis, E.M. Changes in fatty acid composition and electrolyte leakage of 'Hayward' kiwifruit during storage at different temperatures. *Food Chem.* **2008**, *110*, 891–896. [CrossRef]
30. Gao, H.; Lu, Z.M.; Yang, Y.; Wang, D.N.; Yang, T.; Cao, M.M.; Cao, W. Melatonin treatment reduces chilling injury in peach fruit through its regulation of membrane fatty acid contents and phenolic metabolism. *Food Chem.* **2018**, *245*, 659–666. [CrossRef]
31. Nukuntornprakit, O.; Chanjirakul, K.; Doorn, K.G.; Siriphanich, J. Chilling injury in pineapple fruit: Fatty acid composition and antioxidant metabolism. *Postharvest Biol. Technol.* **2015**, *99*, 20–26. [CrossRef]
32. Smirnoff, N. Antioxidant systems and plant response to the environment. In *Environment and Plant Metabolism: Flexibility and Acclimation*; Smirnoff, N., Ed.; Bios Scientific Publishers: Oxford, UK, 1995; pp. 243–317.
33. Xu, F.; Liu, S. Control of postharvest quality in blueberry fruit by combined 1-methylcyclopropene (1-MCP) and UV-C irradiation. *Food Bioproc. Technol.* **2017**, *10*, 1695–1703. [CrossRef]

34. Du, Z.; Bramlage, W.J. Peroxidative activity of apple peel in relation to development of poststorage disorders. *HortScience* **1995**, *30*, 205–209. [CrossRef]

35. Chen, H.-Y.; Jiang, L.-F.; Zeng, J.-H.; Huo, Y.-R.; Li, Y.-X. Combination of carnauba wax-based coating and 1-methylcyclopropene (1-MCP) maintains better "Fuji" apple qualities during storage at low temperature. *J. Food Process. Preserv.* **2020**, *44*, 1–8. [CrossRef]

36. Lurie, S.; Lers, A.; Shacham, Z.; Sonego, L.; Burd, S.; Whitaker, B. Expression of α-farnesene synthase AFS1 and 3-hydroxy-3-methylglutaryl-coenzymea reductase HMG2 and HMG3 in relation to α-farnesene and conjugated trienolsin 'Granny Smith' apples heat or 1-MCP treated to prevent superficial scald. *J. Am. Soc. Hortic. Sci.* **2005**, *130*, 232–236. [CrossRef]

37. Magazin, N.; Gvozdenovic, D.; Keserovic, Z.; Milic, B. Fruit quality of Granny Smith apples picked at different harvest times and treated with 1-MCP. *Fruits* **2010**, *65*, 191–197. [CrossRef]

38. Bai, J.; Baldwin, E.A.; Kevin, L.; Goodner, K.L.; Mattheis, J.P.; Brecht, J.K. Response of four apple cultivars to 1-methylcyclopropene treatment and controlled atmosphere storage. *HortScience* **2005**, *40*, 1534–1538. [CrossRef]

39. Watkins, C.B.; Nock, J.F. Effects of delays between harvest and 1-methylcyclopropene treatment, and temperature during treatment, on ripening of air-stored and controlled atmosphere-stored Apples. *HortScience* **2005**, *40*, 2096–2101. [CrossRef]

40. Miqueloto, A.; Amarante, C.V.T.; Steffens, C.A.; Santos, A.D.; Miqueloto, T.; Silveira, J.P.G. Physiological, physical, chemical and mineral attributes associated with the occurrence of "bitter pit" in apples. *Pesqui. Agropecu. Bras.* **2011**, *46*, 689–696. [CrossRef]

41. Hou, Y.; Li, Z.; Zheng, Y.; Jin, P. Effects of $CaCl_2$ treatment alleviates chilling injury of loquat fruit (*Eribotrya japonica*) by modulating ROS homeostasis. *Foods* **2021**, *10*, 1662. [CrossRef]

ß-Farnesene Exogenous Application as a Novel Damage Induction Model to Fast Explore the Effectiveness of Postharvest Strategies: The Case Study of the 'Rocha' Pear DOP

Cindy Dias [1], Ana Amaro [1], Alexandre Fonseca [2,3], António Ferrante [4], Armando Silvestre [2], Sílvia M. Rocha [3], Nélson Isidoro [5] and Manuela Pintado [1,*]

[1] Centro de Biotecnologia e Química Fina—Laboratório Associado, Escola Superior de Biotecnologia, Universidade Católica Portuguesa-Porto, 4169-005 Porto, Portugal; cdias@ucp.pt (C.D.); aamaro@ucp.pt (A.A.)

[2] CICECO-Instituto de Materiais de Aveiro, Universidade de Aveiro, 3810-193 Aveiro, Portugal; alexandrefonseca@ua.pt (A.F.); armsil@ua.pt (A.S.)

[3] LAQV-REQUIMTE, Departamento de Química, Universidade de Aveiro, 3810-193 Aveiro, Portugal; smrocha@ua.pt

[4] Dipartimento di Scienze Agrarie e Ambientali-Produzione, Territorio, Agroenergia, Università delgi Studi di Milano, 20133 Milano, Italy; antonio.ferrante@unimi.it

[5] Cooperativa Agrícola dos Fruticultores do Cadaval, CRL (COOPVAL), 2550-108 Cadaval, Portugal; nelson.isidoro@coopval.com

* Correspondence: mpintado@ucp.pt

Abstract: Since the prohibition of diphenylamine, replacement strategies have been needed for long-term disorder prevention, namely superficial scald (SC), in fruit. However, as this disorder only appears after months under cold storage, the assessment of effective strategies to prevent this disorder requires long periods. To tackle this challenge, we report in this paper a rapid and reliable system to induce symptoms, such as SC, based on storage under a β-farnesene-enriched atmosphere. Using this model, SC symptoms in 'Rocha' pear were induced after 15 d at 20 °C. As proof of concept, this model system allowed the study of the efficiency of antioxidant natural-based coatings on 'Rocha' pear quality maintenance. Pears treated with the coatings were submitted to 4 months of commercial storage under normal atmosphere conditions and the results were compared with those obtained using the induction model system. A PCA of chemical data allowed us to conclude that the model developed simulates the potential of certain strategies to prevent disorders.

Keywords: β-farnesene; damage induction model; postharvest quality; 'Rocha' pear quality

1. Introduction

Given their perishable nature, pears are preserved using cold storage after harvest, which can be extended, in general, up to 10 months under a controlled atmosphere (CA) [1]. However, prolonged cold exposure can trigger postharvest physiological disorders, decreasing the shelf life and marketability of fresh pears. This quality deterioration is usually described as a combination of various necrotic injuries on the peel and/or flesh of pears, referred to as superficial scald (SC) and internal browning, respectively [2,3]. SC is one of the most common and problematic disorder in the postharvest field. The symptoms of this chilling-induced oxidative disease are generated during cold storage, but become intensified when the fruit are transferred to room temperature [4]. It has already been demonstrated that SC appearance in most pear cultivars is associated with the production of α-farnesene and their auto-oxidation into conjugated trienols [5,6]. This oxidative breakdown and redox imbalance lead to cellular disruption by conjugated trienols [7,8]. When this membrane damage occurs, cellular compartmentalization is disrupted allowing polyphenol oxidase (PPO) mediated browning [9]. It has also been proposed that SC is

a consequence of an imbalance between the fruit capacity to produce and/or regenerate antioxidants and hence scavenge oxidative species during cold storage [10,11].

Until 2013, the standard postharvest procedure in the postharvest industry to reduce the incidence of SC was the application of the antioxidant diphenylamine (DPA) combined with CA storage [12]. However, DPA use was forbidden, in 2011, due to the environmental and health hazardous effects already reported [13]. Since then, different approaches have been attempted to control this postharvest crop quality, such as CA storage, intermittent warming, and treatments with 1-methylcyclopropene (1-MCP) [3,14]. Nevertheless, the negative outcomes associated with these techniques, such as cost and sensorial quality constrains, demonstrated that these treatments are not as effective as DPA and not universally feasible per se, and also that their effect depends on the pear cultivar [15].

In recent years, the use of edible coatings has shown high potential to delay fruit quality deterioration during cold storage due to their potential in reducing respiration rates due to the formation of a gas barrier on the fruit surface [6,16–19]. In addition, such coatings can be loaded with food-compatible antioxidants, which can delay the occurrence of SC [3,6]. Such natural antioxidants can possibly scavenge oxidation processes by binding free radicals, protecting fruit from the oxidative process associated with superficial scald [7], and have been studied among several vegetable crops [20]. For instance, Sharma and Rao [21] reported that xanthan-gum-based edible coating loaded with cinnamic acid led to a reduction in the oxidative browning process on pears.

Effective research about new alternatives to prevent SC development has been hindered by the lack of an experimental system that can rapidly induce this disorder and allow several repetitions. Generally, as SC manifestations occur generally after 4 to 6 months in cold storage, the time necessary to achieve conclusions about new strategies success is frequently restrictive. To overcome this limitation, various attempts have been developed to artificially induce SC in a short period, focused on changing the air composition at room temperature, but usually without success [22]. Later, flushing with N_2 (anaerobiosis creation) after several days proved to provoke SC on apples [23,24]. Recently, Karagiannis et al. [4] found that a cold storage atmosphere enriched with ozone (O_3) induced scalding symptoms in 'Granny Smith' apples, but the technique failed regarding time, economic and environmental factors.

Since natural intrinsic α-farnesene oxidation is one of the reactions believed to explain the occurrence of SC symptoms, it is a hypothesis that the exogenous application of its isomer, β-farnesene, and its oxidation products, are also likely to induce similar disorder development. β-farnesene is one of the major isomers belonging to the farnesene family of acyclic sesquiterpenes found in the volatile emissions of a wide range of fruits and plants [25–27]. Additionally, its extraction and purification are less expensive than α-farnesene. In this context, the current study is designed to develop a novel approach to induce tissue damage based on the creation of a β-farnesene atmosphere through the natural volatilization of a pure β-farnesene solution. This model may be useful as a model for the quick exploration of the effectiveness of new treatments for superficial scald mitigation.

The aim of this work is to assess the reliability of β-farnesene enrichment in the storage atmosphere as a model system to study the SC physiological disorder in pears. The efficacy of the model was validated using pears treated with two natural extracts with different antioxidant potential: the methanolic leaf extract of *Arbutus unedo* L. tree, which demonstrated a high antioxidant activity and a subsequent potential to inhibit SC and quality preservation effect on 'Rocha' pear; and the methanolic apple byproduct extract from apple pomace with a weaker antioxidant activity [6,28]. To validate the results of 'Rocha' pear quality treated with these two natural-based extracts under the induction model, the treated pears were tested under common storage conditions during 4 months under normal atmosphere. Biochemical data supporting the hypothesis that β-farnesene-induced scald involves similar physiological and biochemical mechanisms to those which contribute to naturally occurring superficial scald are also presented.

2. Materials and Methods

2.1. Material

HPLC-grade methanol (≥99.9% purity) was supplied by Honeywell Riedel-de Haën AG, Seelze, Germany. ABTS (2,20-azinobis (3-ethylbenzothiazoline-6-sulfonic acid, di-ammonium salt), food grade pectin from citrus peels, sodium carbonate, ascorbic acid, polyvinylpolypyrrolidone (PVPP), phenylmethanesulfonyl fluoride (PMSF), EDTA, cat-echol and guaiacol were purchased from Sigma-Aldrich, Missouri, EUA, and potassium persulfate and Folin–Ciocalteu from Merck, Damstadt, Germany. Glycerol was supplied by Fisher Chemical, New Hampshire, EUA. β-farnesene (99%) was kindly provided by Amyris, California, EUA.

2.2. Natural Extracts Screening and Selection

For validation of the β-farnesene atmosphere model system, two levels of potential an-tioxidant activity were defined (higher and lower antioxidant capacity compared to ascorbic acid). This selection, among different plants and byproducts, was performed in a previous work [28]. The natural extract with the highest antioxidant capacity was *A. unedo* L. tree leaf and the worse was the apple byproduct. For further analysis, concentrations of 9.5 g L^{-1} and 16 g L^{-1} were used for *A. unedo* L. leaf and the apple byproduct, respectively.

2.3. Fruit Material and Extract Material

Pear fruits (*Pyrus communis* L. 'Rocha') were harvested at optimal maturation stage from a 30-year-old commercial orchard in Cadaval (39°25' N; 8°54' W; 120 m), Portugal, in August 2018. The pears were transported immediately after harvest to a commercial packinghouse and hand-sorted to select undamaged fruit. The fruit were then stored at 4 °C and 95% RH until processing. The pear fruits were kindly provided by COOPVAL (Bombarral, Portgual).

Fresh *A. unedo* L. leaf was provided by Medronhalva, LDA, and stored at—20 °C. Before extraction, the leaf was freeze dried and ground into a fine powder (IKA A10 analyt-ical grinder). The apple byproduct was provided by INDUMAP-Fruit's Industrialization, Portugal, stored at—80 °C upon arrival, and used directly for extraction after thawed. The extraction procedure was performed according to [6]. Each plant material (1:20 *m/v*) was consecutively extracted three times with methanol for 1 h under constant stirring at 25 °C with the renewal of the solvent between extractions. The suspensions were then vacuum filtered, MeOH was removed in a rotary evaporator (Büchi rotavapor R-114) and the extracts were freeze dried to obtain the final extract.

2.4. Preparation of the Pectin-Based Coating and Fruit Coating

Pectin coating was prepared according to the method reported by Oms-Oliu, Soliva-Fortuny, and Martín-Belloso [29] with some modifications. The coating was prepared by dissolving pectin (3% *w/v*) in distilled water and heating at 60 °C while stirring until the solution became clear. After cooling down to room temperature, the chosen natural extracts were dissolved in the coating at the concentration previously optimized (9.5 g L^{-1} and 16 g L^{-1} were used for *A. unedo* L. leaf and the apple byproduct, respectively). The pears were dipped into the coating solution for 2 min and allowed to drain for 1 min and to dry at room temperature for 2 h. Uncoated pears were used as experimental controls, and pears coated without the incorporation of natural-based extracts (i.e., only pectin) were used as procedural controls.

2.5. β-Farnesene-Atmosphere-Based Model

2.5.1. Model System Optimization

To induce the occurrence of tissue damage, samples of 6 pears were equally distributed in polypropylene boxes with 5 L (24.5 cm × 13 cm × 16 cm) capacity and exposed to differ-ent volumes of pure β-farnesene (optimization results in Section 3.2) under a controlled temperature (25 °C). After the selection of the β-farnesene volume (150 mL), the protective

potential of the antioxidant coatings under the β-farnesene atmosphere was evaluated. The pears were removed from cold storage and dipped in the different postharvest treatment coatings and allowed to dry before being exposed to pure β-farnesene. The pears were randomly divided into two lots with 24 fruit each, 1 lot was packed in 4 plastic boxes, hermetically covered and used as control (i.e., without β-farnesene), and the other lot was packed with the optimized volume of β-farnesene. The 24 pears of each lot were divided into 4 experimental conditions (experimental control; procedural control; *A. unedo* L. leaf coating (AL.C); and apple byproduct coating). This experimental design was performed in triplicate. Quality measurements were performed immediately after coating dryness (0 d) and then at 15 d of storage under each condition and atmosphere. Visual inspection for damage development was assessed daily.

2.5.2. Model System Validation Using a Pilot Scale Storage of Pears

Further reproducibility of the results, obtained with the β-farnesene-atmosphere induction model system, was achieved with a pilot scale storage of pears across a 4 month commercial storing period at Cooperativa Agrícola dos Fruticultores do Cadaval (COOP-VAL). Pears from this time had already 4 months of cold storage since harvest. The pears were randomly divided into 3 groups of 50 fruit each. The pears of the first group were treated with AL.C, whereas the second group was treated with the coating without incorporation of natural-based extracts (procedural control) and the third group remained untreated (experimental control). The fruits from each group were cold stored (0 °C, 95% RH), a normal 'Rocha' pear storage strategy at the agricultural cooperative. Randomly, 10 pears from the 3 different treatments were sampled and analyzed for quality and superficial scald development at 5 different storage times (0, 1, 2, 3 and 4 months). Following cold storage, the pears were allowed to ripen for 7 days at room temperature (18–20 °C), hence simulating the marketing period. In parallel for each treatment and each sampling, three replicates of two pears each were isolated and subsequently frozen in liquid nitrogen and stored at—80 °C for biochemical analysis.

2.6. Determination of Pears Physicochemical Parameters

Fruit quality was evaluated in terms of firmness, surface color, total soluble solids, pH and scald incidence. Fruit surface color was measured with a CR-400 colorimeter (Konica Minolta, Osaka, Japan) using the D65 illuminant and the CIE (Commission Internationale de l'Eclairage) parameters (L*, a*, b*). Hue was calculated as hue angle ($h° = \arctan (b*/a*)$). Photos were also taken daily to report the pears' overall appearance. Two measurements were performed on opposite sides of the widest part of each fruit. Firmness (expressed as N) was measured using a texturometer (T.A. XT plus Texture Analyser, Stable Micro Systems, Cardiff, UK) fitted with a 5 mm diameter probe. Force calibration was performed with a 5 kg load cell and height calibration was performed for each pear. The soluble solids content (SSC) was measured in the fruit juice by a digital refractometer PR1ATAGO CoLTD (Japan). For pH measurements, a sensION™ PH31, HACH (Spain) was used. SC incidence was recorded visually in each sampling day and calculated as a percentage of the total number of fruit affected per condition per month [30].

2.7. Antioxidant Capacity and Phenolic Content (Extraction and Quantification)

The extraction of antioxidant compounds from pears was performed according to Salta et al. [31] with some modifications. Thawed pear samples (5 g) were previously homogenized in a Moulinex stirrer and then extracted with 50 mL methanol (3×), while stirring for 15 min. The mixture was filtered with two layers of Miracloth and the liquid extract evaporated under vacuum at 50 °C using a rotary evaporator (Büchi Rotavapor R-114). The concentrated extract was volumetrically adjusted to 10 mL for further analysis with methanol. All the extractions were performed in triplicate with two biological replicates and reading in duplicate.

The total antioxidant capacity was determined by the 3-ethylbenzothiazoline-6-sulfonic acid diammonium salt (ABTS) free radical scavenging assay, as described elsewhere [32]. After the addition of 1.0 mL ABTS solution to 10 µL of the sample, the mixture absorbance reading was performed after 6 min at 743 nm. With the calibration curve, previously prepared with ascorbic acid as a standard, the result was expressed as ascorbic acid equivalent concentration (AEAC) per g of pear on a fresh weight basis.

2.8. Determination of the PPO Enzyme Activity of Pears

PPO was extracted and analyzed as described by Galeazzi and Sgarbieri [33]. Pear tissue (10 g) was homogenized for 2 min in an ice bath with 10 mL of 200 mmol L^{-1} sodium phosphate buffer pH 6.5, 0.25% (*v/v*) Triton X-100 and 2% (*w/v*) of PVPP, using an Ultra-Turrax. The obtained solution was centrifuged at $4000\times g$ for 20 min at 4 °C. The supernatant was filtered through two layers of Miracloth and used as enzyme extract. For the activity determination, the enzyme extract was mixed with the reaction buffer, which consisted of a 200 mmol L^{-1} catechol and 200 mmol L^{-1} of sodium phosphate buffer pH 6.5. The catechol oxidation rate was evaluated at 420 nm for 3 min at room temperature.

All the extractions were performed in triplicate with two biological replicates and readings in duplicate. Enzymatic activities were expressed as the change in unit of activity (U) per milligram of enzyme responsible for a change in 1 absorbance unit per minute. The total protein content in the enzyme extracts was determined using the Pierce Coomassie Plus Protein Assay Kit (Pierce ThermoScientific Inc., Rockford, IL, USA), based on the method of Bradford, following the manufacturer's instructions. Bovine serum albumin was used as a standard.

2.9. Statistical Analysis

Differences between extracts antioxidant activities were tested by the one-way analysis of variance (ANOVA). One-way analysis of variance was applied to determine differences between treatments in both atmospheres (i.e., in the presence and absence of β-farnesene). Additionally, a two-way analysis of variance was performed to assess differences on the pilot scale assay using the treatment and month of storage as independent factors. Fisher's least significant difference (LSD) was conducted for mean comparisons. Differences with a probability value of <0.05 were considered significant and all data were reported as mean ± SD. ANOVA analyses were conducted using STATISTIC software (StatSoft v.8, US). A principal component analysis (PCA) of the chemical parameters was performed using Statgraphics Centurion XVII.

3. Results and Discussion

3.1. Selection of Natural-Based Extracts of Antioxidant Action

The processing of plant foods results in byproduct production, which can be considered rich sources of bioactive compounds, notably compounds with antioxidant properties. Among the bioactive compounds present in plants, phenolic compounds are widely appreciated for their strong antioxidant potential, due to their double bounds and ability to delocalize electrons removing free radicals [31,34,35]. Therefore, in a previous study [28], an initial screening of natural-based extracts with antioxidant activity to be used in edible coatings to prevent pear SC was carried out. The results allowed the selection of the extracts with the highest and lowest antioxidant potential compared to ascorbic acid. In particular, the samples selected were *A. unedo* L. leaf extract (highest antioxidant capacity) and apple byproduct extract (lowest antioxidant capacity). Indeed, in a previous work, we demonstrated the high variety of phenolic compounds found in *A. unedo* L. leaf, which could justify their considerable antioxidant activity [28,35,36]. Additionally, in a previous study [6], AL.C demonstrated to preserve 'Rocha' pear quality during cold-storage.

Although apple byproducts extracts have been reported to be rich in phenolic acids [28], the obtained results show that they display a poor antioxidant activity [37]. Hence, because of their different behavior regarding antioxidant capacity, and therefore their different

potential in reducing pear scald, these extracts were used as a case study to test the β-farnesene-atmosphere model system developed in this study.

3.2. β-Farnesene-Atmohphere Model System Optimization and Evaluation

Since α-farnesene oxidation is one of the main biochemical reactions responsible for the appearance of scald symptoms [5], it was our objective to create a simple and fast model system to induce SC damage through the application of the α-farnesene isomer, β-farnesene, under a controlled temperature (25 °C). Various attempts to find the optimal β-farnesene volume, to induce SC in the manner of the naturally occurring SC, in the 5 L headspace boxes were performed (data not shown). The optimization of β-farnesene volume was carried out because we observed that much higher volumes than 150 mL led to the rapid injury of the fruit skin. As it was used in the case of the pure substance in a closed system and considering the vapor pressure 1.333 Pa at 25 °C [38], the more energetic β-farnesene molecules diffused, i.e., evaporated, from the liquid to the gaseous phase until reaching saturation. This equilibrium allowed the contact of β-farnesene with pears responsible for the appearance of physiological damage. A volume of 150 mL, at the center of each 5 L box and without stirring, with six fruits placed at represented in Figure 1 for 15 d, were determined as the conditions to induce physiological damage in pears, i.e., 30 mL β-farnesene per L of container capacity and 25 mL β-farnesene per pear. The effect of the antioxidant edible coatings in the quality preservation of pear under the β-farnesene-atmosphere model system was then evaluated (Figure 2 and Table 1).
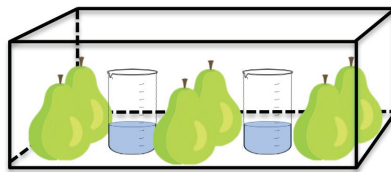
Figure 1. Experimental design of β-farnesene damage induction model system.
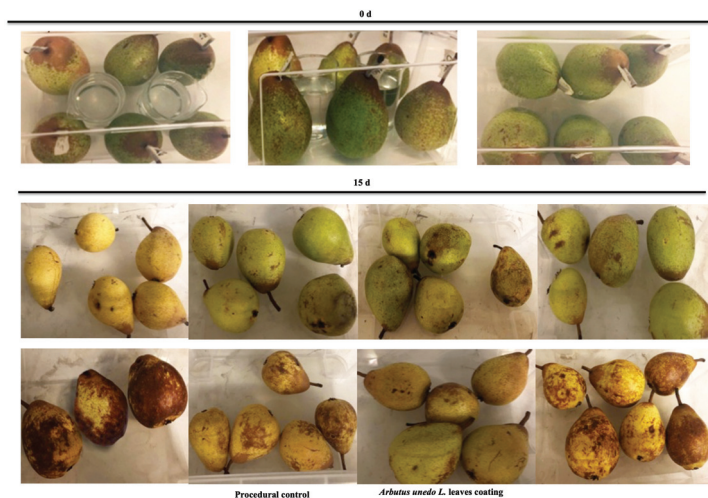
Figure 2. 'Rocha' pear fruit at the initial (0 d) and final (15 d) stage of β-farnesene damage induction model system.

Table 1. Lightness, hue angle, firmness, soluble solid content, pH, scald index, AEAC and PPO activity of 'Rocha' pear at 0 and 15 d storage under the atmosphere without (−) and with (+) β-farnesene. Means ± standard deviation of six determinations followed by the same lower-case letter indicates no differences between conditions at each time point, and by the same upper-case letter indicate no differences between storage months at each condition at $p < 0.05$ (n = 6).

Quality Parameters			0 d	15 d
Lightness (L*)	−	Experimental control	64.58 ± 0.95 a	71.72 ± 2.27 A
		Procedural control	63.21 ± 2.45 a	67.38 ± 3.33 B
		AL.C	66.13 ± 5.20 a	68.87 ± 1.36 B
	+	Experimental control	60.73 ± 2.91 a	79.47 ± 3.36 C
		Procedural control	65.64 ± 1.97 a	72.46 ± 3.26 A
		AL.C	64.66 ± 5.57 a	67.87 ± 3.36 B
Hue angle ($h°$)	−	Experimental control	106.74 ± 3.07 a	87.20 ± 0.80 A
		Procedural control	103.91 ± 3.30 ab	93.81 ± 1.50 C
		AL.C	103.83 ± 3.42 ab	97.76 ± 4.39 D
	+	Experimental control	104.97 ± 4.66 ab	82.88 ± 1.45 E
		Procedural control	105.35 ± 2.47 ab	88.03 ± 0.88 A
		AL.C	102.21 ± 1.80 b	103.82 ± 4.40 B
Firmness (N)	−	Experimental control	33.26 ± 1.67 a	6.28 ± 0.29 A
		Procedural control	34.24 ± 1.77 a	8.04 ± 0.39 B
		AL.C	35.90 ± 5.30 a	11.58 ± 2.26 C
	+	Experimental control	36.40 ± 3.24 a	6.38 ± 0.78 A
		Procedural control	33.85 ± 1.67 a	7.65 ± 0.39 AB
		AL.C	36.59 ± 3.04 a	9.81 ± 1.47 D
SSC (%)	−	Experimental control	12.13 ± 1.26 a	14.15 ± 0.59 AC
		Procedural control	12.42 ± 0.43 a	13.62 ± 0.45 AB
		AL.C	13.85 ± 0.55 b	13.38 ± 0.37 B
	+	Experimental control	13.42 ± 0.45 b	14.27 ± 0.60 C
		Procedural control	12.45 ± 0.31 a	13.40 ± 0.32 B
		AL.C	12.52 ± 0.38 a	13.02 ± 0.74 B
pH	−	Experimental control	5.66 ± 0.17 ac	4.79 ± 0.05 A
		Procedural control	5.67 ± 0.22 ac	5.48 ± 0.16 B
		AL.C	5.88 ± 0.17 b	5.14 ± 0.24 C
	+	Experimental control	5.96 ± 0.15 b	4.79 ± 0.17 A
		Procedural control	5.82 ± 0.13 ab	5.17 ± 0.09 C
		AL.C	5.60 ± 0.10 c	4.72 ± 0.10 A
SC incidence (%)	−	Experimental control	0	0
		Procedural control	0	0
		AL.C	0	0
	+	Experimental control	0	100
		Procedural control	0	83.30
		AL.C	0	16.67
AEAC (g kg^{-1})	−	Experimental control	0.64 ± 0.08 a	0.56 ± 0.02 A
		Procedural control	0.61 ± 0.06 a	0.19 ± 0.04 B
		AL.C	0.67 ± 0.09 a	0.60 ± 0.01 C
	+	Experimental control	0.60 ± 0.10 a	0.69 ± 0.01 D
		Procedural control	0.62 ± 0.04 a	0.23 ± 0.03 B
		AL.C	0.66 ± 0.03 a	0.62 ± 0.04 C
PPO (U.mgprotein^{-1})	−	Experimental control	2.95 ± 0.66 a	3.11 ± 0.43 A
		Procedural control	2.72 ± 0.34 ac	2.75 ± 0.38 AC
		AL.C	3.52 ± 0.48 b	2.28 ± 0.34 B
	+	Experimental control	2.64 ± 0.45 ac	2.95 ± 0.43 AC
		Procedural control	2.41 ± 0.11 c	2.59 ± 0.23 BC
		AL.C	2.67 ± 0.42 ac	1.67 ± 0.19 D

3.2.1. Visual Pear SC-Like Symptom Evaluation

The results reported in Figure 2 and Table 1 show that it is possible to produce typical pear SC-like symptoms within 15 d by exposing the fruit to the atmosphere containing β-farnesene. It is clear from Figure 2, by comparison with the controls in the presence and absence of β-farnesene, that under this conditions damage can be observed after 15 d of storage on β-farnesene-treated pears. It is clear from Figure 2 that the β-farnesene atmosphere accelerated the senescence of the fruit since pears exposed to the β-farnesene atmosphere showed a more damaged surface. In contrast, coated pears showed a greener and healthier surface compared to the control pears, which suggests the protection given by the coatings. α-farnesene biosynthesis appears to promote ethylene production [39]. Similarly, β-farnesene could induce the ethylene biosynthesis responsible for faster senescence.

The application of edible coatings to pears can create a barrier to gas diffusion inside the fruit, leading to a reduction in the senescence process, which can explain the greener surface of coated pears not exposed to β-farnesene [16]. However, the application of an external stress to the fruit resulted in scald-affected and more senescent fruits. Pears with AL.C substantially reduced such visible injury (Figure 2). Additionally, and as expected by its lower antioxidant activity, pears treated with the apple byproduct coating showed higher levels of damage. These results are in agreement with the antioxidant activity of these two extracts, which may be responsible for the protective effect observed. While *A. unedo* L. leaf extract presented a higher antioxidant potential and, therefore, was more effective to reduce tissue injury and senescence, the apple byproduct with a much lower antioxidant activity did not prevent pear damage. Uncoated pears were the ones showing more browning injuries.

The extract with higher antioxidant content, *A. unedo* L. leaf extract, reduced peel damage. Additionally, the antioxidants of this extract coating allowed the fruit to be more protected. Thus, the physicochemical data present in Table 1 supports the visual evaluation performed regarding the effect of AL.C on the protection of fruit from damage, since the apple byproduct was not visually so effective.

3.2.2. Physicochemical Properties of Pears
Color

Initially, immediately after the application of the coating on pears, L* was measured (Table 1). In fact, at application time, the color of pears with AL.C was not different from the controls showing that the optimized concentration of *A. unedo* L. tree leaf extract in the coating had a seamless effect on the pears' color (Figure 2). In fact, the development of edible coatings with optical clarity is desirable, assuring a seamless effect when applied to the fruit [40]. After 15 d of storage, there was an increase in L* and a decrease in h° values (Table 1) in all conditions and storage conditions, which is characteristic of 'Rocha' pear ripening [12,41]. Nevertheless, surface color was affected by the presence of β-farnesene. Higher ΔL* and higher Δh° values indicate faster ripening and damage development [3] and were observed in pears under β-farnesene conditions, particularly in the experimental control, compared to pears under no β-farnesene atmosphere. Additionally, it is clear from the differences between the coated pears and the experimental control under no β-farnesene atmosphere that coatings slowed the ripening process (lower Δh° compared to the control). In pears, the decrease in L* values is a result of chlorophyll degradation and the accumulation of carotenoids. The treatment with edible coatings inhibited the chlorophyll breakdown of various horticultural products, including pears [42]. Pears with the AL.C demonstrated (in both storage conditions) the maintenance of a lower ΔL* and Δh° values, as proved by differences with the control, confirming its protective role. Oms-Oliu et al. [29] also observed that the incorporation of antioxidants into coatings effectively maintained the h° values of freshly cut pears.

Firmness

Firmness is one of the main fresh pear quality parameters. Its decrease is associated with transpiration and respiration processes during storage and cell wall degradation, which promote moisture and turgor loss, leading to fruit softening [40,43]. After 15 d of storage, a rapid softening trend was evident in all samples, although the rate of decrease was different. Despite not statistically different from the uncoated pear, pears coated only with pectin showed a lower firmness loss, which can be due to the coating effect itself (i.e., limited gas diffusion (low O_2), which limits the degradation of the pectins present in the peel). Pears with AL.C better maintained firmness compared to uncoated and pectin-coated pears (Table 1), which indicates the potential use of AL.C on delaying fruit senescence. The higher firmness preservation observed can be attributed to the limited gas diffusion (low O_2) after the application of the edible coating plus the enrichment with antioxidants, which limit the activities of oxidizing enzymes [44]. These enzymes are responsible for turning insoluble protopectins into the more soluble pectic acid and pectin, which, consequently, leads to less membrane integrity degradation [45,46]. Under the β-farnesene atmosphere, a higher firmness loss was observed, probably due to the external stress promoted by β-farnesene, but the same behavior was observed for all conditions.

Soluble Solids Content (SSC) and pH

It is well known that sugars are an important parameter defining fruit maturity and quality. Therefore, it is crucial that the postharvest treatment minimizes cellular processes to maintain the total soluble solids for a prolonged time. After the application of the coating, SSC values generally increased after 15 d of storage, as part of the natural ripening. It was expected that SSC values found in pears stored in the presence of β-farnesene were higher, because of the metabolism induction pattern observed with the other quality parameters, but no differences between the two storage conditions (with and without β-farnesene) were observed. On the other hand, differences were found between the coated and uncoated pears, stored in both conditions, especially between the pears treated with AL.C and the control. This lower accumulation of sugars in the treated fruit can be explained by the effect of the coating in reducing the respiration and metabolic activities associated with the hydrolysis of starch into sugar [3,17]. A decrease in the pH was observed, regardless of the storage conditions and atmosphere. An increase in pH values was expected in highly respiring fruit, such as in control conditions, particularly under the β-farnesene atmosphere since organic acids, such as malic and citric acids, are the primary substrates for respiration [47]. Inversely, in coated pears, the expected decrease in pH was observed since the coating delayed the ripening process and therefore the respiration avoiding the faster degradation of organic acids. The same results were obtained by Sharma and Rao [21], where xanthan-gum coatings were applied to freshly cut pears.

SC Index

At the initial sampling date, none of the conditions exhibited scald symptomatic pears. SC-like damage appeared after 15 d of storage only on pears under the β-farnesene atmosphere treatment. The presence of this α-farnesene isomer affected 100% of the control fruit, 83.30% of pears from the procedural control, and 16.67% of pears treated with AL.C. The analysis of the results suggests that it seems that β-farnesene volatilization effectively promoted stress and injuries in pear skins, leading to the appearance of SC-like signs. However, some protection was detected when pears were treated with AL.C. It is known that edible coatings created an atmosphere inside the fruit similar to the modified atmosphere, i.e., restriction O_2 entering, thus slowing down ethylene production and oxidative metabolism [3]. Additionally, as SC can be regulated by α-farnesene oxidation, the treatment with coatings with higher antioxidant capacity can explain the protection offered by AL.C. Thus, it appears that the bioactive compounds present in AL.C may be responsible for this protective effect, since the apple byproduct coating did not exert the same results (Figure 2). In fact, antioxidant systems might inhibit the occurrence of

oxidation injuries by neutralizing scald-related oxidation reactions [48,49]. Sharma and Rao [21] reported that xanthan-gum-based edible coatings incorporated with cinnamic acid lead to a reduction in the oxidative browning process. Given all this, it is possible to hypothesize that AL.C was able to protect pears from β-farnesene oxidation damages.

3.2.3. Antioxidant Activity of Pears

A higher antioxidant activity was observed in AL.C treated pears, which was maintained during storage. These results are supported by Correa-Betanzo et al. [50], who stated that the application of edible coatings helped to preserve the antioxidant activity of berry cactus fruit. The edible coating by itself (i.e., only pectin) led to a decrease in the antioxidant capacity of the pear as observed on Table 1. However, it is notable that the presence of the antioxidants from A.L. enhanced the antioxidant capacity of the fruit. These results are in agreement with Oms-Oliu et al. [29], which also demonstrated that the use of polysaccharide-based edible coatings by themselves did not contribute to the enhancement of the antioxidant capacity of freshly cut pears. Lindo-García et al. [30] presented that, although having initial higher antioxidant potential, a higher disorder incidence in controls was observed, demonstrating that the initial intrinsic antioxidant potential of the fruit was not directly related to the development of SC. The total antioxidant activity of pears varied between the AL.C treatment and the control.

3.2.4. Oxidative Enzyme Activity of Pears

In this experiment, the PPO activity of pears under the β-farnesene atmosphere showed coherence with the color changes observed, since oxidation via this enzyme is believed to be one of the major causes of skin browning [51]. In this regard, compared to the control, the treatment with AL.C suppressed the PPO activity, which corroborated the lower scald-like percentage observed. Conversely, the other conditions showed an increase in the enzyme activity, which explains the higher L* and lower h° values obtained. Additionally, pears under the β-farnesene atmosphere demonstrated higher increments of PPO activity corroborating the hypothesis of injury development. The natural antioxidants present in AL.C can potentially counteract oxidation-linked damages associated with PPO activity through its inhibition [21,52]. Additionally, the maintenance of higher membrane integrity in pears treated with AL.C explains the lower activity of PPO in pears treated with AL.C since this enzyme is localized in vacuoles. Thus, the lower cell membrane degradation promoted by these coatings contributes to reducing PPO activity, exhibiting less SC-like symptoms.

3.3. β-Farnesene-Atmosphere Model System Validation in Storage Conditions

Normally, in commercial storage, SC appears after 4–6 months of cold storage [5]. Therefore, a simulated commercial long-term storage trial was executed across 4 months to conclude about the reproducibility of the results obtained with the 15 d β-farnesene induction model system. Since, in the induction model experiment, AL.C demonstrated a potential protection function against damage development, the results focused on SC development and quality parameters in the coated pears with AL.C and controls (Figure 3).

3.3.1. Physicochemical Properties of Pears
Color

At the end of 4 month storage, AL.C preserved a higher chlorophyll pigment than both controls, which resulted in fewer variations of L* and h° values (Figure 3A,B). As stated before, these lower variations on color parameters could show the reduction in senescence and superficial scald incidence [53], which corroborates the results obtained previously. This limitation of color degradation is in accordance with a recent study on 'Bartlett' pears, which showed the positive effect of chitosan coating in reducing senescence [54].
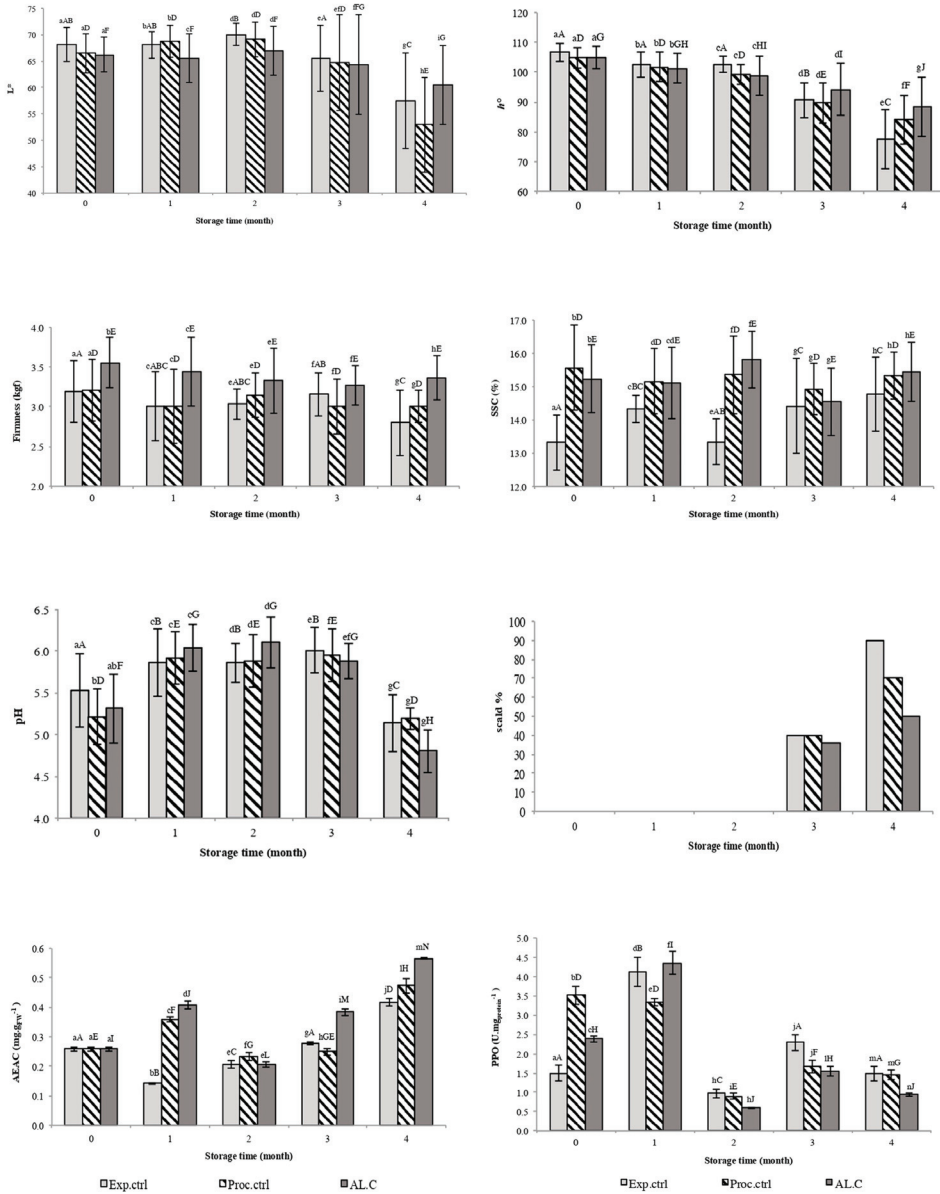
Figure 3. Color parameters (L* (**A**) and hue (**B**)), firmness (**C**), soluble solid content (SSC (**D**)), pH (**E**), scald index (**F**), AEAC (**G**) and PPO (**H**) activity of 'Rocha' pear at 0, 1, 2, 3 and 4 months of commercial storage. Exp. ctrl: experimental control; Proc. ctrl: procedural control; AL.C: *Arbutus Unedo* leaf coating. Error bars represent the standard deviations of the means (n = 10 for A, B, C, D, E, F; n = 6 for G and H). Same lower-case letter indicates no differences between conditions at each time point, and the same upper-case letter indicates no differences between storage months at each condition at $p < 0.05$.

Firmness

A retention of firmness on pears with AL.C was observed, and firmness loss was higher in uncoated pears (Figure 3C). It suggests that AL.C treatment slowed down the ripening process probably due to the oxygen barrier effect and to the indirect inhibition of the catalytic activity of carbohydrate-degrading enzymes. Therefore, once again, it demonstrates the reduction in the ripening and quality loss of pears [12,55].

SSC and PH

In the case of SSC, it is known that organic acids are degraded during ripening, while the sugar content increases [55]. As shown in Figure 3D, this increase was observed only in uncoated pears. Coated pears did not change the SSC content during storage. This lower variation of sugars in treated fruit might be to the effect of coating, which reduced respiration and the metabolic activity of pears, therefore less sugar was consumed [43]. The data regarding the effect of pectin coating incorporated with antioxidants on pH are presented in Figure 3E. As shown, there is an increment until the 3rd month and then a decrease, but without differences between the coated and uncoated pears. This decrease at the end of storage was also noticed on coated pears under the β-farnesene atmosphere and could be explained by the coating influence on respiration activity, which thereby delays the degradation of organic acids, such as the malic and citric ones [47].

Scald Index

The percentage of the SC surface was recorded as the total number of affected fruits in each condition. SC evaluation in uncoated pears indicates that, at the 3rd month, SC symptoms started to appear, and a remarkable increase is achieved at the end of storage, with uncoated pears reaching 90% of scald. Scald is lower in coated pears especially in pears with AL.C. This data are consistent with the findings obtained using the β-farnesene induction model system developed in this work. Given that scald is known to be the result of an oxidative process [5], antioxidants may play a decisive role in SC prevention. This corroborates that the higher antioxidant activity observed in pears with AL.C (Figure 3F) can give some protection against superficial scald development.

3.3.2. Antioxidant Activity of Pears

The data presented in Figure 3G show the changes in the antioxidant activity of coated and uncoated pears. In general, antioxidant activity increased until the end of storage. It is known that, in apples, the increase in antioxidant activity during storage is due to the biosynthesis of phenolic compounds [56]. However, higher antioxidant activity was detected in pears with AL.C, whereas a lower antioxidant activity was noticed in control fruit. These results validated the effects obtained previously under the induction model system atmosphere. The application of this postharvest technique helped to preserve the antioxidant activity better than control fruit. Likewise, the addition of antioxidants into the coating could explain the higher antioxidant activity observed.

3.3.3. Oxidative Enzyme Activity of Pears

The activity of polyphenol oxidase (PPO) enzyme was measured in uncoated and coated pears during storage. In this experiment, it was not possible to set a clear tendency about PPO activity over time. However, it is noticeable that, until the end of storage, there is a decline in PPO activity especially in pears with AL.C (Figure 3H). According to Ghasemnezhad et al. [57], the lower activity of the PPO enzyme can be interpreted as the inhibition of enzymatic browning and, therefore, less superficial scald development. The same conclusions were obtained by Kou et al. [58]. Additionally, the higher membrane integrity and greener surface observed in pears with AL.C explain the lower PPO activity measured. Overall, these findings relate to the lower SC development and validate the β-farnesene model as adequate for the quick exploration of the effectiveness of antioxidant coatings against superficial scald development in the 'Rocha' pear.

3.4. Principal Component Analysis of the Experiment

The principal component analysis (PCA) was performed to summarize and understand the relation between the results obtained under the induction model system with β-farnesene and commercial storage. As expressed before, the principal aim of this work was to create a simple and fast method to enhance the appearance of SC and to achieve conclusions regarding an effective treatment against SC in a short time frame. To prove the reliability of the model system, the same selected antioxidant coatings and controls were tested under a 4 month commercial storage. Figure 4A shows that the first and second principal components described 79% of the variability (53.32 and 25.68%, respectively). Figure 4B shows that the first and second principal components described 60.353% of the variability (37.368 and 22.986%, respectively). Both principal component analyses clearly separated the different conditions, which were mainly dependent on the presence of a higher antioxidant content, i.e., AL.C coating is separated from the other conditions. These PCA results corroborate the conclusions obtained in both assays. It is also clear that pears with AL.C are negatively related to PPO activity and L* values and positively related with firmness, which explains the observed capacity in reducing SC incidence in both assays (Table 1 and Figure 3). Hence, the PCA results demonstrate the reliability of the model system developed in this study, as proved by the similarity of the biochemical data obtained in both assays. Additionally, AL.C could delay ripening and reduce the SC of coated pears. Although previous results suggested that edible coatings enriched with natural antioxidants provide a defense against oxidative reactions and SC [43,52], not all antioxidant extracts demonstrated positive results, so the AL.C composition demonstrates a high potential for its application in the future as a solution to inhibit SC.
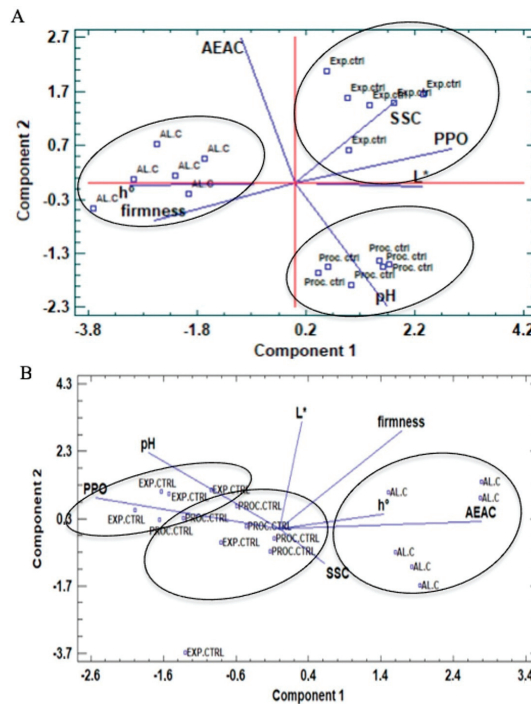
Figure 4. (**A**) PCA analysis biplot for the quality parameters of the β-farnesene atmosphere trial at the end of storage. (**B**) PCA analysis biplot for the quality parameters of the commercial trial at the end of storage. Exp. ctrl: experimental control; Proc. ctrl: procedural control; AL.C: *Arbutus Unedo* leaf coating.

4. Conclusions

This work evaluated an innovative damage induction model system to study SC prevention in postharvest pears through the exposure of fruit to a β-farnesene-enriched atmosphere. The conditions used were found to induce similar SC symptoms in 15 d. This innovative SC induction model represents a no-equipment, simple, rapid, reliable and inexpensive method to test the efficacy of treatments or postharvest strategies to prevent SC and, eventually, other postharvest disorders. The application of the natural extracts to 'Rocha' pears as in this case study permitted the demonstration of the model consistency along with the 4 month commercial storage at low temperatures, which opens the possibility of the application of this model induction to other fruit crops. With this model system and as expected, the protection offered by AL.C was corroborated, which enhanced the quality of pears and reduce injury under the β-farnesene atmosphere, and the same observations were obtained in the commercial trial. In this paper, it was demonstrated for the first time that the generation of a β-farnesene atmosphere can constitute a convenient injury induction model system to fast-track the effectiveness of new treatments and their doses to be applied in the postharvest sector, particularly in the fruit sector.

References

1. Saquet, A.A.; Almeida, D.P.F. Ripening physiology and biochemistry of 'Rocha' pear as affected by ethylene inhibition. *Postharvest Biol. Technol.* **2017**, *125*, 161–167. [CrossRef]
2. Leisso, R.S.; Gapper, N.E.; Mattheis, J.P.; Sullivan, N.L.; Watkins, C.B.; Giovannoni, J.J.; Schaffer, R.J.; Johnston, J.W.; Hanrahan, I.; Hertog, M.L.A.T.M.; et al. Gene expression and metabolism preceding soft scald, a chilling injury of 'Honeycrisp' apple fruit. *BMC Genom.* **2016**, *17*, 798. [CrossRef]
3. Deng, Z.; Jung, J.; Simonsen, J.; Wang, Y.; Zhao, Y. Cellulose Nanocrystal Reinforced Chitosan Coatings for Improving the Storability of Postharvest Pears Under Both Ambient and Cold Storages. *J. Food Sci.* **2017**, *82*, 453–462. [CrossRef] [PubMed]
4. Karagiannis, E.; Tanou, G.; Scossa, F.; Samiotaki, M.; Michailidis, M.; Manioudaki, M.; Laurens, F.; Job, D.; Fernie, A.R.; Orsel, M.; et al. Systems-Based Approaches to Unravel Networks and Individual Elements Involved in Apple Superficial Scald. *Front. Plant Sci.* **2020**, *11*, 8. [CrossRef]
5. Lurie, S.; Watkins, C.B. Superficial scald, its etiology and control. *Postharvest Biol. Technol.* **2012**, *65*, 44–60. [CrossRef]
6. Fonseca, A.M.A.; Dias, C.; Amaro, A.L.; Isidoro, N.; Pintado, M.; Silvestre, A.J.D.; Rocha, S.M. The Impact of Plant-Based Coatings in "ROCHA" Pear Preservation during Cold Storage: A Metabolomic Approach. *Foods* **2020**, *9*, 1299. [CrossRef]
7. Sarkar, D.; Ankolekar, C.; Greene, D.; Shetty, K. Natural preservatives for superficial scald reduction and enhancement of protective phenolic-linked antioxidant responses in apple during post-harvest storage. *J. Food Sci. Technol.* **2018**, *55*, 1767–1780. [CrossRef]
8. Karagiannis, E.; Michailidis, M.; Tanou, G.; Samiotaki, M.; Karamanoli, K.; Avramidou, E.; Ganopoulos, I.; Madesis, P.; Molassiotis, A. Ethylene –dependent and –independent superficial scald resistance mechanisms in 'Granny Smith' apple fruit. *Sci. Rep.* **2018**, *8*, 11436. [CrossRef] [PubMed]
9. Pedreschi, R.; Franck, C.; Lammertyn, J.; Erban, A.; Kopka, J.; Hertog, M.; Verlinden, B.; Nicolaï, B. Metabolic profiling of 'Conference' pears under low oxygen stress. *Postharvest Biol. Technol.* **2009**, *51*, 123–130. [CrossRef]

10. Li, Q.; Cheng, C.; Zhang, X.; Wang, C.; Yang, S. Preharvets bagging and postharvest calcium treatment affects superficial scald incidence and calcium nutrition during storage of 'Chili' pear (*Pyrus bretschneideri*) fruit. *Postharvest Biol. Technol.* **2020**, *163*, 111149. [CrossRef]
11. Silva, F.J.P.; Gomes, M.H.; Fidalgo, F.; Rodrigues, J.A.; Almeida, D.P.F. Antioxidant properties and fruit quality during long-term storage of 'Rocha' pear: Effect of maturity and storage conditions. *J. Food Qual.* **2010**, *33*, 1–20. [CrossRef]
12. Almeida, D.P.; Carvalho, R.; Dupille, E. Efficacy of 1-methylcyclopropene on the mitigation of storage disorders of "Rocha" pear under normal refrigerated and controlled atmospheres. *Food Sci. Technol. Int.* **2016**, *22*, 399–409. [CrossRef]
13. Drzyzga, O. Diphenylamine and derivatives in the environment: A review. *Chemosphere* **2003**, *53*, 809–818. [CrossRef]
14. Dias, C.; Amaro, A.L.; Salvador, Â.C.; Silvestre, A.J.D.; Rocha, S.M.; Isidoro, N.; Pintado, M. Strategies to preserve postharvest quality of horticultural crops and superficial scald control: From diphenylamine antioxidant usage to more recent approaches. *Antioxidants* **2020**, *9*, 356. [CrossRef]
15. Rosenbloom, R.A.; Wang, W.; Zhao, Y. Delaying ripening of 'Bartlett' pears (Pyrus communis) during long-term simulated industrial cold storage: Mechanisms and validation of chitosan coatings with cellulose nanocrystals Pickering emulsions. *LWT* **2020**, *122*, 109053. [CrossRef]
16. Panahirad, S.; Dadpour, M.; Peighambardoust, S.H.; Soltanzadeh, M.; Gullón, B.; Alirezalu, K.; Lorenzo, J.M. Applications of carboxymethyl cellulose- and pectin-based active edible coatings in preservation of fruits and vegetables: A review. *Trends Food Sci. Technol.* **2021**, *110*, 663–673. [CrossRef]
17. Baraiya, N.S.; Rao, T.V.R.; Thakkar, V.R. Improvement of Postharvest Quality and Storability of Jamun Fruit (*Syzygium cumini* L. var. Paras) by Zein Coating Enriched with Antioxidants. *Food Bioprocess Technol.* **2015**, *8*, 2225–2234. [CrossRef]
18. Poverenov, E.; Rutenberg, R.; Danino, S.; Horev, B.; Rodov, V. Gelatin-Chitosan Composite Films and Edible Coatings to Enhance the Quality of Food Products: Layer-by-Layer vs. Blended Formulations. *Food Bioprocess Technol.* **2014**, *7*, 3319–3327. [CrossRef]
19. Gago, C.; Antão, R.; Dores, C.; Guerreiro, A.; Miguel, M.G.; Faleiro, M.L.; Figueiredo, A.C.; Antunes, M.D. The Effect of Nanocoatings Enriched with Essential Oils on "Rocha" Pear Long Storage. *Foods* **2020**, *9*, 240. [CrossRef] [PubMed]
20. Kähkönen, M.P.; Hopia, A.I.; Vuorela, H.J.; Rauha, J.P.; Pihlaja, K.; Kujala, T.S.; Heinonen, M. Antioxidant activity of plant extracts containing phenolic compounds. *J. Agric. Food Chem.* **1999**, *47*, 3954–3962. [CrossRef]
21. Sharma, S.; Rao, T.V.R. Xanthan gum based edible coating enriched with cinnamic acid prevents browning and extends the shelf-life of fresh-cut pears. *LWT-Food Sci. Technol.* **2015**, *62*, 791–800. [CrossRef]
22. Brooks, C.; Cooley, J.; Fisher, D. Nature and control of apple scald. *J. Agric. Res.* **1919**, *XVIII*, 211–241.
23. Bauchot, A.D.; Reid, S.J.; Ross, G.S.; Burmeister, D.M. Induction of apple scald by anaerobiosis has similar characteristics to naturally occurring superficial scald in 'Granny Smith' apple fruit. *Postharvest Biol. Technol.* **1999**, *16*, 9–14. [CrossRef]
24. Dilley, D.R.; Dedolph, R.R.; Maclean, D.C.; Dewey, D.H. Apple Scald Induction by Anaerobiosis. *Nature* **1963**, *200*, 1229–1230. [CrossRef]
25. Jaoui, M.; Lewandowski, M.; Offenberg, J.H.; Docherty, K.S.; Kleindienst, T.E. Ozonolysis of α/β-farnesene mixture: Analysis of gas-phase and particulate reaction products. *Atmos. Environ.* **2017**, *169*, 175–192. [CrossRef]
26. Kumar, D.; Suryavanshi, P.; Padalia, R.C.; Chauhan, A.; Venkatesha, K.T.; Tiwari, A.K.; Singh, V.R.; Singh, S.; Upadhyay, R.K. Evaluation of harvesting time and standardization of distillation duration for higher essential oil content and quality in German chamomile (*Chamomilla recutita* L.). *J. Spices Arom. Crops* **2020**, *29*, 140–147. [CrossRef]
27. Jaoui, M.; Lewandowski, M.; Docherty, K.S.; Corse, E.W.; Lonneman, W.A.; Offenberg, J.H.; Kleindienst, T.E. Photooxidation of farnesene mixtures in the presence of NOx: Analysis of reaction products and their implication to ambient PM2.5. *Atmos. Environ.* **2016**, *130*, 190–201. [CrossRef]
28. Dias, C.; Fonseca, A.M.A.; Amaro, A.L.; Vilas-Boas, A.A.; Oliveira, A.; Santos, S.A.O.; Silvestre, A.J.D.; Rocha, S.M.; Isidoro, N.; Pintado, M. Natural-Based Antioxidant Extracts as Potential Mitigators of Fruit Browning. *Antioxidants* **2020**, *9*, 715. [CrossRef] [PubMed]
29. Oms-Oliu, G.; Soliva-Fortuny, R.; Martín-Belloso, O. Edible coatings with antibrowning agents to maintain sensory quality and antioxidant properties of fresh-cut pears. *Postharvest Biol. Technol.* **2008**, *50*, 87–94. [CrossRef]
30. Lindo-García, V.; Giné-Bordonaba, J.; Leclerc, C.; Ubach, D.; Larrigaudière, C. The relationship between ethylene- and oxidative-related markers at harvest with the susceptibility of pears to develop superficial scald. *Postharvest Biol. Technol.* **2020**, *163*, 111135. [CrossRef]
31. Salta, J.; Martins, A.; Santos, R.G.; Neng, N.R.; Nogueira, J.M.F.; Justino, J.; Rauter, A.P. Phenolic composition and antioxidant activity of Rocha pear and other pear cultivars—A comparative study. *J. Funct. Foods* **2010**, *2*, 153–157. [CrossRef]
32. Gião, M.S.; González-Sanjosé, M.L.; Rivero-Pérez, M.D.; Pereira, C.I.; Pintado, M.E.; Malcata, X.F. Infusions of Portuguese medicinal plants: Dependence of final antioxidant capacity and phenol content on extraction features. *J. Sci. Food Agric.* **2007**, *87*, 2638–2647. [CrossRef] [PubMed]
33. Galeazzi, M.A.M.; Sgarbieri, V.C. Substrate Specificity and Inhibition of Polyphenoloxidase (PPO) From a Dwarf Variety of Banana (*Muss Cavendishii*, L.). *J. Food Sci.* **1981**, *46*, 1404–1406. [CrossRef]
34. Gatto, M.A.; Sergio, L.; Ippolito, A.; Di Venere, D. Phenolic extracts from wild edible plants to control postharvest diseases of sweet cherry fruit. *Postharvest Biol. Technol.* **2016**, *120*, 180–187. [CrossRef]

35. Tenuta, M.C.; Deguin, B.; Loizzo, M.R.; Dugay, A.; Acquaviva, R.; Malfa, G.A.; Bonesi, M.; Bouzidi, C.; Tundis, R. Contribution of Flavonoids and Iridoids to the Hypoglycaemic, Antioxidant, and Nitric Oxide (NO) Inhibitory Activities of *Arbutus unedo* L. *Antioxidants.* **2020**, *9*, 184. [CrossRef] [PubMed]

36. Malheiro, R.; Sá, O.; Pereira, E.; Aguiar, C.; Baptista, P.; Pereira, J.A. *Arbutus unedo* L. leaves as source of phytochemicals with bioactive properties. *Ind. Crops Prod.* **2012**, *37*, 473–478. [CrossRef]

37. Du, G.; Zhu, Y.; Wang, X.; Zhang, J.; Tian, C.; Liu, L.; Meng, Y.; Guo, Y. Phenolic composition of apple products and by-products based on cold pressing technology. *J. Food Sci. Technol.* **2019**, *56*, 1389–1397. [CrossRef]

38. The Good Scents Company. (E)-Beta-Farnesene. Available online: www.thegoodscentscompany.com/data/rw1053891.html (accessed on 20 August 2021).

39. Wang, Q.; Liu, H.; Zhang, M.; Liu, S.; Hao, Y.; Zhang, Y. MdMYC2 and MdERF3 Positively Co-Regulate α-Farnesene Biosynthesis in Apple. *Front. Plant Sci.* **2020**, *11*, 512844. [CrossRef]

40. Guerreiro, A.C.; Gago, C.M.L.; Faleiro, M.L.; Miguel, M.G.C.; Antunes, M.D.C. The use of polysaccharide-based edible coatings enriched with essential oils to improve shelf-life of strawberries. *Postharvest Biol. Technol.* **2015**, *110*, 51–60. [CrossRef]

41. Gago, C.M.L.; Miguel, M.G.; Cavaco, A.M.; Almeida, D.P.F.; Antunes, M.D.C. Combined effect of temperature and controlled atmosphere on storage and shelf-life of 'Rocha' pear treated with 1-methylcyclopropene. *Food Sci. Technol. Int.* **2015**, *21*, 94–103. [CrossRef]

42. Hussain, P.R.; Meena, R.S.; Dar, M.A.; Wani, A.M. Carboxymethyl Cellulose Coating and Low-Dose Gamma Irradiation Improves Storage Quality and Shelf Life of Pear (*Pyrus Communis* L., Cv. Bartlett/William). *J. Food Sci.* **2010**, *75*, M586–M596. [CrossRef]

43. Ali, U.; Kanwar, S.; Yadav, K.; Basu, S.; Mazumder, K. Effect of arabinoxylan and β-glucan stearic acid ester coatings on post-harvest quality of apple (Royal Delicious). *Carbohydr. Polym.* **2019**, *209*, 338–349. [CrossRef]

44. Matabura, V.V. Modelling of firmness variability of Jonagold apple during postharvest storage. *J. Food Sci. Technol.* **2021**, *89*, 1–12. [CrossRef]

45. Baraiya, N.S.; Rao, T.V.R.; Gol, N.B. Influence of Polysaccharide-Based Edible Coatings on the Shelf Life and Nutritional Quality of Tomato Fruit. *Glob. Sci. Books* **2012**, *6*, 22–27.

46. Tesfay, S.Z.; Magwaza, L.S. Evaluating the efficacy of moringa leaf extract, chitosan and carboxymethyl cellulose as edible coatings for enhancing quality and extending postharvest life of avocado (*Persea americana* Mill.) fruit. *Food Packag. Shelf Life* **2017**, *11*, 40–48. [CrossRef]

47. Yaman, Ö.; Bayoındırlı, L. Effects of an Edible Coating and Cold Storage on Shelf-life and Quality of Cherries. *LWT-Food Sci. Technol.* **2002**, *35*, 146–150. [CrossRef]

48. Torres, C.A.; Sepulveda, G.; Mejía, N.; Defilippi, B.G.; Larrigaudière, C. Understanding the key preharvest factors determining 'Packham's Triumph' pear heterogeneity and impact in superficial scald development and control. *Postharvest Biol. Technol.* **2021**, *172*, 1111399. [CrossRef]

49. Ding, R.; Du, B.; Zhang, Y. Conjugated trienols and programmed cell death are more closely related to superficial scald than reactive oxygen species in apple fruit stored at low temperature. *Sci. Hortic.* **2019**, *246*, 597–603. [CrossRef]

50. Correa-Betanzo, J.; Jacob, J.K.; Perez-Perez, C.; Paliyath, G. Effect of a sodium caseinate edible coating on berry cactus fruit (*Myrtillocactus geometrizans*) phytochemicals. *Food Res. Int.* **2011**, *44*, 1897–1904. [CrossRef]

51. Deng, Y.; Wu, Y.; Li, Y. Effects of high O$_2$ levels on post-harvest quality and shelf life of table grapes during long-term storage. *Eur. Food Res. Technol.* **2005**, *221*, 392–397. [CrossRef]

52. Xiao, C.; Zhu, L.; Luo, W.; Song, X.; Deng, Y. Combined action of pure oxygen pretreatment and chitosan coating incorporated with rosemary extracts on the quality of fresh-cut pears. *Food Chem.* **2010**, *121*, 1003–1009. [CrossRef]

53. Pastor, C.; Sánchez-González, L.; Marcilla, A.; Chiralt, A.; Cháfer, M.; González-Martínez, C. Quality and safety of table grapes coated with hydroxypropylmethylcellulose edible coatings containing propolis extract. *Postharvest Biol. Technol.* **2011**, *60*, 64–70. [CrossRef]

54. Jung, J.; Deng, Z.; Zhao, Y. Mechanisms and performance of cellulose nanocrystals Pickering emulsion chitosan coatings for reducing ethylene production and physiological disorders in postharvest 'Bartlett' pears (*Pyrus communis* L.) during cold storage. *Food Chem.* **2020**, *309*, 125693. [CrossRef]

55. Kowalczyk, D.; Kordowska-Wiater, M.; Zięba, E.; Baraniak, B. Effect of carboxymethylcellulose/candelilla wax coating containing potassium sorbate on microbiological and physicochemical attributes of pears. *Sci. Hortic.* **2017**, *218*, 326–333. [CrossRef]

56. Leja, M.; Mareczek, A.; Ben, J. Antioxidant properties of two apple cultivars during long-term storage. *Food Chem.* **2003**, *80*, 303–307. [CrossRef]

57. Ghasemnezhad, M.; Zareh, S.; Rassa, M.; Sajedi, R.H. Effect of chitosan coating on maintenance of aril quality, microbial population and PPO activity of pomegranate (*Punica granatum* L. cv. Tarom) at cold storage temperature. *J. Sci. Food Agric.* **2013**, *93*, 368–374. [CrossRef] [PubMed]

58. Kou, X.; Wu, M.; Li, L.; Wang, S.; Xue, Z.; Liu, B.; Fei, Y. Effects of CaCl2 dipping and pullulan coating on the development of brown spot on "Huangguan" pears during cold storage. *Postharvest Biol. Technol.* **2015**, *99*, 63–72. [CrossRef]

Postharvest Treatment of 'Florida Prince' Peaches with a Calcium Nanoparticle–Ascorbic Acid Mixture during Cold Storage and Its Effect on Antioxidant Enzyme Activities

Lo'ay A. A. [1], Hamed Ismail [2] and Hazem S. Kassem [3,*]

[1] Pomology Department, Faculty of Agriculture, Mansoura University, Mansoura 35516, Egypt; Loay_Arafat@mans.edu.eg
[2] Department of Food Science, Ontario Agricultural College, University of Guelph, Guelph, ON N1G 2W1, Canada; ismailh@uoguelph.ca
[3] Department of Agricultural Extension and Rural Society, College of Food and Agriculture Sciences, King Saud University, Riyadh 11451, Saudi Arabia
[*] Correspondence: hskassem@ksu.edu.sa; Tel.: +966-58104-5671

Abstract: Chilling injury (CI) is a physiological disorder resulting from low storage temperatures that affects the fruit quality and marketing of the 'Florida Prince' peach. In this study, the exogenous application of a mixture of calcium nanoparticles (CaNPs) and ascorbic acid was found to significantly alleviate the symptoms of CI in peaches during cold storage. Fruits were treated with CaNPs plus different concentrations of ascorbic acid (AA; 0, 3, 6, and 9 mM). Peaches were immersed in CaNP–AA for 15 min before being stored at 4 ± 1 °C and $95 \pm 1\%$ RH for 30 days. We observed that the 9 mM CaNP–AA treatment lowered the values for the CI index, ion leakage, and malondialdehyde (MDA) content and increased antioxidant enzyme activities (AEAs), such as for ascorbate oxidase (APX), catalase (CAT), superoxide dismutase (SOD), and glutathione reductase (GR). Furthermore, the treatment reduced the accumulation of both H_2O_2 and $O_2^{\bullet-}$ and increased the level of DPPH reduction throughout the duration of cold storage. Our results suggest that 9 mM CaNP–AA treatment suppresses the incidence of CI in peach fruit throughout cold storage, possibly because 9 mM CaNP–AA is at least partly involved in enhancing the antioxidant system via its effect on antioxidant substances. The results indicate that applying the 9 mM CaNP–AA treatment afforded peaches with enhanced tolerance against cold storage stress.

Keywords: peach; cold storage; quality; calcium nanoparticles; antioxidant enzymes

1. Introduction

From the genus *Prunus*, the *Prunus persica* L. Batsch cv. 'Florida Prince' peach is the first early stone fruit crop to have been cultivated in Egypt. It displays high acclimation to local ecological conditions. A superior yield and fruit quality in comparison with others are recorded for this peach cultivar [1]. The area used for peach cultivation in Egypt is about 24,707 ha, corresponding to a total production of 360,723 tons [2]. Peaches decay easily during marketing processes, losing their value and quality after harvest. This decline occurs for several reasons, such as the rapid ripening of fruits, their sensitivity to mechanical injuries that occur throughout various handling processes, and their susceptibility to rapid infection from fungal diseases [3]. Therefore, for the reasons mentioned above, cold storage is an important way to reduce the rapid ripening of fruits and control the spread of diseases [4]. However, prolonged cold storage of peach fruits leads to biophysical changes in the cell walls that may later manifest as cold injury symptoms [5]. Symptoms of cold injury in peach fruits include the appearance of brown spots that vary in size and shape as well as the collapse of the interior tissue [6]. With an increase in storage duration, there is a tendency for greater development of chilling injury symptoms in fruit, reducing consumer acceptance [7].

Numerous studies conducted on CI symptoms have attempted to understand their prevalence and to mitigate their severity, frequently via treatments. Such studies tested the effect of cold storage of fruit [8], heat treatment of fruits to activate the action of antioxidants before cold storage [9], the use of Ultra-Violet (UV-C) [10] or salicylic acid to relieve the symptoms of cold injury [11], and the treatment of fruits with methyl jasmonate [12]. These studies aimed to reduce the occurrence of cold injury symptoms and control the quality of peaches during storage.

Recent research has examined the use of nano-calcium technology in the field of postharvest treatments for diminishing the phenomenon of CI symptoms during the cold storage of fruits [13]. Strengthening nano-calcium treatment by including antioxidants such as ascorbic acid (AA) plays an active role in countering the CI phenomenon. Generally, CI is directly correlated with the formation of reactive oxygen species (ROS) in fruit tissue throughout the storage period [14]. However, the AA present in plant cells reacts directly with ROS produced in cells [15], especially hydroxyl radicals [16]. Therefore, it increases the tolerance of fruit to the impact of the cold [17]. Furthermore, AA changes the oxidative state of alpha-tocopheroxyl radicals to normalize the action of plasma membranes on the plant cell membrane [18]. It also works to efficiently sustain antioxidant enzyme activity, which creates an equilibrium between the generation of ROS and antioxidants in the cell under chilling stress [19].

Calcium ions (Ca^{++}) are the main basis of pectin accumulation for supporting the cell wall and middle lamella to produce calcium pectate gel [20]. Calcium ions also balance the cell membrane and thus participate in firmness [21]. However, fruit firmness deteriorates considerably under the highest individually applied calcium chloride doses. Hence, using the authorized dose of calcium chloride (1%) is important because the application of high calcium chloride concentrations may cause stress on the tissues and thus a rapid increase in both the respiration rate and ethylene production [22]. Excessive respiration and ethylene production are associated with an increase in enzymatic breakdown, which leads to ripening and senescence [23]. Therefore, the tissues likely become softer than those of the untreated fruits. To the best of our knowledge, no prior studies have examined the role of calcium nanoparticles combined with ascorbic acid in protecting peach fruit during low-temperature storage. Therefore, this paper aims to assess the influence of calcium nanoparticles blended with ascorbic acid on CI increase in the 'Florida Prince' peach cultivar, and investigate the change model in fruit quality, chilling injury, and antioxidant enzyme potential throughout long periods of refrigeration.

2. Materials and Methods

2.1. Fruit Materials and Postharvest Treatments

The 'Florida Prince' peaches were from a commercial farm in Dakahlia province, Egypt (30.04° N, 31.25° E). Fruits were picked at commercial maturity (128 days after the full bloom stage) and included if they were free from peel defects and were uniform in size and shape. Fruits (600) were picked and delivered 2 h after harvesting. They were divided into two main batches. The first batch (300 fruits) was used for physical measurements, i.e., the chilling injury symptoms index, water loss, and fruit skin color (hue angle). This batch was divided into five lots of 60 fruits each for treatments, for which there were three replicates (e.g., 3 × 20 fruits). The second batch was used for the chemical analysis and had the same fruit distribution among the treatments as previously described.

2.2. Synthesis of Metal Calcium Nanoparticles (CaNPs) with Ascorbic Acid (AA)

Calcium nanoparticles (CaNPs) were prepared according to the procedure reported by Yugandhar and Savithramma [24]. A slight modification was made by adding AA at 3, 6, and 9 mM into a solution of CaCl (50 mM). Using distilled water, all weights of ascorbic acid were blended in a solution of calcium chloride at a concentration of 50 mM. The reaction mixture was spun on a checker at 5000 revolutions per minute for 1 h and then allowed to cool to room temperature for 2–3 days.

UV-vis spectroscopy was used to characterize the nanoparticles. The reduction of pure Ca^{++} particles and the subsequent topping of calcium nanoparticles were measured using ATI Unicom UV-vis spectroscopic analysis vision software ver. 3.20 by comparing the UV-vis spectra of the response blend at various wavelengths. The combined metal nanoparticles' UV-vis spectra were measured between 240–440 nm. The investigation was successfully conducted at a temperature of 25 °C using quartz cuvettes with a 1 cm optical path (Figure 1).
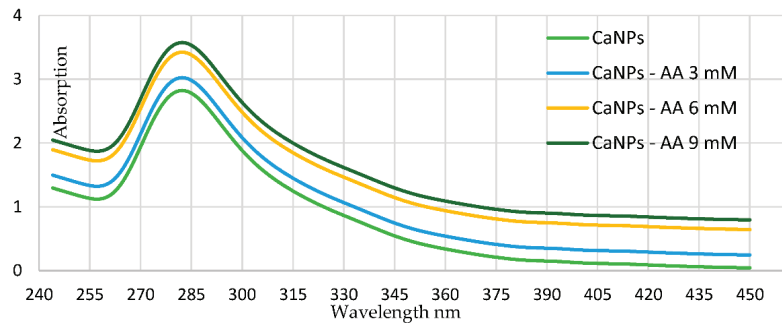
Figure 1. The UV-visible absorption spectra of the structure of calcium nanoparticles (CaNPs) mixed with various combinations of ascorbic acid (0, 3, 6, and 9 mM), displaying a peak at 282 nm.

The Zeta Potential test was used to determine the nanoparticles' (NPs) surface state and forecast the nanoparticle solution's long-term stability. The technique was used to define the CaNPs blended with ascorbic acid (AA) surface charge at the Central Laboratory, Electron Microscope Unit, Faculty of Agriculture, Mansoura University, Mansoura, Egypt, using Malvern Instruments Ltd. and Zeta Potential Ver. 2.3. The CaNP–AA mixture has an electrical charge on its surface, attracting a thin layer of ions with opposite directions to the surface. The Zeta Potential of nanoparticles provides information about their properties. Nanoparticles have two layers of ions that move as the solution diffuses. The electric potential at the end of the double layer is referred to as the Zeta Potential of the particles, and it varies between +100 and 100 mV. CaNPs containing AA were synthesized and had a Zeta Potential of -4.74 mV (higher stability). NPs with Zeta Potentials greater than or equal to +25 mV had a high degree of stability (Figure 2).
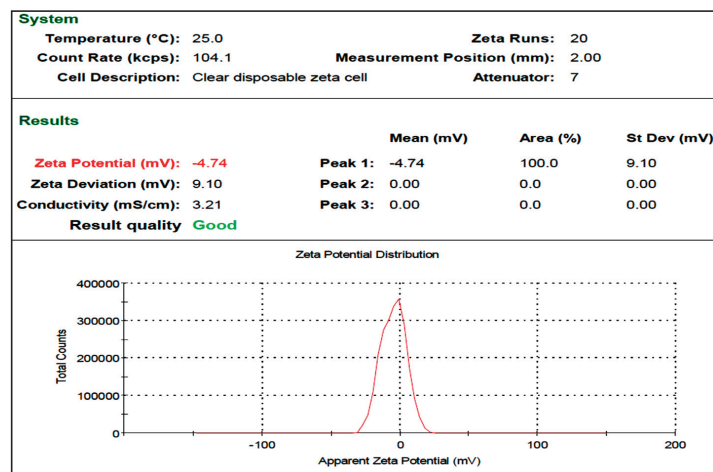
Figure 2. Zeta Potential determination technique for calcium nanoparticles with added ascorbic acid.

The nanoparticles' characterization was determined using transmission electron microscopy (JEOL TEM-2100) coupled to a CCD camera at a 200 kV acceleration voltage. Nanoparticles were defined according to size, shape, surface area, particle structure, and morphological characteristics. The integrated metal nanoparticles were created by suspending them on copper-coated carbon networks and allowing the dissolvable to dissolve gradually before chronicling the TEM images. TEM measurements were taken at Mansoura University's Central Laboratory, Electron Microscope Unit, Faculty of Agriculture, Mansoura, Egypt (Figure 3).
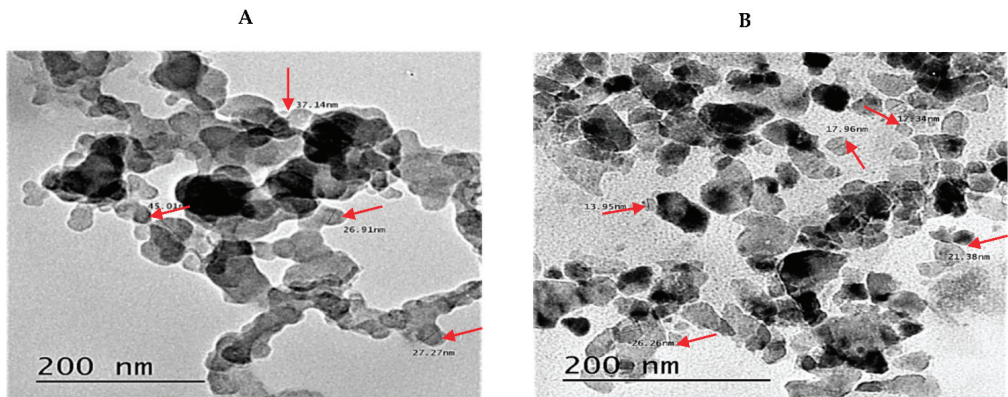
Figure 3. Transmission electron microscopy (TEM) images of the manufactured nanoparticles at 200 nm. The size of the CaNP particles (**A**) was between 27.27 and 45.01 nm. However, after mixing with ascorbic acid, the CaNPs reached about 13.95–21.38 nm in diameter (**B**). The particles were orbicular in appearance, and a few were tetragonal. The CaNPs particles tended to aggregate more in isolation than when mixed with ascorbic acid.

2.3. CaNP–AA Application Protocol

CaNPs were applied to the batches via five application approaches. The treatments were as follows: control, 0 mM CaNP–AA, 3 mM CaNP–AA, 6 mM CaNP–AA, and 9 mM CaNP–AA. Next, batches were soaked in the CaNP–AA treatments for 15 min at 4 °C, then placed into cold storage (4 ± 1 °C and air relative humidity, RH% 95 ± 1) for 30 days.

2.4. Chilling Injury Index, Water Loss%, and Fruit Skin Color

CI symptoms in peaches appear as brown shrunken areas/spots that increase in number and size as the duration of cold storage increases. The CI symptoms were inspected and scored on a scale from 0 (no injury) to 5 (very severe injury) based on necrotic spot area and browning intensity [25]. The CI index was computed according to the following formula:

$$CI - index = \sum_{k=5}^{n} \frac{(CI\ level) * (Number\ fruit\ at\ this\ level)}{Total\ number\ of\ fruit}$$

Water loss (WL%) was assessed by the following equation: WL% = $(W_{t=0} - W_t / W_{t=0})$ × 100; where $W_{t=0}$ is the initial weight of each fruit and W_t is their weight after five days [17]. However, the fruit skin color hue angle measurement was evaluated at intervals throughout the duration of storage by collecting images. To calculate the hue angle of peach, RGB signals were obtained using software ImageJ Ver. 1.43u (USA), according to Khojastehnazhand et al. [26].

2.5. Total Soluble Solid Content (SSC%), Total Acidity (TA%), and SSC/TA Ratio

The SSC% of peach juice was measured with a digital refractometer (PR32 ALAGO Co., Japan) at room temperature and was represented as a percentage. For TA%, peach

juice (20 mL) was used for titration with NaOH (0.1 N) [27]. The outcome was presented as a percentage according to the following formula:

$$TA\% = \frac{[0.1 \text{ M NaOH} * \text{ vol. of NaOH (in liter)} * 192.43]}{wt \text{ of sample}} * 100$$

where 192.43 g/mol is the molecular weight of citric acid.

The SSC/TA ratio was computed to judge peach maturity [25].

2.6. Fruit Pigments and Fruit Firmness (N)

The total anthocyanin in the fruit material was extracted using methanol mixed with 1% hydrochloric acid. After grinding in liquid N_2, the samples were incubated at room temperature overnight. The extracts were then centrifuged at $16,000 \times g$ for 16 min and their absorbance at 530 and 657 nm was measured using a spectrophotometer set at 421 nm [28].

The freeze-dried materials were first pulverized in a ball mill to extract the carotene, then 5 mL of N,N-dimethylformamide (DMF) was added to 0.8 g of this powder. To ensure a thorough extraction of carotene, the sample powder was immersed in DMF for 16 min at 4 °C [29], and then stored at 4 °C for 16 h. Finally, 1 mL of the suspension was centrifuged at $16,000 \times g$ for 5 min at 4 °C to remove all particles, and the supernatant solution was measured using a spectrophotometer [30].

Fruit firmness measurements were taken using a Zwick Universal Testing Machine equipped with a 60° conical probe 6.35 mm in diameter. The apparatus determined the force needed by the mechanical probe to penetrate 8 mm into the tissue of fruits at a speed of 3 mm s^{-1} [31].

2.7. Antioxidant Enzyme Activities (AEAs)

To determine catalase (CAT) activity, fruit pulp (2 g) was homogenized with 20 mL of a solution of 100 mM potassium phosphate (KH_2PO_4). The mixture was centrifuged ($30,000 \times g$) twice for 25 min at 4 °C. The clear extraction quantity was utilized for observations of the CAT activity in a final volume of 5 mL that contained 1 mL of the catalase extract (400–800 mg protein). A unit of CAT activity was defined as the amount of the compound that could oxidize 1 mM H_2O_2 min^{-1} at 25 °C [32].

Ascorbate peroxidase (APX) was isolated from 2 g of fruit pulp tissue ground with 20 mL of 50 mM potassium phosphate (KH_2PO_4). Additionally, EDTA, ascorbic acid (AA, 1 mM), and polyvinylpolypyrrolidone (PVPP, 1%) were added at 5 °C. The materials were mixed and centrifuged twice at $35,000 \times g$ for 30 min at 4 °C, and the clarified supernatant was utilized to monitor the APX activity in a final quantity of 3 mL. This included 150–300 mL of the clear fraction (40/240 mg protein). A unit of APX was characterized as the amount of the compound that oxidized 1 mM of ascorbate min^{-1} at 25 °C [33].

Glutathione reductase (GR) was separated from 1 g of peach pulp tissue ground in 25 mL of a 100 mM KH_2PO_4 buffer (pH 7.4) containing 0.6 mM EDTA at 5 °C. The mixture was centrifuged twice at $25,000 \times g$ for 25 min at 5 °C. An aliquot of the clear supernatant was applied to observe the GR activity in a final volume of 4 mL [34]. It contained 100 mL of the accelerator extract (40–80 mg protein). Each GR unit was defined as the amount of accelerator that oxidized 1 mM of NADPH min^{-1}. Moreover, the activity was counted on the standard curve as reported in [35].

Superoxide dismutase (SOD) was isolated from 1 g of peach pulp tissue ground in 10 mL of 50 mM KH_2PO_4 with the addition of 1.33 mM of diethylenetriamine penta-acetic acid (DTPA, $C_{14}H_{23}N_3O_{10}$) at 4 °C, then the mixture was centrifuged twice at $30,000 \times g$ for 30 min at 4 °C. The clear supernatant was used to detect SOD activity [36] in a final volume of 4 mL, which contained 70–80 mL of the mixture concentrate (24–56 mg of protein). A unit of SOD was described as the quantity of the substances that produced a half-maximal decrease. All the macromolecules were prepared and examined for calculating the catalyst activity [37].

2.8. Lipid Peroxidation, Malondialdehyde (MDA) Accumulation, and Ion Leakage%

Peach pulp (3 g) was ground and combined with 30 mL of metaphosphoric acid (HPO_3, 5%) and 500 µL of butylated hydroxytoluene (2%) in ethanol; then, the mixture was homogenized. 1,1,3,3-Tetra-ethoxy-propane (Sigma-Aldrich, St. Louis, MO, USA) was used to vary the amount of TBARS from 0 to 20 mM relative to 0–1 mM malondialdehyde (MDA) as a calibration standard to evaluate MDA accumulation product for the peach samples. The stoichiometry of MDA was calculated throughout the acid-heating step of the assay [38].

The ion leakage (IL%) of all peach samples was measured initially (M_0) by using an INE-DDSJ-318 conductivity meter. Later, after 3 h, all samples were heated at 100 °C in a water bath for 30 min to measure the total leakage after the samples reached room temperature (M_1) [39]. The percentage of IL% was calculated by the following formula:

$$IL\% = M_0 \text{ reding after 3 h} - M_1 \text{ (reading after heating)}/M_0 \times 100$$

2.9. Ethylene and Respiration Assessment

Ethylene concentrations and CO_2 respiration were determined at 5-day intervals in five peaches. For all experimental treatments, fruits were placed and sealed in 1000 mL glass jars with a 1-h gap between each interval of cold storage duration (in days). Gas chromatography techniques were used to extract gas samples from the headspace atmosphere surrounding the fruit and analyze them for ethylene and carbon dioxide (GC). Ethylene concentrations were determined using a GC-6000 Vega Series from Carlo Erba Ins., Milano, Italy, while CO_2 concentrations were determined using a GC PBI-Dansensor Checkmate-9900 from Denmark [40].

2.10. H_2O_2 and $O_2^{\bullet-}$ Production Rate and DPPH Reduction

One gram of fruit tissue was added to 3 mL of a KH_2PO_4 buffer 50 mM (pH 7.8) under cooling at 4 °C. The reagent was combined with polyvinylpyrrolidone (PVP 1% w/v) and immediately centrifuged at 10,000 rpm at 4 °C for 15 min. The $O_2^{\bullet-}$ production rate was determined by observing the development of NO_2 from hydroxylamine with the introduction of $O_2^{\bullet-}$ [41]. A linear curve with NO_2 was utilized to establish the $O_2^{\bullet-}$ formation rate from the response of $O_2^{\bullet-}$ with hydroxylamine. $O_2^{\bullet-}$ production was determined as nmol min^{-1} g^{-1} FW.

In the H_2O_2 assay, 1 g of the fruit pulp sample was added to 6 mL of 100% $(CH_3)_2CO$ and immediately centrifuged at 10,000× g for 15 min at 4 °C, then 1 mL of the clarified supernatant was combined with 0.1 mL of 5% $Ti(SO_4)_2$ and 0.2 mL of a NH_4OH solution. The hydrogen peroxide sample was accelerated, and the residue was reduced by adding 4 mL of 2 M H_2SO_4 after centrifugation at 10,000× g for 20 min, then the absorbance was quantified on a photometer at 415 nm. The H_2O_2 content was calculated from a standard curve and the fixation rate was shown as ηmol g^{-1} FW [42].

The inhibitory activity of DPPH was examined in the peach pulp sample and the dismutation of radical activity technique was applied. The scavenging results of flavedo samples of DPPH radicals were given as percentages. In brief, a 2 mL sample of peach extract (with methanol) was combined with 2 mL of 0.16 mM DPPH methanolic solvent. Afterward, samples were shaken for 1 min and stored for 30 min at room temperature in dark conditions. Subsequently, samples were evaluated on a photometer at a wavelength absorbance of 517 nm. The final amount of the DPPH radical was assumed by applying the formula of [43].

2.11. Statistical Analysis

The experiment was conducted during two growth seasons (2018–2019) using the Co-Stat software package (Ver. 6.303; 789 Lighthouse Ave PMB 320, Monterey, CA 93940, USA). The chilling injury, water loss, and peach skin color profile were analyzed in a randomized complete block design for the effect of fruit color maturity stages (applied to the same fruit

throughout the storage period). A factorial analysis displayed the main comparisons and the interaction effect of storage time and CaNP–AA under refrigeration. The appropriate significant differences among CaNP–AA treatments were tested by utilizing Duncan's multiple range test at the 5% level.

3. Results

3.1. Synthesis of Metal Calcium Nanoparticles (CaNPs)

We observed that the formation of calcium nanoparticles (CaNPs) blended with ascorbic acid at different concentrations was synthesized, and we confirmed treatments at a peak at 282 nm by UV-visible absorption spectra (Figure 1). Another technique to prove the formation of nanoparticles was using the Zeta Potential test for calcium nanoparticles with added ascorbic acid (Figure 2). To be certain, we used Transmission Electron Microscopy (TEM) images at 200 nm. The size of the CaNP particles (Figure 3A) was between 27.27 and 45.01 nm. However, after mixing with ascorbic acid, the CaNPs reached about 13.95–26.26 nm in diameter (Figure 3B).

3.2. CI Index, Water Loss%, and Peach Skin Color

Figure 4 shows the changes in the CI index, water loss, and peach skin color ($h°$) as physical features of peach quality throughout a cold storage period of several weeks. CaNP–AA treatments had a significant influence when studied as a factor. Regarding the various CaNP–AA applications, a significantly greater increase in CI incidence and water loss occurred, while peach skin color declined, in the untreated fruit compared with fruit treated throughout the 30 days. Nevertheless, fruit subjected to the 9 mM CaNP–AA treatment presented significantly lower CI incidence and water loss and the highest preservation of peach skin color ($h°$) compared with other CaNP–AA treatments throughout the storage period. Moreover, the 9 mM CaNP–AA treatment minimized CI incidence over the full storage period (30 days). This began on the 20th day (1.01), then increased slightly up until the end of storage (1.19). The outcomes indicated a reduction in the rate of water loss (19.57%) and a slight decline in the skin color of the fruit ($h° = 75.31$) on the 30th day of the cold storage period. The change in physical parameters could be due to the cold temperature stress effects, which enhanced the formation of reactive oxygen species (ROS).

3.3. Total Soluble Solids (SSC%), Total Acidity (TA%), and SSC/TA Ratio

Figure 5 depicts the differentiation in chemical quality, i.e., SSC%, TA%, and SSC/TA ratio, as a function of storage duration in days for 'Florida Prince' peach. Evidently, SSC% increased significantly in the control fruit during the storage period. However, the CaNP–AA at 9 mM treatments presented a different trend. We observed the lowest changes in SSC% compared to untreated and treated fruit. The chemical quality elements revealed a significant interaction ($p < 0.001$) when storage time (days) and CaNP–AA treatments were examined.

The chemical quality results for fruit treated with the control treatment showed a gradual increase in SSC% and the SSC/TA ratio throughout the 30 days. Nevertheless, reductions in total TA% throughout storage duration in fruit treated with 9 mM CaNP–AA were seen. This produced the lowest changes in both SSC and the SSC/TA ratio throughout the cold storage period compared with other treatments and the initial values at harvest time, with 11.82% SSC and an SSC/TA ratio of 12.23%. However, a stable TA value (0.960%) was maintained on the 30th day of the storage period compared with the initial value (1.016%) at harvest time.

3.4. Fruit Pigments (Anthocyanin and Carotene) and Fruit Firmness (N)

Figure 6 displays the variation in fruit pigment (i.e., anthocyanin (peel; mg 100 g^{-1} FW) and carotene (pulp; μg 100 g^{-1} FW)) and firmness (N) as a function of storage duration in days for 'Florida Prince' peach. Evidently, both pigments decreased significantly in all CaNP–AA mixtures and control fruit throughout the storage period, as did fruit firmness. The 9 mM CaNP–AA treatment significantly reduced the fruit pigment degradation and

firmness throughout 30 days compared with the initial value at harvest time. Fruit pigments on the 30th day were 14.06 mg 100 g^{-1} FW and 1.94 μg 100 g^{-1} FW compared with the initial values of 14.67 mg 100 g^{-1} FW and 2.00 μg 100 g^{-1} FW, respectively. Furthermore, fruit firmness was recorded at 61.87 N, compared with an initial value of 63.26 N.
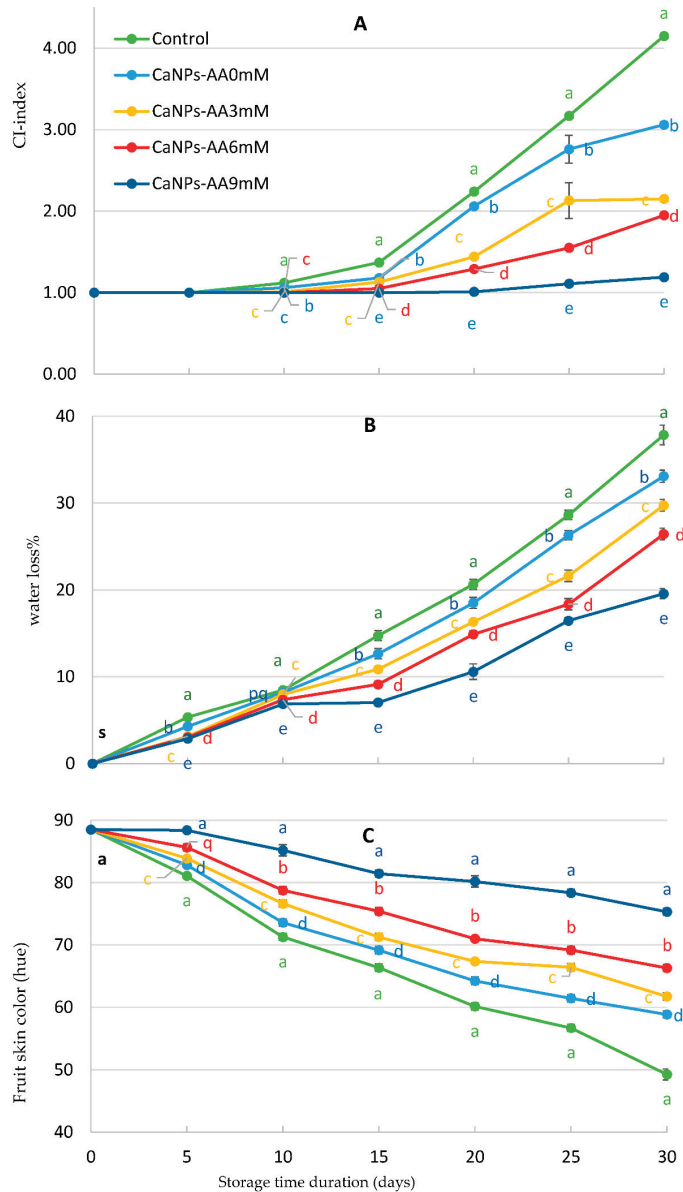
Figure 4. The chilling injury index (**A**), water loss percentage (**B**), and fruit skin color (hue) (**C**) of 'Florida Prince' peaches immersed in CaNPs mixed with ascorbic acid at different concentrations (0, 3, 6, and 9 mM) and stored at a low temperature (4 °C and 95% RH) for 30 days. Error bars represent standard errors and different letters indicate significant differences at $p \leq 0.05$ among treatments for each storage period.
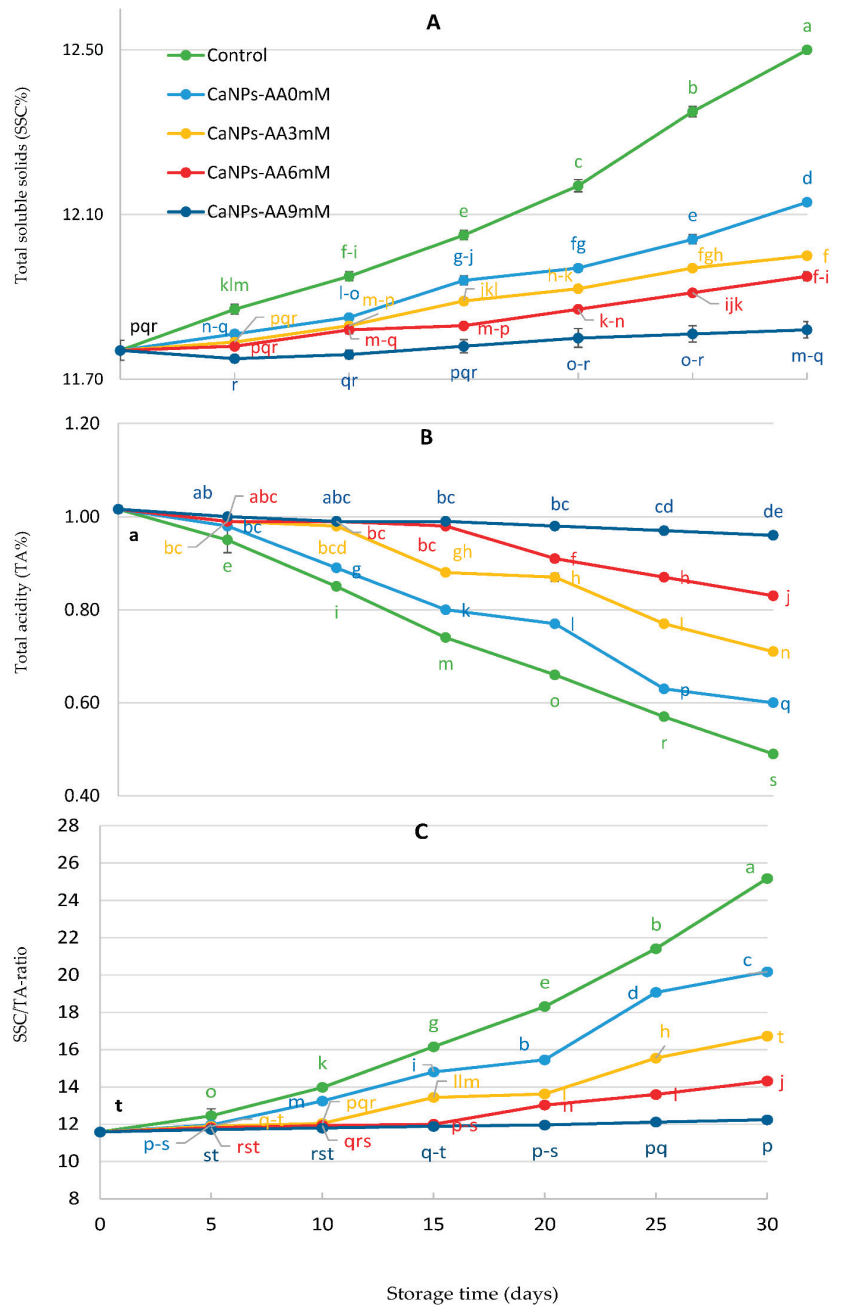
Figure 5. The total soluble solid content (SSC%) (**A**), total acidity percentage (TA%) (**B**), and SSC/TA ratio (**C**) of 'Florida Prince' peaches immersed in CaNPs mixed with ascorbic acid at different concentrations (0, 3, 6, and 9 mM) and stored at a low temperature (4 °C and 95% RH) for 30 days. Error bars represent standard errors and different letters indicate significant differences at $p \leq 0.05$ among treatments for each storage period.
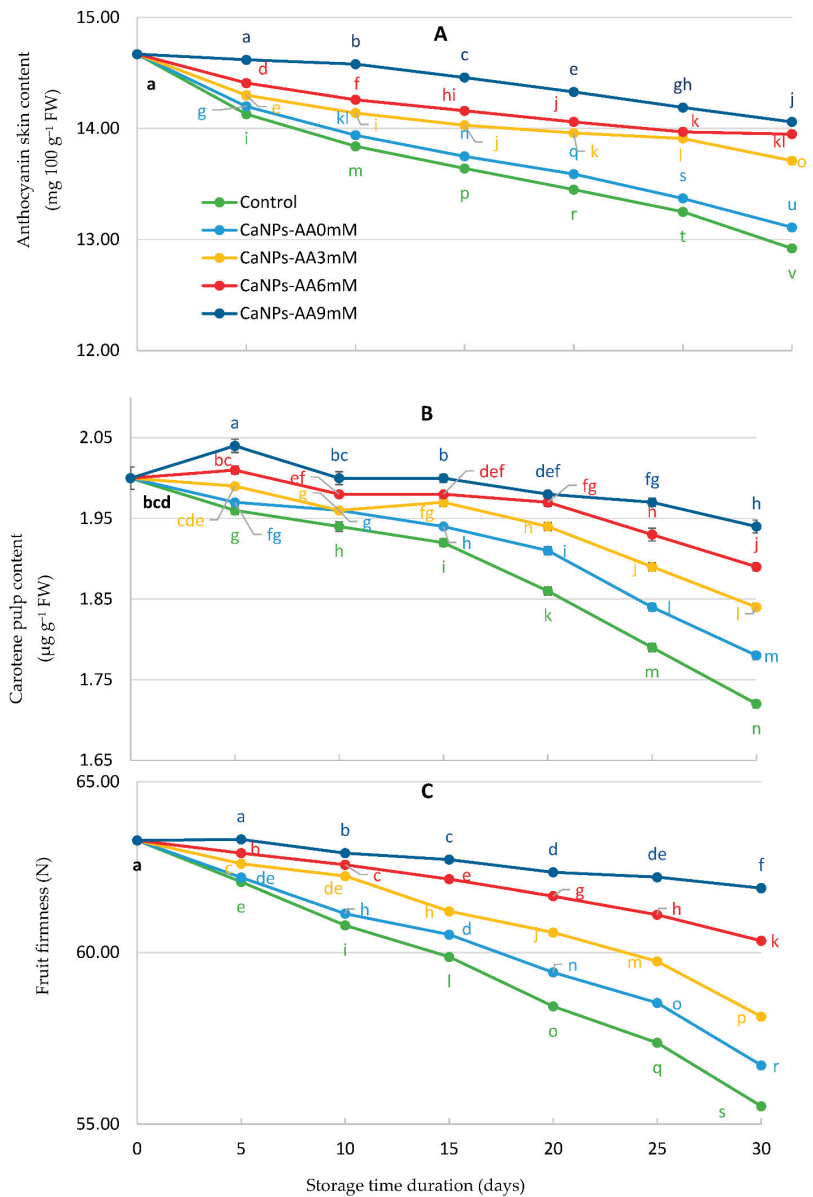
Figure 6. Fruit pigments (i.e., anthocyanin (**A**) and carotene (**B**)) and fruit firmness (**C**) of 'Florida Prince' peaches immersed in CaNPs mixed with ascorbic acid at different concentrations (0, 3, 6, and 9 mM) and stored at a low temperature (4 °C and 95% RH) for 30 days. Error bars represent standard errors and different letters indicate significant differences at $p \leq 0.05$ among treatments for each storage period.

3.5. Antioxidant Enzyme Activity (AEA)

Figure 7 displays the antioxidant enzyme activities (AEAs) as a function of storage time in weeks. Apparently, the AEAs displayed a significant interaction at 5% when the CaNP–AA treatments and storage time duration (days) were considered as an experimental factor.
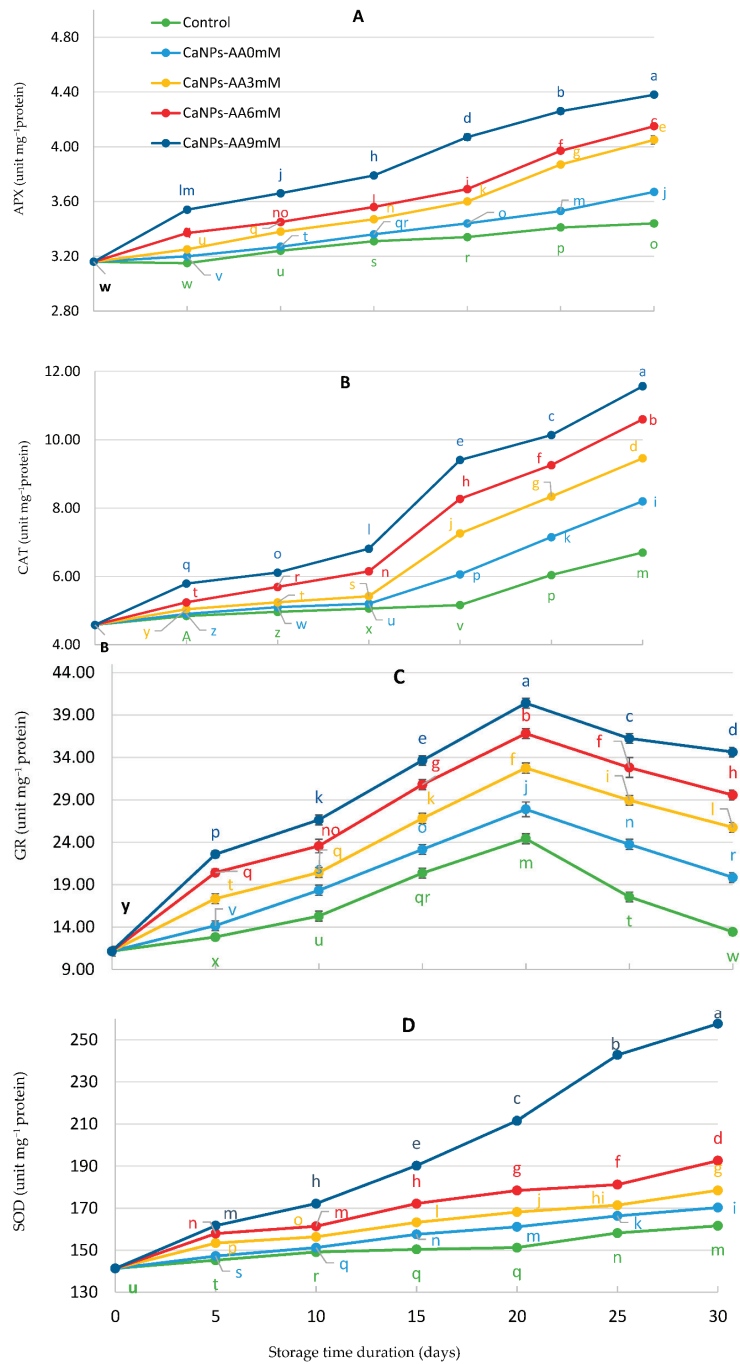
Figure 7. The AEAs, such as APX (**A**), CAT (**B**), GR (**C**), and SOD (**D**), of 'Florida Prince' peaches immersed in CaNPs mixed with ascorbic acid at different concentrations (0, 3, 6, and 9 mM) and stored at a low temperature (4 °C and 95% RH) for 30 days. Error bars represent standard errors and different letters indicate significant differences at $p \leq 0.05$ among treatments for each storage period.

The AEAs continued to increase differently until the end of the storage period. The changes in overall levels of AEAs for all treatments increased slightly throughout the first 20 days, then they became different up to the end of the cold storage period for all treatments.

However, the GR activity increased up to the 20th day and then declined in all treatments until the end of the experiment. Obviously, exogenous treatment with 9 mM CaNP–AA increased the AEAs in peach. The activity increased (APX, 4.38; CAT, 11.57; SOD 257.68) until the 30th day, but GR (40.40) increased up to the 20th day and then declined (34.63 units g^{-1} protein) until the end of the experiment.

3.6. Estimation of Malondialdehyde (MDA), Ion Leakage (IL%), Ethylene Production, and Respiration Rate

In peach pulp, MDA accumulation and IL% significantly ($p > 0.01$) and dramatically increased throughout the duration of storage, dependent on the CaNP–AA treatment (Figure 8). A significant interaction among storage factors, storage duration (weeks), and CaNP–AA treatment was considered as an experimental factor. MDA content and IL% clearly increased in the CaNP–AA treatments compared with the initial values. Furthermore, differences among the CaNP–AA treatments appeared on the 10th day and became more pronounced during the storage duration until the end of the experiment. Certainly, the lowest values of MDA and IL% were identified in peaches treated with 9 mM CaNP–AA (MDA = 0.24 and IL = 23.37%) on the 30th day of the storage period compared with other treatments. However, the control treatment exhibited the highest accumulation of MDA (0.44) and IL (44.85%) in the same time interval. Moreover, the ethylene evolution and respiration rate in peach increased gradually and independently in the CaNP–AA treatments up to the maximum peak on the 10th and 5th days of storage. Both then declined until the end of storage time. However, it can be seen in Figure 5 that respiration showed an increase in CO$_2$ rate until the end of storage. The increases in CO$_2$ were independent and based on the CaNP–AA treatments. However, lower ethylene production and CO$_2$ over the 30 days was observed in the control.
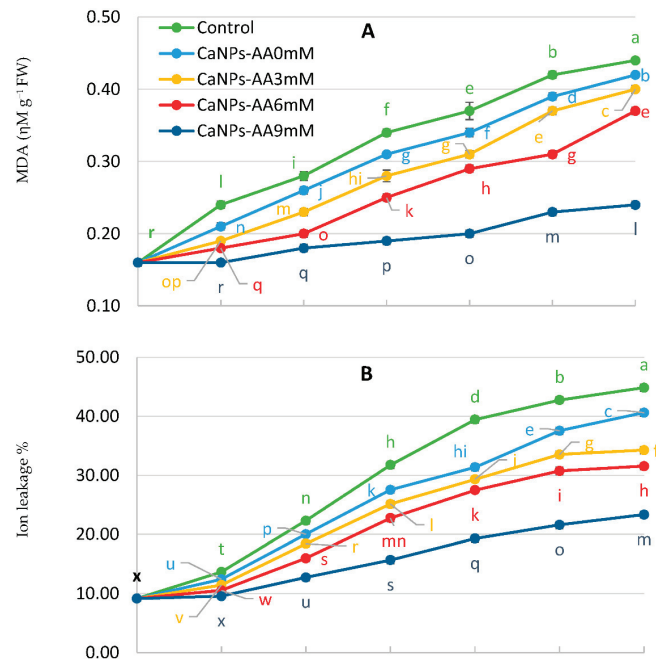
Figure 8. *Cont.*
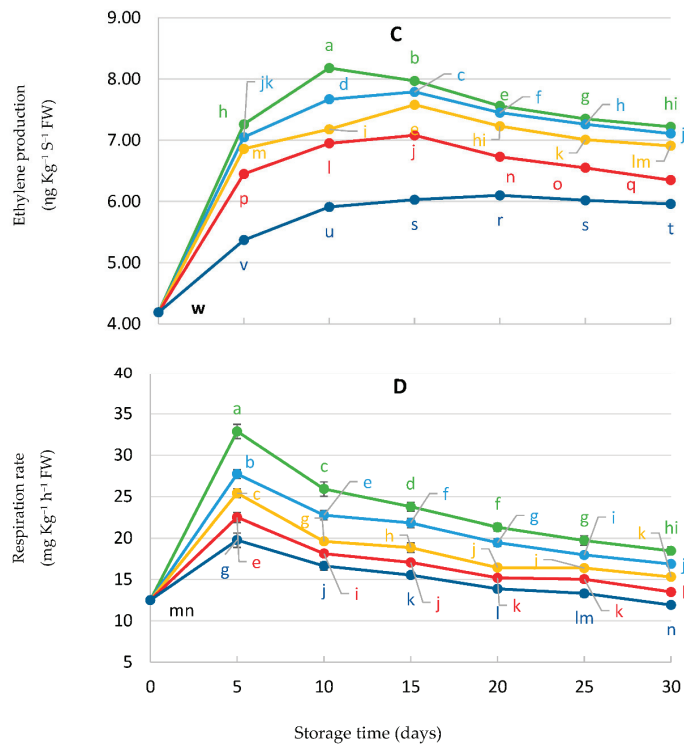
Figure 8. MDA (**A**), IL% (**B**), ethylene (**C**), and respiration rate (**D**) of 'Florida Prince' peaches immersed in CaNPs mixed with ascorbic acid at different concentrations (0, 3, 6, and 9 mM) and stored at a low temperature (4 °C and 95% RH) for 30 days. Error bars represent standard errors and different letters indicate significant differences at $p \leq 0.05$ among treatments for each storage period.

3.7. H_2O_2 and $O_2^{\bullet-}$ Production and DPPH Reduction

Differences in H_2O_2 and $O_2^{\bullet-}$ generation rates and antioxidant performance (utilizing the DPPH technique) could be seen as a function of time in days. The parameters produced a significant effect ($p < 0.003$) when the storage time and CaNP–AA applications were used as experimental factors (Figure 9).

H_2O_2 and $O_2^{\bullet-}$ generation in peach pulp increased continuously from the time of fruit collection up to the 30th day of the experiment. Consequently, increases and differences were independently associated with CaNP–AA applications on the 30th day of storage time. The 9 mM CaNP–AA treatment produced the lowest H_2O_2 (0.12 mM min^{-1} g^{-1} FW) and $O_2^{\bullet-}$ (0.34 mM g^{-1} FW) amounts throughout the storage period compared with different CaNP–AA treatments on the 30th day. The assessment of AEAs by utilizing the DPPH decrease demonstrated that their activity improved spontaneously and slowly in all CaNP–AA treatments throughout the storage period. In any case, the control displayed the greatest reduction in DPPH (41.86%) on the 30th day of the trial.
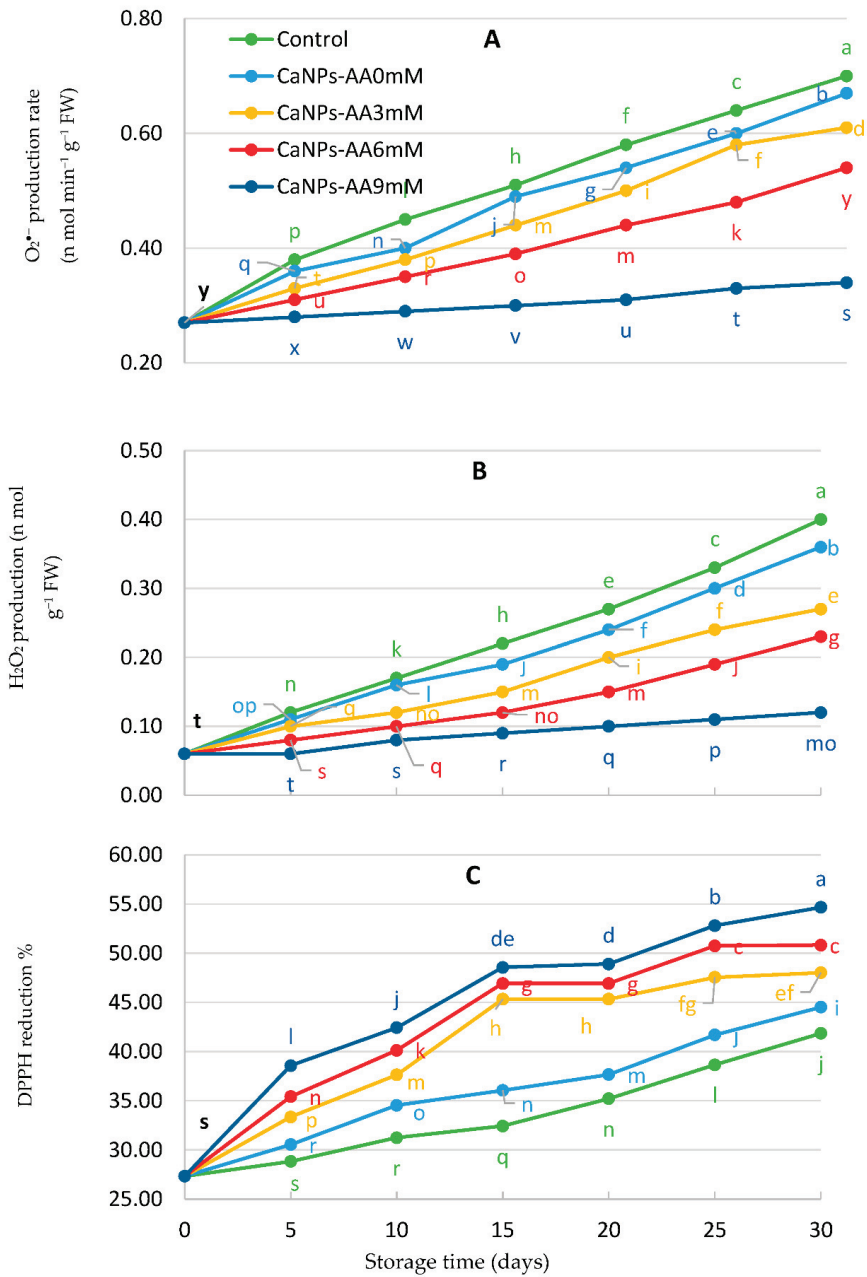
Figure 9. H_2O_2 (**A**), $O_2^{\bullet-}$ (**B**) production rates, and DPPH reduction (**C**) in 'Florida Prince' peaches immersed in CaNPs mixed with ascorbic acid at different concentrations (0, 3, 6, and 9 mM) and stored at a low temperature (4 °C and 95% RH) for 30 days. Error bars represent standard errors and different letters indicate significant differences at $p \leq 0.05$ among treatments for each storage period.

4. Discussion

This study examined the effectiveness of CaNP–AA treatment for reducing chilling injury in peaches during cold storage. Chilling injury has been recognized as a physiological disorder caused by low temperatures [44]. A variation was observed during 30 days of cold storage stress in peach fruit. Usually, low temperatures generate reactive oxygen species (ROS) during long-term cold storage [43]. The most abundant ROS produced is the hydroxyl radical ($\cdot$OH), which reacts with lipids and proteins of the plasma cell membrane [45]. Over a long period of cold storage, malondialdehyde (MDA) and protein carbonyl groups (PCG) terminate the lipid and protein of the cell membrane [46]. Consequently, cell membrane structure and function are lost [13] and cell death occurs [15]. With cell death, CI symptoms appear [45] via an equilibrium between ROS formation and antioxidant system activity under low temperatures [15,19]. Our results confirmed that the most severe symptoms of CI were observed in untreated fruit compared with CaNP–AA treatments. We observed that the 9 mM CaNP–AA treatment minimized CI symptoms and water loss. These results were due to the efficacy of AA at 9 mM for quenching ROS formation and preventing cell damage [15,47]. The reduction in CI incidence was reflected in fruit color (hue angle) (Figure 4). This may demonstrate that the presence of AA in combination with CaNP application preserved the water content during cold storage [48]. The results are consistent with other previous studies on peaches [49,50], which confirmed the positive influence of CaNP–AA treatment on minimizing chilling injury symptoms and improving fruit quality during cold storage.

In the present study, 9 mM CaNP–AA produced fewer changes in SSC and TA than other treatments (Figure 5). The SSC and TA remained at the same level as the initial values, which could be due to the role of AA as an antioxidant that decreased the oxidation reaction [51]. The SSC/TA ratio is an indicator of the good taste and flavor of peach fruit [52].

The changes in both SSC% and TA% in stressed peach fruit during cold storage after CaNP–AA treatment can be attributed to the conversion of organic acids to sugar [53]. Moreover, the highest SSC% seen throughout the storage period may have occurred as a consequence of decreasing AA and acidity under prolonged storage [17]. Furthermore, it could be associated with increases in starch enzyme activities that change organic acids to sugar, as described previously [54]. Similar results were observed in sweet orange fruit [55], lime [56], and pawpaw [57] stored at low temperatures.

The results revealed that fruit treated with 9 mM CaNP–AA maintained better fruit pigmentation and fruit firmness than the control (Figure 6). Based on the fruit quality data, it is clear that with the 9 mM L^{-1} CaNP–AA treatment, no adverse effects were observed in the fruit. However, higher AA doses (9 mM L^{-1}) were more effective at reducing the decline in peach quality. Thus, the 9 mM CaNP–AA application maintained the fruit pigments and firmness of peach fruit under cold storage. These findings may be linked to the physiological roles of calcium and AA in the CaNP–AA mixture. Calcium is essential for maintaining cell wall stability and integrity, as well as determining fruit quality [58]. Calcium has been demonstrated to be effective at preserving the quality of fruit [58], increasing antioxidant capacity [59], preventing softening [58], alleviating chilling injury [60], controlling postharvest decay [61], and delaying the fruit ripening process [62]. Previously, calcium lactate had better textural and sensory properties on peaches than calcium chloride and calcium propionate [58]. Supplementing CaNPs with AA provided additional benefits, such as quenching ROS [63], maintaining fruit quality throughout cold storage [64], delaying fruit ripening, and reducing microbial infection [65]. These results are in line with the findings of Campos-Vargas et al. [66] on 'O'Henry' peaches.

In our study, APX, CAT, GR, and SOD activities were more strongly activated in 9 mM CaNP–AA-treated fruit. According to several reports, APX donates an electron to free radicals and converts H_2O_2 to oxygen and water, thereby mitigating oxidative damage [67]. The activity of the APX enzyme is directly proportional to the amount of AA [68]. Thus, the increased activity in 9 mM CaNP–AA-treated peaches could be a result of stable AA

concentrations in the fruit. Additionally, findings have shown that both CAT and SOD are essential enzymes for reducing ROS damage in litchi fruit [69]. Reduced CAT and SOD activity are typically associated with increased fruit senescence [70]. The increased CAT and SOD activity may be attributed to the fruit treated with 9 mM CaNP–AA producing fewer $O_2^{\bullet-}$ and H_2O_2 radicals. Their activities were enhanced with CaNP–AA treatments based on the concentration of AA. Certain differences in AEAs among the CaNP–AA applications can be revealed. The presence of AA in combination with CaNP mixture at a high concentration (9 mM) improved AEAs during cold storage. The CaNPs also increased AA to quench ROS formation throughout storage [71]. However, the AA works indirectly as a quencher of ROS [27]. Moreover, AA might be forced to balance the production of ROS and AEAs [19]. Hence, AA can be used as a stabilizer of the network of AEAs [15]. The results are in line with other studies conducted on peach [49,72], persimmon fruit [73], and banana [44].

Calcium (Ca^{2+}) is an essential mineral for fruit and plays an important role in forming cell walls and membranes [74]. A second messenger in plant signal transduction, Ca^{2+} is implicated in stress responses [75]. Furthermore, different calcium-binding proteins perceive transitory increases in cytosolic Ca^{2+} under cold stress and trigger varied physiological responses [76]. Calcium in the form of $CaCl_2$ treatment reduced peel browning caused by freezing injury in pear fruit by inhibiting membrane lipid peroxtion and increasing SOD activity and expression [77]. It reduced chilling injury symptoms in winter jujube fruit [78]. By modulating SOD, POD, CAT, and the AsA-GSH cycle, $CaCl_2$ increased chilling tolerance in green peppers [79]. A previous study on loquat fruit found that $CaCl_2$ treatment increased cold tolerance by regulating energy metabolism and accumulating osmotic substances [72,80].

In this work, MDA accumulation was the most prevalent side effect of lipid peroxidation, a process that can cause cellular membrane damage [81]. Elevated ROS levels can lead to more lipid peroxidation, leading to damaged membranes and decreased storage capacity [82]. Due to the reduction in oxidative damage and senescence, 9 mM CaNP–AA-treated peaches showed reduced MDA and IL% concentrations. CaNPs were paired with AA to minimize ethylene and respiration. In this context, further investigations are required to determine how these two methods achieved such positive results.

The results were obtained due to the decline in oxygen-consuming respiration under cold storage, which diminishes both H_2O_2 and $O_2^{\bullet-}$ production [83]. Furthermore, the increase in AEAs (Figure 4) may diminish both the production of H_2O_2 and $O_2^{\bullet-}$ correlated with improved SOD activity, as indicated by Lo'ay and El-Khateeb [17]. The relationship between both CAT and APX in the network, besides other antioxidants [15], could be strongly connected to the quenching of both H_2O_2 and $O_2^{\bullet-}$ or the minimization of the effects of both [41].

5. Conclusions

CI significantly impairs the storage of peach fruits, as measured by fruit loss over the course of a cold storage period. The 9 mM CaNP–AA treatment clearly ameliorated CI in peach fruit by improving AEAs and minimizing ion leakage. Thus, treatment with AA at 9 mM L^{-1} together with CaNPs suppressed the incidence of CI during cold stress, particularly in terms of ROS. It also activated antioxidant enzymes, which was reflected by the low MDA content throughout the cold storage period. Our results suggest that a mixture of AA with CaNPs could be used as a tool adjuvant to maintain fruit quality traits under cold storage.

Conflicts of Interest: The authors declare no conflict of interest.

References

1. El-Boray, M.S.; Shalan, A.M.; Khouri, Z.M. Performance of Peach Trees cv. Florida Prince under Different Foliar Concentrations of NPK-humate in Presence or Absence of Adjuvants. *Trends Hortic. Res.* **2016**, *6*, 5–17.
2. FAOSTAT. *Peach Production in Egypt*; FAO: Rome, Italy, 2017.
3. Jin, P.; Zhu, H.; Wang, L.; Shen, T.; Zheng, Y. Oxalic acid alleviates chilling injury in peach fruit by regulating energy metabolism and fatty acid contents. *Postharvest Biol. Technol.* **2014**, *161*, 87–93. [CrossRef]
4. Wang, C.Y. *Chilling Injury of Horticultural Crops*; CRC Press: Boca Raton, FL, USA, 1990.
5. Lurie, S.; Crisosto, C.H. Chilling injury in peach and nectarine. *Postharvest Biol. Technol.* **2005**, *37*, 195–208. [CrossRef]
6. Brummell, D.A.; Dal Cin, V.; Crisoto, C.H.; Labavith, J.M. Cell wall metabolism during the development of chilling injury in cold-stored peach fruit: Association of mealiness with arrested disassembly of cell wall pectins. *J. Exp. Bot.* **2004**, *55*, 2041–2052. [CrossRef] [PubMed]
7. Cao, S.; Hu, Z.; Zheng, Y.; Lu, B. Synergistic effect of heat treatment and salicylic acid on alleviating internal browning in cold-stored peach fruit. *Postharvest Biol. Technol.* **2010**, *58*, 93–97. [CrossRef]
8. Fernandez-Trujillo, J.P.; Martinez, J.A.; Artes, F. Modified atmosphere pack affect the incidence of cold storage disorder and keep 'flat' peach quality. *Food Res. Int.* **1998**, *31*, 571–579. [CrossRef]
9. Ebel, R.C.; Woods, F.M.; Himelrick, D. Effect of UV-C on ripening and postharvest quality of peach. *HortScience* **1999**, *34*, 504. [CrossRef]
10. Feng, L.; Zheng, Y.H.; Zhang, Y.F.; Wang, F.; Zhang, L.; Lu, Z.X. Methyl jasmonate reduces chilling injury and maintains postharvest quality in peaches. *Agric. Sci. China* **2003**, *11*, 1246–1252.
11. Girardi, C.L.; Corrent, A.R.; Lucchetta, L.; Zanuzo, M.R.; Da Costa, T.S.; Brachmann, A.; Twymand, R.M.; Nora, F.R.; Nora, L.; Silva, J.A.; et al. Effect of ethylene, intermittent warming and controlled atmosphere on postharvest quality and occurrence of woolliness in peach (*Prunus persic* cv. Chiripa) during cold storage. *Postharvest Biol. Technol.* **2005**, *38*, 25–33. [CrossRef]
12. Wang, L.; Chen, S.; Kong, W.; Li, S.; Archbold, D.D. Salicylic acid pretreatment alleviates chilling injury and affects the antioxidant system and heat shock proteins of peaches during cold storage. *Postharvest Biol. Technol.* **2006**, *41*, 244–251. [CrossRef]
13. Lo'ay, A.A.; Ameer, N.M. Performance of calcium nanoparticles blending with ascorbic acid and alleviation internal browning of 'Hindi Be-Sennara' mango fruit at a low temperature. *Sci. Hortic.* **2019**, *254*, 199–207. [CrossRef]
14. Wismer, W.V.; Worthing, W.M.; Yada, R.Y.; Marangoni, A.G. Membrane lipid dynamics and lipid peroxidation in the early stages of low-temperature sweetening in tubers of Solanum tuberosum. *Physiol. Plant.* **1998**, *102*, 396–410. [CrossRef]
15. Foyer, C.H.; Ruban, A.V.; Noctor, G. Viewing oxidative stress through the lens of oxidative signaling rather than damage. *Biochem. J.* **2017**, *474*, 877–883. [CrossRef] [PubMed]
16. Hossain, Z.; Nouri, M.Z.; Komatsu, S. Plant Cell Organelle Proteomics in Response to Abiotic Stress. *J. Proteome Res.* **2012**, *11*, 37–48. [CrossRef] [PubMed]
17. Lo'ay, A.A.; El-Khateeb, A.Y. Antioxidant enzyme activities and exogenous ascorbic acid treatment of 'Williams' banana during long-term cold storage stress. *Sci. Hortic.* **2018**, *234*, 210–219. [CrossRef]
18. Purvis, A.C. Regulatin of oxidative stress in horticultural crops. *HortiScience* **2004**, *39*, 930–932. [CrossRef]
19. Foyer, C.H.; Noctor, G. Oxidant and antioxidant signalling in plants: A re-evaluation of the concept of oxidative stress in a physiological context. *Plant Cell Environ.* **2005**, *28*, 1056–1071. [CrossRef]
20. Manganaris, G.A.; Vasilakakis, M.; Diamantidis, G.; Mignani, I. Effect of calcium additives on physicochemical aspects of cell wall pectin and sensory attributes of canned peach (*Prunus persica Batsch* cv Andross). *J. Sci. Food Agric.* **2005**, *85*, 1773–1777. [CrossRef]
21. Fan, X.; Niemera, B.A.; Matthheis, J.P.; Zhuang, H.; Olson, D.W. Quality of fresh-cut apple slices as affected by low-dose ionizing radiation and calcium ascorbate treatment. *J. Food Sci.* **2005**, *70*, 143–149. [CrossRef]
22. Luna-Guzman, I.; Cantwell, M.; Barrett, D.M. Fresh-cut cantaloupe: Effects of calcium chloride dips and heat treatments on firmness and metabolic activity. *Postharvest Biol. Technol.* **1999**, *17*, 201–213. [CrossRef]
23. Mishra, S. *Calcium Chloride Treatment of Fruits and Vegetables*; Tetre Technologies Inc.: The Woodlands, TX, USA, 2002.
24. Yugandhar, P.; Savithramma, N. Biosynthesis, characterization and antimicrobial studies of green synthesized silver nanoparticles from fruit extract of Syzygium alternifolium (Wt.) Walp. an endemic, endangered medicinal tree taxon. *Appl. Nanosci.* **2016**, *6*, 223–233. [CrossRef]
25. Schirra, M. Behaviour of 'star Ruby' grapefruit under chilling and non-chilling storage temperature. *Postharvest Biol. Technol.* **1992**, *2*, 315–327. [CrossRef]

26. Khojastehnazhand, M.; Omid, M.; Tabatabaeefar, A. Development of a lemon sorting system based on color and size. *Afr. J. Plant Sci.* **2010**, *4*, 122–127.
27. Lo'ay, A.A.; Dawood, H.D. Active chitosan/PVA with ascorbic acid and berry quality of 'Superior seedless' grapes. *Sci. Hortic.* **2017**, *224*, 286–292. [CrossRef]
28. Mehrtens, F.; Kranz, H.; Bednarek, P.; Weisshaar, B. The Arabidopsis Transcription Factor MYB12 Is a Flavonol-Specific Regulator of Phenylpropanoid Biosynthesis. *Plant Physiol.* **2005**, *138*, 1083–1096. [CrossRef] [PubMed]
29. Mínguez-Mosquera, M.I.; Jarén-Galán, M.; Hornero-Méndez, D.; Garrido-Fernández, J.; Gallardo-Guerrero, M.L.; Gandul-Rojas, B. Decoloration of vegetable oils and oleoresins with recovery of unaltered pigments. *J. Am. Oil Chem. Soc.* **1991**, *68*, 809–813. [CrossRef]
30. Biehler, E.; Mayer, F.; Hoffmann, L.; Krause, E.; Bohn, T. Comparison of 3 Spectrophotometric Methods for Carotenoid Determination in Frequently Consumed Fruits and Vegetables. *J. Food Sci.* **2010**, *75*, C55–C61. [CrossRef] [PubMed]
31. Wang, J.; Teng, B.; Yu, Y. The firmness detection by excitation dynamic characteristics for peach. *Food Control* **2006**, *17*, 353–358. [CrossRef]
32. Kar, M.; Mishra, D. Catalase, peroxidase, and polyphenoloxidase activities during rice leaf senescence. *Plant Physiol.* **1976**, *57*, 315–319. [CrossRef]
33. Asada, K. Assay of ascorbate-specific peroxidase. *Methods Enzymol.* **1984**, *105*, 427–429.
34. Smith, I.S.; Vierheller, T.L.; Thorne, C.A. Assay of glutathione reductase in crude tissue homogenates using 5,5%-dithiobis (2-nitrobenzoic acid). *Anal. Biochem.* **1988**, *175*, 408–413. [CrossRef]
35. Carlberg, I.; Mannervik, B. Glutathione reductase. *Methods Enzymol.* **1985**, *113*, 484–490.
36. Oberley, L.W.; Spitz, D.R. Nitroblue tetrazolium. In *Handbook of Methods for Oxygen Radical Research*; Greenwald, R.A., Ed.; CRC Press: Boca Raton, FL, USA, 1986.
37. Bradford, M.M. A rapid and sensitive method for the quantitation of microgram quantities of protein utilizing the principle of protein-dye binding. *Anal. Biochem.* **1976**, *72*, 248–254. [CrossRef]
38. Iturbe-Ormaetxe, I.; Escuredo, P.R.; Arrese-Igor, C.; Becana, M. Oxidative damage in pea plants exposed to water deficit or paraquat. *Plant Physiol.* **1998**, *116*, 173–181. [CrossRef]
39. Lo'ay, A.A.; Taha, N.A.; El-Khateeb, Y.A. Storability of 'Thompson Seedless' grapes: Using biopolymer coating chitosan and polyvinyl alcohol blending with salicylic acid and antioxidant enzymes activities during cold storage. *Sci. Hortic.* **2019**, *249*, 314–321. [CrossRef]
40. Lo'ay, A.A. Chilling Injury in Mangoes. Ph.D. Thesis, Wageningen University, Wageningen, The Netherlands, 2005.
41. Yang, H.; Wu, F.; Cheng, J. Reduced chilling injury in cucumber by nitricoxide and the antioxidant response. *Food Chem.* **2011**, *127*, 1237–1242. [CrossRef]
42. Xu, M.; Dong, J.; Zhang, M.; Xu, X.; Sun, L. Cold-induced endogenous nitric oxide generation plays a role in chilling tolerance of loquat fruit during postharvest storage. *Postharvest Biol. Technol.* **2012**, *65*, 5–12. [CrossRef]
43. Yen, G.C.; Chen, H.Y. Antioxidant activity of various tea extracts in relation to their antimutagenicity. *J. Agric. Food Chem.* **1995**, *43*, 27–32. [CrossRef]
44. Chen, L.-L.; Shan, W.; Cai, D.-L.; Chen, J.-Y.; Lu, W.-J.; Su, X.-G.; Kuang, J.-F. Postharvest application of glycine betaine ameliorates chilling injury in cold-stored banana fruit by enhancing antioxidant system. *Sci. Hortic.* **2021**, *287*, 110264. [CrossRef]
45. Lo'ay, A.A.; Doaa, M.H. The potential of vine rootstocks impacts on 'Flame Seedless' bunches behavior under cold storage and antioxidant enzyme activity performance. *Sci. Hortic.* **2020**, *260*, 108844. [CrossRef]
46. Hodges, D.M.; Lester, G.E.; Munro, K.D.; Toivonen, P.M.A. Oxidative stress: Importance for postharvest quality. *HortScience* **2004**, *39*, 924–929. [CrossRef]
47. Wang, C.Y. Reducing chilling injury and maintaining quality of horticultural crops with natural products and their derivatives. *Acta Hortic.* **2006**, *712*, 285–290. [CrossRef]
48. Kondo, S.; Kittikorn, M.; Kanlayanarat, S. Preharvest antioxidant activities of tropical fruit and the effect of low temperature storage on antioxidants and jasmonates. *Postharvest Biol. Technol.* **2005**, *36*, 309–318. [CrossRef]
49. Liu, H.; Jiang, W.; Cao, J.; Ma, L. A combination of 1-methylcyclopropene treatment and intermittent warming alleviates chilling injury and affects phenolics and antioxidant activity of peach fruit during storage. *Sci. Hortic.* **2018**, *229*, 175–181. [CrossRef]
50. Zhu, L.Q.; Zhou, J.; Zhu, S.H. Effect of a combination of nitric oxide treatment and intermittent warming on prevention of chilling injury of 'Feicheng' peach fruit during storage. *Food Chem.* **2010**, *121*, 165–170. [CrossRef]
51. Giménez, M.; Olarte, C.; Sanz, S.; Lomas, C.; Echávarri, J.F.; Ayala, F. Influence of Packaging Films on the Sensory and Microbiological Evolution of Minimally Processed Borage (*Borrago officinalis*). *J. Food Sci.* **2003**, *68*, 1051–1058. [CrossRef]
52. De Reuck, K.; Sivakumar, D.; Korsten, L. Integrated application of 1-methylcyclopropene and modified atmosphere packaging to improve quality retention of litchi cultivars during storage. *Postharvest Biol. Technol.* **2009**, *52*, 71–77. [CrossRef]
53. Baldwin, E.A.; Niesperos, M.O.; Shaw, P.E.; Burns, J.K. Effect of coatings and prolonged storage conditions on fresh orange flavour volatiles, degrees brix and ascorbic acid levels. *J. Agric. Food Chem.* **1995**, *43*, 1321–1331. [CrossRef]
54. Kader, A.A. *Postharvest Technology of Horticulture Crops*, 3rd ed.; University of California Agriculture & Natural Resources: Irvine, CA, USA, 2002.
55. Shahid, M.N.; Abbasi, N.A. Effect of bee wax coatings on physiological changes in fruits of sweet orange CV. "Blood Red". *Sarhad J. Agric.* **2011**, *27*, 385–394.

56. Verma, P.; Dashora, L.K. Post-harvest physiconutritional changes in Kagzi Limes (*Citrus aurantifolia* S.) treated with selected oil emulsions and diphenyl. *Plant Food Hum. Nutr.* **2000**, *55*, 279–284. [CrossRef]
57. Galli, F.; Archbold, D.D.; Pomper, K.W. Pawpaw fruit chilling injury and antioxidant protection. *J. Am. Soc. Hortic. Sci.* **2009**, *134*, 466–471. [CrossRef]
58. Wang, Y.; Long, L.E. Physiological and biochemical changes relating to postharvest splitting of sweet cherries affected by calcium application in hydrocooling water. *Food Chem.* **2015**, *181*, 241–247. [CrossRef] [PubMed]
59. Naser, F.; Rabiei, V.; Razavi, F.; Khademi, O. Effect of calcium lactate in combination with hot water treatment on the nutritional quality of persimmon fruit during cold storage. *Sci. Hortic.* **2018**, *233*, 114–123. [CrossRef]
60. Gerasopoulos, D.; Drogoudi, P.D. Summer-pruning and preharvest calcium chloride sprays affect storability and low temperature breakdown incidence in kiwifruit. *Postharvest Biol. Technol.* **2005**, *36*, 303–308. [CrossRef]
61. Sugar, D.; Basile, S.R. Orchard calcium and fungicide treatments mitigate effects of delayed postharvest fungicide applications for control of postharvest decay of pear fruit. *Postharvest Biol. Technol.* **2011**, *60*, 52–56. [CrossRef]
62. Madani, B.; Mohamed, M.T.M.; Watkins, C.B.; Kadir, J.; Awang, Y.; Shojaei, T.R. Preharvest calcium chloride sprays affect ripening of Eksotika II'papaya fruits during cold storage. *Sci. Hortic.* **2014**, *171*, 6–13. [CrossRef]
63. Fang, T.; Zhen, Q.; Liao, L.; Owiti, A.; Zhao, L.; Korban, S.S.; Han, Y. Variation of ascorbic acid concentration in fruits of cultivated and wild apples. *Food Chem.* **2017**, *225*, 132–137. [CrossRef]
64. Lin, L.; Li, Q.P.; Wang, B.G.; Cao, J.K.; Jiang, W.B. Inhibition of core browning in 'Yali' pear fruit by post-harvest treatment with ascorbic acid. *J. Hortic. Sci. Biotechnol.* **2007**, *82*, 397–402. [CrossRef]
65. Sogvar, O.B.; Koushesh Saba, M.; Emamifar, A. Aloe vera and ascorbic acid coatings maintain postharvest quality and reduce microbial load of strawberry fruit. *Postharvest Biol. Technol.* **2016**, *114*, 29–35. [CrossRef]
66. Campos-Vargas, R.; Becerra, O.; Baeza-Yates, R.; Cambiazo, V.; González, M.; Meisel, L.; Orellana, A.; Retamales, J.; Silva, H.; Defilippi, B.G. Seasonal variation in the development of chilling injury in 'O'Henry' peaches. *Sci. Hortic.* **2006**, *110*, 79–83. [CrossRef]
67. Gupta, A.S.; Webb, R.P.; Holaday, A.S.; Allen, R.D. Overexpression of Superoxide Dismutase Protects Plants from Oxidative Stress (Induction of Ascorbate Peroxidase in Superoxide Dismutase-Overexpressing Plants). *Plant Physiol.* **1993**, *103*, 1067–1073. [CrossRef] [PubMed]
68. Elia, M.R.; Borraccino, G.; Dipierro, S. Soluble ascorbate peroxidase from potato tubers. *Plant Sci.* **1992**, *85*, 17–21. [CrossRef]
69. Duan, X.; Liu, T.; Zhang, D.; Su, X.; Lin, H.; Jiang, Y. Effect of pure oxygen atmosphere on antioxidant enzyme and antioxidant activity of harvested litchi fruit during storage. *Food Res. Int.* **2011**, *44*, 1905–1911. [CrossRef]
70. Ali, S.; Khan, A.S.; Malik, A.U.; Shahid, M. Effect of controlled atmosphere storage on pericarp browning, bioactive compounds and antioxidant enzymes of litchi fruits. *Food Chem.* **2016**, *206*, 18–29. [CrossRef]
71. Rapisarda, P.; Bianco, M.L.; Pannuzzo, P.; Timpanaro, N. Effect of cold storage on vitamin C, phenolics and antioxidant activity of five orange genotypes [*Citrus sinensis* (L.) *Osbeck*]. *Postharvest Biol. Technol.* **2008**, *49*, 348–354. [CrossRef]
72. Hou, Y.; Li, Z.; Zheng, Y.; Jin, P. Effects of CaCl$_2$ Treatment Alleviates Chilling Injury of Loquat Fruit (*Eribotrya japonica*) by Modulating ROS Homeostasis. *Foods* **2021**, *10*, 1662. [CrossRef]
73. Niazi, Z.; Razavi, F.; Khademi, O.; Aghdam, M.S. Exogenous application of hydrogen sulfide and γ-aminobutyric acid alleviates chilling injury and preserves quality of persimmon fruit (*Diospyros kaki*, cv. Karaj) during cold storage. *Sci. Hortic.* **2021**, *285*, 110198. [CrossRef]
74. Hocking, B.; Tyerman, S.D.; Burton, R.A.; Gilliham, M. Fruit Calcium: Transport and Physiology. *Front. Plant Sci.* **2016**, *7*, 569. [CrossRef]
75. Ranty, B.; Aldon, D.; Cotelle, V.; Galaud, J.-P.; Thuleau, P.; Mazars, C. Calcium Sensors as Key Hubs in Plant Responses to Biotic and Abiotic Stresses. *Front. Plant Sci.* **2016**, *7*, 327. [CrossRef]
76. Yuan, P.; Yang, T.; Poovaiah, B.W. Calcium Signaling-Mediated Plant Response to Cold Stress. *Int. J. Mol. Sci.* **2018**, *19*, 3896. [CrossRef]
77. Zhang, L.; Wang, J.-W.; Zhou, B.; Li, G.-D.; Liu, Y.-F.; Xia, X.-L.; Xiao, Z.-G.; Fei, L.; Ji, S.-J. Calcium inhibited peel browning by regulating enzymes in membrane metabolism of 'Nanguo' pears during post-ripeness after refrigerated storage. *Sci. Hortic.* **2019**, *244*, 15–21. [CrossRef]
78. Wei, D.; Zhao, X.-h. Calcium maintained higher quality and enhanced resistance against chilling stress by regulating enzymes in reactive oxygen and biofilm metabolism of Chinese winter jujube fruit. *J. Food Biochem.* **2020**, *44*, 13161. [CrossRef] [PubMed]
79. Zhang, X.; Ma, M.; Ye, B.; Liu, L.; Ji, S. Calcium ion improves cold resistance of green peppers (*Capsicum annuum* L.) by regulating the activity of protective enzymes and membrane lipid composition. *Sci. Hortic.* **2021**, *277*, 109789. [CrossRef]
80. Li, Z.; Wang, L.; Xie, B.; Hu, S.; Zheng, Y.; Jin, P. Effects of exogenous calcium and calcium chelant on cold tolerance of postharvest loquat fruit. *Sci. Hortic.* **2020**, *269*, 109391. [CrossRef]
81. Wang, C.F.; Cheng, Z.M.; Li, Y. Effect of postharvest treatments on physiology and quality of litchi and their economics. *Acta Hortic.* **1996**, *429*, 503–507. [CrossRef]
82. Shewfelt, R.L.; del Rosario, B.A. The role of lipid peroxidation in storage disorders of fresh fruits and vegetables. *HortScience* **2000**, *35*, 575–579. [CrossRef]
83. Tang, T.; Huang, D.W.; Zhou, C.Q.; Li, X.; Xie, Q.J.; Liu, F.S. Molecular cloning and expression patterns of copper/zinc superoxide dismutase and manganese superoxide dismutase in *Musca domestica*. *Gene* **2012**, *505*, 211–220. [CrossRef]

Influence of Solution Combination for Postharvest Treatment Stage on Vase Life of Cut Hydrangea Flowers (*Hydrangea macrophylla* cv. 'Verena')

Haejo Yang [1]**, Sooyeon Lim** [1]**, Ji-Hyun Lee** [1]**, Ji-Weon Choi** [1] **and Il-Sheob Shin** [2,*]

[1] Postharvest Technology Division, National Institute of Horticultural and Herbal Science, RDA, Wanju 55365, Korea; gowh1231@korea.kr (H.Y.); sylim84@korea.kr (S.L.); leejh80@korea.kr (J.-H.L.); jwcnpri@korea.kr (J.-W.C.)

[2] Pear Research Institute, National Institute of Horticultural and Herbal Science, RDA, Naju 58216, Korea

* Correspondence: shinis3@korea.kr

Abstract: Vase life is one of the most important factors that determines the marketability of cut flowers and is greatly affected by the water balance. The vase life of cut hydrangea flowers varies greatly depending on the postharvest solution management. Therefore, this study investigated the vase life of freshly harvested hydrangea (*Hydrangea macrophylla* 'Verena') according to the three types of preservative solutions (tap water (TW), 1% Chrysal Professional III (CPIII), 2% sucrose + 250 mg/L 8-hydroxquinoline + 100 mg/L citric acid (SHQC)) and the combination solutions (pretreatment; TW, 0.1% Chrysal RVB (RVB), Floralife Quick Dip (FQ), transport; TW, CPIII, Floralife Clear (FC), preservative; CPIII, FC) for each distribution stage (pretreatment–transport–consumer). In the preservative comparison experiment, compared with the control, SHQC and CPIII significantly increased the vase life in 2019 (0.7 days, 3.4 days) and 2020 (1.4 days, 3.1 days), respectively. In the comparative experiment, by solution combination, the group (RVB, FQ) using the pretreatment significantly extended the vase life by 5.9 days and 4.6 days compared with the TW. These results confirm the importance of preservative solutions and pretreatment, suggesting that appropriate pretreatment and preservatives should be used to improve the marketability of cut hydrangea flowers.

Keywords: cut flower; preservative solution; pretreatment; transport; sucrose

1. Introduction

Hydrangea (*Hydrangea* spp.) is an ornamental plant widely used in the garden as a potted plant and also for cut flower production. Especially, *Hydrangea macrophylla* is the most cultivated cultivar among the Hydrangea species. Hydrangea inflorescences are classified into two types: hortensia and lace caps, depending on the arrangement of decorative and nondecorative flowers. Hortensia-type hydrangea, which has a high market share in the cut flower market, is classified into two stages: fresh stage and antique stage, depending on the harvest stage [1].

Vase life of cut hydrangea flowers harvested in the fresh stage is usually short, between 7 and 15 days [2]. Vase life is one of the most important quality factors affecting the marketability and customers' satisfaction of cut hydrangea flowers [3]. An important factor in determining the quality of cut flowers is known as vase life, which is affected by water absorption and evaporation [4]. Water absorption and evaporation of cut hydrangea flowers in all cut flowers is associated with catabolism, such as respiration, and decreases due to vascular occlusions by air embolism and microorganisms. In particular, microorganisms block the ends of cut flowers' stems, inhibiting solution uptake and shortening vase life [1,5]. To solve this problem, some studies have been conducted to extend the vase life of cut flowers by adding various preservatives to vase water [6–10]. In addition, the most important problem after harvesting cut flower hydrangea is that if the water supply is not

maintained, air embolism may occur. Air embolism in xylem conduits can partially or completely block the water transport path between roots and sinks for water in plants [11]. Wilting is sometimes caused by air embolism and is a criterion for the end of vase life, and the vase life of cut hydrangeas is shortened due to sepal browning and wilting [12]. To prevent wilting by air embolism, cut flowers should be pretreated immediately after harvesting, have moisture managed during transport, and obtain preservative solution treatment at the consumer stage.

In many previous studies, aluminum sulfate, 8-hydroxyquinolin, 8-hydroxyquinolin sulfate (8-HQS), 8-hydroxyquinolin citrate, ethanol, and sodium hypochlorite are typically used as preservatives. In particular, 8-HQS is one of the essential preservatives used in cut flowers and has been reported to have a positive effect [13–15]. 8-HQS mainly acts as an antibacterial agent and has been reported as a mechanism to increase moisture by physiologically reducing stem blockage in sterile tissue absorption [16]. Sucrose is the most commonly used sugar to extend the vase life of cut flowers, and exogenous application of sucrose can supply large amounts of respiratory substrate to cut flowers and induce the flowering of flowers that are harvested at the bud stage. It is also known to improve water relationships by acting as osmotically active molecules [17].

However, although many studies on the effects of 8-HQS and sucrose have been reported, studies comparing the effects of 8-HQS and sucrose with preservatives commercially used in actual farmhouses are lacking.

The market for hydrangea is largely divided into domestic and export, and is commonly subdivided into harvest–transport–sale. In order to maintain the quality of cut flowers, proper vase solution treatment (pretreatment after harvesting, water container during transportation, preservative solution after purchase) should be performed at each distribution stage.

We aimed to compare the effects of currently used preservatives and scientifically reported preservatives on the vase life of cut hydrangea flowers, and further investigate the effect of each combination of pretreatment, transport, and preservative treatment.

2. Materials and Methods

2.1. Plant Materials

The hydrangea cultivar used in this experiment were those that are widely sold in Korea, and all were harvested in fresh stages. The cut hydrangea flower samples were 'Verena' grown in a farm in Gangjin, Jeollanam-do, South Korea (34°34′06″ N 126°50′08″ E). The flowers were harvested at the commercial stage, where about 80% of the florets showed the colors of the cultivar in June of 2019 and 2020. The harvested flowers were immediately pretreated in a cold storage at 4 °C for 24 h. After pretreatment, they were recut to a length 60 cm and put in a water container and transported to the postharvest laboratory within three hours. Then, the flowers were stored 72 h at 4 °C to transport conditions during simulated export. After simulated transport, the flower stems were recut to a length of 48 cm and five upper leaves were held on each stem for vase life evaluation.

2.2. Treatment Solutions

In this study, the first experiment is a comparative experiment with 3 types of preservation solutions, and the second experiment is a comparative experiment with 4 types of solution combinations for each postharvest treatment stage. The postharvest treatment stage was divided into a pretreatment stage at the farm, a transport stage during distribution, and a stage for preserving cut flowers after purchase.

For comparison by preservative solution treatment, the pretreatment and transportation solution were treated with tap water (TW), and then the preservation solution was used. The preservative solutions used were 1% Chrysal Professional III (CPIII), 2% sucrose + 250 mg/L 8-hydroxquinoline + 100 mg/L citric acid (SHQC), and TW as control. Preservative solution treatment was carried out by putting 700 mL of preservative solution prepared in advance in a glass bottle (1000 mL).

For comparison by solution combinations for each postharvest treatment stage, the pretreatment solution used were 0.1% Chrysal RVB (RVB), Floralife Quick Dip (FQ), and TW as control. For pretreatment, after the hydrangea flowers were harvested, they were immediately transferred to storage set at 4 °C and immersed in the pretreatment solution for 24 h. The transport solution used were CPIII, Floralife Clear (FC), and TW as control. The pretreated flowers were put in a water container containing transport solution, and then packed in a cardboard box and stored at 4 °C for 72 h, which was simulated transport with consideration for the transport period from packaging to sales. The preservative solution used were CPIII and FC. All solutions were prepared fresh at the initiation of the study. The conditions of the vase life evaluation room included a fluorescent lamp turned on for 12 h from 6 am to 6 pm every day with a room temperature of 22 ± 1 °C, and relative humidity of 60 ± 5%.

2.3. Relative Fresh Weight, Solution Uptake, Water Balance, and Vase Life

Fresh weight and solution uptake were measured once every 2 days. Fresh weight was calculated by subtracting the weight of the vase and solution from the total weight of the vase, solution, and flower. Relative fresh weight was calculated as the rate of fresh weight change, which was calculated as a percentage of fresh weight at the day of measurement compared with fresh weight at the day of initial.

$$\text{Relative fresh weight (\% of initial)} = (W_t/W_0) * 100 \tag{1}$$

$$W_t = \text{the weight of flower stem (g) at the day of measurement} \tag{2}$$

$$W_0 = \text{the weight of flower stem (g) at the day of initial} \tag{3}$$

Solution uptake was investigated by subtracting the weight of the vase and solution on the day of measurement from the weight of the vase and solution on the previous day. Total solution uptake was calculated by adding up all daily solution uptakes. Water balance was investigated by subtracting transpiration from solution uptake, and transpiration was investigated by subtracting the total weight (sum of the weight of the vase, solution, and cut flower) on the day of measurement from the total weight on the previous day. Vase life was defined by the duration from the initial experiment to the occurrence of wilting, browning, and drying. The degree of flower wilting, browning, drying and vase life of flowers was determined according to the morphological stages and appearance of symptoms such as drying, brown edges, wilting flower, and bent neck (Figure 1).

(**a**)	(**b**)

Figure 1. The main senescence symptoms of cut hydrangea flowers 'Verena' (**a**) browning (**b**) wilting.

2.4. Statistical Analysis

The experiment with preservative solution 3 treatment and postharvest solution combination 4 treatments was conducted in completely randomized design (CRD) with three replicates and three flowers for each replication. For statistical analysis, data were subjected to Brown–Forsythe and Welch analysis of variance (ANOVA) using the SPSS 20 (SPSS Inc., Chicago, IL, USA), while the significance of differences was assessed using Duncan's multiple range test ($p < 0.05$).

3. Results

3.1. Relative Fresh Weight Due to Preservative Solution

Fresh weight results were expressed as relative fresh weight with the results for each preservative solution treatment shown in Figure 2. Relative fresh weight in SHQC treatment increased sharply until 8 days (2019) and 10 days (2020), respectively (Figure 2). As a result, in 2019, TW and CPIII treatment maintained, as compared with initial weights, whereas the SHQC treatment increased at 8 days (Figure 2a). As a result, in 2020, a pattern similar to the 2019 result was shown, and the TW and CPIII treatment maintained the initial weight, while the SHQC treatment increased the fresh weight compared with the initial weight. (Figure 2b).

Figure 2. Changes in the relative fresh weight of cut hydrangea flowers 'Verena' kept in each preservative solution treatment in (**a**) 2019 and (**b**) 2020. Vertical bars indicate standard deviation of means (*n* = 9). TW, tap water; CPIII, 1% Chrysal Professional III; and SHQC, 2% sucrose + 250 mg/L 8-hydroxquinoline + 100 mg/L citric acid.

3.2. Solution Uptake and Total Solution Uptake Due to Preservative Solution

Solution uptake decreased until the 10th day after preservative solution treatment in all treatments, and TW treatment was the the lowest until 6 days after treatment, but there was no significant difference between treatments. In addition, CPIII treatment and SHQC treatment maintained solution uptake as much as the initial solution uptake level until the end of vase life (Figure 3a). Total solution uptake in 2019 was 199.08 g/stem in CPIII treatment, which was higher than tap water treatment (138.00 g/stem) and SHQC treatment (163.54 g/stem) (Table 1). As a result, in 2020, the initial solution uptake of the three treatments was 15.3, 15.9, and 16.3 g/stem, respectively, and the difference in absorption between TW, CPIII, and SHQC treatments was 0.6~1 g/stem, which was similar. Changes in solution uptake during the preservation period of cut flowers were 8.9, 11.4, and 12.0 g/stem at 19 days, respectively. The difference in solution uptake between TW and treatment with CPIII and SHQC ranged from 2.5 g/stem to 3.1 g/stem, and there was

a statistically significant difference between the control and treatment groups (Figure 3b). In 2020, the total solution uptake of CPIII and SHQC was 135.28 and 132.71 g/stem, respectively, which was statistically significantly higher than TW treatment (Table 1).
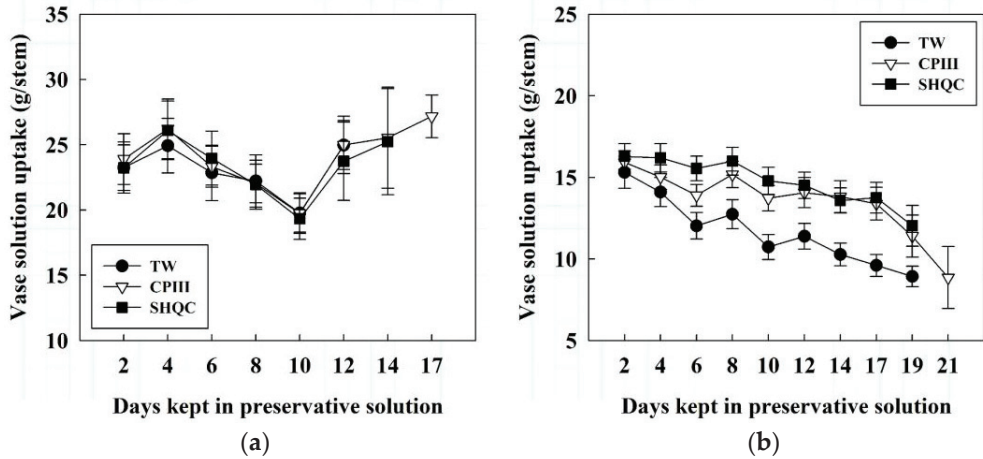
Figure 3. Changes in the vase solution uptake of cut hydrangea flowers 'Verena' kept in each preservative solution treatment in (**a**) 2019 and (**b**) 2020. Vertical bars indicate standard deviation of means (*n* = 9). TW, tap water; CPIII, 1% Chrysal Professional III; and SHQC, 2% sucrose + 250 mg/L 8-hydroxyquinoline + 100 mg/L citric acid.

Table 1. Total solution uptake of cut hydrangea flowers 'Verena' kept in each preservative solution treatment in 2019 and 2020.

Year	Pretreatment Solution	Transport Solution	Preservative Solutions	Total Solution Uptake (g/stem)	F/*p* Value	Brown–Forsythe Value
2019	TW	TW	TW [z]	138.00 b [y]	4.759/0.058 [ns x]	0.095
	TW	TW	CPIII	199.08 a		
	TW	TW	SHQC	163.54 ab		
2020	TW	TW	TW	105.12 b	4.206/0.27 *	0.028
	TW	TW	CPIII	135.28 a		
	TW	TW	SHQC	132.71 a		

[z] Abbreviations: TW = tap water; CPIII = 1% Chrysal Professional III; SHQC = 2% sucrose + 250 mg/L 8-hydroxquinoline + 100 mg/L citric acid. [y] a, ab, b: Mean separation within columns by Duncan's multiple ranges test at *p* < 0.05. [x] Minimum vase life and maximum vase life (day). ns, *: Nonsignificant or significant at *p* < 0.05, respectively.

3.3. Water Balance Due to Preservative Solution

The water balance results according to the preservative solution treatment showed a similar trend to the 2019 and 2020 results, and the water balance in the SHQC treatment was maintained longer than that of other treatments. The number of days to maintain the water balance was the date at which water balance value changed from a positive value to a negative value. As a result, in 2019, the number of days to maintain water balance in SHQC treatment was 8, which was maintained for 2–4 days longer than 6 days for CPIII treatment, and 4 days for TW (Figure 4a). In the study conducted in 2020, the number of days of maintaining water balance in SHQC treatment was 10, which was 2–4 days longer than 8 days for CPIII treatment, and 6 days for TW (Figure 4b).
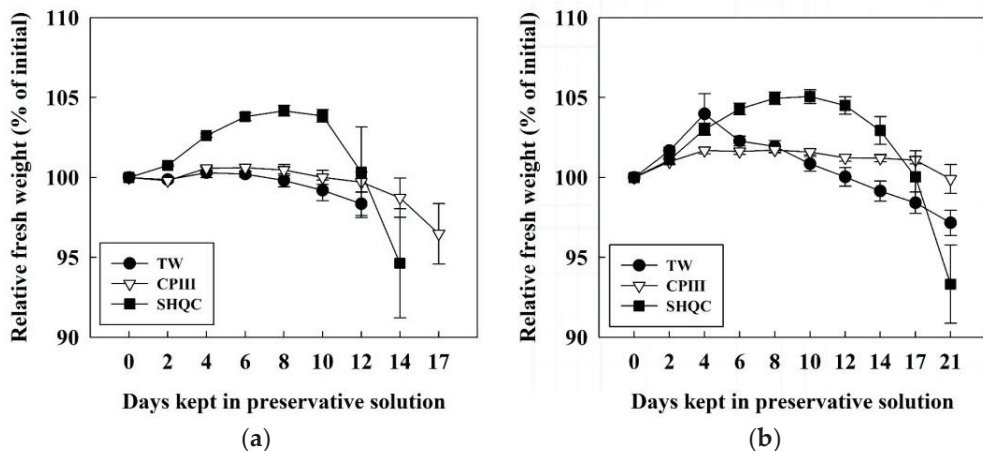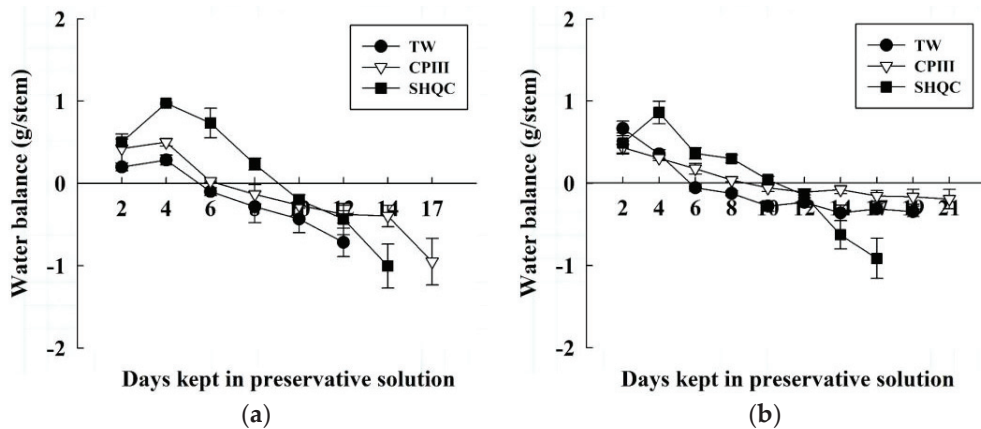
Figure 4. Changes in the water balance of cut hydrangea flowers 'Verena' kept in each preservative solution treatment in (**a**) 2019 and (**b**) 2020. Vertical bars indicate standard deviation of means (*n* = 9). TW, tap water; CPIII, 1% Chrysal Professional III; and SHQC, 2% sucrose + 250 mg/L 8-hydroxyquinoline + 100 mg/L citric acid.

3.4. Vase Life Due to Preservative Solution

The use of a preservative was effective in extending the vase life following the treatment with a preservative solution (Table 2). As a result, in 2019, the vase life of CPIII treatment and SHQC treatment was extended by 0.7–3.4 days as compared with the TW treatment. The minimum vase life of CPIII treatment was 18 days and the maximum vase life was 23 days, which exceeded the vase life of TW and SHQC treatment. In the 2020 results, the vase life was extended with the CPIII treatment and SHQC treatment as compared with the TW. In both 2019 and 2020, CPIII treatment and SHQC treatment with a preservation solution at the consumer stage was effective in extending the vase life of cut hydrangea flowers.

Table 2. Vase life and main factor of senescence of cut hydrangea flowers 'Verena' kept in each preservative solution treatment in 2019 and 2020.

| Year | Pretreatment Solution | Transport Solution | Preservative Solutions | Vase Life (days) | | | | F/*p* Value | Brown–Forsythe Value |
				Average	Min. [x]	Max.	MF [r]		
2019	TW [z]	TW	TW	17.3 b [y]	17	18	B	3.652/0.092 [ns]	0.163
	TW	TW	CPIII	20.7 a	18	23	B/W		
	TW	TW	SHQC	18.0 ab	17	19	W		
2020	TW	TW	TW	20.9 b	20	21	B	6.316/0.006 **	0.012
	TW	TW	CPIII	24.0 a	21	28	B/W		
	TW	TW	SHQC	22.3 ab	20	24	W/B		

[z] Abbreviations: TW = tap water; CPIII = 1% Chrysal Professional III; SHQC = 2% sucrose + 250 mg/L 8-hydroxyquinoline + 100 mg/L citric acid. [y] a, ab, b: Mean separation within columns by Duncan's multiple ranges test at *p* < 0.05. [x] Minimum vase life and maximum vase life (day). [r] Main factor in determining the vase life of cut flowers (B, browning; W, wilting). ns, **: Nonsignificant or significant at *p* < 0.01, respectively.

3.5. Relative Fresh Weight Due to Combination of Postharvest Solution

The results of relative fresh weight by solution combination for each postharvest treatment stage are shown in Figure 5a. There was a slight difference in the maintenance period of fresh weight for each treatment. As compared with other treatments, the RVB–CPIII–CPIII combination had the longest fresh weight maintenance period of 23 days and showed a difference of about 5 days. During vase life, the RVB–CPIII–CPIII combination was higher than those without pretreatment. It was similar to the FQ–FC–FC combination, and there was no significant difference.
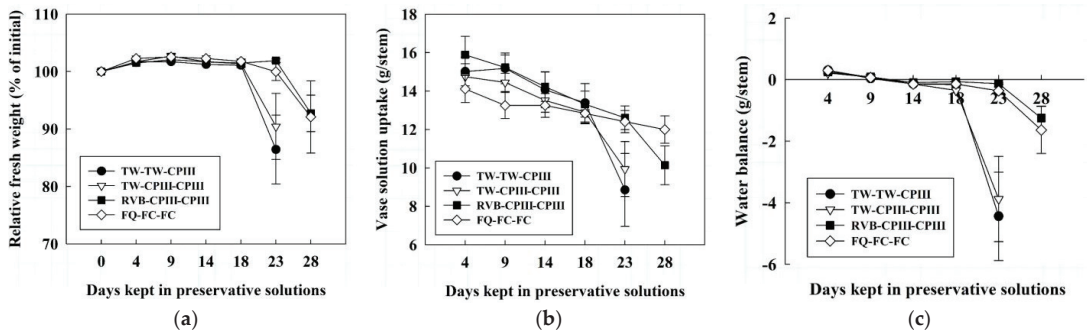
Figure 5. Changes in the relative fresh weight in (**a**) vase solution uptake, (**b**) water balance, and (**c**) cut hydrangea flowers 'Verena' by solution combination for each postharvest treatment stage in 2020. Vertical bars indicate standard deviation of means (*n* = 9). TW, tap water; CPIII, 1% Chrysal Professional III; RVB, 0.1% Chrysal RVB; FQ, Floralife Quick Dip; and FC, Floralife Clear. The order of TW–TW–CPIII indicates the order of pretreatment solution, transport solution, and preservation solution.

3.6. Solution Uptake and Total Solution Uptake Due to Combination of Postharvest Solution

The results of solution uptake and total solution uptake by solution combination for each postharvest treatment stage are shown in Table 3 and Figure 5b. Solution uptake gradually decreased during the preservation period of cut flowers commonly for all treatments. In particular, the solution uptake of cut flowers treated with the TW–TW–CPIII and TW–CPIII–CPIII combination decreased sharply from 18 days. On the other hand, the RVB–CPIII–CPIII combination and FQ–FC–FC combination maintained solution uptake during vase life as compared with other combinations. This finding was statistically significant both by using Duncan's multiple range test between absolute values, and with repeated measurements. The total solution uptake by each postharvest solution was 164.92 g/stem in the RVB–CPIII–CPIII combination, which was the highest as compared with other treatments, but there was no statistically significant difference between treatments.

Table 3. Total solution uptake of cut hydrangea flowers 'Verena' by solution combination for each postharvest treatment stages in 2020.

Pretreatment Solutions	Transport Solutions	Preservative Solutions	Total Solution Uptake (g/stem)	F/*p* Value	Brown–Forsythe Value
TW [z]	TW	CPIII	141.18 a [y]		
TW	CPIII	CPIII	143.78 a	2.024/0.130 [ns]	0.133
RVB	CPIII	CPIII	164.98 a		
FQ	FC	FC	158.48 a		

[z] Abbreviations: TW = tap water; CPIII = 1% Chrysal Professional III; RVB = 0.1% Chrysal RVB; FQ = Floralife Quick Dip; FC = Floralife Clear. [y] a: Mean separation within columns by Duncan's multiple ranges test at *p* < 0.05.). ns: Nonsignificant at *p* < 0.01, respectively.

3.7. Water Balance Due to Combination of Postharvest Solution

The results of water balance according to the solution management in the overall process from preharvest treatment to preservation solution showed a dramatic effect depending on the treatment (Figure 5c). The effect of maintaining the water balance according to the treatment of the transport solution used in the distribution stage was insignificant. The number of days for maintaining water balance between the TW–TW–CPIII combination and the TW–CPIII–CPIII combination was the same 9 days; therefore there was no difference between TW and CPIII used as a transport solution. However, due to the use of pretreatment, the number of days for maintaining water balance was slightly extended. The number of days for maintaining water balance of the RVB–CPIII–CPIII and

the FQ–FC–FC combination with the pretreatment was 23, which was extended by 5 more days than the TW–TW–TW and the TW–CPIII–CPIII combination without pretreatment. In addition, there was a difference in the time when the water balance value rapidly decreased, depending on whether or not pretreatment was used. The combination with pretreatments such as RVB and FQ started to decrease from day 18, while the combination without pretreatment decreased sharply from day 18.

3.8. Vase Life Due to Combination of Postharvest Solution

The effect of pretreatment performed in the postharvest treatment stage was clearly different in the results of vase life according to the 4 groups of postharvest solution combinations (Table 4, Figure 6). The average vase life of the group pretreated with RVB and FQ were 29.9 and 28.6 days, respectively, which was longer than that of the group without pretreatment. In particular, the vase life of the RVB–CPIII–CPIII combination was 27 days at the minimum and 35 days at the maximum, which exceeded the vase life range of the TW–TW–CPIII combination. Through these results, it was confirmed that the use of an appropriate pretreatment agent is an important factor to extend vase life and improve quality.

Table 4. Vase life and main factor of senescence of cut hydrangea flowers 'Verena' by solution combination for each postharvest treatment stage in 2020.

Pretreatment Solution	Transport Solution	Preservative Solution	Vase Life (Days)				F/p Value	Brown–Forsythe Value
			Average	Min. [x]	Max.	MF [r]		
TW [z]	TW	CPIII	24.0 b [y]	21	28	W		
TW	CPIII	CPIII	25.0 b	20	29	B	9.674/0.000 ***	0.000
RVB	CPIII	CPIII	29.9 a	27	35	B		
FQ	FC	FC	28.6 a	23	31	B		

[z] Abbreviations: TW = tap water; CPIII = 1% Chrysal Professional III; RVB = 0.1% Chrysal RVB; FQ = Floralife Quick Dip; and FC = Floralife Clear. [y] a: Mean separation within columns by Duncan's multiple ranges test at $p < 0.05$. [x] Minimum vase life and maximum vase life (day). [r] Main factor in determining the vase life of cut flowers (W, wilting; B, browning). ***: significant at $p < 0.001$, respectively.
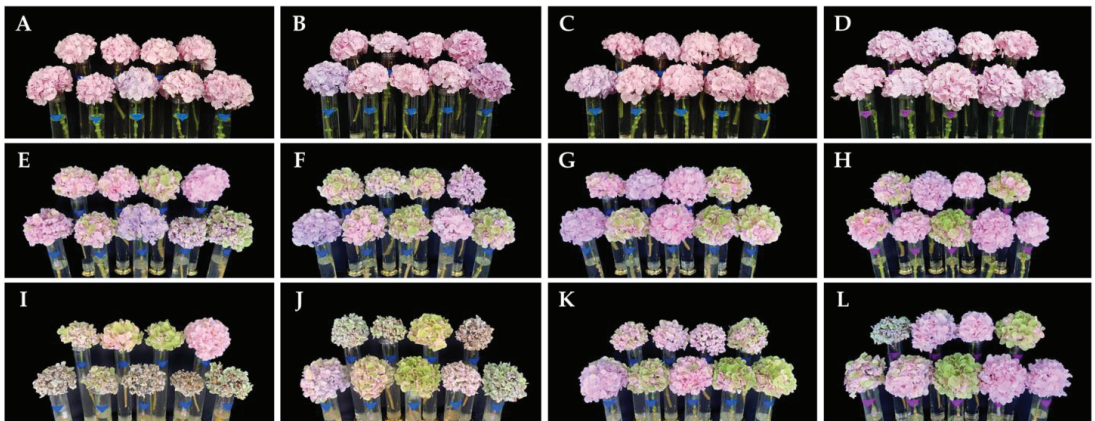
Figure 6. Appearance of cut hydrangea flowers 'Verena' by solution combination for each postharvest treatment stage in 2020. (**A–D**): First day after preservative solution, (**E–H**): 22nd day after preservative solution, (**I–L**): 29th day after preservative solution (**A,E,I**): TW–TW–CPIII, (**B,F,J**): TW–CPIII–CPIII, (**C,G,K**): RVB–CPIII–CPIII, (**D,H,L**): FQ–FC–FC.

4. Discussion

Cut hydrangea flowers are sensitive to water stress, and when water is insufficient, the water balance of the calyx changes to a negative value. The main causes of water stress are interruption of water supply and vascular occlusion at the tip of the stem [18]. Most cut flowers, including cut hydrangea flowers, have a high initial solution uptake rate,

but decrease over time, mainly due to vascular blockage by microorganisms and air embolism [9]. The impact of kept water relations on extending the vase life is constructed on the conclusion that cut hydrangeas are sensitive to water shortage caused by disturbing the postharvest water balance [9,12,19]. If these causes persist, they wither and the quality of the cut flowers deteriorates, which is the standard for the end of the vase life [1]. Asrar [13] reported that solution uptake through preservative treatment improved the water balance and freshness of flowers and reduced premature wilting, thereby improving the vase life of cut flowers, which is similar to our comparative results of preservative treatment. In our study, we observed the vase life of cut hydrangea flowers according to the combination of a preservation solution at the consumer stage and solution combination for each postharvest treatment stage after harvest for the purpose of improving the marketability of cut hydrangea flowers. For hydrangeas grown in Korea, it usually takes 2–3 days for export to the destination country. During this period, water management should be focused on the pretreatment stage immediately after harvest and the transportation stage. Pretreatment immediately after harvest is an essential step as it artificially supplies nutrient moisture to cut flowers whose supply of moisture and nutrients is interrupted [20]. In addition, the use of preservatives as a post-treatment concept to help prolong the flower viewing period at the consumer stage is also effective in extending the vase life. In particular, the various chemical solutions used in this study, such as RVB, CPIII, SHQC, FQ, and FC, generally have a specific purpose, so proper use is required. Previous studies reported that there was a strong correlation between solution uptake and fresh weight [5,21], and the combined effect of sucrose and antibacterial agents on the fresh weight of cut flowers was significantly greater than that of single treatment [22]. Sucrose supply is known to increase vase life, and it has been reported that it may act as an osmotic active molecule constituting a water relationship, as well as a nutrient source for tissues [23–25]. Similar to these reports, in our study, RVB as a pretreatment and SHQC as a preservative solution absorbed more solution than TW treatment and improved water balance. In addition, SHQC treatment with 2% sucrose significantly increased the fresh weight as compared with TW treatment. These results at fresh weight are similar to those of solution uptake positively affected by 8-HQ with 2% sucrose. Ku and Cho [26] also used 8-HQS to increase vase life of cut hydrangeas. They performed three different experiments [1% and 3% sucrose + 250 mg/L 8-HQS, varying pH levels (3.5–5.5 and 7.5), organic acids (citric and ascorbic)] and 3% sucrose + 250 mg/L 8-HQS. As a result, it was reported that 8-HQS (pH 3.5), or 3% sucrose + 250 mg/L 8-HQS + 100 mL citric acid, was effective in improving the cut flower quality of hydrangeas. As such, the maintenance of the water balance according to the increase in solution uptake and the decrease in transpiration can have a positive effect on fresh weight by preventing the water loss of cut flowers. In addition, pretreatment using RVB, which consists of sucrose and disinfectant, and transportation and preservation processing using CPIII, which is used for a different purpose than RVB, is one of the postharvest management technologies that must be performed in the entire distribution process, from harvesting to sales. When managing in this way, it was confirmed that the effect of maintaining the marketability was excellent.

5. Conclusions

This study was set up to highlight the importance of using the right pretreatment and preservatives at farms and in distribution stages by showing the potential effects on maintaining the commerciality of cut hydrangea flowers and extending the vase life. In the preservation solution comparison experiment, treatment with 1% CPIII and SHQC significantly extended the vase life of cut hydrangea flowers by 3.1 days and 1.4 days, respectively, as compared with control. In the comparative experiment of solution combination for each postharvest treatment stage, the pretreatment group using RVB and FQ significantly extended the vase life of cut hydrangea flowers to 5.9 and 4.6 days, respectively, as compared with control group (TW–TW–CPIII). These results show that using a pretreatment solution is effective in improving the quality of cut hydrangea flowers after long-term distribution.

However, SHQC used in the preservation solution comparison experiment was conducted to explore the possibility of replacing commercial preservatives, but did not obtain beneficial results, such as extending the vase life of cut hydrangea flowers and maintaining freshness. Therefore, new research on finding the optimal combination of sucrose, 8-HQS, and citric acid, and developing eco-friendly pretreatments and preservatives using natural materials should be performed.

Author Contributions: Conceptualization, I.-S.S. and H.Y.; methodology, I.-S.S. and H.Y.; validation, J.-H.L., S.L. and J.-W.C.; investigation, H.Y.; resources, I.-S.S.; data curation, J.-H.L., S.L. and J.-W.C.; writing—original draft preparation, H.Y.; writing—review and editing, I.-S.S. and H.Y.; visualization, H.Y.; supervision, I.-S.S.; project administration, I.-S.S. All authors have read and agreed to the published version of the manuscript.

Data Availability Statement: Data is contained within the article. The data presented in this study are available in article.

Conflicts of Interest: The authors have declared that no conflicts of interest exist.

References

1. Kitamura, Y.; Kato, Y.; Yasui, T.; Aizawa, H.; Ueno, S. Relation between increases in stomatal conductance of decorative sepals and the quality of antique-stage cut hydrangea flowers. *Hort. J.* **2017**, *86*, 87–93. [CrossRef]
2. Thomas, D.; Gollnow, B. *What Cut Flower Is That? The Essential Care and Handling Guide for Cut Flower Professionals*; Kingston, Australia Government, Rural Industries Research and Development Corporation: Kingston, Australia, 2014; p. 197.
3. da Costa, L.C.; Finger, F.L. Flower opening and vase life of gladiolus cultivars: The sensitivity to ethylene and the carbohydrate content. *Ornam. Hortic.* **2016**, *22*, 147–153. [CrossRef]
4. Kitamura, Y.; Ueno, S. Inhibition of transpiration from the inflorescence extends the vase life of cut hydrangea flowers. *Hort. J.* **2015**, *84*, 156–160. [CrossRef]
5. Alaey, M.; Babalar, M.; Naderi, R.; Kafi, M. Effect of pre-and postharvest salicylic acid treatment on physio-chemical attributes in relation to vase-life of rose cut flowers. *Postharvest Biol. Technol.* **2011**, *61*, 91–94. [CrossRef]
6. Abreu, M.E.; Munné-Bosch, S. Salicylic acid may be involved in the regulation of drought-induced leaf senescence in perennials: A case study in field-grown Salvia officinalis L. plants. *Environ. Exp. Bot.* **2008**, *64*, 105–112. [CrossRef]
7. Bahran Kinfe, L.G.; Yosief, R.; Mehari, S.; Maekele, S.; Rao, G.S. Impact of different preservative solutions on extending vase life of rose (Rosa hybrid) cut flowers. *Bioscience* **2018**, *11*, 3562.
8. Lü, P.; Cao, J.; He, S.; Liu, J.; Li, H.; Cheng, G.; Joyce, D.C. Nano-silver pulse treatments improve water relations of cut rose cv. Movie Star flowers. *Postharvest Biol. Technol.* **2010**, *57*, 196–202. [CrossRef]
9. Mashhadian, N.V.; Tehranifar, A.; Bayat, H.; Selahvarzi, Y. Salicylic and citric acid treatments improve the vase life of cut chrysanthemum flowers. *J. Agric. Sci. Technol.* **2012**, *14*, 879–887.
10. Pun, U.K.; Ichimura, K. Role of sugars in senescence and biosynthesis of ethylene in cut flowers. *Jpn. Agric. Res. Q.* **2003**, *37*, 219–224. [CrossRef]
11. Van Ieperen, W.; Nijsse, J.; Keijzer, C.J.; Van Meeteren, U. Induction of air embolism in xylem conduits of pre-defined diameter. *J. Exp. Bot.* **2001**, *52*, 981–991. [CrossRef] [PubMed]
12. Kazaz, S.; Doğan, E.; Kılıç, T.; Şahin, E.G.E.; Seyhan, S. Influence of holding solutions on vase life of cut hydrangea flowers (*Hydrangea macrophylla* Thunb.). *Fresenius Environ. Bull.* **2019**, *28*, 3554–3559.
13. Asrar, A.W.A. Effects of some preservative solutions on vase life and keeping quality of snapdragon (*Antirrhinum majus* L.) cut flowers. *J. Saudi Soc. Agric. Sci.* **2012**, *11*, 29–35. [CrossRef]
14. Edrisi, B.; Sadrpoor, A.; Saffari, V.R. Effects of chemicals on vase life of cut carnation (*Dianthus caryophyllus* L. 'Delphi') and microorganisms population in solution. *J. Ornam. Hortic.* **2015**, *2*, 1–11.
15. Seyf, M.; Khalighi, A.; Mostofi, Y.; Naderi, R. Study on the effect of aluminum sulfate treatment on postharvest life of the cut rose 'Boeing' (*Rosa hybrida* cv. Boeing). *J. Hortic. Sci. Biotechnol.* **2012**, *16*, 128–132.
16. Elhindi, K.M. Evaluation of several holding solutions for prolonging vase-life and keeping quality of cut sweet pea flowers (*Lathyrus odoratus* L.). *Saudi J. Biol. Sci.* **2012**, *19*, 195–202. [CrossRef]
17. Ichimura, K.; Hisamatsu, T. Effects of continuous treatment with sucrose on the vase life, soluble carbohydrate concentrations, and ethylene production of cut snapdragon flowers. *J. Jpn. Soc. Hortic. Sci.* **1999**, *68*, 61–66. [CrossRef]

18. Kazaz, S.; Kılıç, T.; Doğan, E.; Sekmen, Ş. Vase life extension of cut hydrangea (*Hydrangea macrophylla*) flowers. *J. Hortic. Sci. Biotechnol.* **2020**, *95*, 325–330. [CrossRef]
19. Rafi, Z.N.; Ramezanian, A. Vase life of cut rose cultivars 'Avalanche' and 'Fiesta' as affected by Nano-Silver and S-carvone treatments. *S. Afr. J. Bot.* **2013**, *86*, 68–72. [CrossRef]
20. Reid, M.S. *Handling of Cut Flowers for Export*; Proflora Bulletin; 2009; pp. 1–26. Available online: https://ucanr.edu/sites/Postharvest_Technology_Center_/files/231308.pdf (accessed on 14 October 2021).
21. Amin, O.A. II-Effect of some chemical treatments on keeping quality and vase life of cut chrysanthemum flowers. *Middle East J. Agric. Res.* **2017**, *6*, 221–243.
22. Ichimura, K.; Shimizu-Yumoto, H. Extension of the vase life of cut roses by treatment with sucrose before and during simulated transport. *Bull. Natl. Inst. Flor. Sci.* **2007**, *7*, 17–27.
23. Elgimabi, M.E.N.E. Vase life extension of Rose cut flowers (Rosa Hybrida) as influenced by silver nitrate and sucrose pulsing. *Am. J. Agric. Biol. Sci.* **2011**, *6*, 128–133. [CrossRef]
24. Yagi, M.I.; Eldeen, M.; Elgemaby, N.E. Effect of bactericides and sucrose pulsing on longevity and vase life of rose cut flowers. *Int. J. Sci. Basic Appl. Res.* **2014**, *14*, 117–129.
25. Norikoshi, R.; Shibata, T.; Niki, T.; Ichimura, K. Sucrose treatment enlarges petal cell size and increases vacuolar sugar concentrations in cut rose flowers. *Postharvest Biol. Technol.* **2016**, *116*, 59–65. [CrossRef]
26. Ku, B.S.; Cho, M.S. Vase life and quality as affected by various holding solution of cut *Hydrangea macrophylla. Flower Res. J.* **2014**, *22*, 12–20. [CrossRef]

MDPI

Article

Ethephon-Induced Abscission of Oil Palm Fruits at Optimal Bunch Ripeness and Retting Period to Improve Commercial Seed Production

Jaime Yoke-Sum Low, Po-Yee Fong *, Chee-Keng Teh, Ai-Ling Ong, Chin-Ming Lim and David Ross Appleton

Biotechnology & Breeding Department, Sime Darby Plantation R&D Centre, Serdang 43400, Selangor, Malaysia; jaime.low.yokesum@simedarbyplantation.com (J.Y.-S.L.); teh.chee.keng@simedarbyplantation.com (C.-K.T.); ong.ailing.sdtc@simedarbyplantation.com (A.-L.O.); lim.chin.ming@simedarbyplantation.com (C.-M.L.); david.ross.appleton@simedarbyplantation.com (D.R.A.)
* Correspondence: fong.po.yee@simedarbyplantation.com; Tel.: +60-3-9842-2641; Fax: +60-3-8943-1867

Abstract: Oil palm seed producers typically require 10 months of various processes from pollination to seed germination to produce commercial *dura* × *pisifera* hybrid seeds. Conventional forced fruit shedding from underripe fresh fruit bunches (FFB) usually causes seed damage and an extended retting period (incubation for natural fruit abscission from spikelets), eventually leading to bunch rot and disease infection. As a fruit ripening agent, ethephon has been explored to hasten fruit abscission in many fruit crops and oil palm. Nevertheless, the previous studies in oil palm only focused on fruit shedding from FFB to improve oil extraction rate in oil mills without considering the actual FFB ripeness and retting period, which are critical for oil palm seed production. In this study, the application of ethephon containing buffer (adjusted to pH 9.0) to underripe FFB at 145 days after pollination (DAP), 135 DAP and 125 DAP resulted in 50% more fruit abscission after a 72-h incubation. Considering the minimal seed loss upon FFB harvest (<1%) and 50% reduction in retting period, underripe FFB at around 145 DAP was found to be optimum for seed production using ethephon treatment. The treatment, however, made negligible improvement in fruit detachment for ripe FFB at 150 DAP and older. Importantly, seed germination and culling rate at nursery stages were not significantly affected by the ethephon treatment. Hence, ethephon application can improve commercial seed production practices for oil palm.

Keywords: fresh fruit bunch; postharvest technology; ethephon; retting period; germination; seed abnormality

1. Introduction

Oil palm (*Elaeis guineensis* Jacq.) is an important oil crop which supplies 35% of the global vegetable oils and fats [1]. Currently, oil palms have an economic life exceeding 20 years and can produce 10 times more oil per hectare than other oil crops [2]. One of the contributing factors to current yields is the switch in the 1960s of commercial *dura* planting to *dura* x *pisifera* hybrids (DxP), also termed *tenera*. This resulted in an increment of 30% oil yield in Southeast Asia [3,4]. Since then, the demand for palm oil has been increased with a rapid growth of world population especially in Malaysia has become the second largest producer and exporter of crude palm oil (CPO) [5,6]. The CPO production in Malaysia increased significantly from 92,000 tons in 1960 to 16.99 million tons in 2010, 19.4 million tons in 2020 and expected to increase to 19.6 million tons in 2021 [7,8]. This explains why commercial DxP seed production for planting in Malaysia has almost doubled from 1995 to 130 million in 2012 [9,10]. A cycle of seed production typically requires 10 months to complete various processes including controlled pollination, bunch harvesting, retting (incubation for natural fruit abscission), fruit shedding, dormancy breaking and germination (Figure 1). Therefore, improvement in production efficiency and

seed recovery is important to ensure a continuous supply of high quality seeds to growing markets and improve the profitability of seed producers.
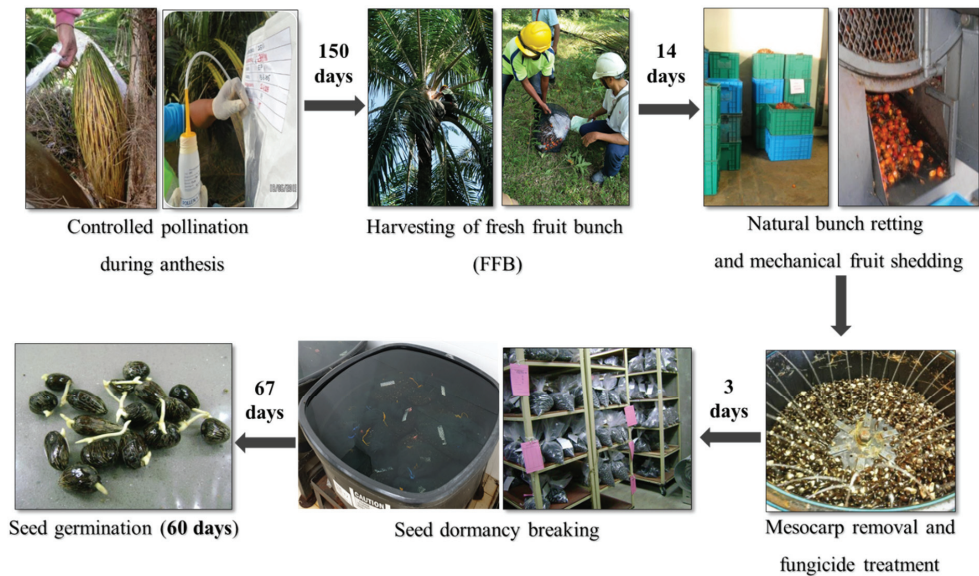
Figure 1. A process flow that involves various processes in a 10-month period for oil palm seed production. Conventional bunch retting allows natural abscission of fruits from spikelets, in which the process may take up to 14 days before fruit shedding by mechanical means.

A fresh fruit bunch (FFB) normally bears 1000 to 4000 fruits tightly wedged in the leaf axil of a palm. Similar to fruit crops such as red raspberry [11] and apple [12], abscission of oil palm fruits directly correlates to overall bunch ripeness [13]. The ripeness of commercial FFB for typical harvest standard is based on a minimum five naturally abscised fruits—known as loose fruits on the ground, which usually happens around 150–160 days after pollination (DAP), although it may not achieve the optimal oil extraction rates. This, however, does not apply to commercial seed production where harvesting is typically on the underripe FFB not more than 150 DAP for minimal loss of loose fruits during transport. Recovery of the loose fruit is totally restricted because some fruits can potentially originate from unintended parentage, causing genetic contamination. In a seed production facility, the fruits are mechanically shed from the spikelets of underripe FFB that have been retted for more than 10 days (Figure 1). Long retting period can increase the risk of fungal infection on seeds that may later reduce seed germination [14]. As a solution, ethylene can be used to accelerate uniform FFB ripeness and fruit abscission in oil palm.

Ethylene currently can be commercially obtained in the form of ethephon (2-chloroethylphosphonic acid) and it is widely used as an artificial ripening agent in many fruit crops. One example, ethylene has been applied in date fruits (*Phoenix dactylifera* L.) to increase ripening rate and facilitate early harvesting [15,16]. Indeed, the application of ethephon is not new to oil palm FFB, but it is only limited to accelerate fruit abscission to increase oil extraction rate in oil mills [17–20]. However, the applicability of ethephon/ethylene to increase the efficiency of oil palm seed production has yet to be reported. The current bunch ripeness standard with five or more loose fruits does not actually reflect the optimal time for underripe FFB harvest for seed production. Hence, our aim is (1) to evaluate the optimal FFB ripeness at the actual DAP for ethephon application to accelerate fruit abscission, (2) to allow the retting period to be shortened, and (3) to evaluate the

impact of ethephon on seed germination and culling rates at the nursery stages were also studied.

2. Materials and Methods

2.1. Plant Materials

A total of 66 FFB derived from commercial Deli *dura* x AVROS *pisifera* origin were harvested from four seed gardens, namely PT100, PT101, PT105 and PT116 located at Dusun Durian Estate, Sungai Sedu Estate, Klanang Bharu Estate and East Estate in Selangor State, Malaysia which are maintained by Sime Darby Plantation Seeds and Agricultural Services Sdn. Bhd. (SDPSAS). The FFB were harvested at five different bunch ripeness stages, including 125, 135, 145, 150 and 160 DAP. At each DAP, the FFB was divided into two groups i.e., ethephon-treated and nontreated control as summarized in Table 1. The sample size for 160 DAP was small (6 FFB) because most of the bunches harvested were rotten due to being overripe. For recording purposes, each FFB was sealed with a netting bag to prevent loss of loose fruits during the harvesting process. Bunch weight and the number of loose fruits upon harvesting were recorded. The percentage of loose fruits of each FFB was then calculated based on the total number of fruits per FFB harvested.

Table 1. Number of fresh fruit bunch (FFB) harvested across different bunch ripeness.

Days after Pollination (DAP)	Number of FFB	
	Control	Ethephon-Treated
125	9	10
135	6	8
145	6	6
150	7	8
160	3	3
Total	31	35

2.2. Ethephon Treatment, Quantification of Loose Fruits and Retting Period

Approximately 200 mL of 0.5% (*v/v*) ethephon buffer adjusted to pH 9.0 with 5M sodium hydroxide was sprayed on each FFB [21]. Both ethephon-treated and control FFB (without buffer treatment) were placed into different covered boxes to prevent mixing of loose fruits during the retting process. The number of loose fruits were first counted after 72 h of incubation. Subsequently, the retting period of each FFB was observed daily and determined when all fruits were fully shed from a bunch using the mechanical method. The percentage of loose fruits detached after 72 h was calculated based on the total number of fruits per FFB.

2.3. Ethephon Effect on Seed Germination and Culling Rate for 145 DAP

The ethephon-treated and the nontreated fruits from 145 DAP were processed according to Malaysian Standard, namely MS 157:2005 [22] to produce germinated seeds. After dormancy breaking, the seed germination took place for 60 days with routine inspection and recording for every 10-day interval. The final percentage of seed germination of each FFB was calculated based on the total germinated seeds after 60 days. The seed germination of ethephon-treated FFBs and controls were then compared. A total of 100 seeds per FFB which were randomly selected from the ethephon-treated and the control FFB from 145 DAP was sown in a nursery. The first and second rounds of culling were carried out after 3 months and 9 months, respectively. The final percentage of culling per bunch was calculated based on the total seeds sowed.

2.4. Statistical Analysis

All comparisons were analyzed using the Kruskal–Wallis test in the Minitab 20 program [23]. Comparisons were conducted to address (a) the effect of FFB ripeness on fruit

abscission upon harvesting, (b) the effect of ethephon treatment on fruit abscission after 72-h incubation and retting period across FFB ripeness, and (c) the effect of postethephon treatment on seed germination and culling at nursery. A significant difference was defined at the $p = 0.05$ threshold. All boxplots were constructed using *R 3.5.3* with package *ggplot2*.

3. Results

3.1. Effect of FFB Ripeness on Fruit Abscission upon Harvesting

Minimal loose fruits were observed upon FFB harvesting at 125 DAP and 135 DAP (Figure 2). Fruit abscission only started with loose fruit median = 0.27% at 145 DAP and significantly increased to 9.9% and 16.8% loose fruits at 150 DAP and 160 DAP, respectively with $p < 0.0005$.
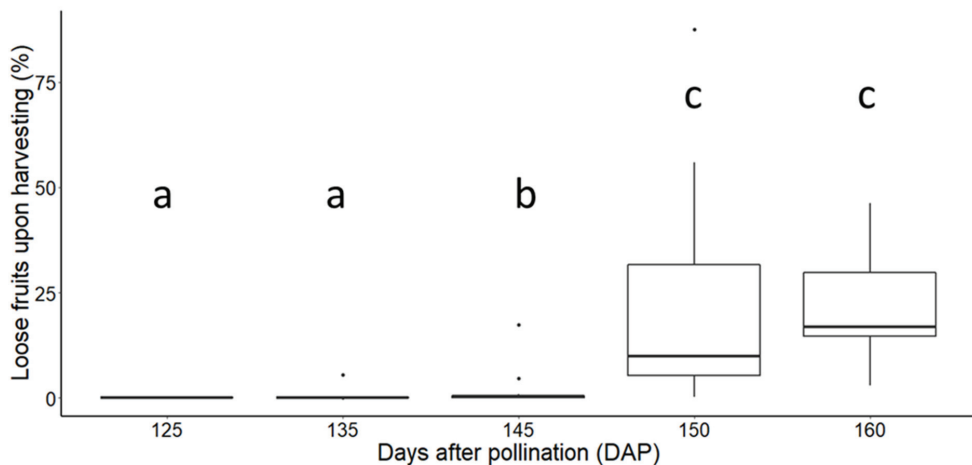
Figure 2. The boxplots represent median values, 25th–75th percentile of loose fruit percentage upon harvesting across FFB ripeness. Significant differences in loose fruit among the five DAP are denoted by a, b, and c based on Kruskal-Wallis test at the $p = 0.05$ threshold. Nineteen FFB harvested at 125 DAP have 0 loose fruit. Thirteen FFB harvested at 135 DAP have zero loose fruit with 1 outlier has 5.53% loose fruits. Ten FFB harvested at 145 DAP have less than 1.0% loose fruits, with 2 outliers having loose fruits 4.66% and 17.42%.

3.2. Effect of Ethephon Treatment on Fruit Abscission after 72-h Incubation and Retting Period across FFB Ripeness

The loose fruit percentage of 72-h postethephon treatment and the control across FFB ripeness is shown in Figure 3. Ethephon-induced loose fruits (median = 28.4%) started as early as 125 DAP, which was significantly 315 folds higher than that of the control FFB (median = 0.09%) with $p < 0.0005$. Subsequently, loose fruits of ethephon-treated FFB increased rapidly at 135 DAP (median = 51.4%) and peaked at 145 DAP (median = 53.4%), whereas the control FFB only peaked at median = 31.9% at 160 DAP which was delayed by 15 days and was 50% lower in loose fruits. In addition, the ethephon-induced loose fruit percentage at 150 DAP (median = 36.1%) and 160 DAP (median = 40.1%) dropped to a comparable level of control FFB.

Overall, the retting period reduced as FFB ripeness increased regardless of ethephon-treated and control FFB (Figure 4). Retting of the ethephon-treated FFB at 125 DAP was successfully reduced to a median of 9 days, while 3 more days were required by the control FFB. The trend continued and reached the bottom at a median of 4.5 days of retting for the ethephon-treated FFB at 145 DAP, which was significantly 50% shorter than that of the control FFB with $p = 0.023$. However, the gap of retting period between ethephon-treated and control FFB at 150 DAP and 160 DAP become comparable with p value of 0.109 and 0.197, respectively.
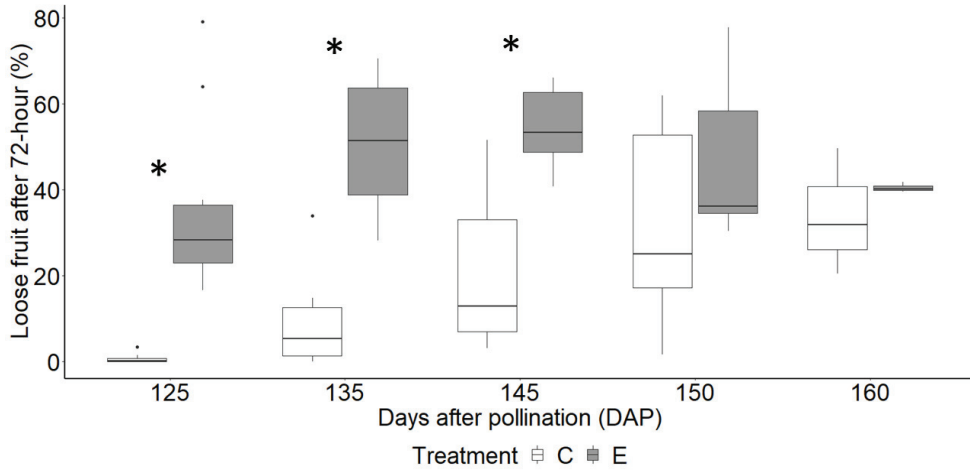
Figure 3. The boxplots represent median values, 25th–75th percentile of loose fruit percentage of ethephon-treated (E) and control (C) FFB after 72-h incubation across FFB ripeness. Significant difference in loose fruits between E and C are denoted by asterisk (*) based on the Kruskal–Wallis test at the *p* = 0.05 threshold.
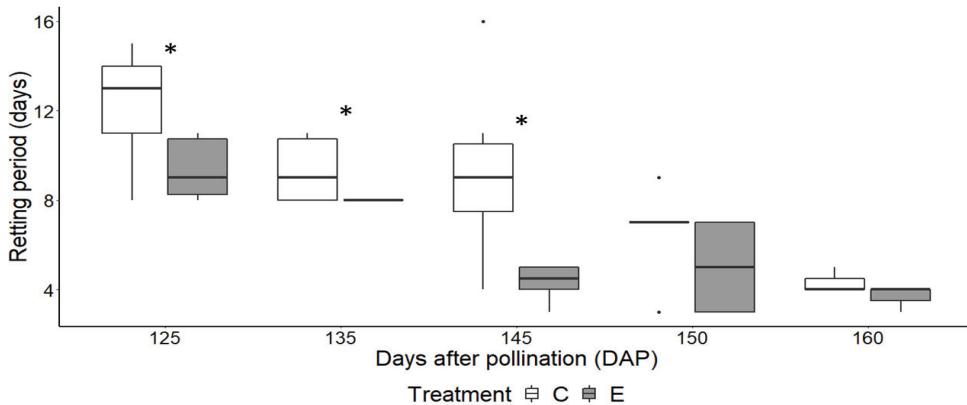
Figure 4. The boxplots represent median values, 25th–75th percentile of retting period (days) between ethephon-treated (E) and control (C) FFB across FFB ripeness. Significant difference in retting period between E and C are denoted by asterisk (*) based on the Kruskal–Wallis test at the *p* = 0.05 threshold. Eight FFB harvested at 135 DAP were retted at 8 days. Seven FFB harvested at 150 DAP completed retting process at 7 days, with 2 outliers retted at 3 days and 9 days.

3.3. Effect of Posttreatment with Ethephon on Seed Germination and Culling at Nursery for 145 DAP

In this study, only FFB from 145 DAP were selected for seed germination and culling recording. This is based on the lowest retting period at 145 DAP with minimal loose fruits upon harvesting. The seed germination of ethephon-treated FFB recorded a median of 79% and control FFB recorded a median of 74% and showed no significant difference with *p* = 0.8102. Grass leaf (or narrow leaf) and juvenile were the major abnormalities culled from 3-month-old and 6-month-old seedlings. Again, the final culling percentage of the ethephon-treated (culling median = 19.98%) and the control (culling median = 15.29%) was not significantly different with *p* = 1.000.

4. Discussions

Oil palm as a perennial crop usually requires 12–20 years to complete a selective breeding cycle [24]. Consequently, improvement of oil palm planting material is much slower than annual crops. This is partly the result of infrequent replanting with typical 25 years per cycle in oil palm. The recent advancement of genomics and molecular breeding in oil palm, however, is expediting the breeding progress to produce high-yield planting materials such as GenomeSelect[TM] to bring improvements to oil yield in existing fields without further expansion and clearance of forest land [24,25]. Moreover, the rapid introduction of elite planting materials motivates early replanting for the oil palm industry to take advantage of better oil yield and to reduce labor shortage, especially for FFB harvested from tall palms. For instance, Sime Darby Plantation is accelerating 5% annual replanting with the GenomeSelect[TM] material to fully cover its 0.32 million hectare of total land bank in Malaysia by 2023 [26]. A similar trend in oil palm industry is foreseeable. Hence, oil palm seed producers need to improve their production efficiency and seed quality to cope with the high demand for seeds.

In this study, natural fruit abscission was found to initiate at 145 DAP and peaked within 150–160 DAP, inferring full FFB ripeness. The primary abscission zone of a ripe oil palm fruit is sensitive to ethylene, which induces cell separation and abscission in the abscission zone [27]. Therefore, FFB harvest for seed production should be carried out before 150 DAP for minimal loose fruits on the ground or being caught in the axil of lower fronds, which can also lead to seed lot contamination. The findings coincide with the SDPSAS current standard operating procedure. A seed garden is usually planted with *dura* palms and only those with high yield performance are certified as mother palms based on MS 157:2005 (Malaysian Standard, 2005). Recovery of loose fruits in the seed garden may pose a risk of mixing with open-pollinated *dura* seeds derived from the same mother palms or neighboring nonmother palms, leading to *dura* contamination. Planting of thick-shelled *dura* contaminants can immediately lead to a 25% reduction in oil yield compared to the commercial thin-shelled DxP hybrids and the impact remains throughout the 20–25 years of economic life of the commercial palm [28]. To safeguard seed purity, *SHELL* and SNP-based legitimacy assays are now available to detect and remove the *dura* contaminants as early as the seed stage [29,30], but preventing the 10% loose fruits through early FFB harvest before 150 DAP is clearly more effective to completely avoid the risk of genetic contamination and seed loss. Mesh netting can be a good solution to secure the loose fruits during FFB harvest. Still, the method requires more manpower and eventually incur unnecessary production cost.

A major challenge was to enhance efficiency of fruit shedding from underripe FFB younger than 150 DAP. The fruits were not ready to abscise from FFB during the underripe stage and it would require a prolonged FFB retting. Without ethephon-treatment, the underripe FFB spent a median of 9 days to complete the retting process at 145 DAP and recorded the longest retting with a median of 13 days at 125 DAP. Oil palm FFB usually start to rot due to fungal and maggot infestation after a week of retting (Supplementary Figure S1). In such conditions, mycelia have enough time to grow over the seeds and penetrate through the germ pores to the surface of the testa near to the embryo, affecting respiration activity during seed germination [31]. Our target, hence, is to keep the retting period shorter than a week to avoid the fungal infection. Applying high mechanical shedding force is possible to forcibly remove fruits from the spikelets, but it also increases the risk of seeds cracking. Again, this would expose the kernel (endosperm) to microbial colonization, causing further complications with disease control in the subsequent seed processes. Even worse is the 10-month effort of seed production and monetary loss.

Many studies have shown that the application of exogenous ethylene can expedite ripening and fruit abscission in various fruit crops such as banana [32], tomato [33], apple [34], persimmon [35] and even oil palm [18,36]. However, the previous studies in oil palm were mainly focused on the response to ethephon of commercial FFB in the oil mill without knowing their actual fruit ripeness. We close the gap with similar results

in this study by evaluating seed maturity, viability and damage. Ethephon-induced fruit abscission started as early as 72-h posttreatment on underripe FFB at 125 DAP and fruit abscission peaked at 145 DAP with 50% loose fruits. For the untreated control bunches, the peak of fruit abscission coincided with the typical 150-DAP ripeness, as expected. This suggests that FFB retting at 145 DAP can be shortened significantly from 9 days to 4 days, enabling a mechanical shedding method e.g., vibration, which was tested by Ismail and colleagues in the oil mill to minimize seed damage [37]. By consolidating the assayed parameters, we found that around 145 DAP is the optimum FFB ripeness for ethephon treatment. The 145-DAP FFB produced less than 1% seed loss upon harvest in a seed garden and only required a median of 4 days of retting, compared to 10–14 days of conventional interval. Apart from excessive 9.9% seed loss and risk of seed legitimacy, ethephon treatment on ripe FFB (>150 DAP) was found to be expendable because the endogenous ethylene probably had sufficed the requirement for fruit ripening and abscission during seed production [11,20].

In early studies, possible roles of ethephon in dormancy breaking in oil palm [38] and macaw palm [39] were reported. Loblolly pine seeds were found to be sensitive to higher ethephon concentration at 10% (v/v), which significantly reduced 40% of seed germination and increased culling beyond 10% [40]. To further understand the effect of ethephon residues on the treated oil palm FFB, the germinated seeds tested in this study were sown and monitored throughout the prenursery (3 months) and main nursery (9 months) stages. The result, however, indicated that the ethephon treatment did not significantly affect germination and culling in oil palm because the concentration used was 200 times lower than the reported concentration in loblolly pine seeds. More importantly, the observed percentage of culling was still within the normal range i.e., about 25% [41]. This is possibly due to the physical barrier of endocarp (or shell) preventing excessive exogenous ethylene released from ethephon to reach the embryo [42]. Grass leaf and juvenile spotted seedling palms are the major abnormal phenotypes at the prenursery and main nursery based on the industry standard in MPOB-created Code of Practice (CoP) 1001:2015 [43–45]. The levels of these "abnormalities" were also in concordance with a previous study reported by United Plantations Bhd. [46] with or without ethephon. These "abnormalities" are mostly resulted from bad planting, such as deep or inverted planting or from insufficient water supply [47].

5. Conclusions

Ethephon was found to be effective in expediting fruit abscission (50%). This study also has provided evidence that the ethephon treatment can be a powerful method to improve the current commercial seed production of oil palm with minimal seed loss (0.27%) and reduced retting period from 9 days to 4 days, provided it is applied on the optimal FFB ripeness, which is around 145 DAP. Furthermore, the use of ethephon has no obvious adverse effect on germination and culling at nursery stages. The assayed oil palm seedlings have been field planted and a further evaluation of ethephon effect on FFB yield could be conducted when the yield recording is completed after 6 years. This study has paved a way for a future study on ethylene gas which is cheaper and leaves fewer residues as an alternative for commercial seed production, as has been widely used in fruit industry.

References

1. Meijaard, E.; Garcia-Ulloa, J.; Sheil, D.; Wich, S.A.; Carlson, K.M.; Juffe-Bignoli, D.; Brooks, T.M. *Oil Palm and Biodiversity: A Situation Analysis by the IUCN Oil Palm Task Force*, 1st ed.; International Union for Conservation of Nature and Natural Resources (IUCN): Gland, Switzerland, 2018. [CrossRef]
2. Ghulam Kadir, A.P. Oil palm economic performance in Malaysia and R&D progress in 2019. *J. Oil Palm Res.* **2020**, *32*, 159–190. [CrossRef]
3. Corley, R.H.V.; Tinker, P.B. The Origin and Development of the Oil Palm Industry. In *The Oil Palm*; Corley, R.H.V., Tinker, P.B., Eds.; Wiley Blackwell: Oxford, UK, 2015; pp. 1–29. [CrossRef]
4. Hardon, J.J.; Corley, R.H.V.; Lee, C.H. Breeding and selecting the oil palm. In *Improving Vegetatively Propagated Crops*; Abbot, A.J., Atkin, R.K., Eds.; Academic Press: London, UK, 1987; pp. 63–81.
5. Choong, C.G.; McKay, A. Sustainability in the Malaysian palm oil industry. *J. Clean. Prod.* **2014**, *85*, 258–264. [CrossRef]
6. Henry Ezechi, E.; Muda, K. Overview of trends in crude palm oil production and economic impact in Malaysia. *Sriwij. J. Environ.* **2019**, *4*, 19–26. [CrossRef]
7. Wong, E.L.; The EdgeTM Markets. MPOC: Palm Oil Production to Increase to 19.6 Million Tonnes in 2021. 2021. Available online: https://www.theedgemarkets.com/article/mpoc-palm-oil-production-increase-196-million-tonnes-2021 (accessed on 1 June 2021).
8. Abdullah, R. World palm oil supply, demand, price and prospects: Focus on Malaysian and Indonesian Palm Oil Industries. *Oil Palm Ind. Econ. J.* **2011**, *11*, 13–25.
9. Rajanaidu, N.; Ainul, M.M.; Kushairi, A.; Din, A. Historical review of oil palm breeding for the past 50 years—Malaysian Journey. In Proceedings of the International Seminar on Oil Palm Breeding—Yesterday, Today and Tomorrow, Kuala Lumpur, Malaysia, 18 November 2013; pp. 11–28.
10. Teh, C.-K.; Global Engage. Is Palm Oil Sustainable for People? 2018. Available online: https://www.global-engage.com/agricultural-biotechnology/is-palm-oil-sustainable-for-people/ (accessed on 7 September 2021).
11. Burdon, J.N.; Sexton, R. The Role of Ethylene in the Shedding of Red Raspberry Fruit. *Ann. Bot.* **1990**, *66*, 111–120. [CrossRef]
12. Eccher, G.; Begheldo, M.; Boschetti, A.; Ruperti, B.; Botton, A. Roles of Ethylene Production and Ethylene Receptor Expression in Regulating Apple Fruitlet Abscission. *Plant Physiol.* **2015**, *169*, 125–137. [CrossRef]
13. Mohanaraj, S.N.; Donough, C.R. Harvesting practices for maximum yield in oil palm: Results from a re-assessment at IJM Plantations, Sabah. *Oil Palm Bull.* **2016**, *72*, 32–37.
14. Mora, S.; Chinchilla, C.; Sánchez, A.; Escobar, R. Germinated oil palm (*Elaeis guineensis*) seeds: Process innovations to improve seed quality and performance of nursery plants. *Planter* **2007**, *83*, 435–446.
15. Al-Saif, A.; Alebidi, A.I.; Alobeed, R.; Soliman, S.S. Preharvest Ethephon spray on fruit quality and increasing the rate of ripening of date palm fruit (*Phoenix dactylifera* L.) cv. Helali. *Prog. Nutr.* **2017**, *19*, 97–103. [CrossRef]
16. Rouhani, I.; Bassiri, A. Effect of Ethephon on Ripening and Physiology of Date Fruits at Different Stages of Maturity. *J. Hortic. Sci.* **2015**, *52*, 289–297. [CrossRef]
17. Juntaraniyom, T.; Tongkum, P.; Eksomtramage, T.; Chuntanalurg, O. Use of calcium carbide and ethephon to stimulate fruit drop of oil palm. *Songklanakarin J. Sci. Technol.* **1996**, *18*, 293–299.
18. Nualwijit, N.; Lerslerwong, L. Post harvest ripening of oil palm fruit is accelerated by application of exogenous ethylene. *Songklanakarin J. Sci. Technol.* **2014**, *36*, 255–259.
19. Nurniwalis, A.W.; Zubaidah, R.; Siti Nor, A.A.; Suhaimi, N.; Massawe, F. Isolation and Characterisation of an ethylene receptor (ERS-Type) from Oil Palm (*Elaeis guineensis* Jacq.) Mesocarp. *J. Oil Palm Res.* **2018**, *30*, 251–264. [CrossRef]
20. Tranbarger, T.J.; Dussert, S.; Joët, T.; Argout, X.; Summo, M.; Champion, A.; Cros, D.; Omore, A.; Nouy, B.; Morcillo, F. Regulatory Mechanisms Underlying Oil Palm Fruit Mesocarp Maturation, Ripening, and Functional Specialization in Lipid and Carotenoid Metabolism. *Plant Physiol.* **2011**, *156*, 564–584. [CrossRef] [PubMed]
21. Mat Hassan, N.S.; Kua, S.F.; Noor Haizat, A.H.; Mustaner, M.; Mohd Hakimi, N.I.N.; Syed Hilmi, S.M.H.; Balakrishnan, A.; Tan, B.A.; Lim, C.M.; Jaime Low, Y.S.; et al. *Process for Producing Crude Palm Fruit Oil and Virgin Palm Fruit Oil*; Intellectual Property Corporation of Malaysia: Kuala Lumpur, Malaysia, 2021.
22. Malaysian Standard. *MS 157:2005 Oil Palm Seeds for Commercial Planting—Specification (Third Revision)*; Department of Standards Malaysia: Selangor, Malaysia, 2005.

23. *Minitab 20 Statistical Software*; Minitab Inc.: State College, PA, USA, 2020.

24. Soh, A.C.; Mayes, S.; Roberts, J.; Zaki, N.M.; Madon, M.; Schwarzacher, T.; Heslop-Harrison, P.; Ithnin, M.; Amiruddin, M.D.; Ramli, U.S.; et al. Molecular Genetics and Breeding. In *Oil Palm Breeding: Genetics and Genomics*; Aik, C.S., Mayes, S., Roberts, J., Eds.; CRC Press: Atlanta, FL, USA, 2017; pp. 225–281.

25. Bernama. Sime Darby Plantation: 'Genomeselect' Oil Palm Seeds Boost Yields on Existing Land. *Malay Mail*. 21 July 2020. Available online: https://www.malaymail.com/news/money/2020/07/21/sime-darby-plantation-genomeselect-oil-palm-seeds-boost-yields-on-existing/1886671 (accessed on 10 December 2020).

26. Shankar, A.C.; The Edge Markets. Sime Darby Plantation Plans to Fully Use GenomeSelect Seeds for Oil Palm Replanting from 2023. 2020. Available online: https://www.theedgemarkets.com/article/sime-darby-plantation-plans-fully-use-genomeselect-seeds-oil-palm-replanting-2023 (accessed on 20 August 2020).

27. Roongsattham, P.; Morcillo, F.; Jantasuriyarat, C.; Pizot, M.; Moussu, S.; Jayaweera, D.; Collin, M.; Gonzalez-Carranza, Z.H.; Amblard, P.; Tregear, J.W.; et al. Temporal and spatial expression of polygalacturonase gene family members reveals divergent regulation during fleshy fruit ripening and abscission in the monocot species oil palm. *BMC Plant Biol.* **2012**, *12*, 150. [CrossRef]

28. Chalil, D.; Basyuni, M.; Barus, R.; Putri, L.A. Smallholders' willingness to pay for dura marking oil palm seeds. *E3S Web Conf.* **2018**, *52*, 11. [CrossRef]

29. Singh, R.; Low, E.T.; Ooi, L.C.; Ong-Abdullah, M.; Ting, N.C.; Nagappan, J.; Nookiah, R.; Amiruddin, M.D.; Rosli, R.; Manaf, M.A.; et al. The oil palm SHELL gene controls oil yield and encodes a homologue of SEEDSTICK. *Nature* **2013**, *500*, 340–344. [CrossRef]

30. Teh, C.-K.; Lee, H.-L.; Abidin, H.; Ong, A.-L.; Mayes, S.; Chew, F.-T.; Appleton, D. A practical genome-enabled legitimacy assay for oil palm breeding and seed production. *BMC Plant Biol.* **2019**, *19*, 470. [CrossRef]

31. Dikin, A.; Kamaruzaman, S.; Zainal Abidin, M.A.; Idris Abu, S. Biological control of seedborne pathogen of oil palm, Schizopyllum commune Fr. with antagonistic bacteria. *Int. J. Agric. Biol.* **2003**, *5*, 507–512.

32. Pongprasert, N.; Srilaong, V.; Sugaya, S. An alternative technique using ethylene micro-bubble technology to accelerate the ripening of banana fruit. *Sci. Hortic.* **2020**, *272*, 109566. [CrossRef]

33. Wu, Q.; Bai, J.; Tao, X.; Mou, W.; Luo, Z.; Mao, L.; Ban, Z.; Ying, T.; Li, L. Synergistic effect of abscisic acid and ethylene on color development in tomato (*Solanum lycopersicum* L.) fruit. *Sci. Hortic.* **2018**, *235*, 169–180. [CrossRef]

34. Lv, J.; Zhang, M.; Zhang, J.; Ge, Y.; Li, C.; Meng, K.; Li, J. Effects of methyl jasmonate on expression of genes involved in ethylene biosynthesis and signaling pathway during postharvest ripening of apple fruit. *Sci. Hortic.* **2018**, *229*, 157–166. [CrossRef]

35. Kou, J.; Wei, C.; Zhao, Z.; Guan, J.; Wang, W. Effects of ethylene and 1-methylcyclopropene treatments on physiological changes and ripening-related gene expression of 'Mopan' persimmon fruit during storage. *Postharvest Biol. Technol.* **2020**, *166*, 111185. [CrossRef]

36. Suryanto, H.; Bardaie, M.Z. Effective treatment to hasten oil palm fruitlets abscission using ethephon. *AMA Agric. Mech. Asia Afr. Lat. Am.* **1994**, *25*, 40–44.

37. Ismail, W.I.W.; Yip, L.W.; Razali, M.H. Determination of the optimum frequency for Elaeis guineensis Jacq. detachment. *Afr. J. Agric. Res.* **2011**, *6*, 5656–5663.

38. Herrera, J.; Alizaga, R.; Guevara, E. Use of chemical treatments to induce seed germination in oil palm *Elaeis guineensis* Jacq. *ASD Oil Palm Pap.* **1998**, *18*, 1–16.

39. Bicalho, E.M.; Pintó-Marijuan, M.; Morales, M.; Müller, M.; Munné-Bosch, S.; Garcia, Q.S. Control of macaw palm seed germination by the gibberellin/abscisic acid balance. *Plant Biol.* **2015**, *17*, 990–996. [CrossRef] [PubMed]

40. Vanangamudi, K.; Zope, J.S.; Elam, W.W. Effect of Ethephon on Dormancy and Germination of Loblolly Pine (*Pinus taeda*) seed. *J. Trop. For. Sci.* **1999**, *11*, 503–506.

41. Heriansyah, C.; Tan, C. Nursery practices for production of superior oil palm planting materials. *Planter* **2005**, *81*, 159–171.

42. Wan, C.K.; Hor, H.L. A Study on the Effects of Certain Growth Substances on Germination of Oil Palm (*Elaeis quineensis* Jacq.) Seeds. *Pertanika* **1983**, *6*, 45–48.

43. Laksono, N.D.; Setiawati, U.; Nur, F.; Rahmaningsih, M.; Anwar, Y.; Rusfiandi, H.; Sembiring, E.H.; Forster, B.; Subbarao, A.S.; Zahara, H. *Nursery Practices in Oil Palm: A Manual*; CABI: Wallingford, UK, 2019; p. 120.

44. Mathews, J.; Tan, T.H.; Yong, K.K.; Chong, K.M.; Ng, S.K.; IP, W.M. Managing oil palm nursery: IOI's experience. *Planter* **2010**, *86*, 771–785.

45. MPOB. *Code of Good Nursery Practice for Oil Palm Nurseries*; MPOB CoP 1001:2015; MPOB: Kajang, Malaysia, 2016.

46. Sharma, M.; Vijiandran, J.; Applanaidu, M. Oil palm nursery management—A perspective from UP Bhd. In Proceedings of the International Seminar on Oil Planting Materials for Local & Overseas Joint Ventures, Hotel Istana, Asgard Information Services. Kuala Lumpur, Malaysia, December 2007.

47. Corley, R.H.V.; Tinker, P.B. Seed Germination and Nurseries. In *The Oil Palm*; Corley, R.H.V., Tinker, P.B., Eds.; Wiley Blackwell: Oxford, UK, 2016; p. 674.

Article

Extending Shelf Life and Maintaining Quality of Tomato Fruit by Calcium Chloride, Hydrogen Peroxide, Chitosan, and Ozonated Water

Said A. Shehata [1], Said Z. Abdelrahman [2], Mona M. A. Megahed [3], Emad A. Abdeldaym [1], Mohamed M. El-Mogy [1] and Karima F. Abdelgawad [1,*

[1] Vegetable Crops Department, Faculty of Agriculture, Cairo University, Giza 12613, Egypt; said_shehata2@yahoo.com (S.A.S.); emad.abdeldaym@agr.cu.edu.eg (E.A.A.); elmogy@agr.cu.edu.eg (M.M.E.-M.)
[2] Department of Postharvest Handling of Vegetables, Agriculture Research Center, Giza 12613, Egypt; profdrsaid.zakaria@yahoo.com
[3] Horticulture Department, Faculty of Agriculture, Aswan University, Aswan 81528, Egypt; monamahrouse98@gmail.com
* Correspondence: karima.abdelgawad@agr.cu.edu.eg

Abstract: Tomatoes are perishable fruit that makes them deteriorate rapidly during the post-harvest chain. Therefore, the effect of calcium chloride ($CaCl_2$), chitosan, hydrogen peroxide (H_2O_2), and ozonated water on the storage abil\ity and quality of tomato fruit (*Solanum lycopersicum* L. cv. 448) stored at 10 °C for 28 d was studied. Weight loss, firmness, fruit color, total soluble solids (TSS), titratable acidity, total carotenoids, and ascorbic acid content (AsA) of treated tomato fruit were recorded. Our results revealed that all tested treatments significantly extended the shelf-life and maintained quality of tomato fruit compared to the control. Chitosan and $CaCl_2$ were the most effective treatments in maintaining quality attributes. Furthermore, a correlation study suggested that AsA and total carotenoids played a vital role in conserving tomato fruit quality during storage. PC1 had strong positive loading for pH, appearance, firmness, AsA, TSS, carotene, fruit color (L* & b*) and a strong negative loading for lycopene content, color (a), weight loss, and color index. PC2 had high positive loading for total acidity and total sugar content.

Keywords: *Solanum lycopersicum*; antioxidants; storage; quality; postharvest

1. Introduction

Tomato (*Solanum lycopersicum* L.) is considered one of the most important vegetable crops worldwide for fresh market and processed products due to its health and economic importance [1]. It has been reported that tomato fruit have a considerable value of the most important antioxidants such as lycopene, carotenoids, vitamin C, and minerals, which can play a vital role for suppressing the development of some human diseases including prostate, colon, and breast cancers [2]. Additionally, consumption about 100 g of tomato can supply the human body with 40% of the recommended daily dosage of vitamin C which can enhance the immune system, lower blood pressure and cholesterol [3]. Furthermore, tomatoes are classified as a climacteric fruit and deteriorate rapidly after harvest due to soft textures and its susceptibility to microbial infection. Tomatoes are harvested at various maturity stages, including green mature, breaker, turning, light red, and full red. The most preferred stages for consumers are the light and full red stages, which decay vastly after harvest. Fruit and vegetables quality is mainly affected by postharvest conditions such as transportation and storage conditions [4]. Some previous postharvest application has been utilized to extend the shelf-life of tomatoes during storage such as using hydrogen sulfide [5], chitosan coating [6], abscisic acid [7], and the use of essential oils [8]. Previous studies showed that $CaCl_2$ reduced the fruit decay ratio and improved the hardness of

tissues and cell walls [9]. Chitosan is inexpensive and a natural compound which is obtained from chitin. Edible coating of chitosan alone or combined with essential oils provides an excellent antimicrobial agent, minimizing the fruit respiration and water loss rates [10,11]. Furthermore, the efficiency of oxidative substances, including ozone and H_2O_2 on stored vegetables and fruit, was mentioned previously in few reports [12,13]. However, to our knowledge, the effect of exogenous application of H_2O_2 and ozonated water on postharvest behavior of tomato fruit has not been reported before. Therefore, the aim of this study was to evaluate the effect of chitosan, $CaCl_2$, H_2O_2, and ozonated water as postharvest treatments on maintaining postharvest quality and prolonging the shelf life of tomato fruit during refrigerated storage.

2. Materials and Methods

2.1. Experimental Design and Treatments

Fruit of tomato hybrid cv. 448 (Syngenta company for seeds) were harvested at the breaker stage from a private farm (Abo Shalaby) in Ismailia Governorate, Egypt (30.5831° N, 32.2654° E). The tomato fruit were transported within one hour to the postharvest laboratory of the Vegetable Department, Faculty of Agriculture, Cairo University. Fruit free from any defects, diseases, unripe/immature, and uniform in size and weight (150 g, round type and large size) were chosen for the experiments. Selected tomato fruits were washed with tap water and then immersed in the following different solutions for 5 min. at room temperature: chitosan (0.5%) [10], calcium chloride (1%) [9], hydrogen peroxide (0.12%) [13], and ozonated water (1%) [12]. The control group was left without any treatments. The treated fruit where then left until fully dried at room temperature, packed in polystyrene trays (40 cm × 20 cm), and then covered by polyethylene sheet. Each tray had about 450 g (three fruit) of tomato fruit. The trays were stored for 28 days at 10 °C plus 2 days at 20 °C and 90–95% relative humidity (RH) in complete darkness. All measured parameters were recorded at time intervals of 0, 7, 14, 21, and 28 d. after applying treatments. The experiment was repeated twice with three replicates for each one and the averages were used.

2.2. Preparation Treatments Solutions

Chitosan 0.5% (*w:v*) (Qualikems, Vadodara, India) was dissolved in acetic acid 1% (*v:v*) (El-Nasr Company, Helwan, Egypt) then stirred using a magnetic stirrer for 6 h. in accordance to Xiao et al. [14]. Ozonated water was provided by an O_3 generator 101 (Cosemar Ozono, Madrid, Spain). Calcium chloride (Loba Chemie, Mumbai, India) was prepared at 1% by dissolving 1 g in 100 mL distilled water. Hydrogen peroxide 0.12% (*v:v*) was prepared by mixing 0.12 mL of hydrogen peroxide (Qualikems, Vadodara, India) in 100 mL distilled water in a homogenizer.

2.3. Appearance, Weight Loss, Color Parameters, and Firmness Determination

Appearance was evaluated using a scale from 9 to 1, where 9 = excellent, 7 = good (minor defect), 5 = fair (slightly to moderately objectionable defects), 3 = poor (excessive defect), 1 = unacceptable (extremely defect). Samples were submitted to six professional panelists from the vegetables department, Faculty of Agriculture, Cairo University, Giza, Egypt, for general appearance evaluation. Fruit rated 3 or below were considered as unmarketable. It was recorded for both the shriveling, wilting, color, change, and decay or any visible deterioration as described by Ali et al. [15]. Treated fruit were weighed after drying and at every sampling time to measure weight loss percentage as described by Awad et al. [16]. Fruit color was determined using a Chroma meter CR-400 (Konica Minolta, INC, Tokyo, Japan) for the estimation of L* (lightness), a* (change color from red to green), and b* (change color from yellow to blue). The color index (CI) was calculated according to Voss [17]. Fruit firmness was measured using a digital food pressure tester (Force Gauge Model M4-200 MARK) with a 2 mm diameter flat probe. Five fruits per

treatment were used to measure firmness at three points on the equatorial region. The results were expressed in kg·cm^{-2}.

2.4. Total Soluble Solids (TSS), Ascorbic Acid (AsA), and Titratable Acidity (TA) Determination

Total soluble solids (TSS) were evaluated using a digital refractometer (model PAL-1, Atago, Tokyo, Japan) and the values of TSS were expressed as °Brix. Ascorbic acid of tomato samples was determined using titration methods [18]. Briefly, ten gram of tomato fruit tissue was mixed with 90 mL of oxalic acid (6%) (Nice Chemical Ltd., Kochi, India). The sample was then filtered using a filter paper, 25 mL of filtrated solution was titrated by 2,6–dichlorophenol indophenol (Loba Chemie, Mumbai, India). The values were reported as mg/g fresh weight (FW).

The percentage of titratable acidity (TA) in tomato samples was determined by using 5 g of treated tomato fruit and homogenized with 50 mL of distilled water, then filtered. The aliquot was titrated with 0.1 N NaOH (El-Nasr Company, Giza, Egypt) using phenolphthalein as an indicator [19]. The values were reported as the percentage of citric acid, according to the following formula:

Acidity% = [(Titre value × Normality × m.eq.wt. of acid)/(Volume of sample)] × 100.

2.5. Total Sugar, Lycopene, and Carotenoid Contents Determination

Total sugar content was determined using the phenol-sulphuric acid (El-Nasr Company, Giza, Egypt) according to the method described by Shehata et al. [11]. Lycopene and carotenoid contents were measured according to the method described by Abdelgawad et al. [1]. Tomato samples were homogenized and one gram was mixed with a 10 mL mixture of Acetone-Hexane (4:6 *v:v* Merk, Darmstadt, Germany). The solution was then left to separate into distinct and non-polar layers. The spectrophotometer (Unico, UV2000, Rochester, NY, USA) was used to measurement of absorbance at 663, 645, 505, and 453 nm, and then lycopene and carotenoid content calculated according to the following equations:

Lycopene = −0.0458 × A 663 + 0.204 × A 645 + 0.372 × A 505 − 0.0806 × A 453,

B-carotene = 0.216 × A 663 − 1.22 × A 645 − 0.304 × A 505 + 0.452 × A 453.

2.6. Statistical Analysis

The data of experiments were subjected to the two-way analysis of variance (ANOVA) using the M.Stat software (Version 2.1, Michigan State University, East Lansing, MI, USA). Means of different treatments were compared by the Duncan test at 5% (LSD). The principal component analysis of the different applied solutions and physiochemical properties of tomato fruit, during the storage periods, were performed and displayed on the correlation heat map.

3. Results and Discussion

3.1. Appearance, Weight Loss, Color Parameters, and Firmness

Appearance was influenced by storage periods and treatments whereas the interaction was not significant (Table 1). As shown in Figure 1A, appearance of tomato fruit significantly reduced by increasing the storage period. Similar findings were confirmed by previous study [11]. They found that general appearance of strawberries decreased with increasing of storage period. The decrease in appearance during storage could be due to wilting, shriveling, color change, and deterioration [3]. All treatments significantly delayed the deterioration in fruit appearance (shriveling and color deterioration) during storage periods (Figure 1B). Both CaCl$_2$, and H$_2$O$_2$ treatments showed better appearance than other treatments or the control. Additionally, the difference between ozonated water treatment and the control was not significant. Previous study has shown that chitosan coating improves the external appearance and visual quality of fruits and vegetables, which

is consistent with our findings [20]. Additionally, CaCl$_2$ application conserved the appearance during storage [9,21]. The positive effect of chitosan could be attributed to its ability in reducing the respiration rate, moisture loss, ethylene production, delay product ripening, and inhibit the growth and development of undesirable microbes [22]. The beneficial effects of chitosan in conserving the appearance of tomato fruit during refrigerated storage could be also due to the reduction of lycopene degradation by chitosan treatment [20]. A strong negative correlation between appearance and weight loss was observed (Table 2).

Table 1. Analysis of variance (mean square) of tomato fruit attributes (appearance, weight loss, firmness, TSS and pH) stored at 10 °C for 28 days + 2 day at 20 °C and 90–95% RH.

Source	Appearance	Weight Loss (%)	Firmness (Kg/cm)	TSS	pH
Storage period (S)	57.42 ***	1973.2 ***	14.03 ***	6.87 ***	1.09 ***
Treatment (T)	1.48 **	110.29 ***	4.14 ***	6.94 ***	1.88 ***
S × T	0.703 [ns]	14.26 **	0.147 [ns]	1.08 ***	0.106 [ns]

[ns], **, *** not significant or significant at, $p \leq 0.01$, $p \leq 0.001$, analysis of variance.

Table 2. Pearson's correlation analysis between the physicochemical properties of tomato fruit.

Variables	Weight Loss	Appearance	Firmness	TSS	L*	a*	b*	pH	TA	AsA	Lycopene	Carotene	CI
Appearance	−0.91												
Firmness	−0.90	0.90											
TSS	−0.09	−0.14	0.13										
L*	−0.38	0.53	0.55	−0.21									
a*	0.78	−0.72	−0.82	−0.11	−0.29								
b*	−0.36	0.32	0.45	0.11	0.59	−0.31							
pH	−0.36	0.49	0.33	−0.36	−0.08	−0.42	−0.10						
TA	0.16	−0.47	−0.20	0.80	−0.35	0.04	0.02	−0.53					
VC	−0.80	0.72	0.85	0.23	0.54	−0.84	0.53	0.17	0.06				
Lycopene	0.85	−0.72	−0.88	−0.38	−0.33	0.83	−0.49	−0.16	−0.15	−0.88			
Carotene	−0.20	0.11	0.37	0.32	0.41	−0.49	0.36	−0.23	0.37	0.66	−0.44		
CI	0.73	−0.76	−0.85	0.00	−0.69	0.86	−0.57	−0.28	0.16	−0.86	0.76	−0.57	
Sugars	0.33	−0.57	−0.41	0.70	−0.54	0.22	−0.25	−0.51	0.89	−0.15	0.05	0.21	0.41

Values in bold are different from 0 with a significance level alpha = 0.05.
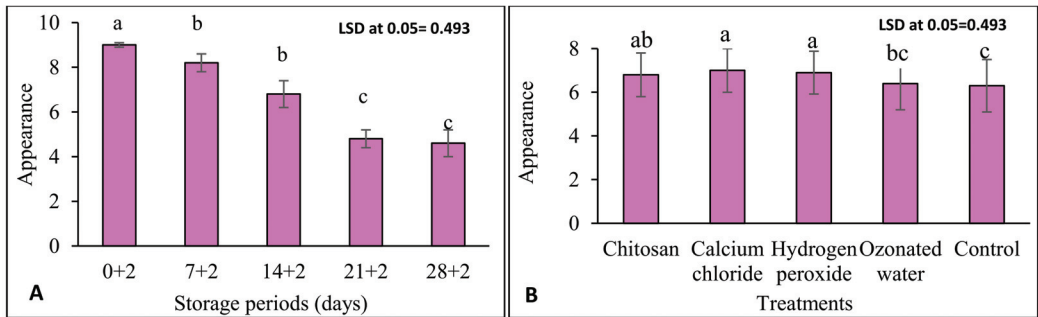
Figure 1. Appearance of tomato fruit as affected by storage periods (**A**) and treatments (**B**).

Weight loss is the most important factor for the quality and shelf-life of horticulture crops [18]. As shown in Table 1 and supplementary Table S1, weight loss, was affected by storage period, treatments, and their interactions. As expected, the weight loss increased during the storage period for all treatments (Figure 2A). After 7 + 2 days of storage and shelf-life until the end of storage, the percentage of weight loss of tomato fruit treated with CaCl$_2$, chitosan, ozonated water, and H$_2$O$_2$ was significantly ($p < 0.05$) lower than non-treated fruit (control) as well as reduced progress of ripening. The lowest value of weight loss was observed in chitosan treatment compared to all other treatments.
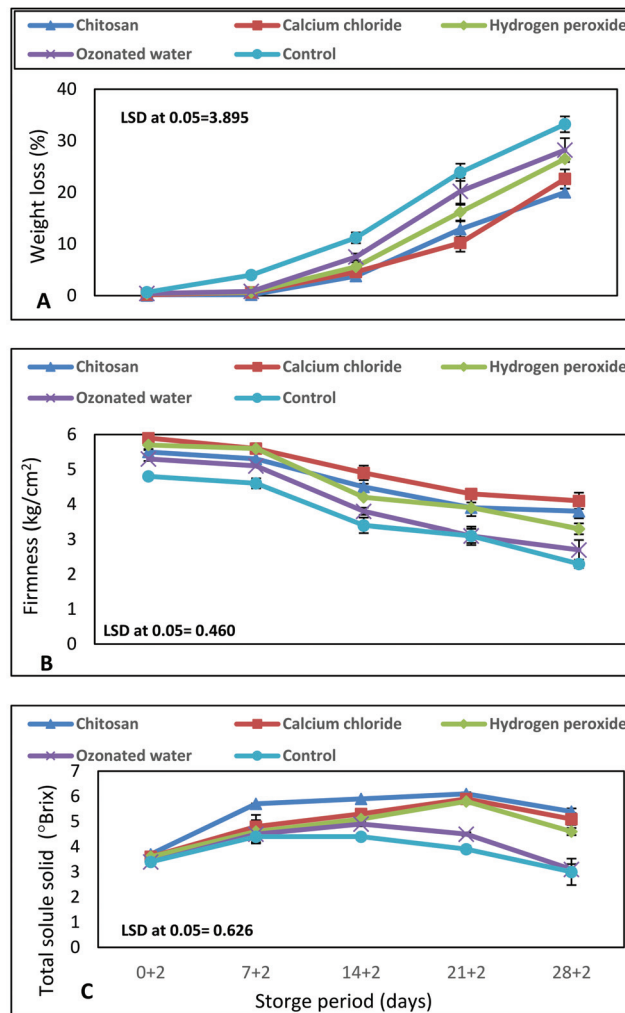
Figure 2. Weight loss% (**A**), firmness (**B**), and total soluble solid (°Brix) (**C**) of treated tomato fruit as affected by the interaction between the treatments and storage periods.

High relative air humidity and low temperature were employed to decrease posthar-vest water loss [23]. Thus, preventing water loss which could increase shelf-life of the fresh products. Weight loss was increased with increasing storage periods in all treatments and the control (Figure 2A). The high weight loss percentage at the end of storage period was related to the two days at shelf-life at 20 °C. It has been reported that water loss from fresh products causes unfavorable metabolic changes in plant cells which activate the enzymes. These enzymatic activities accelerate senescence and decrease the nutritional values [24]. Thus, the use of edible coating such as chitosan could help to prevent senescence and extend shelf-life. It is clear from current and previous reports that coating tomatoes with chitosan reduces weight loss when compared to the control fruit, most likely as a result of covering the cuticles on the fruit surfaces with chitosan [20]. The positive role of chitosan application in reducing weight loss of tomato fruit could be due to its ability to form a thin semipermeable film on the outer surface of the fruit which reduces transpiration [25].

Some previous studies have found that chitosan is effective for delaying weight loss in other commodities such as strawberries [26] and cucumber [27] which is in agreement with our results.

Moreover, the reduction in weight loss by $CaCl_2$ treatment could be due to the role of calcium in the creation of calcium pectate hydrogel, which holds more water and slows the dehydration process [28]. In our study, ozonated water treatment reduced weight loss compared to the control. This result is in agreement with Rodini et al. [29] who found that ozone treatment reduced weight loss of tomato fruit during storage at 20 °C for 9 d. Ozonated water treatment could reduce weight loss from tomato fruit by maintaining the cell wall and reducing pectin solubilization [30].

Firmness is considered one of the most important indicators of tomato quality [31]. Maturation process of tomato fruit affects the firmness and the composition of the cell wall polysaccharides [32]. In this study and previous studies, firmness of all tomato samples decreased with increasing storage time (Figure 2B and supplementary Table S1). This reduction in firmness is mainly due to the activity of some endogenous enzymes related to cell wall degradation [33]. Furthermore, softening changes have been linked to the degradation of the middle lamella of cortical parenchyma cells, which results in a significant increase in pectin solubilization [34]. During the entire storage period, the tomato fruit treated with chitosan and $CaCl_2$ were firmer than other treatments and the control. Chitosan and $CaCl_2$ treatments showed reduced ripening of fruits compared to other treatments and the control. Calcium is a key cation in plant nutrients which is required for maintaining firmness of the cell wall and middle lamella. It has been reported that application of exogenous calcium to fruit tissue maintains the structure of the cell wall and middle lamella which conserves firmness during cold storage [35]. In this study and previously, application of chitosan can also prevent the loss of tomatoes firmness under cold storage conditions [36]. This result might be due to the role of chitosan in reducing oxygen availability in tissue which reduces the activity of the enzymes responsible for firmness loss such as pectin-esterase and polygalacturonase resulting in higher firmness during storage [37]. It has been well known that H_2O_2 is an economical, safe, and sanitizing agent used for fruit and vegetables [38]. A strong negative correlation was recorded between firmness and the other parameters including a*, lycopene content, and color index. On the other hand, a positive correlation was found between firmness and L*, b*, and vitamin C (Table 2).

3.2. Total Soluble Solids and pH

Total soluble solids were gradually increased in chitosan, calcium chloride, and hydrogen peroxide treatments with extended storage period until 21 + 2 days of storage plus shelf-life, and then decreased until the end of the storage period (Figure 2C and supplementary Table S1). On the other hand, total soluble solids in ozonated water and control treatments were increased until the 14 + 2 days of storage period and then gradually decreased until the end of storage period. The increment in TSS might be due to the solubilization of cellulous and hemi-cellulous in cell wall [39] or water loss [18]. The decline of TSS at the end of the storage period could be due to the use of sugar in the respiratory process which decreases the level of TSS in all treatments and the control [40].

At the last two periods of storage, TSS values of chitosan, $CaCl_2$, and H_2O_2 treated fruit were higher than control and other treatments. Total soluble solids consist of some compounds such as sugar, vitamins, and acids which are mainly used for the respiration process. Previous work and our study indicated that chitosan application reduces the loss of TSS during storage [41]. It has been reported that TSS of tomatoes were increased and then decreased during the cold storage, which is in agreement with the results of this study [42]. Chitosan could preserve TSS by reducing the respiration process during cold storage [31]. It is reported that $CaCl_2$ treatment reduce respiration process [28]. As a result, the amount of TSS which is used for respiration in fruit treated with $CaCl_2$ is lower than untreated fruit. In this study, hydrogen peroxide was used as a disinfectant and it decrease

the loss of TSS during storage. This result is in agreement with previous work where H_2O_2 treatment also delayed the decline of TSS in muskmelon fruit [43]. In this study, positive correlation was noted between TSS and TA or total sugar (Table 2).

As shown in Figure 3A, the pH of tomato juice progressively decreased with increasing storage period. This result is in agreement with previous study on tomatoes. They noted a decrease in pH values until 21 days of refrigerated storage at 10 °C [34]. Figure 3B shows that a minimum value of pH was recorded in fruit treated with chitosan and $CaCl_2$. Negative correlation between pH and both TA and total sugar was observed (Table 2).
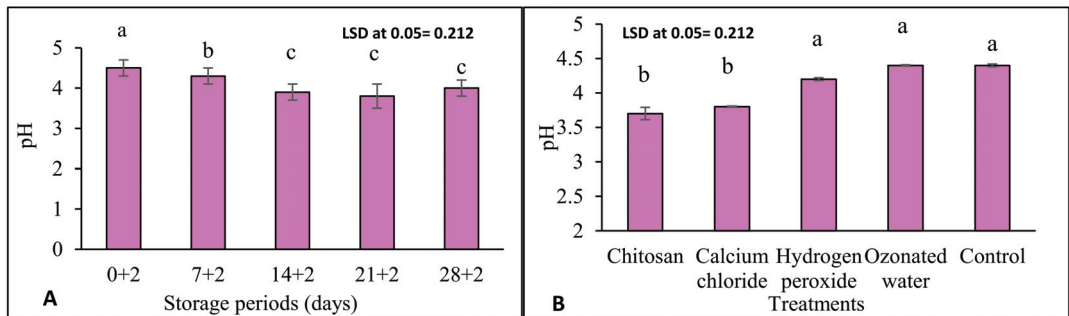
Figure 3. pH of tomato fruit as affected by storage periods (**A**) and treatments (**B**).

3.3. Surface Color Evaluation

Color is one of the major visual quality parameters that effects consumer acceptance of fresh products including tomato fruit. All color parameters L* (lightness), a* (green/red), b* (yellow/blue), and color index (CI) were significantly affected by the storage period, treatment, and their interaction (Table 3).

Table 3. Analysis of variance (mean square) of tomato fruit surface color.

Source	L*	a*	b*	Color Index
Storage period (S)	229.70 ***	741.40 ***	144.44 ***	1290.73 ***
Treatment (T)	68.32 ***	337.33 ***	44.19 ***	550.22 ***
S × T	36.84 ***	18.94 ***	29.57 ***	51.28 ***

*** significant at $p \leq 0.001$, analysis of variance.

The lightness (L*) of tomatoes fruit is one of the most important colorimetric parameters that is strongly affected during storage. The values of L* and b* of tomato fruit significantly decreased with increasing storage period, showing darker and less yellowing of fruits (Figure 4A,C and supplementary Table S1). This result is agreeing with Breda et al.'s study [24]. The reduction of L* during cold storage could be related to the surface dehydration which decrease surface glossiness [44]. Red color is one of the most attractive visual parameter to consumers [45]. Red color is gradually developed during tomato fruit ripening and maturation due to the degradation of chlorophyll and formation of lycopene pigment [46]. The values of a* and CI increased with increasing the storage period, showing redder and mature fruit (Figure 4B,D and supplementary Table S1). Chitosan treatment was the most effective treatment for conserving higher L* and b* values and lower a* and CI values during the entire storage period. This result indicated that chitosan treatment retarded the repining development (Figure 4). Our result is in agreement with previous works who indicated that chitosan treatment conserved higher L* and b* values [47,48] and a lower color (less red color) index during storage [49]. It was found that chitosan coating treatment reduced O_2 levels and increased CO_2 levels within tomato fruit which retarded ripening and color development [24,50]. As a result, the lower respiration rate can help to slow down the deterioration process and preserve fruit quality

after harvest. Additionally, application of chitosan as an edible coating on fruit surface could provide an additional gloss on fruit surface which increases and conserve the L* during cold storage [51]. Positive correlation was found between L* from one side and b*, vitamin C, and carotene from other side (Table 2). Additionally, a negative correlation between L* and both CI and total sugar was observed.
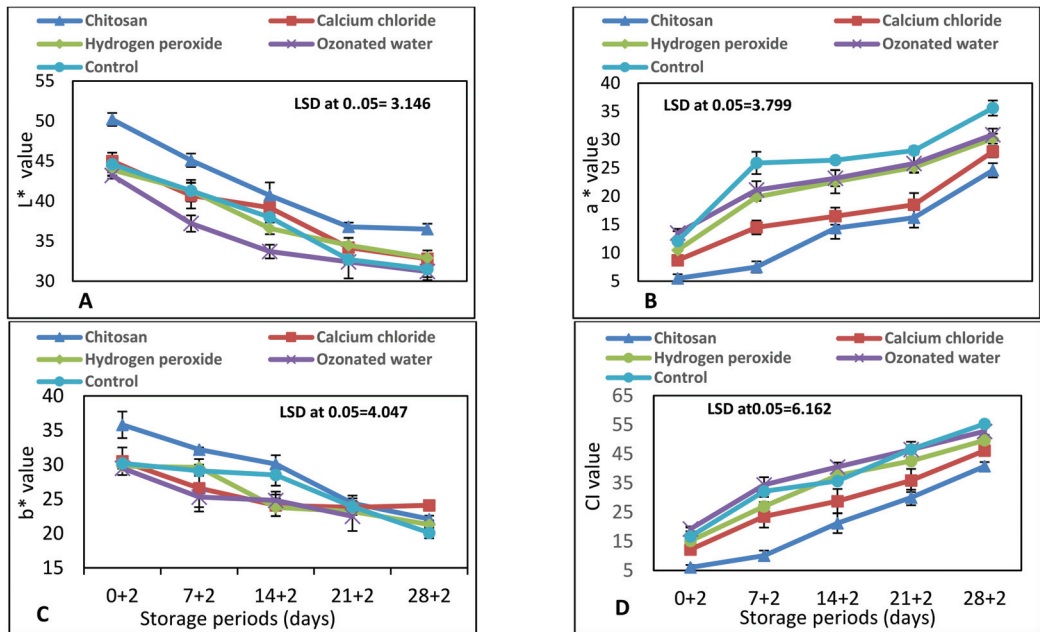
Figure 4. Values of L* (**A**), a* (**B**), b* (**C**), and CI (**D**) of tomato fruit as affected by the interaction between the treatments and storage periods.

3.4. Titratable Acidity and Ascorbic Acid

Titratable acidity and AsA, significantly affected by treatment, storage period and their interaction (Table 4). As shown in Figure 5A and supplementary Table S1, the content of TA in all treatments and the control increased constantly with increasing the storage period until 21 days of storage then decreased which is in agreement with previous work [36]. This increase in TA at the beginning of storage could be due to the increase of Cl^- ion [52]. Moreover, the reduction in TA content after 21 + 2 of storage might be attributed to the use of titratable acids in the respiration process and its metabolism [53]. In contrast with our results, previous work reported that TA in tomatoes decreased with increasing storage time [29]. The differences with our results may be due to the fact that our TA measurement was carried out after two days at 20 °C as a shelf-life. Thus, the increase in TA was recorded due to the high temperature of shelf-life storage which enhances the accumulation of titratable acids [54]. Chitosan treatment slowed the loss of TA in tomato fruit during refrigerated storage which is in agreement with previous results on pear fruit [37] and pineapple [55]. This result may be due to reduction of respiration rate by chitosan coating [37] via changes in the internal O_2 and CO_2 composition of the tissue. Additionally, it was reported that $CaCl_2$ treatment reduces the respiration process [56]. Thus, the amount of TA which is used in respiration process in tomato fruit treated with $CaCl_2$ is lower than untreated fruit. A strong positive correlation between TA and total sugar was observed (Table 2).

Table 4. Analysis of variance (mean square) of tomato fruit chemical properties.

Source	Titratable Acidity (%)	Ascorbic Acid (%)	Lycopene (mg/g)	Carotenoid (mg/g)	Sugar Content (mg/100 g)
Storage period (S)	0.104 ***	58.07 ***	0.046 ***	0.006 ns	17.213 ***
Treatment (T)	0.040 ***	46.95 ***	0.028 ***	0.542 ***	2.599 ***
S × T	0.004 **	2.77 ***	0.001 ***	0.007 ns	0.222 ***

ns, **, *** not significant or significant at $p \leq 0.01$, $p \leq 0.001$, analysis of variance
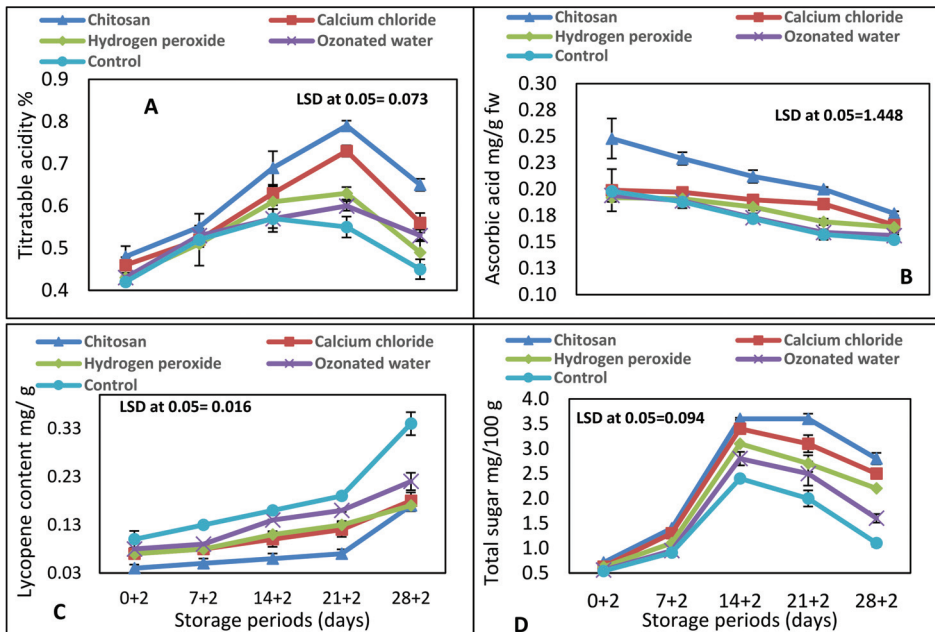
Figure 5. Titratable acidity (%) (**A**), ascorbic acid (**B**), lycopene (**C**), and total sugar contents (**D**) of tomato fruit as affected by the interaction between the treatments and storage period.

Ascorbic acid is the most important antioxidant compound present in tomato fruit [57]. Some pre and postharvest factors can affect AsA levels such as light during refrigerated storage [58]. They also noted that A_SA content was dependent on the maturity stage. Ascorbic acid content significantly decreased with the increasing of storage period for all treatments and the control (Figure 5B and supplementary Table S1). This decrease could be due to the use of AsA in respiration process [37] or the oxidation of AsA [38]. Figure 5B shows that chitosan coating was the most effective treatment for reducing the loss of vitamin C during storage followed by $CaCl_2$ and H_2O_2, respectively. It has been reported that chitosan coating maintained AsA in tomatoes [48] and some other fruit during storage such as papaya [59]. This result could be due to the low O_2 permeability of the chitosan coating resulting in lower respiration process [27,48] which conserved AsA from the loss. A strong negative correlation between AsA and lycopene content and CI was observed (Table 2).

3.5. Lycopene, Total Sugar Contents, and Carotenoids Contents

Lycopene is the pigment mainly accountable for the distinguishing red color of ripe tomato fruit. As shown in Figure 5C and supplementary Table S1, lycopene content was increased with increasing storage time in all treatments and the control. However, the increase in lycopene content was lower in fruit treated with chitosan, $CaCl_2$, H_2O_2,

and ozonated water than the untreated fruit. This result could be attributed to the role of chitosan and CaCl$_2$ for reducing respiration and maturity process [27,55] leading to slowing down of fruit ripening and lycopene biosynthesis. Some previous reports are in accordance with our results [36,48], they found that chitosan treatment increased retention of lycopene content during refrigerated storage of tomato fruit.

One of the most basic factors for evaluating fruit ripening in the fruit is total sugars [36]. In this study, total sugar content in tomato fruit for all treatments increased with prolongation of the storage period until the 14th day of storage and then decreased until the end of storage (Figure 5D and supplementary Table S1). These findings were consistent with previous works, who found that the sugar content of tomatoes increased as they matured from pink stage to red ripen [60,61]. The increase in total sugar content in tomato fruit during the first period of storage might be explained by the moisture loss during storage [62]. The decline in total sugar content in tomato fruit after 14 d from storage might be due to the consumption of total sugar in respiration process during storage [36]. Chitosan and CaCl$_2$ treatments maintained the highest level of total sugar content in tomato fruit throughout storage period as compared to the control. The previously observed result might be related to the hypotheses that chitosan and CaCl$_2$ control respiration process and their related metabolic activities leading to an accumulation of sugar content [55,63]. In this study, tomato fruit treated with H$_2$O$_2$, and ozonated water conserved higher total sugar content than the control.

Carotenoids have a dual role in tomato fruit. They act as antioxidants (thus alleviating oxidative stress) and they are of high value for human intake [64]. Chitosan and CaCl$_2$ treated fruit conserved significantly higher carotenoid content and delayed repining than the control and other treatments during storage period (Figure 6). The favorable effect of chitosan treatment on carotenoids retention until the end of refrigerated storage is consistent with previous studies on tomato [61,62]. This result may be related to the role of chitosan for reducing respiration rate which resulted in higher carotenoid content during storage. Furthermore, chitosan could preserve carotenoid from oxidation during storage [64]. CaCl$_2$ treatment conserved carotenoid content in tomato fruit during storage which could be due to its role for reducing respiration metabolism [55] resulting in higher carotenoid content. Negative correlation between lycopene and carotenoids content was observed while a strong positive correlation was recorded between lycopene and CI (Table 2).
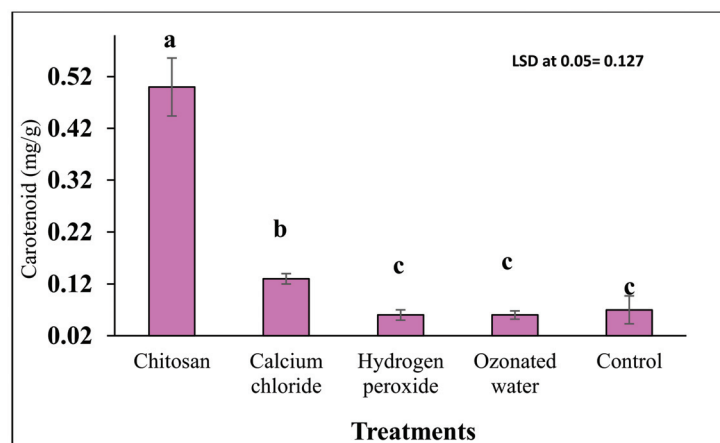
Figure 6. Carotenoid content (mg·g^{-1} fresh weight) of tomato fruit as affected by treatments.

4. Correlation Study

Principal component analysis (PCA), Pearson's correlation analysis, and Heatmap of the changes in physicochemical properties of tomato fruits during storage were presented in Table 2 and Figure 7. Considering the variances in the tomatoes quality, conserved at 10 °C for 28 days plus two days at 20 °C, treated with chitosan (CH) at 0.5%, calcium chloride (CaCl$_2$) at 1%, hydrogen peroxide (H$_2$O$_2$) at 0.12%, Ozonated water (O$_3$), 14 indexes of tomato fruits during storage periods were integrated using two-dimensional principal component analysis (PCA) with the SPSS 20.0 software. PCA was used to additional integrate and analyze the findings of postharvest quality indicators of tomato fruits. Principal components (PCs) denote 74.08% of the total variance of the data set. The contribution rate of PC1 and PC2 was 23.84% and 50.25% of the variance in the data set, respectively. PC1 had strong positive loading for pH, general appearance (appearance), firmness, AsA (V.C), TSS, carotene, fruit color (L* & b*) and a strong negative loading for lycopene content, color (a*), weight loss, and color index (CI).
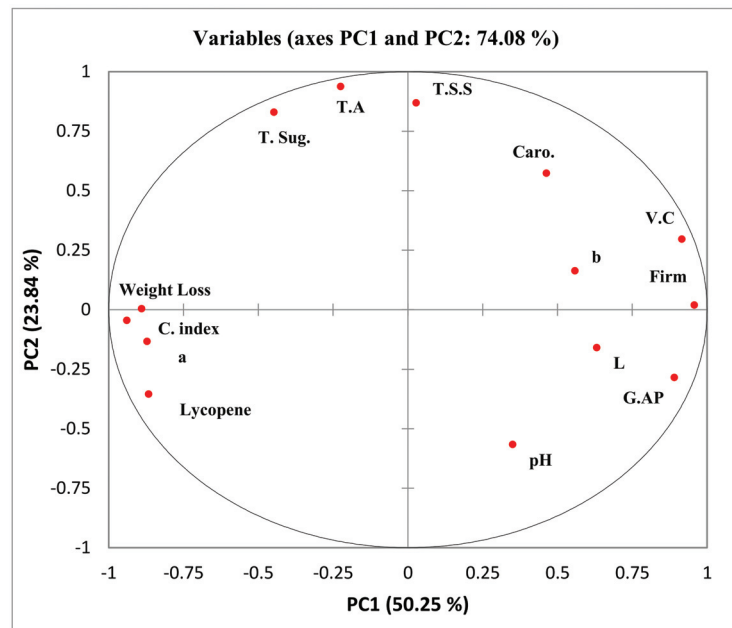
Figure 7. Principal component analysis of the main physicochemical quality of post-harvest tomato fruit.

PC2 had high positive loading for total acidity and total sugar content. Correlation-based method using the Pearson coefficient was used to observe the positive and negative correlations between the physiochemical parameters of treated and stored tomato fruits. Significant correlations (in bold number) and insignificant relationships (unbold number) are presented in Table 2. Pearson correlation analysis showed that a general appearance had a significant positive correlation with fruit firmness, L*, AsA, and total carotenoids. Meanwhile, it had a negative correlation with weight loss, a value, total sugar, lycopene, and color index and TA which is indicated to fruit ripening. Carotenoids significantly and positively correlated with VC, L* value, appearance and negatively with C. index, a* value, lycopene content of tomato fruits.

In Figure 8 (heatmap), it can be clearly seen the changes in physicochemical properties of treated tomato fruits during storage periods. Generally, general appearance, pH, vitamin C, firmness, TSS, carotenoids, L value and b value of tomato fruits were gradually

reduced with the storage period; fruit weight loss, sugar content, color index, and lycopene were slowly increased. At the end of storage periods (28 + 2 d), highest content of vitamin C, firmness, TSS, carotenoids, L* value and b* of tomato fruits treated with chitosan and CaCl$_2$. Furthermore, these treatments also reduced the content of lycopene, value a, and color index than other treatments. This finding indicated that the treatment with chitosan and CaCl$_2$ were effective to delay the color changes, retard the ripening process and senescence of tomato fruit (Figure 6). Moreover, both treatments also maintained the well-appearance and alleviated decline the nutrient contents of tomatoes, such as vitamin C, total sugar, and total carotenoids.
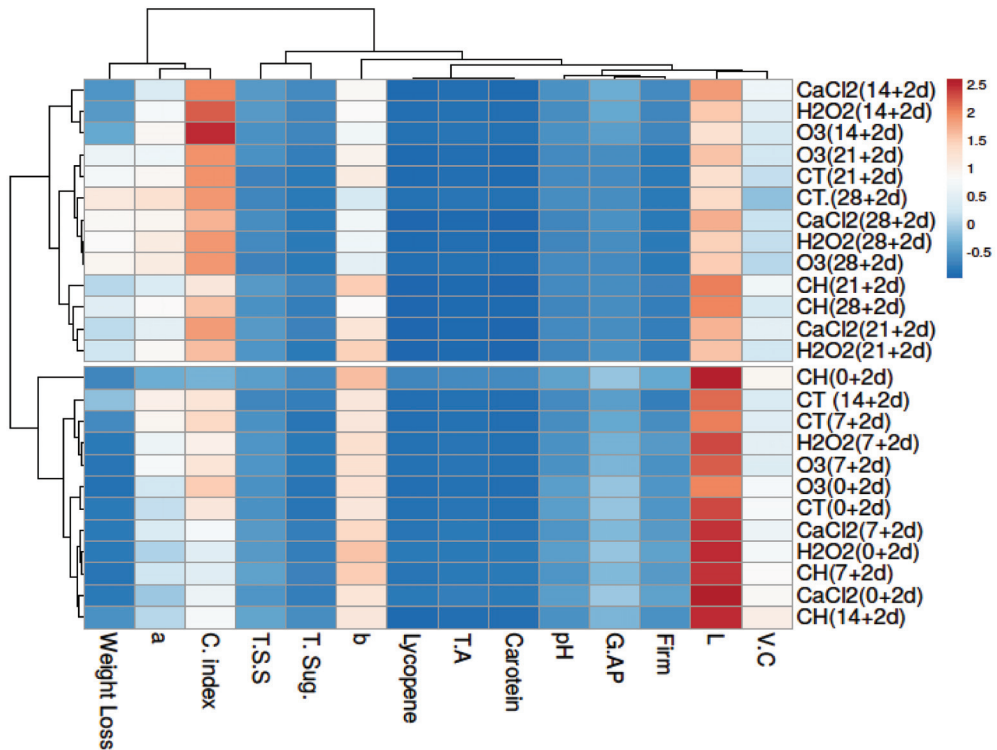
Figure 8. Correlation heat map between physiochemical quality of tomato fruit after 28 days of storage at 10 °C and following 2 days of storage at 20 °C. Positive relationships are presented in red color and negative relationships in blue color.

5. Conclusions

The results of this study indicate that tomato fruit treated with chitosan or CaCl$_2$ were the most applicable treatments for retarding tomato fruit repining and extending shelf-life. Both treatments have a positive and favorable effect in preserving the physiochemical properties of tomato fruit during preservation. Treatments with chitosan or CaCl$_2$ reduced storage-induced alterations such as weight loss, TSS, firmness, pH, CI, and total lycopene and carotenoids while preserving the contents of sugars. The multivariate statistical analyses showed that the firmness and content of L*, a*, b*, TA, pH, carotenoids, lycopene, sugar, and TSS correlated with CI and general appearance. It can be concluded that these physiochemical qualities can be used as indicators for CI and appearance based on multivariate statistical analyses. However, treated tomato fruit had lower CI and higher appearance and nutrient value, particularly in those treated with chitosan and CaCl$_2$

solutions. Finally, it implied that both previous treatments might be effective in regulating the ripening and delaying senescence of post-harvest fruit under cold storage conditions.

References

1. Abdelgawad, K.F.; El-Mogy, M.M.; Mohamed, M.I.A.; Garchery, C.; Stevens, R.G. Increasing Ascorbic Acid Content and Salinity Tolerance of Cherry Tomato Plants by Suppressed Expression of the Ascorbate Oxidase Gene. *Agronomy* **2019**, *9*, 51. [CrossRef]
2. Tsaniklidis, G.; Charova, S.N.; Fanourakis, D.; Tsafouros, A.; Nikoloudakis, N.; Goumenaki, E.; Tsantili, E.; Roussos, P.A.; Spiliopoulos, I.K.; Paschalidis, K.A.; et al. The role of temperature in mediating postharvest polyamine homeostasis in tomato fruit. *Postharvest Biol. Technol.* **2021**, *179*, 111586. [CrossRef]
3. Zeng, C.; Tan, P.; Liu, Z. Effect of exogenous ARA treatment for improving postharvest quality in cherry tomato (*Solanum lycopersicum* L.) fruits. *Sci. Hortic.* **2020**, *261*, 108959. [CrossRef]
4. Al-Dairi, M.; Pathare, P.B.; Al-Yahyai, R. Effect of Postharvest Transport and Storage on Color and Firmness Quality of Tomato. *Horticulturae* **2021**, *7*, 163. [CrossRef]
5. Yao, G.-F.; Li, C.; Sun, K.-K.; Tang, J.; Huang, Z.-Q.; Yang, F.; Huang, G.-G.; Hu, L.-Y.; Jin, P.; Hu, K.-D.; et al. Hydrogen Sulfide Maintained the Good Appearance and Nutrition in Post-harvest Tomato Fruit by Antagonizing the Effect of Ethylene. *Front. Plant Sci.* **2020**, *11*, 584. [CrossRef]
6. Zhu, Y.; Li, D.; Belwal, T.; Li, L.; Chen, H.; Xu, T.; Luo, Z. Effect of Nano-SiOx/Chitosan Complex Coating on the Physicochemical Characteristics and Preservation Performance of Green Tomato. *Molecules* **2019**, *24*, 4552. [CrossRef]
7. Tao, X.; Wu, Q.; Aalim, H.; Li, L.; Mao, L.; Luo, Z.; Ying, T. Effects of Exogenous Abscisic Acid on Bioactive Components and Antioxidant Capacity of Postharvest Tomato during Ripening. *Molecules* **2020**, *25*, 1346. [CrossRef]
8. Tzortzakis, N.; Xylia, P.; Chrysargyris, A. Sage Essential Oil Improves the Effectiveness of Aloe vera Gel on Postharvest Quality of Tomato Fruit. *Agronomy* **2019**, *9*, 635. [CrossRef]
9. El-Mogy, M.M.; Parmar, A.; Ali, M.R.; Abdel-Aziz, M.E.; Abdeldaym, E.A. Improving postharvest storage of fresh artichoke bottoms by an edible coating of Cordia myxa gum. *Postharvest Biol. Technol.* **2020**, *163*, 111143. [CrossRef]
10. Peralta-Ruiz, Y.; Tovar, C.D.; Sinning-Mangonez, A.; Coronell, E.A.; Marino, M.F.; Chaves-Lopez, C. Reduction of Postharvest Quality Loss and Microbiological Decay of Tomato "Chonto" (*Solanum lycopersicum* L.) Using Chitosan-E Essential Oil-Based Edible Coatings under Low-Temperature Storage. *Polymers* **2020**, *12*, 1822. [CrossRef]
11. Shehata, S.A.; Abdeldaym, E.A.; Ali, M.R.; Mohamed, R.M.; Bob, R.I.; Abdelgawad, K.F. Effect of Some Citrus Essential Oils on Post-Harvest Shelf Life and Physicochemical Quality of Strawberries during Cold Storage. *Agronomy* **2020**, *10*, 1466. [CrossRef]
12. Mustapha, A.T.; Zhou, C.; Wahia, H.; Amanor-Atiemoh, R.; Otu, P.; Qudus, A.; Fakayode, O.A.; Ma, H. Sonozonation: Enhancing the antimicrobial efficiency of aqueous ozone washing techniques on cherry tomato. *Ultrason. Sonochem.* **2020**, *64*, 105059. [CrossRef] [PubMed]
13. Kim, H.J.; Fonseca, J.M.; Kubota, C.; Choi, J.H. Effect of Hydrogen Peroxide on Quality of Fresh-Cut Tomato. *J. Food Sci.* **2007**, *72*, S463–S467. [CrossRef]
14. Xiao, C.; Zhu, L.; Luo, W.; Song, X.; Deng, Y. Combined action of pure oxygen pretreatment and chitosan coating incorporated with rosemary extracts on the quality of fresh-cut pears. *Food Chem.* **2010**, *121*, 1003–1009. [CrossRef]

15. Ali, M.R.; Parmar, A.; Niedbała, G.; Wojciechowski, T.; El-Yazied, A.A.; El-Gawad, H.G.A.; Nahhas, N.E.; Ibrahim, M.F.M.; El-Mogy, M.M. Improved Shelf-Life and Consumer Acceptance of Fresh-Cut and Fried Potato Strips by an Edible Coating of Garden Cress Seed Mucilage. *Foods* **2021**, *10*, 1536. [CrossRef]

16. Awad, A.H.R.; Parmar, A.; Ali, M.R.; El-Mogy, M.M.; Abdelgawad, K.F. Extending the Shelf-Life of Fresh-Cut Green Bean Pods by Ethanol, Ascorbic Acid, and Essential Oils. *Foods* **2021**, *10*, 1103. [CrossRef]

17. Voss, D.H. Relating colourimeter measurement of plant colour to the royal horticultural society colour chart. *HortScience* **1992**, *27*, 1256–1260. [CrossRef]

18. Shehata, S.A.; El-Mogy, M.M.; Mohamed, H.F.Y. Postharvest quality and nutrient contents of long sweet pepper enhanced by supplementary potassium foliar application. *Int. J. Veg. Sci.* **2019**, *25*, 196–209. [CrossRef]

19. Perdones, Á.; Escriche, I.; Chiralt, A.; Vargas, M. Effect of chitosan-lemon essential oil coatings on volatile profile of strawberries during storage. *Food Chem.* **2016**, *197*, 979–986. [CrossRef]

20. Kibar, H.F.; Sabir, F.K. Chitosan coating for extending postharvest quality of tomatoes (*Lycopersicon esculentum* Mill.) maintained at different storage temperatures. *AIMS Agric. Food* **2018**, *3*, 97–108. [CrossRef]

21. Safari, Z.S.; Ding, P.; Nakasha, J.J.; Yusoff, S.F. Combining Chitosan and Vanillin to Retain Postharvest Quality of Tomato Fruit during Ambient Temperature Storage. *Coatings* **2020**, *10*, 1222. [CrossRef]

22. Velickova, E.; Eleonora, W.; Margarida, M.O.-M.; Slobodanka, K.; Vitor, D.A. Impact of chitosan-beeswax edible coatings on the quality of fresh strawberries (Fragaria ananassa cv Camarosa) under commercial storage conditions. *LWT-Food Sci. Technol.* **2013**, *52*, 80–92. [CrossRef]

23. Fanourakis, D.; Aliniaeifard, S.; Sellin, A.; Giday, H.; Körner, O.; Rezaei Nejad, A.; Delis, C.; Bouranis, D.; Koubouris, G.; Kambourakis, E.; et al. Stomatal behavior following mid- or long-term exposure to high relative air humidity: A review. *Plant Physiol. Biochem.* **2020**, *153*, 92–105. [CrossRef]

24. Breda, C.A.; Morgado, D.L.; de Assis, O.B.G.; Duarte, M.C.T. Effect of chitosan coating enriched with pequi (Caryocar brasiliense Camb.) peel extract on quality and safety of tomatoes (*Lycopersicon esculentum* Mill.) during storage. *J. Food Process. Preserv.* **2017**, *41*, e13268. [CrossRef]

25. Lin, Y.; Li, N.; Lin, H.; Lin, M.; Chen, Y.; Wang, H.; Ritenour, M.A.; Lin, Y. Effects of chitosan treatment on the storability and quality properties of longan fruit during storage. *Food Chem.* **2020**, *306*, 125627. [CrossRef] [PubMed]

26. Ribeiro, C.; Vicente, A.A.; Teixeira, J.A.; Miranda, C. Optimization of edible coating composition to retard strawberry fruit senescence. *Postharvest Biol. Technol.* **2007**, *44*, 63–70. [CrossRef]

27. Olawuyi, I.F.; Park, J.; Lee, J.J.; Lee, W.Y. Combined effect of chitosan coating and modified atmosphere packaging on fresh-cut cucumber. *Food Sci. Nutr.* **2019**, *7*, 1043–1052. [CrossRef]

28. Turmanidze, T.; Gulua, L.; Jgenti, M.; Wicker, L. Potential antioxidant retention and quality maintenance in raspberries and strawberries treated with calcium chloride and stored under refrigeration. *Braz. J. Food Technol.* **2017**, *20*. [CrossRef]

29. Rodoni, L.; Casadei, N.; Concellón, A.; Chaves Alicia, A.R.; Vicente, A.R. Effect of Short-Term Ozone Treatments on Tomato (*Solanum lycopersicum* L.) Fruit Quality and Cell Wall Degradation. *J. Agric. Food Chem.* **2010**, *58*, 594–599. [CrossRef]

30. Sauqi, A.; Sjah, T.; Desiana, R.Y. Combination of ozone and packaging treatments maintained the quality and improved the shelf life of tomato fruit. In *IOP Conference Series: Earth and Environmental Science*; IOP Publishing: Bristol, UK, 2018; Volume 102, p. 012027. [CrossRef]

31. Mostofi, Y.; Toivonen, P.M.A.; Lessani, H.; Babalar, M.; Lu, C. Effects of 1-methylcyclopropene on ripening of greenhouse tomatoes at three storage temperatures. *Postharvest Biol. Technol.* **2003**, *27*, 285–292. [CrossRef]

32. Saladié, M.; Matas, A.J.; Isaacson, T.; Jenks, M.A.; Goodwin, S.M.; Niklas, K.J.; Xiaolin, R.; Labavitch, J.M.; Shackel, K.A.; Fernie, A.R.; et al. A reevaluation of the key factors that influence tomato fruit softening and integrity. *Plant Physiol.* **2007**, *144*, 1012–1028. [CrossRef]

33. Seymour, G.B.; Taylor, J.E.; Tucker, G.A. *Biochemistry of Fruit Ripening*; Chapman & Hall: London, UK, 1993.

34. García, M.; Casariego, A.; Díaz, R.; Roblejo, L. Effect of edible chitosan/zeolite coating on tomatoes quality duringrefrigerated storage. *Emir. J. Food Agric.* **2014**, *26*, 238–246. [CrossRef]

35. Gago, C.M.L.; Guerreiro, A.C.; Miguel, G.; Panagopoulos, T.; da Silva, M.M.; Antunes, M.D.C. Effect of Calcium chloride and 1-MCP (Smartfresh™) postharvest treatment on 'Golden Delicious' apple cold storage physiological disorders. *Sci. Hortic.* **2016**, *211*, 440–448. [CrossRef]

36. Benhabiles, M.S.; Tazdait, D.; Abdi, N.; Lounici, H.; Drouiche, N.; Goosen, M.F.A.; Mameri, N. Assessment of coating tomato fruit with shrimp shell chitosan and *N,O*-carboxymethyl chitosan on postharvest preservation. *J. Food Meas. Charact.* **2013**, *7*, 66–74. [CrossRef]

37. Hesami, A.; Kavoosi, S.; Khademi, R.; Sarikhani, S. Effect of Chitosan Coating and Storage Temperature on Shelf-Life and Fruit Quality of Ziziphus Mauritiana. *Int. J. Fruit Sci.* **2021**, *21*, 509–518. [CrossRef]

38. de Siqueira Oliveira, L.; Eça, K.S.; de Aquino, A.C.; Vasconcelos, L.B. Chapter 4—Hydrogen Peroxide (H$_2$O$_2$) for Postharvest Fruit and Vegetable Disinfection. In *Postharvest Disinfection of Fruit and Vegetables*; Siddiqui, M.W., Ed.; Academic Press: Cambridge, MA, USA, 2018; pp. 91–99.

39. Hernández-Muñoz, P.; Almenar, E.; Valle, V.D.; Velez, D.; Gavara, R. Effect of chitosan coating combined with postharvest calcium treatment on strawberry (Fragaria × ananassa) quality during refrigerated storage. *Food Chem.* **2008**, *110*, 428–435. [CrossRef]

40. Gol, N.B.; Patel, P.R.; Rao, T.V.R. Improvement of quality and shelf-life of strawberries with edible coatings enriched with chitosan. *Postharvest Biol. Technol.* **2013**, *85*, 185–195. [CrossRef]
41. Chiabrando, V.; Giacalone, G. Effect of different coatings in preventing deterioration and preserving the quality of fresh-cut nectarines (cv Big Top). *CyTA-J. Food* **2013**, *11*, 285–292. [CrossRef]
42. Gharezi, M.; Joshi, N.; Sadeghian, E. Effect of post-harvest treatment on stored cherry tomatoes. *J. Nutr. Food Sci.* **2012**, *2*, 157. [CrossRef]
43. Chen, G.; Chen, J.; Feng, Z.; Mao, X.; Guo, D. Physiological responses and quality attributes of Jiashi muskmelon (Cucurbitaceae, *Cucumis melo* L.) following postharvest hydrogen peroxide treatment during storage. *Eur. J. Hortic. Sci.* **2015**, *80*, 288–295. [CrossRef]
44. Perdones, Á.; Tur, N.; Chiralt, A.; Vargas, M. Effect on tomato plant and fruit of the application of biopolymer–oregano essential oil coatings. *J. Sci. Food Agric.* **2016**, *96*, 4505–4513. [CrossRef] [PubMed]
45. Arias, R.; Lee, T.C.; Logendra, L.; Janes, H. Correlation of lycopene measured by HPLC with the L, a, b color readings of a hydroponic tomato and the relationship of maturity with color and lycopene content. *J. Agric. Food Chem.* **2000**, *48*, 1697–1702. [CrossRef] [PubMed]
46. Wu, M.; Kubota, C. Effects of high electrical conductivity of nutrient solution and its application timing on lycopene, chlorophyll and sugar concentrations of hydroponic tomatoes during ripening. *Sci. Hortic.* **2008**, *116*, 122–129. [CrossRef]
47. Meena, M.; Pilania, S.; Pal, A.; Mandhania, S.; Bhushan, B.; Kumar, S.; Gohari, G.; Saharan, V. Cu-chitosan nano-net improves keeping quality of tomato by modulating physio-biochemical responses. *Sci. Rep.* **2020**, *10*, 21914. [CrossRef]
48. Ghaouth, A.E.; Ponnampalam, R.; Castaigne, F.; Arul, J. Coating to Extend the Storage Life of Tomatoes. *HortScience* **1992**, *27*, 1016–1018. [CrossRef]
49. Gago, C.; Antão, R.; Dores, C.; Guerreiro, A.; Miguel, M.G.; Faleiro, M.L.; Figueiredo, A.C.; Antunes, M.D. The Effect of Nanocoatings Enriched with Essential Oils on 'Rocha' Pear Long Storage. *Foods* **2020**, *9*, 240. [CrossRef]
50. Souty, M.; Reich, M.; Breuils, L.; Chambroy, Y.; Jacquemin, G.; Audergon, J.M. Effects of Postharvest Calcium Treatments on Shelf-life and Quality of Apricot Fruit. In *X International Symposium on Apricot Culture 384*; Acta Horticulturae: Leuven, Belgium, 1995; pp. 619–624.
51. Baldwin, E.A.; Hagenmaier, R.D. Introduction. In *Edible Coatings and Films to Improve Food Quality*; Baldwin, E.A., Hagenmaier, R.D., Bai, J., Eds.; CRC Press: New York, NY, USA, 2011; pp. 1–12.
52. Sogvar, O.B.; Saba, M.K.; Emamifar, A. Aloe vera and ascorbic acid coatings maintain postharvest quality and reduce microbial load of strawberry fruit. *Postharvest Biol. Technol.* **2016**, *114*, 29–35. [CrossRef]
53. Toor, R.K.; Savage, G.P. Changes in major antioxidant components of tomatoes during post-harvest storage. *Food Chem.* **2006**, *99*, 724–727. [CrossRef]
54. Ibrahim, S.M.; Nahar, S.; Islam, J.; Islam, M.; Hoque, M.; Khan, M.A. Effect of Low Molecular Weight Chitosan Coating on Physico-chemical Properties and Shelf life Extension of Pineapple (*Ananas sativus*). *J. For. Prod. Ind.* **2014**, *3*, 161–166.
55. Robert, A.S.; William, S.C.; Carl, E.S. Postharvest Calcium Infiltration Alone and Combined with Surface Coating Treatments Influence Volatile Levels, Respiration, Ethylene Production, and Internal Atmospheres of 'Golden Delicious' Apples. *J. Am. Soc. Hortic. Sci. Jashs* **1999**, *124*, 553–558. [CrossRef]
56. El-Mogy, M.M.; Garchery, C.; Stevens, R. Irrigation with salt water affects growth, yield, fruit quality, storability and marker-gene expression in cherry tomato. *Acta Agric. Scand. Sect. B—Soil Plant Sci.* **2018**, *68*, 727–737. [CrossRef]
57. Zhang, Y.; Ntagkas, N.; Fanourakis, D.; Tsaniklidis, G.; Zhao, J.; Cheng, R.; Yang, Q.; Li, T. The role of light intensity in mediating ascorbic acid content during postharvest tomato ripening: A transcriptomic analysis. *Postharvest Biol. Technol.* **2021**, *180*, 111622. [CrossRef]
58. Ali, A.; Muhammad, M.T.M.; Sijam, K.; Siddiqui, Y. Effect of chitosan coatings on the physicochemical characteristics of Eksotika II papaya (*Carica papaya* L.) fruit during cold storage. *Food Chem.* **2011**, *124*, 620–626. [CrossRef]
59. Sinaga, R.M. Effect of maturity stages on quality of tomato cv. Money marker. *Bull. Penelit. Hortic.* **1986**, *13*, 43–53.
60. Moneruzzaman, K.M.; Hossain, A.B.M.S.; Sani, W.; Alenazi, M. Effect of harvesting and storage conditions on the postharvest quality of tomato (*Lycopersicon esculentum* Mill). *Aust. J. Crop Sci.* **2009**, *3*, 113–121.
61. Migliori, C.A.; Salvati, L.; Di Cesare, L.F.; Lo Scalzo, R.; Parisi, M. Effects of preharvest applications of natural antimicrobial products on tomato fruit decay and quality during long-term storage. *Sci. Hortic.* **2017**, *222*, 193–202. [CrossRef]
62. Zhang, J.; Zhang, S.; Yu, Y.; Ren, Y. Cherry tomato preservation using chitosan combined with zinc/cerium ion. *Int. J. Nutr. Food Sci.* **2014**, *3*, 111–118.
63. Chen, Y.; Fanourakis, D.; Tsaniklidis, G.; Aliniaeifard, S.; Yang, Q.; Li, T. Low UVA intensity during cultivation improves the lettuce shelf-life, an effect that is not sustained at higher intensity. *Postharvest Biol. Technol.* **2021**, *172*, 111376. [CrossRef]
64. Salinas-Roca, B.; Guerreiro, A.; Welti-Chanes, J.; Antunes, M.D.C.; Martín-Belloso, O. Improving quality of fresh-cut mango using polysaccharide-based edible coatings. *Int. J. Food Sci. Technol.* **2018**, *53*, 938–945. [CrossRef]

Article

Effect of Postharvest Transport and Storage on Color and Firmness Quality of Tomato

Mai Al-Dairi [1], Pankaj B. Pathare [1,*] and Rashid Al-Yahyai [2]

[1] Department of Soils, Water and Agricultural Engineering, College of Agricultural & Marine Sciences, Sultan Qaboos University, Muscat 123, Oman; s124911@student.squ.edu.om

[2] Department of Plant Sciences, College of Agricultural & Marine Sciences, Sultan Qaboos University, Muscat 123, Oman; alyahyai@squ.edu.om

* Correspondence: pankaj@squ.edu.om; Tel.: +968-2414-1222

Abstract: Transport duration affects the vibration level generated which has adverse effects on fresh produce during transportation. Furthermore, temperature affects the quality of fresh commodities during storage. This study evaluated physical changes in tomatoes during transportation and storage. Tomatoes were transported at three distances (100, 154, and 205 km) from a local farm and delivered to the Postharvest Laboratory where vibration acceleration was recorded per distance. Tomato was stored at two different temperatures (10 °C and 22 °C) for 12 days. The physical qualities like weight loss and firmness of all tomato samples were evaluated. RGB image acquisition system was used to assess the color change of tomato. The results of vibration showed that over 40% of accelerations occurred in the range of 0.82–1.31 cm/s^2 of all transport distances. Physical quality analyses like weight loss and firmness were highly affected by transportation distance, storage temperature, and storage period. The reduction in weight loss and firmness was the highest in tomatoes transported from the farthest distance and stored at 22 °C. Lightness, yellowness, and hue values showed a high reduction as transport distance increased particularly in tomatoes stored at 22 °C. Redness, total color difference, and color indices increased significantly on tomatoes transported from 205 km and stored at 10 °C and 22 °C. The study indicated that the increase in transportation distance and storage temperature cause higher changes in the physical qualities of tomatoes.

Keywords: quality; vibration; tomato; transportation

1. Introduction

Consumers prefer high-quality fresh produce, which is primarily assessed based on their appearance and taste [1]. For this reason, the fresh produce provided to the market should meet the international standards of quality for freshness, firmness, and other quality characteristics [2,3]. Throughout postharvest operations like harvesting, handling processing, storing, and transporting, fresh produce is subjected to different external forces. Therefore, this reduces product quality and decreasing sale prices as well as losses to the orchardists and growers [4]. Transportation is an essential process during the postharvest supply chain of any fresh produce [5]. However, transportation could cause postharvest losses leading to high economic losses [6] if it is not probably managed. Several factors lead to postharvest losses during transportation including bad roads, non-refrigerated vehicles [7], the surrounding environment [8], and mechanical and physiological properties of fresh produce [6]. During transport, fruits and vegetables are often exposed to rough handling and transported over bad road conditions resulted in damage and mechanical injuries which could increase the losses over the supply chain [9].

The vibration produced by vehicles (truck beds) during road transportation has a significant effect on the damage process of agricultural products like fruits and vegetables [10]. Furthermore, it is one of the main reasons for causing external and internal damages to the fresh produce during the supply chain [11,12]. Transport distance is one

of the essential factors that directly correlate with vibration level where long-distance transportation time resulted in high vibration level. Çakmak et al. [13], Shahbazi et al. [14], and La Scalia et al. [15] recorded high vibration levels and great damage as transit time increased in fig, watermelon, and strawberry respectively. Furthermore, long transport times during fresh produce transportation can accelerate enzymatic and metabolic processes resulted in increasing the mechanical damage risk, therefore, reducing market value [6].

Different physical changes have been investigated on different fresh produce during transportation like an apple [16], fig [13], grape [17], kiwifruit [18], tomato [8,19,20], and strawberry [15]. Most of the results showed that the internal damages produced by vibration during transportation can generate a rapid degradation [21] which can directly affect ripening level and firmness [12]. The vibrated samples of strawberries had a lower shelf life compared to the control (non-vibrated) samples as reported by Dhital et al. [22]. Xu et al. [3] also recorded high color change on lightness in broccoli stressed to two hours vibration.

Fresh produce storage is another essential part of the postharvest supply chain [23]. The majority of microbial, physiological, and biochemical processes contributing to produce quality deterioration are temperature dependence [24]. A high increase in storage temperature rises the rate of respiration [25], transpiration, and the rate of ethylene production. However, a high reduction of storage temperature could be a reason for causing chilling injuries and quality reduction [26].

Tomato (*Solanum lycopersicum* L.) is one of the most widely grown and important fresh produce worldwide. Tomato is a vital source of many nutrients and other healthy minerals that benefit the human body [27]. Weight, firmness, and color are essential quality indicators influenced by postharvest operations [1,25]. These quality aspects affect consumer acceptance and market success [28]. Compared to other fruits and vegetables, tomato is a sensitive produce [29] which is highly perishable due to vibration and impact load during transportation, the market process, and storage temperature [25]. Vibration during transportation causes the tomato to rub and rotate against other products and the packaging containers resulted in softening and other mechanical damages [8,13]. Besides, storage becomes difficult to maintain particularly in high moisture content fresh produce like tomato [23]. Few studies investigated the effect of real-time transportation vibration generated from different distances coupled with varying storage conditions on tomato fruit that can resolve the critical post-harvest losses and problems in perishable commodities. Therefore, this study was performed to investigate the contribution of vibration generated from road transportation of three different distances (100, 154, and 205 km) and storage temperature (10 and 22 °C) in tomato quality aspects including weight, firmness, and color for 12 days storage period.

2. Materials and Methods

2.1. Field Experiments

To compare the influence of vibration level and distance during transit on the quality of fresh produce, a total of 27 wooden boxes (400 × 300 × 110 mm) of bright red color tomatoes with calyx ("Miral" variety) of one harvest were purchased from a farm located in Al-Suwaiq, Sultanate of Oman. Tomato boxes were then transported to three different distances (100 km, 154 km, and 205 km) using 1692 kg non-refrigerated pickup (Model: Hilux, Toyota, Samut Prakan, Thailand) to Postharvest Laboratory, College of Agricultural and Marine Sciences at Sultan Qaboos University, Oman. For each distance, the time required to transport tomato fruit boxes per distance was 75 min, 120 min, and 180 min for 100 km, 154 km, and 205 km, respectively. Tomato wooden boxes were covered by a blue plastic sheet to avoid direct exposure to the sun. This study was carried out during the summer season of June 2020.

2.2. Vibration

In this study, a three-axis USB vibration/acceleration data logger (Model: OM-VIB-101, Spectris plc, Connecticut, Norwalk, CT, USA) was used to record the data of obtained vibration during transportation. This sensor has a −16 to 16 g acceleration range, 0 to 60 Hz frequency range, and ±0.5 g accuracy. This sensor was attached in the top position of the tomato fruit container and was positioned vertically to get more vibration [30] inside tomato boxes. For sampling rate, vibration data were recorded every 1 s of road travel.

The generated signals were simplified on the sensor and then transferred to a personal computer to be later analyzed by shock application (vibration data logger, v2.3). Thousands of vibration signals were recorded in each distance during transit in milligal (mGal) which were later converted to cm/s^2. Moreover, vibration analysis was applied to evaluate the number of obtained accelerations (time-domain) for each distance that occurs during transit. Subsequently, all time-domain signals above $0.13 \, cm/s^2$ were calculated using a histogram which was performed to identify the number of peaks of acceleration during transit for each distance.

2.3. Sample Preparation and Laboratory Experiment

A total of 195 tomato fruits from three distances with similar color, firmness, weight (0.487 ± 0.1 kg), and free from defects were selected for the study analysis. For each distance, tomato fruits were divided into two groups, where the first group stored at ambient room temperature (22 ± 1 °C with 65 ± 5% RH) and the other at refrigerated temperature (10 ± 0.5 °C with 95 ± 1% RH). Each storage condition consists of seven sub-groups where each group consists of five replicates to undergo some physical quality analysis (weight loss percentage, color, and firmness) for the evaluation of their postharvest changes due to transport vibration and storage for 12 days at 2 days interval. Daily monitoring of temperature and relative humidity in the laboratory were measured using a temperature meter (Model: TES 13604, TES Electrical Corp., Taipei, Taiwan).

2.3.1. Tomato Weight Loss %

Weight loss (%) of tomato fruit transported from each distance stored at both conditions was determined for two days intervals to an accuracy of ±0.01 g by using an electric weight balance (Model: GX-4000, A & D Company, Tokyo, Japan). The results were calculated as a percentage of the initial recorded weight of the tomato group from the first day of the experiment.

2.3.2. Tomato Color Change

A total of twenty-five external color readings (per one color parameter) were taken from 5 tomato samples per group at 2 days interval using RGB (Red, Green, Blue) image acquisition system (Figure 1). In this system, a cardboard box was used to cover the whole system to avoid backscattering effects. Furthermore, a white background (stage) was placed to provide high contrast between the tomato sample and the background. Tomato samples were illuminated using two 36 W long fluorescent tubes (Model: Dulux L, OSRAM, Milano, Italy) to provide light with uniform intensity over the sample. Light sources were fixed to be parallel to the tomato platform. Moreover, the image of tomato samples was captured using an RGB color camera (Model: EOS FF0D, Canon Inc., Tokyo, Japan) placed vertically in the center of the cardboard box at a distance of 0.26 m from the tomato sample. The digital camera was connected to the USB port of a personal computer where the images were stored for subsequent processing. A remote shooting software EOS Utility included in the camera was performed to acquire the image in the maximum possible resolution [31]. The captured images were stored in JPG format. Each sample was placed and oriented manually. For image processing, ImageJ software (v. 1.53, National Institute of Health, Bethesda, MD, USA) was applied. RGB mean values were obtained by using the histogram tool (Analyze/Histogram menu). RGB values were later converted to CIEL*a*b* color space which was chosen as it is mostly applied in food quality studies [32]. Total color differences

($\Delta E*$) that indicate the magnitudes of color change in the stored tomato (Equation (1)), chroma that represents the color intensity of stored (Equation (2)), a hue which indicates the purity of tomato color (Equation (3)), color index (CI) (Equation (4)), and tomato color index (COL) (Equation (5)) were also calculated to track red color development of stored tomato fruit transported from different distances using the following equations [33]:

$$\Delta E = \sqrt{\Delta a*^2 + \Delta b^2 + \Delta L*^2} \tag{1}$$

$$Chroma = \sqrt{a*^2 + b*^2} \tag{2}$$

$$Hue = \tan^{-1}\left(\frac{b*}{a*}\right) \tag{3}$$

$$CI = a^*/b^* \tag{4}$$

$$COl = \left(\frac{2000 \times a^*}{L^* \times Chroma}\right) \tag{5}$$
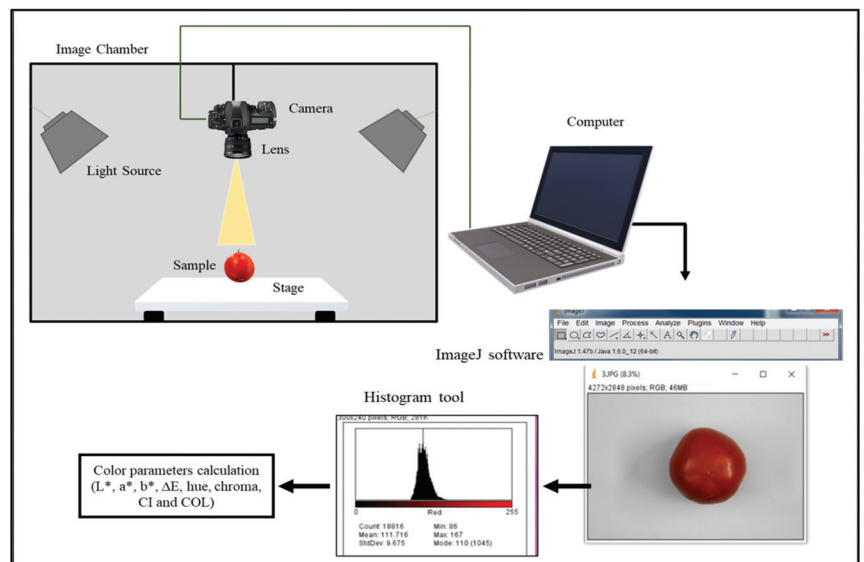
Figure 1. A schematic of a typical RGB image acquisition system.

2.3.3. Tomato Firmness

The firmness of tomato fruit was determined by a digital fruit firmness tester (Model: FHP-803, L.L.C., Franklin, ME, USA) [34] using an appropriate stainless-steel cylinder probe with a 3 mm diameter. Two measurements were taken at opposite positions on each tomato using a total of 5 samples from (10 readings per group) tomato fruit transported from each distance stored at both conditions and was expressed as N.

2.4. Statistical Analysis

SPSS 20.0 (International Business Machine Crop., New York, NY, USA) was used to study the impact of experimental variables, i.e., transport distance (100 km, 154 km, and 205 km), storage condition (10 ± 0.5 °C and 22 ± 1 °C), and storage duration on the physical (weight loss, color, and firmness) quality parameters of tomato by performing three-way analysis of variance (ANOVA) and the mean values were considered at 5% significance level ($p < 0.05$). Mean and standard deviation (S.D) were also reported for all

measured parameters. Tukey's range (HSD) test was applied to determine the significant differences between treatment means. Construction of all graphs was performed using GraphPad Prism software version 9.0.0 (GraphPad Software, Inc., San Diego, CA, USA).

3. Results and Discussions

3.1. Vibration Level Analysis during Transit

To determine vibration levels during transportation, continuous vertical, longitudinal, and lateral accelerations were measured. Minimum and maximum values of acceleration were the same in all three travel distances due to the continuous measurements of the same instrument during transportation. The results of the transport experiment showed that the vertical direction (Z) gave the maximum acceleration value in all three distances with 2.694 cm/s^2 followed by lateral (X) (1.314 cm/s^2) and longitudinal (Y) (1.123 cm/s^2). Therefore, all subsequent analysis was done using vertical vibration level data. Similar findings were observed by Soleimani and Ahmadi [35] who reported that vertical direction can generate high vibration compared to lateral and longitudinal directions.

A histogram of all time-domain vibration data higher than 0.13 g was used to identify the number of acceleration peaks that occurred per distance (Figure 2). The measured time-domain vibration signals were divided into intervals of 0.17 (0.13–2.69 cm/s^2). The maximum number of peaks was highly found in the acceleration interval of 0.99–1.17 cm/s^2 with 1607, 2864, and 4121 peaks for 100, 154, and 205 km, respectively. It was followed by the acceleration interval of 1.17–1.34 cm/s^2 which was also higher during transit of the longest distance with 2505 peaks compared to medium (1935) and short (1365) distances.
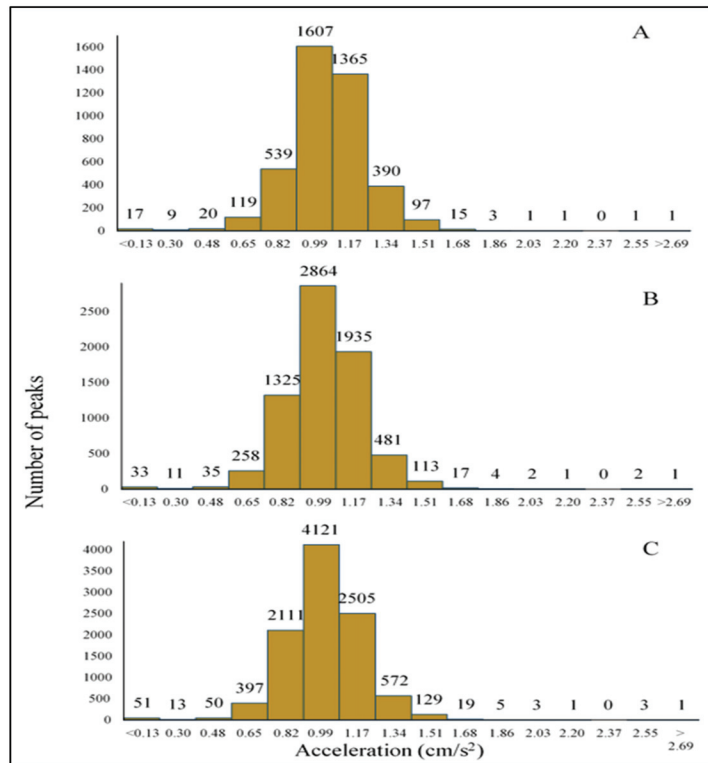
Figure 2. The number of peaks (signals) generated during transport for each acceleration interval (cm/s^2) from (**A**) 100 km (**B**) 154 km and (**C**) 205 km distances using a histogram.

Figure 3 indicates that over 40% of accelerations occurred in the range of 0.82–1.31 cm/s^2 of all transport distances. The percentage of this highest acceleration range was higher in the longest distance with 41% followed by medium 40% and short 38% distance. The maximum accelerations observed during transit (2.96 cm/s^2) showed only 0.03% of acceleration occurrence in all three distances, particularly the shortest distance (100 km). Generally, increasing distance is responsible to increase the acceleration occurrence during transport. The result of the acceleration value measured in the research is close to that reported by Shahbaz et al. [14] who reported that the accelerations of over 97% of vibrations recorded on the transported bins had values below 2 g. They also reported that the intervals of 0.25–0.50 g and 0.50 0.75 g had the highest distribution percentages of vibration accelerations, where the values in these intervals were 35.06 and 23.59% respectively. Besides, increasing the vibration period to 60 min during simulated in-transit vibration resulted in a greater percentage of damage for watermelon with 0.7 g acceleration vibration compared with 0.3 g by 30 min. Wu and Wang [19] observed damage in tomatoes during simulated transit due to vibration when exposed to more than 1 g acceleration.
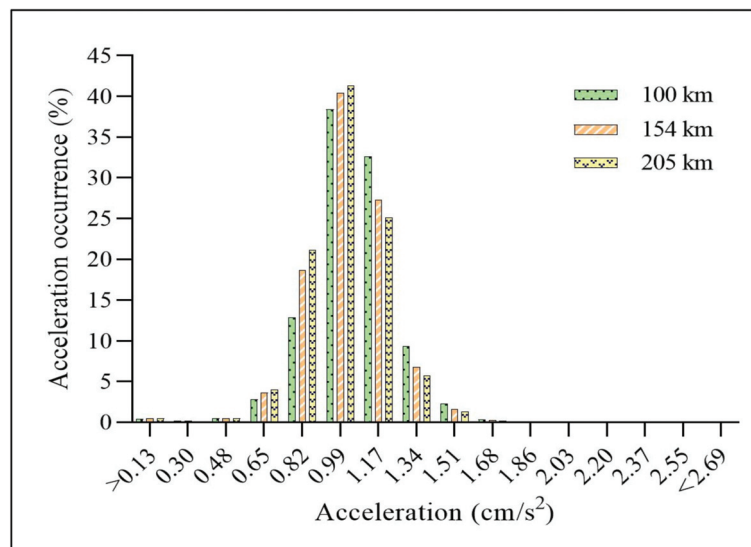
Figure 3. The occurrence percentage of the acceleration intervals (cm/s^2) for 100, 154, and 205 km distances in the vehicle during transportation.

3.2. Effect on Physical Quality Characteristics of Tomato

3.2.1. Weight Loss (%)

Figure 4 shows that the weight loss of tomato fruit was affected by transport distance ($p < 0.0001$), storage temperature ($p = 0.0052$), and storage duration ($p < 0.0072$). An increasing trend in weight loss was observed in all tomato fruits transported from different distances stored at 10 and 22 °C for 12 days storage period. However, weight reduction percentage was significantly higher in tomato transported from the longest distance and stored at 22 °C with 6.91% followed by tomato transported from middle and shortest distances with 6.31% and 5.96%, respectively (Figure 4). Nevertheless, the weight loss of tomatoes transported from the long, medium, and short transport distances and subjected to cold temperature (10 °C) was 3.5%, 3.3%, and 3.09%, respectively over 12 days. Generally, increasing transportation distance and temperature storage at (22 °C) increased the weight reduction of tomato samples during storage. However, low-temperature storage reduced the effect of transportation distance on the weight loss of tomato fruit.

Figure 4. Weight loss (%) of tomatoes from three different distances stored at (A) 10 ± 0.5 °C (95 ± 1%RH) and (B) 22 ± 1 °C (65 ± 5%RH) for 12 days.

These results suggested that tomato fruit transported from the longest distance were stressed due to multiple vibrations compared to others. Exposure to external vibration resulted in a higher respiration rate leading to more weight reduction during storage [16]. Furthermore, Wei et al. [12] reported that fresh produce experienced high weight reduction due to the increment in transport vibration which accelerates water reduction of fresh produce as well as shriveling resulted from intracellular damage. Regarding storage, Endalew [36] stated that storage time and storage temperature had a great effect on the weight loss of tomatoes. Storage at ambient temperature increased the tomato weight loss due to transpiration, respiration [37], and dehydration [38] resulted in water loss leading to an increase in the physical barriers between a fresh produce with the surrounded air [36]. Transpiration occurs in response to the vapor pressure deficit of water that is a function of pressure, air temperature, and relative humidity. Moreover, respiration can prompt weight loss increment due to the alteration of carbon (C) atoms to atmospheric carbon dioxide (CO_2) [7]. In tomato, a higher transpiration rate resulted from higher temperature storage condition compared to lower temperatures lead to shriveling and wilting, thus, reduce consumer acceptability and market-level [36]. Low relative humidity at ambient temperature can also reduce water quantity in the produce which accelerates water reduction [39]. In this study, low temperature storge at 10 °C declined weight reduction of tomato due to the direct impact on vapor pressure and water retention enhancement.

Similarly, Jung et al. [17] experienced 15% and 9% weight loss in the grape group exposed to vibration and control group during 30 days storage. Furthermore, Çakmak et al. [13] found higher mass loss of fig when affected by high vibration frequency and acceleration (16 Hz~2.54 m s^{-2}) compared to fig exposed to 3 Hz~0.56 m s^{-2} at different storage conditions. Wei et al. [12] also revealed a significant weight loss and shrinkage on kiwifruit affected by simulated vibration compared to the non-vibrated kiwifruit after 12 days storage at 25 °C and 75% RH. A progressive increase in weight loss was also reported during storage for 10 days at 34 °C [40] and 8 °C, 12 °C, 20 °C for 20 days [41]. The findings of this study were also in agreement with the findings of Pathare and Al-Dairi [42] who recorded a high percentage of weight reduction in tomato for 10 days storage at room temperature.

3.2.2. Color Change

A significant difference was observed between tomato color lightness (L*) values and transport distance ($p = 0.0445$), storage temperature ($p = 0.0047$), and storage duration ($p = 0.0025$) (Figure 5). During storage, tomato transported from 205 km and stored at 22 °C showed the highest decrease on L* value from 44.30 to 18.10 on Days 0 and 12 respectively. This was followed by tomato transported from 154 km and 100 km from 44.57 and 45.50 to 18.23 and 24.62 respectively (Figure 5). The same scenario was observed on tomato fruit stored at 10 °C, where the highest L* value reported on tomato transported from long followed by medium and short distances. On Day 12, the study reported a 45.88%, 59.08%, and 59.13% reduction in tomato lightness transported from short, medium, and long distances stored at 22 °C compared to only 23.44%, 34.80%, and 35.95% at 10 °C. This indicated that storage at 10 °C slowed down the lightness reduction of tomatoes that could be affected by vibration during different transportation distances. This could be attributed to the repeated vibration stresses during long-distance transportation of tomato resulted in increasing lightness reduction and alteration. Furthermore, the L* value reduction during storage at 22 °C indicated the increment of tomato fruit darkening during storage due to carotenoids synthesis [36]. The slow reduction in lightness (L*) at low storage temperature can occur due to normal ripening resulted from the inhibition of enzymatic activities [43]. The effect of transportation on the fresh produce was also studied by La Scalia et al. [15], where lightness was reduced during storage with no significant effect on vibration duration. Zhou et al. [44] confirmed that pears suffered from transport vibration during long transit time showed high changes on L* stored at ambient temperature. Endalew [36] also stated that the lightness value of tomatoes decreased with the storage time.

Figure 5. L* value of tomatoes from three different distances stored at (A) 10 ± 0.5 °C ($95 \pm 1\%$ RH) and (B) 22 ± 1 °C ($65 \pm 5\%$ RH) for 12 days. Error bars represent standard error (SE) of the mean values $\pm$S.E. of 25 measurements (readings) of 5 tomato replicates. Bars with different letters (per day) are significantly different ($p < 0.05$) performed by the Tukey HSD test and numerical values of A, B, and C are *p*-values.

The increase of 'redness' and decrease of 'greenness' in tomato fruit was associated with the increment in a* value. The results revealed that the red color (a*) of tomato fruit was influenced by the independent variables like transport distance ($p = 0.0343$), storage temperature ($p = 0.0093$), and storage duration ($p = 0.0014$) (Figure 6). Tomato transported

from the longest distance and then stored at 22 °C recorded the highest alternation of a* value from 20.94 on Day 0 to 33.39 on the last day of storage. However, the a* value of tomato transported from the shortest distance increased from 20.05 to 32.21 on Day 0 and Day 12, respectively (Figure 6). Tomatoes stored at 10°C after being transported from 100 km showed the least degree of red color development during storage from 20.05 to 25.74 on Days 0 and 12, respectively, while that from longest distance increased from 20.94 to 28.76 for 12 days storage (Figure 6). In the case of transportation distance, the repeated acceleration occurrence which was recorded from the longest distance could lead to an increase in the ripping process that accelerates redness development in tomato fruit. Tomato kept at room temperature can provide an optimal environment for the tomato to ripe resulted in increasing redness (a*) compared to cold storage conditions [7]. Storage at 22 °C can cause an increase in a* value of tomato due to chlorophyll degradation, lycopene accumulation, and ethylene biosynthesis [45]. Tigist et al. [46] also stated that high temperature tends to increase the red color of tomato compared to low temperature due to the increase in the ripening state of tomato during storage. Regarding transport, La Scalia et al. [15] recorded a small but significant influence of vibration duration on a* value of strawberries. Similarly, Wu and Wang [19] found that tomatoes became redder when exposed to higher acceleration vibration during 60 min of simulated transport. An increase in a* value was obtained during storage, particularly, at 20 °C with a delay in redness development recorded in tomato stored at 2 and 5 °C (Pinheiro et al., 2013). The same scenario was found by Guillén et al. [47], who reported a slow development on a* value of tomato stored for 28 days storage.
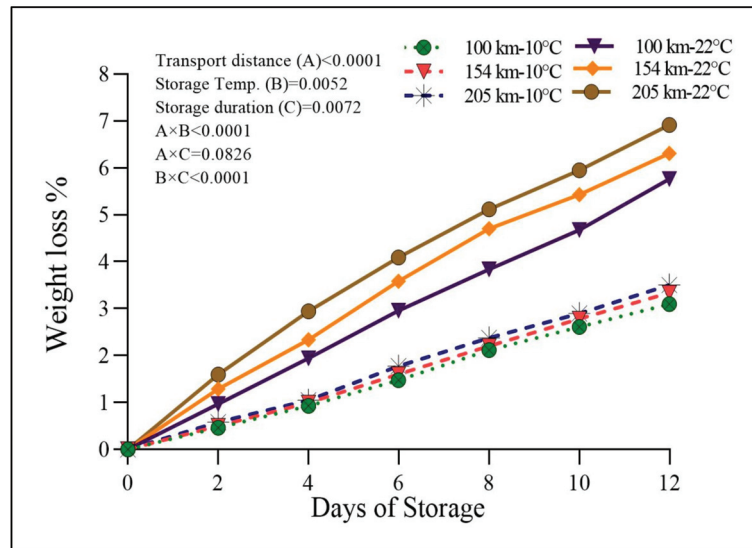

Figure 6. a* value of tomatoes from three different distances stored at (A) 10 ± 0.5 °C (95 ± 1% RH) and (B) 22 ± 1 °C (65 ± 5% RH) for 12 days. Error bars represent standard error (SE) of the mean values ±S.E. of 25 measurements (readings) of 5 tomato replicates. Bars with different letters (per day) are significantly different ($p < 0.05$) performed by the Tukey HSD test and numerical values of A, B, and C are *p*-values.

As shown in Figure 7, the alteration of tomato color yellowness was significantly affected by all three factors such as transport distance ($p = 0.0100$), storage temperature ($p = 0.0032$), and storage duration ($p = 0.0004$). The b* value of all tomato samples transported from all distances decreased dramatically, particularly, at 22 °C with 58.18% followed by medium and short distances by 58.01% and 49.36% respectively for 12 days storage

period. However, the b* value of tomato transported from short, medium, and long distances and stored at 10 °C was significantly lower than those stored at 22 °C with 30.92%, 41.98%, and 41.96%, respectively (Figure 7). The reduction in yellowness (b*) during storage is mostly associated with red color development [36]. As highlighted by Khairi et al. [48], the yellowness (b*) value of tomato was continually decreased as temperature and time increased. The yellow discoloration was also observed on tomato, which reached its minimum b* value after 21 days at 5 and 10 °C [43].

The total color difference is considered as an outcome of alteration in L*, a*, and b* values. Total color differences of tomatoes were statistically significant with transport (*p* = 0.0435), storage temperature (*p* = 0.0078), and storage duration (*p* = 0.0026) (Figure 8). Tomato transported from long distance and stored at ambient temperature had the highest change in total color differences which was ranging between 0 and 32.83 for 12 days storage compared to medium and short distances. Tomato transported from a short distance and stored at 10 °C recorded the lowest range of total color differences from 0 to 14.99 (Figure 8).

Figure 7. b* value of tomatoes from three different distances stored at (A) 10 ± 0.5 °C (95 ± 1% RH) and (B) 22 ± 1 °C (65 ± 5% RH) for 12 days. Error bars represent standard error (SE) of the mean values ±S.E. of 25 measurements (readings) of 5 tomato replicates. Bars with different letters (per day) are significantly different (*p* < 0.05) performed by the Tukey HSD test and numerical values of A, B, and C are *p*-values.
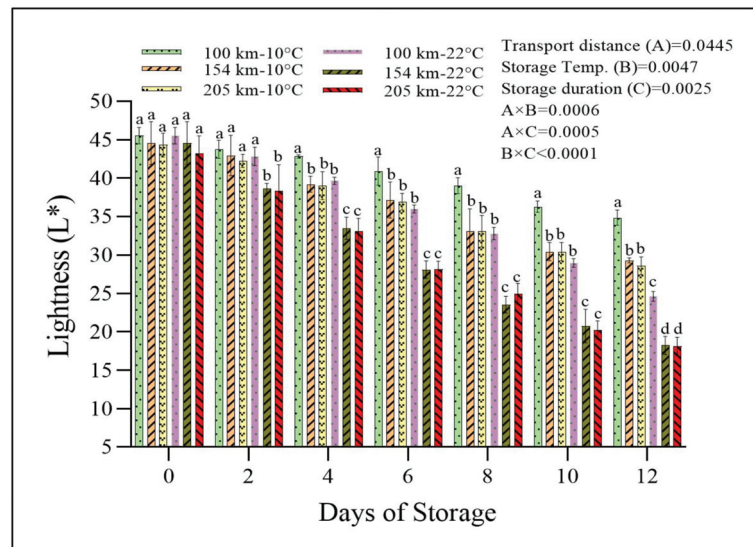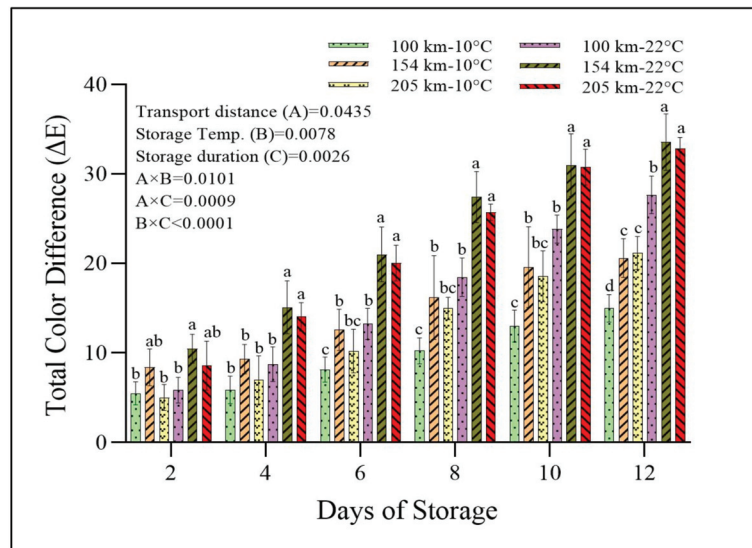
Figure 8. Total color differences (ΔE) value of tomatoes from three different distances stored at (A) 10 ± 0.5 °C (95 ± 1% RH) and (B) 22 ± 1 °C (65 ± 5% RH) for 12 days. Error bars represent standard error (SE) of the mean values ±S.E. of 25 measurements (readings) of 5 tomato replicates. Bars with different letters (per day) are significantly different (*p* < 0.05) performed by the Tukey HSD test and numerical values of A, B, and C are *p*-values.

This study showed a significant interaction between hue value and investigated factors like transportation distance (*p* = 0.0037), storage temperature (*p* = 0.0002), and storage duration (*p* = 0.0004) (Table S1). Hue value maximum reduction percentage was 64.48% by Day 12 in tomato transported from the longest distance and stored at 22 °C (Table 1). The percentage of hue value reduction of tomato transported from medium distance 63.65%, while it was 57.13% on tomato transported from the short distance. The least reduction (33%) was observed on tomatoes transported from the shortest distance and stored at 10 °C (Table 1). As expected, the reduction in hue value of tomato stored at 22 °C was greater than those stored at 10 °C due to the natural relationship found between the rate of biochemical reaction and temperature [49]. Long transport distance also showed a high increase in hue and chroma during storage at ambient storage temperature [44]. There was a significant effect of storage at 4, 20, and 30 °C for 16 days on the intensity (chroma) and purity (hue) of tomato color. In contrast to the current study, storage at a high temperature can retain the purity of color (hue) compared to low temperature [50]. However, there was no statistical difference (*p* > 0.05) between chroma and the investigated factors for 12 days of storage (Table 1 and Table S1). However, La Scalia et al. [15] recorded a significant reduction in chroma value of the vibrated fresh produce (strawberry) stored at cold storage temperature.

Color index (CI) was statistically influenced by transport distance (*p* = 0.0149), storage temperature (*p* = 0.0148), and storage duration (*p* ≤ 0.0001). Besides, a similar scenario was observed with tomato color index (COL) (Table S1). The dramatic increase in tomato CI and COL was mostly shown in tomato stored at 22 °C after it was transported from a 205 km distance (Table 1). However, 100 km transportation distance showed the lowest development of color indices for 12 days storage. According to Tadesse et al. [50], the increase in color indices can indicate the development of a dark red color in the investigated tomato. They recorded a high red color increment in tomatoes stored at 20 and 30 °C than tomatoes stored at low temperature (4 °C) which attributed to lycopene development associated with the internal membrane system of tomato.

Table 1. Chroma, Hue, CI, and COL changes in tomatoes transported from three distances (100 km, 154, and 205 km) stored at ambient (22 °C) and optimum (10 °C) for 12 days storage period. The data were expressed in mean ± standard deviation of 25 measurements (readings) of 5 tomato replicates. Mean values with different letters in a column (per parameter) differ significantly ($p < 0.05$) performed by the Tukey HSD test. Numerical values of A, B, and C are *p*-values. All *p*-values in bold are statistically significant (Tukey HSD test., $p < 0.05$).

Color Quality Parameters	Distances (Km)	ST (°C)	Days of Storage						
			0	2	4	6	8	10	12
Chroma	100	10	33.38 ± 1.70 [a]	33.23 ± 0.53 [a]	32.83 ± 0.67 [a]	31.72 ± 0.73 [a]	31.81 ± 1.00 [a]	32.02 ± 0.60 [ab]	31.65 ± 0.52 [b]
		22		32.68 ± 0.80 [a]	32.82 ± 1.00 [a]	31.06 ± 1.07 [a]	32.43 ± 1.89 [a]	33.79 ± 1.25 [a]	34.93 ± 0.92 [a]
	154	10	33.59 ± 4.17 [a]	32.80 ± 1.38 [a]	32.38 ± 1.32 [a]	32.92 ± 1.68 [a]	32.60 ± 0.54 [a]	31.68 ± 0.55 [b]	32.39 ± 1.22 [b]
		22		32.28 ± 1.28 [a]	31.52 ± 0.84 [a]	30.70 ± 0.94 [a]	32.78 ± 0.66 [a]	33.76 ± 1.51 [a]	34.88 ± 0.87 [a]
	205	10	33.37 ± 0.82 [a]	32.63 ± 1.51 [a]	32.32 ± 0.65 [a]	32.50 ± 1.46 [a]	32.70 ± 0.55 [a]	31.72 ± 1.33 [b]	32.49 ± 1.17 [b]
		22		32.49 ± 1.26 [a]	31.51 ± 0.61 [a]	30.69 ± 0.55 [a]	32.84 ± 0.66 [a]	33.86 ± 0.50 [a]	35.15 ± 0.58 [a]
Hue	100	10	0.92 ± 0.05 [a]	0.90 ± 0.04 [a]	0.85 ± 0.04 [a]	0.77 ± 0.02 [a]	0.71 ± 0.05 [a]	0.67 ± 1.04 [a]	0.61 ± 0.02 [a]
		22		0.86 ± 0.37 [ab]	0.76 ± 0.04 [b]	0.67 ± 0.02 [a]	0.53 ± 0.02 [c]	0.44 ± 0.44 [c]	0.39 ± 0.01 [c]
	154	10	0.88 ± 0.08 [a]	0.87 ± 0.01 [a]	0.80 ± 0.03 [a]	0.70 ± 0.05 [a]	0.61 ± 0.00 [b]	0.53 ± 0.04 [b]	0.49 ± 0.01 [b]
		22		0.80 ± 0.03 [b]	0.65 ± 0.01 [c]	0.54 ± 0.01 [c]	0.39 ± 0.00 [d]	0.34 ± 0.02 [d]	0.32 ± 0.01 [d]
	205	10	0.89 ± 0.02 [a]	0.84 ± 0.03 [a]	0.79 ± 0.04 [a]	0.70 ± 0.05 [a]	0.60 ± 0.03 [b]	0.52 ± 0.04 [b]	0.48 ± 0.02 [b]
		22		0.78 ± 0.03 [b]	0.65 ± 0.02 [c]	0.54 ± 0.03 [a]	0.38 ± 0.01 [d]	0.34 ± 0.02 [d]	0.03 ± 0.02 [d]
CI	100	10	0.75 ± 0.08 [a]	0.79 ± 0.06 [c]	0.88 ± 0.07 [c]	1.02 ± 0.04 [c]	1.15 ± 0.11 [d]	1.25 ± 0.11 [d]	1.41 ± 0.07 [b]
		22		0.86 ± 0.08 [bc]	1.04 ± 0.10 [b]	1.25 ± 0.05 [b]	1.70 ± 0.16 [b]	2.09 ± 0.12 [b]	2.41 ± 0.11 [b]
	154	10	0.82 ± 0.14 [a]	0.84 ± 0.02 [c]	0.97 ± 0.07 [bc]	1.19 ± 0.14 [b]	1.44 ± 0.03 [c]	1.73 ± 0.20 [c]	1.88 ± 0.05 [c]
		22		0.97 ± 0.07 [ab]	1.29 ± 0.03 [a]	1.65 ± 0.07 [b]	2.42 ± 0.06 [a]	2.77 ± 0.20 [a]	3.04 ± 0.19 [a]
	205	10	0.84 ± 0.04	0.88 ± 0.06 [abc]	0.98 ± 0.09 [bc]	1.18 ± 0.13 [b]	1.45 ± 0.10 [c]	1.74 ± 0.22 [bc]	1.94 ± 0.11 [c]
		22		0.99 ± 0.06 [a]	1.31 ± 0.06 [a]	1.67 ± 0.12 [b]	2.47 ± 0.10 [a]	2.82 ± 0.23 [a]	3.21 ± 0.28 [a]
COL	100	10	26.47 ± 2.09 [a]	28.38 ± 2.07 [c]	30.84 ± 1.60 [c]	31.48 ± 1.28 [c]	34.46 ± 1.28 [d]	36.56 ± 0.33 [d]	41.79 ± 1.46 [b]
		22		30.48 ± 1.19 [bc]	36.28 ± 1.70 [b]	43.36 ± 0.99 [b]	52.69 ± 1.37 [b]	55.12 ± 1.37 [b]	63.84 ± 1.40 [b]
	154	10	28.59 ± 3.41 [a]	30.05 ± 1.70 [c]	47.49 ± 2.39 [bc]	41.24 ± 3.32 [b]	50.25 ± 3.32 [c]	56.77 ± 3.17 [c]	60.23 ± 0.80 [c]
		22		36.30 ± 1.63 [ab]	35.17 ± 1.73 [a]	60.96 ± 2.37 [b]	79.01 ± 3.89 [a]	92.17 ± 7.80 [a]	104.35 ± 7.02 [a]
	205	10	28.44 ± 1.69 [a]	31.36 ± 1.43 [abc]	35.93 ± 3.30 [bc]	41.28 ± 2.06 [b]	49.81 ± 2.06 [c]	56.87 ± 3.31 [ab]	60.25 ± 2.07 [c]
		22		37.02 ± 3.22 [a]	48.09 ± 3.15 [a]	61.06 ± 2.68 [b]	75.17 ± 4.50 [a]	93.58 ± 5.84 [a]	106.44 ± 75.38 [a]

ST, storage temperature; CI, color index; COL, tomato color index.

3.2.3. Firmness

Tomato fruit firmness significantly influenced by transport distance ($p = 0.0129$), storage temperature ($p = 0.0012$), and storage duration ($p = 0.0036$) (Figure 9). Overall, firmness decreased drastically during the period of storage at both storage temperatures in all distances of transported tomato. In this study, as distance duration increases, the firmness of the tomato reduces. Firmness reduced by 50.82%, 51.44, and 58.39% for short, medium, and long-stored at 22 °C, respectively (Figure 9). However, the reduction in firmness at 10°C was 28.36%, 33.69%, and 37.12% for the same distances, respectively. The results indicated that the maximum acceleration occurrence can affect the firm state of the longest distance transported tomatoes. The distribution of fresh produce during transportation can cause critical problems affecting ripening and firmness [12]. In terms of storage conditions, ambient temperature can cause a continuous reduction in tomato firmness due to moisture loss through transpiration and enzymatic changes [37] which can degrade tomato cell wall [45,51]. Texture/firmness reduction is attributed to different factors like losses in cell turgor pressure as well as the cell wall and polysaccharides degradation. Besides, the firmness state is closely correlated with the ripening stage of the fresh produce that causes a rapid increase in enzyme activity [16]. Furthermore, Zhou et al. [44] determined that firmness reduction and softening can occur due to the active state of pectic enzymes and cellulose on polysaccharides in the cell wall of the product. Jung and Park [16] experienced a firmness reduction on vibrated tomato with 33.2% compared to 21.9% of the control group for 30 days storage. Zhou et al. [44] also found that pear fruit exposed to less vibration stress retained higher firmness. Pear fruit exposed to high transit time and stored at ambient temperature had a higher softening rate. The findings of this study agreed with the findings reported by Munhuewyi [7], Park et al. [41], and Kabir et al. [25] who recorded similar reduction trends of et tomato firmness at cold and ambient temperature. Al-Dairi et al. [1] also recorded a 67.80% reduction in tomato firmness at ambient temperature for 12 days.
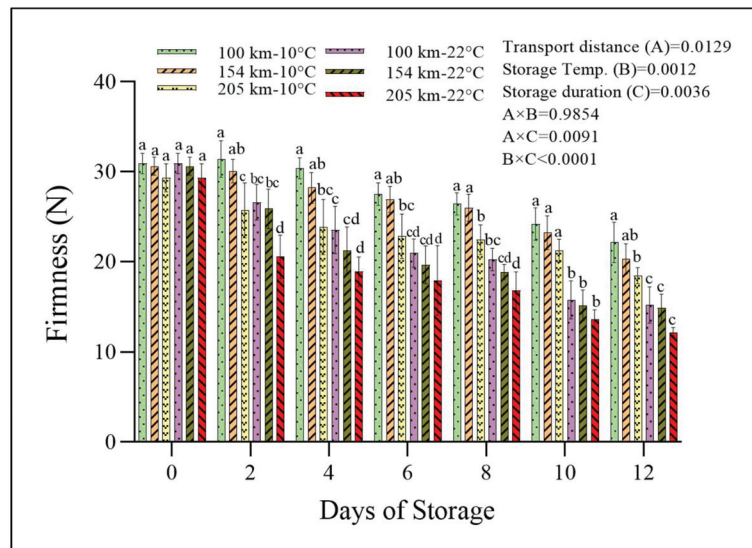
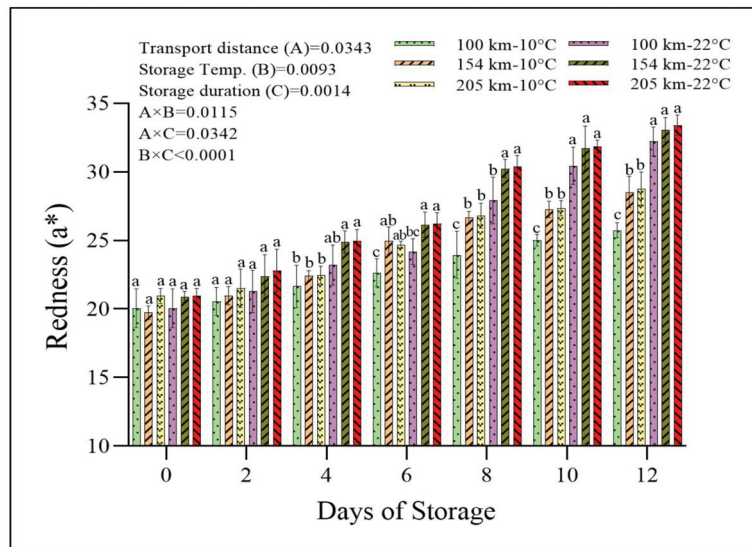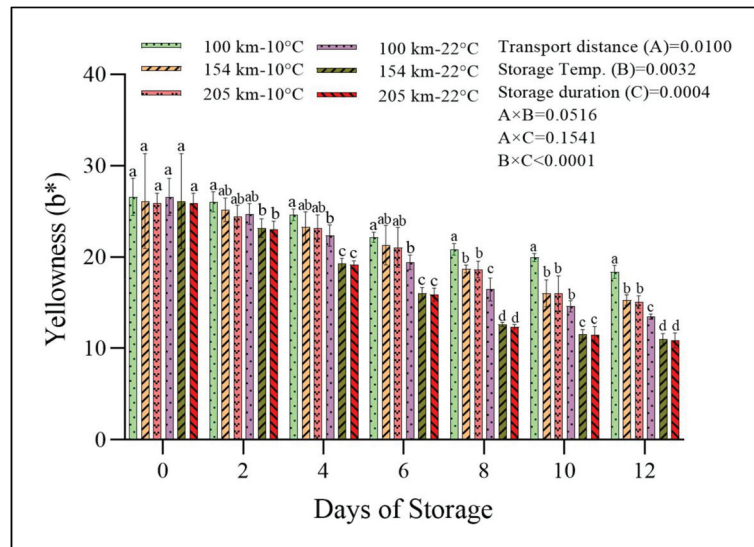**Figure 9.** The firmness of tomatoes from three different distances stored at (A) 10 ± 0.5 °C (95 ± 1% RH) and (B) 22 ± 1 °C (65 ± 5% RH) for 12 days. Error bars represent standard error (SE) of the mean values ±S.E. of 10 measurements (readings) of 5 tomato replicates. Bars with different letters (per day) are significantly different ($p < 0.05$) performed by the Tukey HSD test and numerical values of A, B, and C are *p*-values.

4. Conclusions

The results of this study indicated that vibration generated from different transportation distances significantly affected tomato physical quality parameters. Storage temperature and duration were also found to have a significant impact on the physical quality attributes like weight, color, and firmness. Among all studied distances, long transportation distances highly increased weight and firmness reduction and produced greater color changes during storage. Moreover, storage at ambient temperature conditions (22 °C) accelerated all of these quality changes for 12 days storage period. Nevertheless, storage at a lower temperature (10 °C) showed slower reductions and enhancement of the studied parameters as affected by transport distance, storage time, and storage condition. The results of this study can help the industrial sector to avoid all the critical issues during the transport and storage of fresh produce. In this way, adequate packaging, transportation, and handling facilities, and storage temperature management, need to be available to reduce all expected damages due to transportation and storage.

Informed Consent Statement: Not applicable.

Data Availability Statement: Data is contained within the article.

Conflicts of Interest: The authors declare no conflict of interest.

References

1. Al-Dairi, M.; Pathare, P.B.; Al-Mahdouri, A. Effect of storage conditions on postharvest quality of tomatoes: A case study at market-level. *J. Agric. Marine Sci.* **2021**, *26*, 13–20.
2. Lubes, G.; Goodarzi, M. Analysis of Volatile Compounds by Advanced Analytical Techniques and Multivariate Chemometrics. *Chem. Rev.* **2017**, *117*, 6399–6422. [CrossRef] [PubMed]
3. Xu, D.; Zuo, J.; Li, P.; Yan, Z.; Gao, L.; Wang, Q.; Jiang, A. Effect of methyl jasmonate on the quality of harvested broccoli after simulated transport. *Food Chem.* **2020**, *319*, 126561. [CrossRef] [PubMed]
4. Cui, J.; Yang, M.; Son, D.; Park, S.; Cho, S.-I. Estimation of Tomato Bruising by Mechanical Impact Force Using Multivariate Analysis. *HortScience* **2018**, *53*, 1352–1359. [CrossRef]
5. Al-Dairi, M.; Pathare, P.B.; Al-Yahyai, R. Chemical and nutritional quality changes of tomato during postharvest transportation and storage. *J. Saudi Soc. Agric. Sci.* **2021**. [CrossRef]
6. Cherono, K.; Workneh, T.S. A review of the role of transportation on the quality changes of fresh tomatoes and their management in South Africa and other emerging markets. *Int. Food Res. J.* **2018**, *25*, 2211–2228.
7. Munhuewyi, K. Postharvest Losses and Changes in Quality of Vegetables from Retail to Consumer: A Case Study of Tomato, Cabbage and Carrot. Master's Thesis, Stellenbosch University, Stellenbosch, South Africa, 2012.
8. Idah, P.I.; Gana, Y.M.; Ogbonnaya, C.; Morenikeji, O.O. Simulated transport damage study on fresh tomato (*Lycopersicon esculentum*) fruits. *Agric. Eng. Int. CIGR J.* **2012**, *14*, 119–126.
9. Mutari, A.; Debbie, R. The effects of postharvest handling and storage temperature on the quality and shelf of tomato. *Afr. J. Food Sci.* **2011**, *5*, 340–348.
10. Mvumi, B.; Matsikira, L.T.; Mutambara, J. The banana postharvest value chain analysis in Zimbabwe. *Br. Food J.* **2016**, *118*, 272–285. [CrossRef]
11. Fadiji, T.; Coetzee, C.; Chen, L.; Chukwu, O.; Opara, U.L. Susceptibility of apples to bruising inside ventilated corrugated paperboard packages during simulated transport damage. *Postharvest Biol. Technol.* **2016**, *118*, 111–119. [CrossRef]
12. Wei, X.; Xie, D.; Mao, L.; Xu, C.; Luo, Z.; Xia, M.; Zhao, X.; Han, X.; Lu, W. Excess water loss induced by simulated transport vibration in postharvest kiwifruit. *Sci. Hort.* **2019**, *250*, 113–120. [CrossRef]
13. Çakmak, B.; Alayunt, F.N.; Akdeniz, R.C.; Aksoy, U.; Can, H.Z. The assessment of the quality losses of fresh fig fruits during transportation. *J. Agric. Sci.* **2010**, *16*, 180–193.
14. Shahbazi, F.; Rajabipour, A.; Mohtasebi, S.; Rafie, S. Simulated in-transit vibration damage to watermelons. *J. Agric. Sci. Technol.* **2010**, *12*, 23–34.
15. La Scalia, G.; Aiello, G.; Miceli, A.; Nasca, A.; Alfonzo, A.; Settanni, L. Effect of Vibration on the Quality of Strawberry Fruits Caused by Simulated Transport. *J. Food Process. Eng.* **2016**, *39*, 140–156. [CrossRef]
16. Jung, H.-M.; Park, J.-G. Effects of Vibration Stress on the Quality of Packaged Apples during Simulated Transport. *J. Biosyst. Eng.* **2012**, *37*, 44–50. [CrossRef]
17. Jung, H.M.; Lee, S.; Lee, W.-H.; Cho, B.-K.; Lee, S.H. Effect of vibration stress on quality of packaged grapes during transportation. *Eng. Agric. Environ. Food* **2018**, *11*, 79–83. [CrossRef]
18. Tabatabaekoloor, R.; Hashemi, S.; Taghizade, G. Vibration damage to kiwifruits during road transportation. *Int. J. Agric. Food Sci. Technol.* **2013**, *4*, 467–474.
19. Wu, G.; Wang, C. Investigating the effects of simulated transport vibration on tomato tissue damage based on vis/NIR spectroscopy. *Postharvest Biol. Technol.* **2014**, *98*, 41–47. [CrossRef]
20. Babarinsa, F.; Ige, M. Young's modulus for packaged roma tomatoes under compressive loading. *Int. J. Sci. Eng. Res.* **2012**, *3*, 314–320.
21. Li, Z.; Li, P.; Yang, H.; Liu, J. Internal mechanical damage prediction in tomato compression using multiscale finite element models. *J. Food Eng.* **2013**, *116*, 639–647. [CrossRef]
22. Dhital, R.; Joshi, P.; Becerra-Mora, N.; Umagiliyage, A.L.; Chai, T.; Kohli, P.; Choudhary, R. Integrity of edible nano-coatings and its effects on quality of strawberries subjected to simulated in-transit vibrations. *LWT* **2017**, *80*, 257–264. [CrossRef]
23. Arah, I.K.; Kumah, E.K.; Anku, E.K.; Amaglo, H. An overview of post-harvest losses in tomato production in Africa: Causes and possible prevention strategies. *J. Bio. Agric. Healthc.* **2015**, *5*, 78–88.
24. Majidi, H.; Minaei, S.; Almassi, M.; Mostofi, Y. Tomato quality in controlled atmosphere storage, modified atmosphere packaging and cold storage. *J. Food Sci. Technol.* **2012**, *51*, 2155–2161. [CrossRef] [PubMed]
25. Kabir, S.N.; Rasool, K.; Lee, W.-H.; Cho, S.-I.; Chung, S.-O. Influence of delayed cooling on the quality of tomatoes (*Solanum lycopersicum* L.) stored in a controlled chamber. *AIMS Agric. Food.* **2020**, *5*, 272. [CrossRef]
26. Atanda, S.; Pessu, P.; Agoda, S.; Isong, I.; Ikotun, I. The concepts and problems of post–harvest food losses in perishable crops. *Afr. J. Food Sci.* **2011**, *5*, 603–613.
27. Sarma, P.K. Postharvest losses of tomato: A value chain context of Bangladesh. *Int. J. Agric. Educ. Extn.* **2018**, *4*, 085–092.

28. Barrett, D.M.; Beaulieu, J.C.; Shewfelt, R. Color, Flavor, Texture, and Nutritional Quality of Fresh-Cut Fruits and Vegetables: Desirable Levels, Instrumental and Sensory Measurement, and the Effects of Processing. *Crit. Rev. Food Sci. Nutr.* **2010**, *50*, 369–389. [CrossRef]
29. Al-Dairi, M.; Pathare, P.B. Kinetic modeling of quality changes of tomato during storage. *Agric. Eng. Int. CIGR J.* **2021**, *23*, 183–193.
30. Soleimani, B.; Ahmadi, E. Measurement and analysis of truck vibration levels as a function of packages locations in truck bed and suspension. *Comput. Electron. Agric.* **2014**, *109*, 141–147. [CrossRef]
31. Chero, M.J.S.; Zamora, W.R.M.; Chero, J.A.S.; Villarreyes, S.S.C. Application of the Computer Vision System to the Measurement of the CIE L*a*b* Color Parameters of Fruits. In *Advances in Artificial Intelligence, Software and Systems Engineering*; Ahram, T., Ed.; Advance Intelligent Systems and Computing; Springer: Cham, Switzerland, 2020; Volume 1213. [CrossRef]
32. Al-Dairi, M.; Pathare, P.B.; Al-Mahdouri, A. Impact of vibration on the quality of tomato produced by stimulated transport. In *IOP Conference Series: Earth and Environmental Science*; IOP Publishing: Bristol, UK, 2021; Volume 653, p. 012101. [CrossRef]
33. Pathare, P.B.; Opara, U.L.; Al-Said, F.A. Colour measurement and analysis in fresh and processed foods: A review. *Food Bioprocess Technol.* **2013**, *6*, 36–60. [CrossRef]
34. Jantra, C.; Slaughter, D.C.; Roach, J.; Pathaveerat, S. Development of a handheld precision penetrometer system for fruit firmness measurement. *Postharvest Biol. Technol.* **2018**, *144*, 1–8. [CrossRef]
35. Soleimani, B.; Ahmadi, E. Evaluation and analysis of vibration during fruit transport as a function of road conditions, suspension system and travel speeds. *Eng. Agric. Environ. Food* **2015**, *8*, 26–32. [CrossRef]
36. Endalew, E. Postharvest Loss Assessment of Tomato (*Lycopersicon esculenticon Mill*) (Galilea Cultivar) along the Postharvest Supply Chain, Northwest Ethiopia. Master's Thesis, Bahir Dar University, Bahir Dar, Ethiopia, 2020.
37. Abiso, E.; Satheesh, N.; Hailu, A. Effect of storage methods and ripening stages on postharvest quality of tomato (*Lycopersicom esculenticum Mill*) cv. chali. *Annals. Food Sci. Technol.* **2015**, *6*, 127–137.
38. Fagundes, C.; Moraes, K.; Pérez-Gago, M.; Palou, L.; Maraschin, M.; Monteiro, A. Effect of active modified atmosphere and cold storage on the postharvest quality of cherry tomatoes. *Postharvest Biol. Technol.* **2015**, *109*, 73–81. [CrossRef]
39. Ayomide, O.; Ajayi, O.; Ajayi, A. Advances in the development of a tomato postharvest storage system: Towards eradicating postharvest losses. In *Journal of Physics: Conference Series*; IOP Publishing: Bristol, UK, 2019; Volume 1378, p. 022064.
40. Nirupama, P.; Neeta, B.G.; Rao, T.V.R. Effect of post harvest treatments on physicochemical characteristics and shelf life of tomato (*Lycopersicon Esculenticum Mill.*) fruits during storage. *Am. Eurasian J. Agric. Environ. Sci.* **2010**, *9*, 470–479.
41. Park, M.-H.; Sangwanangkul, P.; Baek, D.R. Changes in carotenoid and chlorophyll content of black tomatoes (*Lycopersicone sculenticum* L.) during storage at various temperatures. *Saudi J. Biol. Sci.* **2018**, *25*, 57–65. [CrossRef] [PubMed]
42. Pathare, P.; Al-Dairi, M. Bruise Damage and Quality Changes in Impact-Bruised, Stored Tomatoes. *Horticulturae* **2021**, *7*, 113. [CrossRef]
43. Žnidarčič, D.; Požrl, T. Comparative study of quality changes in tomato cv. 'Malike' (*Lycopersicon esculenticum Mill.*) whilst stored at different temperatures. *Acta Agric. Slov.* **2006**, *87*, 235–243.
44. Zhou, R.; Su, S.; Yan, L.; Li, Y. Effect of transport vibration levels on mechanical damage and physiological responses of Huanghua pears (*Pyrus pyrifolia Nakai*, cv. Huanghua). *Postharvest Bio. Technol.* **2007**, *46*, 20–28. [CrossRef]
45. Hatami, M.; Kalantari, S.; Delshad, M. Responses of different maturity stages of tomato fruit to different storage Conditions. *Acta Hort.* **2013**, *14*, 857–864. [CrossRef]
46. Tigist, M.; Workneh, T.S.; Woldetsadik, K. Effects of variety on the quality of tomato stored under ambient conditions. *J. Food Sci. Technol.* **2013**, *50*, 477–486. [CrossRef]
47. Guillén, F.; Castillo, S.; Zapata, P.J.; Martínez-Romero, D.; Valero, D.; Serrano, M. Efficacy of 1-MCP treatment in tomato fruit: 2. Effect of cultivar and ripening stage at harvest. *Postharvest Biol. Technol.* **2006**, *42*, 235–242. [CrossRef]
48. Khairi, A.; Falah, M.; Suyantohadi, A.; Takahashi, N.; Nishina, H. Effect of Storage Temperatures on Color of Tomato Fruit (*Solanum Lycopersicum Mill.*) Cultivated under Moderate Water Stress Treatment. *Agric. Agric. Sci. Proc.* **2015**, *3*, 178–183. [CrossRef]
49. Cherono, K.; Sibomana, M.; Workneh, T.S. Effect of infield handling conditions and time to pre-cooling on the shelf-life and quality of tomatoes. *Braz. J. Food Technol.* **2018**, *21*, 1–12. [CrossRef]
50. Tadesse, T.N.; Ibrahim, A.M.; Abtew, W.G. Degradation and formation of fruit color in tomato (*Solanum lycopersicum* L.) in response to storage temperature. *Am. J. Food Technol.* **2015**, *10*, 147–157. [CrossRef]
51. Pinheiro, J.; Alegria, C.; Abreu, M.; Gonçalves, E.M.; Silva, C.L. Kinetics of changes in the physical quality parameters of fresh tomato fruits (*Solanum lycopersicum*, cv. 'Zinac') during storage. *J. Food Eng.* **2013**, *114*, 338–345. [CrossRef]

Article

Effect of Simulated Vibration and Storage on Quality of Tomato

Pankaj B. Pathare * and Mai Al-Dairi

Department of Soils, Water and Agricultural Engineering, College of Agricultural & Marine Sciences,
Sultan Qaboos University, Muscat 123, Oman; s124911@student.squ.edu.om
* Correspondence: pankaj@squ.edu.om or pbpathare@gmail.com; Tel.: +968-2414-1222

Abstract: The influence of simulated transport vibration and storage conditions for 10 days on tomato fruits quality (color, weight, firmness, total soluble solids, and headspace gases) were investigated. Better kinetic models for color changes, weight loss, and firmness of stored tomato fruits were selected. Tomato fruits were divided equally into two main groups where the first one was subjected to vibration at a frequency of 2.5 Hz for two hours and the other group was set as a control (with no vibration stress). Both tomato groups were stored for 10 days at 10 °C and 22 °C storage conditions. The results showed a reduction in total soluble solids, yellowness, weight, lightness in the tomato fruits subjected to vibration at 22 °C storage condition. Ethylene and carbon dioxide increased by 124.13% and 83.85% respectively on the same condition (22 °C). However, storage at 10 °C slowed down the investigated quality changes attributes of both tomato groups (vibrated and control) during storage. The weight loss change kinetics of both tomato groups at both storage temperatures were highly fitted with a zero-order kinetic model. Color and firmness kinetic changes of tomato groups stored at both conditions were described well by zero and first order kinetic models. To validate the appropriateness of the selected model, lightness, redness, yellowness, and firmness were taken as an example. The study revealed that the vibration occurrence and increasing storage temperature cause various changes in the quality attributes of tomatoes.

Keywords: quality; kinetic model; tomato; simulated vibration; storage; transport

Practical Application

The practical application of this research is the understanding of the main causes of damages and quality changes of tomatoes due to vibration generated from the simulated transport at a particular frequency. The use of optimal storage temperature and the other proposed temperature can help to minimize the resulted damages in tomatoes. Improving refrigeration storage conditions in the supply chain of tomatoes is required and very essential to reinforce the quality and shelf life of the product. The mathematical models used in our research with the presence of vibration and control data, storage temperatures, and storage durations helped to predict the effect of simulated vibration and control groups on the quality of tomatoes during the experimental time. Such valuable data can help to discover different strategies and technologies to minimize the deterioration of fresh produce like tomatoes during the supply chain.

1. Introduction

Tomato fruit (*Lycopersicon esculentum,* Mill) is one of the most common and significantly grown fresh produce worldwide and ranked second after potato in terms of area and amount of production as recently reported by FamuyİnI and Sedara [1]. It is a vital source of nutrients and different beneficial minerals and considers as a source of income in most developing countries. The quality of any agricultural product is a significant factor for both the consumers and producers. The quality of tomatoes is highly categorized by weight, color, firmness, and flavor [2]. Tomatoes are climacteric fruits and their physiological attributes make them highly delicate agricultural products [3]. Wu and

Wang [4] highlighted that tomatoes can be affected by postharvest factors like storage, handling, and transportation, etc. Besides, Cherono et al. [5] stated that postharvest losses in tomatoes are as high as 40%.

The quality of fresh produce is reduced during transportation due to biological and physical damages/changes caused by vibration [6]. Vibration generated from transportation caused different external and internal damages to fresh produce. Interior damage is most difficult to recognize via consumers as reported by Wei et al. [7]. Besides, vibration can consider as a critical problem influencing fruit and vegetable sugar content [8], ripening, firmness, browning, core breakdown [7], color redness [4], and headspace gases (O_2, CO_2, C_2H_4) [9]. Walkowiak-Tomczak et al. [10] found that the mechanical vibration of the simulated transport reduced the firmness of 'Gala' and 'Idared' apple by 9 and 13%, respectively, after 14 days of storage. Jung et al. [11] revealed that vibration stress increased the amount of ethylene concentration of packaged grapes (15.3 nL/g·h) compared to the initial stage, while about 9.8 nL/g·h for the packaged grapes with no vibration stress. Tao et al. [12] stated that the vibrated mushrooms showed higher changes in color browning index (89.4) compared to the controls (56.2). Besides, Xu et al. [13] reported that the soluble solids content of blueberries vibrated for 12, 24, and 36 h reduced by 12.9, 21.4, and 28.6%, respectively, and firmness decreased by 28.6, 57.1, and 78.6%, respectively, comparing with the control one. Vibration occurrence can induce both weight and water loss of fresh produce that led to shriveling, which is one of the major physical alterations and cause a direct effect on appearance. Therefore, increasing flesh of fresh tissues [7]. Also, Tao et al. [12] reviewed that mechanical damages generated due to vibration can accelerate the weight loss % in fresh produce, which directly affects the marketability of produce. Jung et al. [11] reported a weight loss of 15% in the vibrated grape group compared to 9% in the control grape group after 30 days storage period. The effect of transport vibration has been studied in the quality of different fresh produce including tomato fruit [4,14], kiwifruit [7], grape fruit [11], broccoli [15], strawberry [16] and mushroom [17].

The quality of fresh produce like tomatoes is highly correlated with storage temperature and storage time [5]. Storage temperature can greatly affect tomato firmness, color, and flavor [18]. Increasing the storage temperature of products can increase the processes of respiration, transpiration, and ethylene rates resulted in a high weight loss percentage [19]. Arah et al. [20] reviewed that tomato fruits contain a high amount of moisture contents; thus, it is difficult to keep and store them at ambient temperature for a long period. Recently, Al-Dairi et al. [2] recorded 16.60% weight loss on tomatoes stored for 12 days at ambient temperature. Low storage temperature condition is considered as a major factor applied for maintaining the quality of postharvest attributes of tomatoes. Furthermore, data on postharvest characteristics of fresh produce are significant and required as an input used for models to predict postharvest behavior and attributes [21].

Kinetic modeling is an essential tool for predicting and controlling the quality attributes alterations in fresh produce [22,23]. It has been highlighted that kinetic modeling has been applied to identify the changes in fresh produce quality characteristics like firmness, color parameters, weight [24], pigments, sugars, and acids [25]. The mathematical modeling depends on the reaction rate like zero-order kinetic models, first-order kinetic models, and higher was applied on different fresh produce [22,24].

This study was carried out to explore the influence of 2 h of simulated transport vibration and storage at 10 °C and 22 °C on tomato's quality attributes like weight loss, color parameters, firmness, TSS, and headspace gases for 10 days storage period. Kinetic models were also applied as a new contribution for predicting the weight loss, color, and firmness kinetic on the stored tomato groups as a function of time.

2. Materials and Method

2.1. Plant Sample and Vibration/Storage Treatments

'Roma' variety tomato fruits packaged in a recycled plastic container with a dimension of (365 × 255 × 155 mm) were purchased from the market and transported to Postharvest

Technology Laboratory of Sultan Qaboos University, Oman. The selected samples (*n* = 63) were similar in color, size, weight (177 ± 0.02 g), firm state, and free of defects and blemishes. Tomato fruits were divided equally into two main groups where the first one was subjected to vibration at 2.5 Hz frequency for two hours and the other group stressed no vibration stress.

The vibrated group were exposed to vibration using an orbital shaker (model: SM25, Edmund Bühler GmbH, Schleswig-Holstein, Germany) [16] to simulate the vibration generated during fresh produce transportation at 2.5 Hz frequency for 120 min at a speed of 150 revolutions per minute (r/min) (205 km distance). The plastic container was tightly fixed in the top of the shaker and 3-axis vibration/acceleration data loggers (Model: OM-VIB101, Spectris plc, Connecticut, Norwalk, CT, USA) were placed vertically inside the container (bottom, middle and top) to record the generated vibration (every 1 s) during simulated transport from three different positions. The resulted vibration signals were later transformed to a personal computer and a shock application (Vibration data logger v2.3) was applied for time-domain vibration analysis of signals. Also, a histogram was used to identify the peaks number generated per accelerometer fixed on each location during the simulated transport experiment.

After conducting the simulated vibration experiment, tomatoes with and without vibration stress were divided equally into two groups at 22 ± 1 °C (65 ± 5% RH) and 10 ± 0.5 °C (95 ± 1% RH). Further objective evaluations of tomato fruit were carried out such as weight loss, firmness, color, total soluble solids (TSS), and headspace gases to study the influence of vibration/control treatments and two storage conditions on the quality of tomatoes at two days intervals for 10 days. For day-0 analysis, three tomato fruits with no vibration were analyzed for all previously mentioned analyses. Besides, daily observations of bruising were recorded. In the current paper, a total of 3 tomato fruits replicates were utilized for each treatment.

2.2. Physical and Physiological Quality Analysis

2.2.1. Weight Loss%

A batch of three tomato fruits for each treatment was weighed on day 0 and the weight loss percentage was recorded on days 2, 4, 6, 8, and 10, relative to day 0.

2.2.2. Color Measurements

The color values of tomato fruits were measured using a computer vision system (Figure 1). A total of 5 readings were taken per sample for color measurements during the experiment at 2 days intervals (60 per day). The system includes a cardboard box utilized to cover the entire system and to avoid the backscattering effect. A lighting system including two long fluorescent lights (36 W) (Model: Dulux L, OSRAM, Milano, Italy) was placed above the sample at an angle of 45°. An RGB digital camera (Model: EOS FF0D, Canon Inc., Tokyo, Japan) was fixed in the top of the cardboard box at 26 cm from the sample. The digital camera involves a remote shooting software EOS Utility used to acquire the image in the maximum required resolution. All captured images were transferred to a personal computer and stored in JPG format for subsequent analysis. ImageJ software (v. 1.53, National Institute of Health, Bethesda, MD, USA) was performed for image processing [6]. All obtained RGB values were transformed to CIEL*a*b* color coordinates. The L* value refers to darkness (0) and lightness (100), a* value is used to donate redness (+) and greenness (-), and the value of b* denotes yellowness (+) and blueness (-). The total color difference (TCD) (Equation (1)) from tomato samples was calculated. Chroma (Equation (2)), hue angle (Equation (3)), and tomato color index (CI) (Equation (4)) indicating color intensity, purity, and red color development index, respectively were also computed [26] as follow:

$$\Delta E* = \sqrt{\Delta a*^2 + \Delta b*^2 + \Delta L*^2} \qquad (1)$$

$$Chroma = \sqrt{a*^2 + b*^2} \qquad (2)$$

$$Hue° = tan^{-1}\left(\frac{b*}{a*}\right) \qquad (3)$$

$$CI = \left(\frac{a*}{b*}\right) \qquad (4)$$
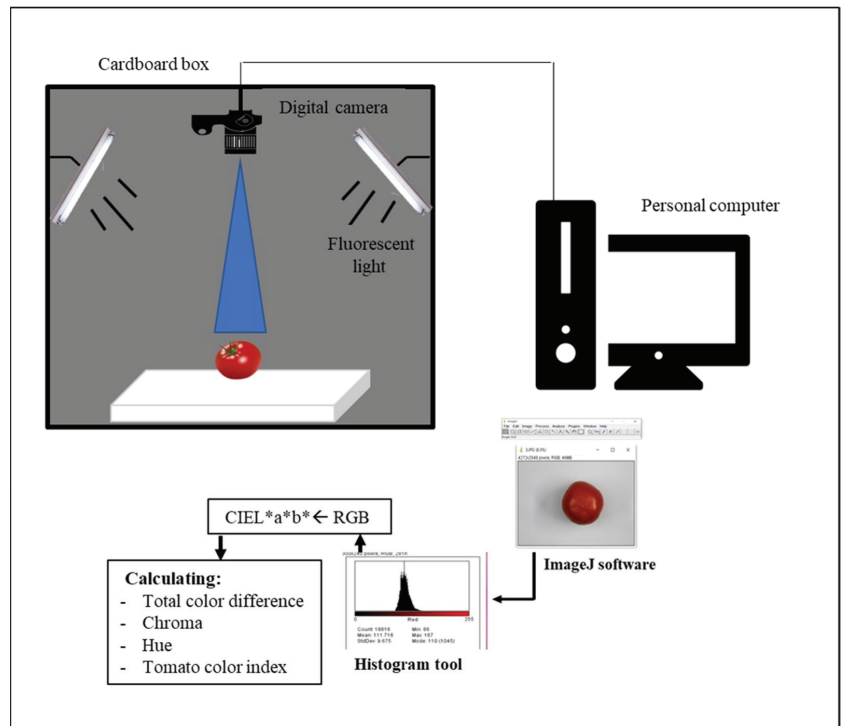
Figure 1. A schematic diagram of computer vision system.

2.2.3. Firmness

To measure the force (N) needed to puncture the tomato surface, a digital fruit firmness tester (Model: FHP-803, L.L.C., Franklin, ME, USA) was used. Both sides were measured in each tomato sample at two days intervals.

2.2.4. Total Soluble Solids (°Brix)

Tomatoes juice was extracted and then analyzed by utilizing a digital refractometer (Model: PR-32 α, ATAGO Co., Ltd., Tokyo, Japan). Clear and pure drops of tomato juice were added to the prism surface of the refractometer and the readings were taken and expressed as °Brix.

2.2.5. Headspace Gases (CO_2, O_2, and C_2H_4)

After the vibration treatment, eight plastic food containers (2.6 L) were prepared as gas collection containers. A total of 6 tomatoes (968.3 ± 25.2 g) were placed inside each container. Oxygen (O_2) and carbon dioxide (CO_2) concentrations were measured using O_2/CO_2 analyzer (Model: 90 2D, Quantek Instruments, Inc., Grafton, Australia). Ethylene (C_2H_4) (ppm) was determined using an ethylene detector (Model: SCS 56, Fricaval89, Valencia, Spain). Both instruments include a needle that is plunged inside the containers

and an electronically timed pump used to pull the needed amount of gases for further analysis. Besides, two replicates were used per treatment to determine O_2, CO_2 (%), and C_2H_4 (ppm) inside the containers for two days intervals.

2.3. Kinetic Model

To determine the physical quality changes of vibrated and non-vibrated tomatoes stored at different storage temperature conditions as a function of time, a kinetic model was applied. The rate of quality change factor was explained by (Equation (5)) [27]:

$$\frac{dC}{dt} = -kC^n \tag{5}$$

where k is the kinetic rate constant at a temperature T, C is the quality factor concentration at time t, and n is the order of the reaction. Most time-dependent relationships for most food materials are likely to be well fitted with the zero-order kinetic model (Equation (6)) or the first-order kinetic model (Equation (7)) follow [28]:

$$C = C_0 \pm kt \tag{6}$$

$$C = C_0 \times \exp\left(\pm kt\right) \tag{7}$$

where C_0 is the initial quality parameter value, C is the quality parameter value at a time and t is the time of storage. Regression analysis such as reduced chi-square (X^2) (Equation (8)), determination of coefficient (R^2) (Equation (9)), and root mean square error (RMSE) (Equation (10)) were done as the main standard to choose the best fit of the studied kinetic models to the current experimental data. Also, the model that effectively fitted tomato fruits quality parameters was defined with the maximum R^2 and lowest X^2 and RMSE. Besides, the following formulas were applied for the estimations of the parameters [23]:

$$X^2 = \frac{\sum_{i=1}^{N} \left(MR_{exp,i} - MR_{pre,i}\right)^2}{N - n} \tag{8}$$

$$R^2 = 1 - \frac{\sum_{i=1}^{N} \left(MR_{pre,i} - MR_{exp,i}\right)^2}{\sum_{i=1}^{N} \left(MR_{pre} - MR_{exp,i}\right)^2} \tag{9}$$

$$RMSE = \sqrt{\frac{1}{N} \sum_{i=1}^{N} \left(MR_{pre,i} - MR_{exp,i}\right)^2} \tag{10}$$

where, $MR_{pre,i}$ and $MR_{exp,i}$ are the ith predicted and experimental values of the quality parameters and MR_{pre} is the average values of predicted quality parameters, n is the numbers of constant model and N is the number of observations. To validate the appropriateness of the selected model, some quality attributes were taken as an example.

2.4. Statistical Analysis

SPSS 20.0 (International Business Machine Crop., New York, NY, USA) was applied to study the influence of vibration/control treatments as well as storage temperature conditions (10 °C and 22 °C) on the physical and physiological attributes of tomatoes for 10 days. For statistical analysis, analysis of variance (ANOVA) was conducted at a 5% significance level. All resulted data were expressed in mean $\pm$ SD.

3. Results and Discussions

3.1. Simulated Vibration Analysis

The accelerometers placed in the three positions of the plastic container recorded thousands of vibration signals. Histogram analysis was applied for all time-domain vibration signals to obtain the peaks number of accelerations per accelerometer (Table 1). The middle position recorded the maximum number of peaks (1664 peaks) at 2.5 Hz for 120 min in the acceleration interval of 0.0275 to 0.0280 m/s^2 with an acceleration occurrence

reached 22.75%. This was followed by the bottom position of the container which generated 1248 peaks in the acceleration interval of 0.0053 to 0.0055 m/s^2. The acceleration interval of 0.0151 to 0.0156 m/s^2 of the top position recorded 896 peaks during the simulated transport experiment. The vibration recorded from each position of the tomato plastic container can indicate that tomato fruits can encounter several damages from each side of the packaging unit during transportation.

3.2. Physiological Weight Loss (%)

Figure 2 shows the weight loss (%) of both tomato groups stored at different storage conditions (10 and 22 °C) during the 10 days of storage. Tomato fruit weight loss was varied significantly ($p < 0.05$) between vibrated and control groups. Also, tomato weight loss was statistically influenced ($p < 0.05$) by storage condition and storage duration. Vibrated tomato fruits stored at ambient temperature (22 °C) had about 4.21% weight loss at the end of storage compared to the control tomato group that had 3.38% of weight loss at the same storage condition. The lowest tomato weight loss was recorded on the control group stored at 10 °C with 1.02% on day 10 of storage. While the vibrated tomatoes stored at 10 °C recorded a 1.39% weight loss on the last day of the study. As reported by Jung et al. [11], vibration can accelerate the increment of both respiration and ethylene rates resulted in a higher reduction in moisture content of the produce, consequently increasing weight reduction as storage duration increased. As stated by Xu et al. [13], vibration can prompt the process of ripening which is highly caused by the promotion of respiration rate and ethylene production. During ripening, an increase in weight loss can be observed due to water movement (water evaporation) from the produce to the surrounding environment. Also, Munhuewyi [29] confirmed that the rate of respiration is one of the main factors that contribute to weight alterations in fresh produce due to the conversion of carbon (C) atoms to atmospheric carbon dioxide (CO_2).
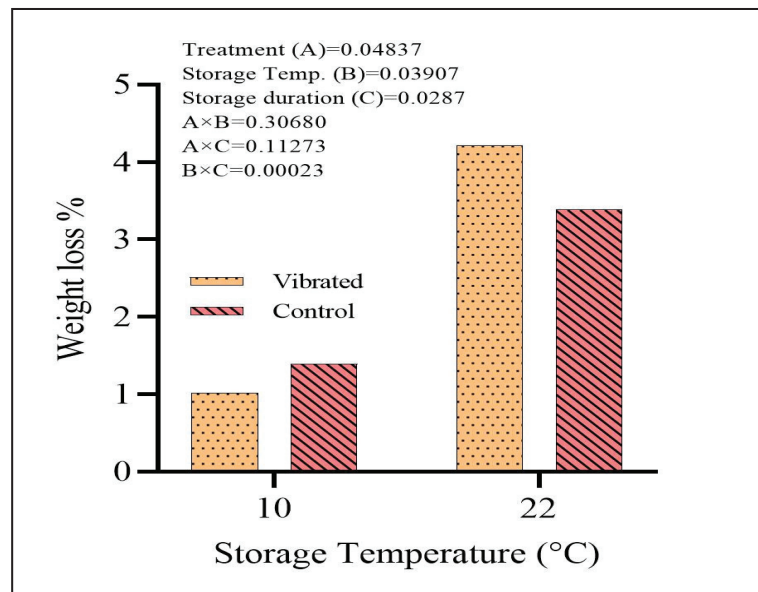
Figure 2. Weight loss (%) of vibrated and non-vibrated (Control) tomato fruits stored at 10 and 22 °C.

Table 1. Vibration accelerations data during simulated transport.

Top	Acceleration Interval (m/s²)	>0.0094	0.0099–0.0104	0.0104–0.0109	0.0109–0.0113	0.0113–0.0118	0.0118–0.0123	0.0123–0.0127	0.0127–0.0132	0.0132–0.0137	0.0137–0.0141	0.0141–0.0146	0.0146–0.0151	0.0151–0.0156	0.0156–0.0160	<0.0160
	Number of Peaks	42	145	203	239	737	595	674	790	374	358	816	839	896	549	57
	Acceleration distribution (%)	0.57	1.98	2.77	3.26	10.07	8.13	9.21	10.80	5.11	4.89	11.15	11.47	12.25	7.50	0.77
Middle	Acceleration Interval (m/s²)	>0.0247	0.252–0.0257	0.0257–0.0261	0.0261–0.0266	0.0266–0.0270	0.0270–0.0275	0.0275–0.0280	0.0280–0.0284	0.0284–0.0289	0.0289–0.0293	0.0293–0.0298	0.0298–0.0302	0.0302–0.0307	0.0307	-
	Number of peaks	78	68	57	139	775	1457	1664	1539	815	245	168	131	85	93	-
	Acceleration distribution (%)	1.06	0.92	0.77	1.90	10.29	19.92	22.75	21.04	11.14	3.34	2.29	1.79	1.16	1.27	-
Bottom	Acceleration Interval (m/s²)	>0.0036	0.0039–0.0042	0.0042–0.0044	0.0044–0.0047	0.0047–0.0050	0.0050–0.0053	0.0053–0.0055	0.0055–0.0058	0.0058–0.0061	0.0061–0.0063	0.0063–0.0066	0.0066–0.0069	0.0069–0.0071	<0.0071	-
	Number of peaks	137	339	616	1156	1213	874	1248	861	327	218	118	66	64	77	-
	Acceleration distribution (%)	1.87	4.63	8.42	15.80	16.58	11.94	17.06	11.77	4.47	2.98	1.61	0.90	0.78	1.05	-

Ghazal et al. [30] also recorded higher weight loss on tomato fruit stressed to vibration compared to the control tomato group due to higher respiration rate and mechanical damages caused by the simulated transport vibration. According to Endalew [31] and Al-Dairi et al. [6], storage at ambient temperature resulted in a greater transpiration rate that leads to wilting, shriveling, and weight reduction in tomatoes. Also, Al-Dairi et al. [2] recorded a low weight loss percentage (3.18%) on tomato fruit stored for 12 days at low temperature (10 °C) which attributed to water retention that occurred at this condition. Regarding weight loss kinetic, Table 2 demonstrates that the zero-order kinetic model gave the highest R^2 ($R^2 \geq 0.9483$) and the lowest values of X^2, and *RMSE* for weight loss of both control and vibrated tomato groups stored at both storage conditions (10 °C and 22 °C).

Table 2. The statistical values of zero-order and first-order models of control and vibrated tomato groups were stored at 10 °C and 22 °C for 10 days storage period.

Quality Parameter	Treatment	Temp.	Zero-Order Model				First-Order Model			
			k	R_2	X^2	*RMSE*	*k*	R^2	X^2	*RMSE*
Weight loss	C	10 °C	0.2111	0.9917	0.0012	0.0331	0.4149	0.9397	0.0325	0.1485
		22 °C	0.6627	0.9909	0.0790	0.1085	0.4357	0.9653	0.8850	0.1167
	V	10 °C	0.2733	0.9982	0.0270	0.0199	0.3537	0.9731	1.1982	0.5357
		22 °C	0.8416	0.9816	0.1660	0.1966	0.4868	0.9735	0.0765	0.1037
L*	C	10 °C	−1.0630	0.9483	0.0213	0.4239	−0.0215	0.9451	0.0001	0.0088
		22 °C	−2.2679	0.9593	0.0817	0.7982	−0.0502	0.9719	0.0003	0.0145
	V	10 °C	−1.9482	0.9720	0.0404	0.5643	−0.0418	0.9668	0.0002	0.0132
		22 °C	−2.6281	0.9604	0.1039	0.9109	−0.0599	0.9733	0.0004	0.0169
a*	C	10 °C	1.3427	0.9836	0.0187	0.2957	0.0481	0.9876	0.0001	0.0092
		22 °C	1.8395	0.9675	0.0683	0.5759	0.0622	0.9512	0.0010	0.0240
	V	10 °C	1.5191	0.9827	0.0246	0.3442	0.0532	0.9835	0.0002	0.0117
		22 °C	2.5830	0.9897	0.0447	0.4506	0.0823	0.9771	0.0008	0.2154
b*	C	10 °C	−1.0147	0.9539	0.0409	0.3811	−0.0430	0.9495	0.0007	0.0190
		22 °C	−1.5240	0.9486	0.1120	0.6059	−0.0786	0.9404	0.0023	0.0337
	V	10 °C	−1.2538	0.9528	0.0627	0.4764	−0.0620	0.9555	0.0010	0.0228
		22 °C	−1.9122	0.9804	0.0593	0.4616	−0.1041	0.9832	0.0011	0.0232
ΔE	C	10 °C	1.8760	0.8446	3.7311	1.3744	0.1539	0.8514	0.0207	0.0909
		22 °C	3.1374	0.9007	4.4746	1.7794	0.1761	0.9962	0.0004	0.0154
	V	10 °C	2.6917	0.9138	3.5762	1.4117	0.2040	0.9220	0.0165	0.0839
		22 °C	4.1489	0.9559	3.5630	1.5219	0.2294	0.9997	6.3×10^{-5}	0.0059
Chroma	C	10 °C	0.4437	0.7822	0.0275	0.3998	0.0126	0.7818	0.0002	0.0113
		22 °C	0.6751	0.8766	0.0307	0.4327	0.0187	0.8767	0.0002	0.0119
	V	10 °C	0.5043	0.8049	0.0308	0.4240	0.0142	0.8053	0.0002	0.0119
		22 °C	1.2289	0.9822	0.0129	0.2825	0.0328	0.9873	6.7×10^{-5}	0.0063
Hue	C	10 °C	−2.6247	0.9867	0.0426	0.5209	−0.0713	0.9809	0.0004	0.0170
		22 °C	−3.6755	0.9707	0.1914	1.0900	−0.1111	0.9784	0.0282	0.0013
	V	10 °C	−3.1014	0.9780	0.0947	0.7948	−0.0880	0.9797	0.0007	0.0217
		22 °C	−4.5943	0.9753	0.2494	1.2480	−0.1525	0.9875	0.0014	0.0293
CI	C	10 °C	0.1284	0.9669	0.0071	0.0405	0.0951	0.9799	0.0163	0.0232
		22 °C	0.2206	0.9671	0.0157	0.0695	0.1411	0.9759	0.0420	0.0378
	V	10 °C	0.1673	0.9708	0.0103	0.0496	0.1162	0.9793	0.0289	0.0288
		22 °C	0.3385	0.9724	0.0302	0.0974	0.1893	0.9872	0.0443	0.0367
Firmness	C	10 °C	−0.1401	0.7796	0.0301	0.1272	−0.0133	0.7610	0.0088	0.0414
		22 °C	−0.2481	0.9665	0.0124	0.0788	−0.0847	0.9572	0.0052	0.0306
	V	10 °C	−0.1822	0.9283	0.0147	0.0865	−0.0585	0.9404	0.0034	0.0251

C indicates the control group; V indicates the vibrated group.

3.3. Color

Figure 3 shows the significant ($p < 0.05$) interaction effect of treatments (vibration/control groups), storage conditions, and storage duration on tomato L* value. With storage time, a decreasing trend of the L* value of all vibrated and non-vibrated tomatoes at both storage temperatures for the 12 days storage was observed due to a reduction in brightness. However, the results of this study showed a higher L* value reduction (37.33) in tomato stressed to vibration compared to the control 39.83 group and stored at 22 °C. Besides, the non-vibrated tomatoes at 10 °C had a better (L*) color value (46.71) than tomatoes stressed to vibration after 10 days of storage. More changes of lightness were observed on tomatoes exposed to vibration due to the repeated vibration motions generated during simulated transport. Besides, the reduction of the color change of the L* value with storage time particularly at 22 °C is due to carotenoids synthesis which leads to tomato darkening [2]. Discoloration of fresh produce due to vibration results in enzymatic browning [32] like polyphenol oxidase (PPO) and peroxidase (POD) [33]. Lightness (L*) change kinetics on Table 2 shows that the zero-order model produced a high R^2 for both control ($R^2 = 0.9483$) and vibrated ($R^2 = 0.9720$) tomato groups stored at 10 °C. However, the first-order model was considered the most appropriate model to represent the L* value change for 10 days for both tomato groups stored at 22 °C. To validate the best model of the L* value of both tomato groups stored at both temperature conditions, the predicted values with the experimental data values were presented and plotted in Figure 4. The predicted values were in a very good correlation with the experimental values ($R^2 > 0.94$) where the predicted data banded around the straight line for all storage conditions and groups which validate the suitability of the selected.

Figure 3. Lightness (L*) value of vibrated and non-vibrated (control) tomatoes stored at (A) 10 °C and (B) 22 °C for 10 days storage. Error bars represent the standard deviation (SD) of the mean values ± S.D of 15 readings per 3 replicates.
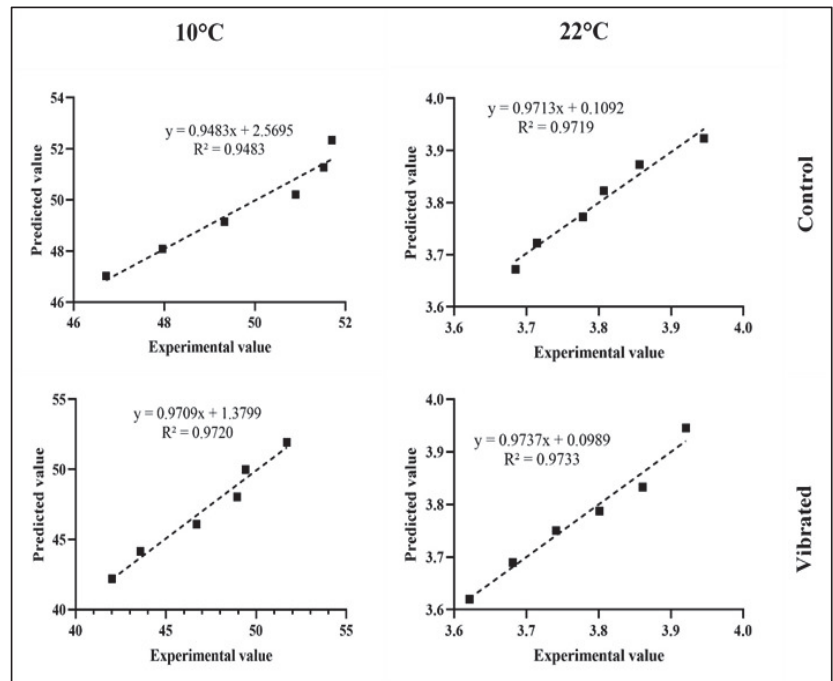
Figure 4. Predicted and experimental results of L* change kinetic of vibrated and non-vibrated (control) tomatoes stored at10 °C and 22 °C.

The redness (a*) was differed ($p < 0.05$) significantly between tomato groups (control and vibrated), storage condition, and storage duration. The redness increased dramatically as storage temperature and duration increased. Besides, vibration showed a higher a* value increment in tomatoes than those exposed to no-vibration. At the end of the 10 days storage period at 22 °C, the a* value percentage of increase in tomato stressed to simulated vibration was 54.14%, while it was 38.66% in tomatoes with no vibration (Figure 5). However, the control tomato group stored at 10 °C showed the lowest percentage of increase in both groups. The increment in redness observed on vibrated tomato samples could be attributed to the high percentage of acceleration occurrence generated from simulated transport resulted in increasing the ripening process of the samples. Besides, higher ethylene and respiration are responsible for vibrated tomato color changes. Also, Dagdelen and Aday [32] indicated an increase in the a* value of peach on the last day of storage due to the increase in respiration rate resulted from the mechanical vibration leading to fruit and color degradation. Wu and Wang [4] observed high red color development in tomatoes exposed to 60 min of simulated transport vibration. Furthermore, high temperature caused a rapid change in the redness value due to lycopene accumulation, rapid ripening, and chlorophyll degradation compared to low storage temperature with storage time [34]. The experimental data of a* value color kinetic of vibrated and control tomato groups stored at 10 °C was highly described by the first-order model. The zero-order kinetic model provided the highest (R^2) for the a* value of vibrated and control tomato groups stored at 22 °C Table 2. The good agreement reported between the predicted values and the experimental values can validate the appropriateness of the models in a* value color kinetic change (Figure 6).
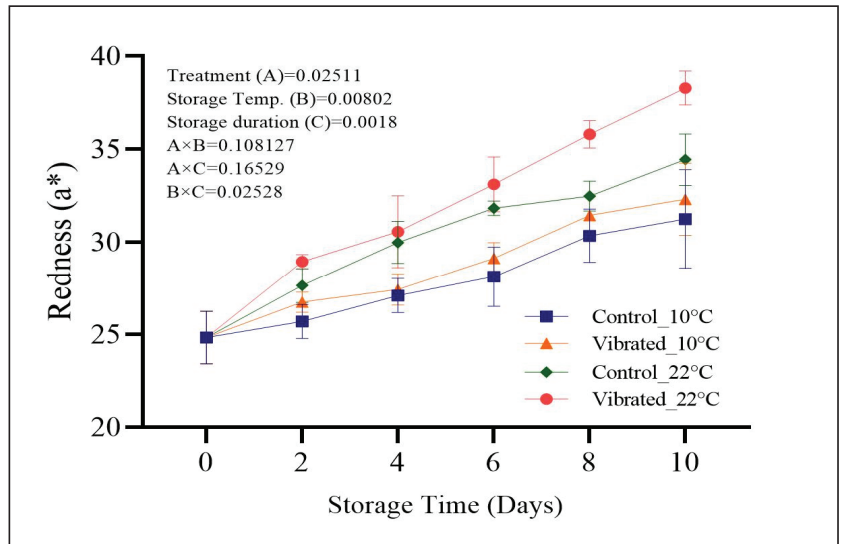
Figure 5. Redness (a*) value of vibrated and non-vibrated (control) tomatoes stored at 10 °C and 22 °C for 10 days storage. Error bars represent the standard deviation (SD) of the mean values ± S.D 15 readings per 3 replicates.
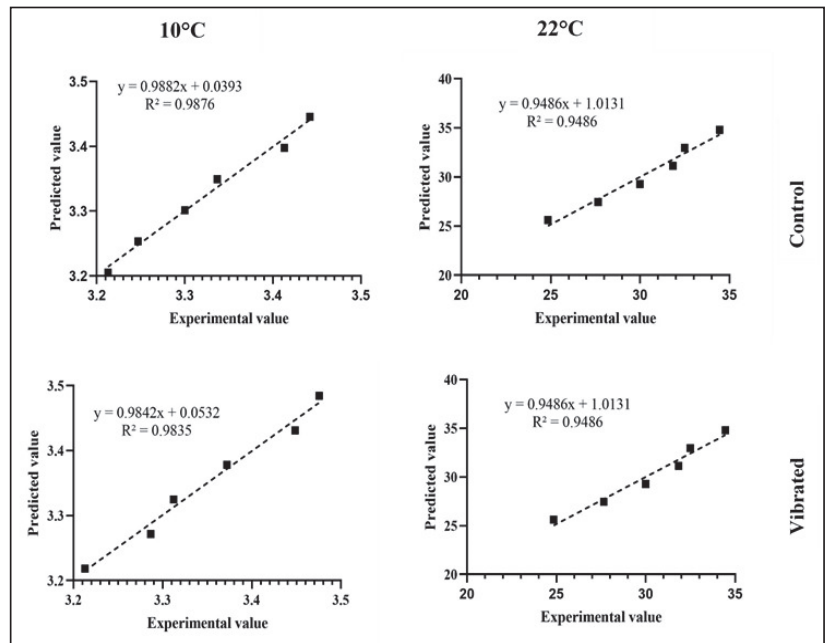
Figure 6. Predicted and experimental results of a* change kinetic of vibrated and non-vibrated (control) tomatoes stored at 10 °C and 22 °C.

The yellowness (b*) color from the two tomato groups decreased with storage temperature and storage period and a considerable b* value difference ($p < 0.05$) between the vibrated and control tomato groups was observed (Figure 7). On the last day of storage,

vibrated tomato stored at 22 °C showed 18.35% more b* value reduction than the control group tomato stored at 10 °C that had the lowest reduction in the b* value among all tomato groups stored at both conditions. Endalew [31] recorded a reduction in the b* value of tomato at a higher temperature during storage due to red color increment. Table 2 shows that the b* value of control tomato groups stored at 10 °C and 22 °C was highly described by the zero-order model. However, the first-order kinetic model was adequately fitted with the b* value of vibrated tomato stored at 10 °C and 22 °C. Figure 8 indicated the correct selection of the kinetic models in the b* color kinetic change which was resulted from the good agreement and relation between the predicted and the experimental data values.
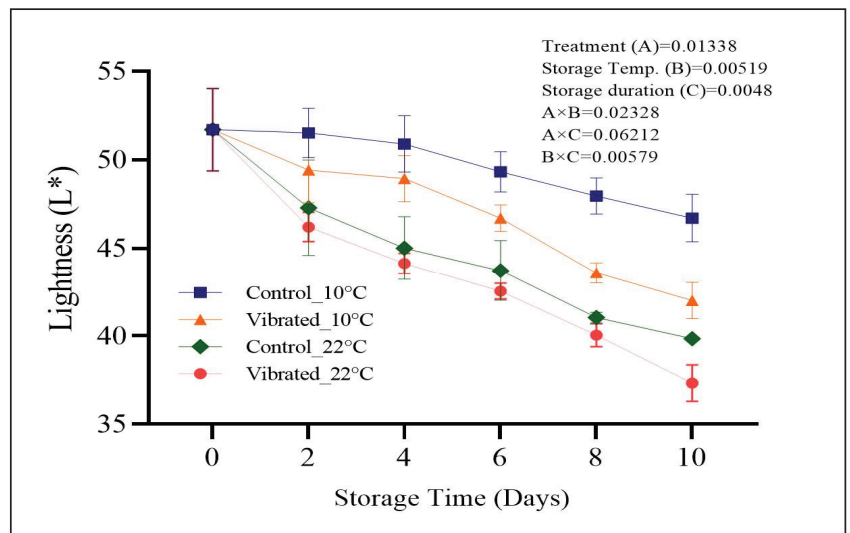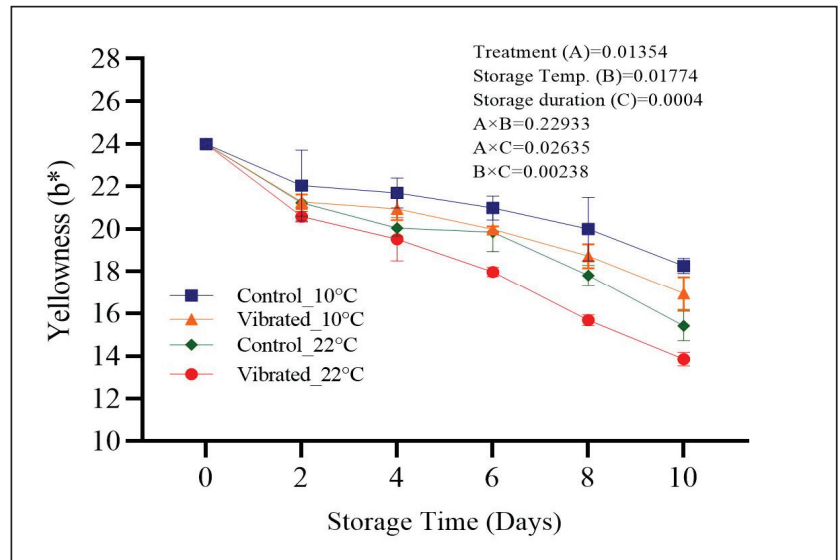

Figure 7. Yellowness (b*) value of vibrated and non-vibrated (control) tomatoes stored at 10 °C and 22 °C for 10 days storage. Error bars represent the standard deviation (SD) of the mean values ± S.D 15 readings per 3 replicates.

The color attributes of total color difference (ΔE), chroma, hue angle, and tomato color index were significantly ($p < 0.05$) varied with storage temperature condition and duration (Figure 9). Also, they were statistically ($p < 0.05$) differed between control and vibrated tomato groups, except with chroma, which had no pronounce ($p > 0.05$) significance between the tomato groups (vibrated and control). The total color difference value of tomato increased with storage time in all storage conditions and groups. The highest ΔE was observed in vibrated tomato group (22.87) followed by the control tomato group (17.86) stored at 22 °C (Figure 9A). On the last day of storage, the ΔE reached 15 and 11.16 on vibrated and control tomato groups stored at 10 °C, respectively (Figure 9A). The reduction in the hue° was higher in tomatoes exposed to vibration and stored at 22 °C with 54.99% than those exposed to no vibration at 10 °C (Figure 9B). Storage at 22 °C offered a faster reduction in hue angle caused due to the natural relation between chemical reactions and temperature that make tomato samples ripen rapidly and convert the green color of tomato to red [5]. During storage days, a fluctuation in chroma value was observed in tomato groups, particularly in those stored at 10 °C (Figure 9C). Despite this, the vibrated tomato group stored at 22 °C showed a dramatic increase in chroma for the 10 days storage period (Figure 9C). As tomato is exposed to vibration and stored at a higher temperature, more color index (CI) can be observed. The initial color index of tomato was 1.03 which later increased and reached 1.91 and 1.71 in vibrated and control tomato groups stored at

10 °C, respectively (Figure 9D). However, the increment was twice higher at 22 °C in the vibrated (2.29) and control (2.24) tomato groups (Figure 9D).

Figure 8. Predicted and experimental results of b* change kinetic of vibrated and non-vibrated (control) tomatoes stored at 10 °C and 22 °C.

Regarding model kinetics, Table 2 shows that the total color difference and tomato color index experimental data of all tomato groups stored at both storage conditions were better predicted by the first-order kinetic model. However, the zero-order model was found suitable to describe chroma and hue angle data of the control tomato group stored at 10 °C. To predict the kinetic changes in hue angle and chroma of vibrated tomato stored at both conditions and control tomato group at 22 °C, a zero-order model was selected (Table 2).

3.4. Firmness (N)

There was a significant difference ($p < 0.05$) in the firmness values between vibrated and control tomato groups. Besides, storage temperature conditions and storage duration were highly significant ($p < 0.05$) with firmness (Figure 10). The initial value of firmness in all tomato groups was 35.51 N. With storage time, the firmness reduced by 24% and 21.95% on vibrated and control tomato groups stored at 10 °C, respectively. When the vibrated and control tomatoes were stored at 22 °C, their firmness state became low with increasing storage duration. At the end of storage, tomatoes subjected to 2 h vibration and stored at 22 °C showed more reduction (44.82%) in firmness compared to those stressed no vibration (35.11%). As highlighted by Wei et al. [7], the vibration generated from simulated transport accelerated the ripening process, thus, reduced firmness with storage time. Dagdelen and Aday [32] reported that higher vibration during transportation can cause more damage to the produce cell wall, therefore, water loss and respiration increased due to structural degradation. In this study, firmness loss was observed in both control and vibrated tomato groups particularly at a storage temperature of 22 °C. This was attributed to the enzymatically controlled processes occurred at room temperature condition which is also link to other metabolic processes like respiration and transpiration as obtained by Cherono and Workneh [35]. Kabir et al. [21] and Al-Dairi et al. [36] found similar trends of firmness reduction at cold and ambient temperature conditions.
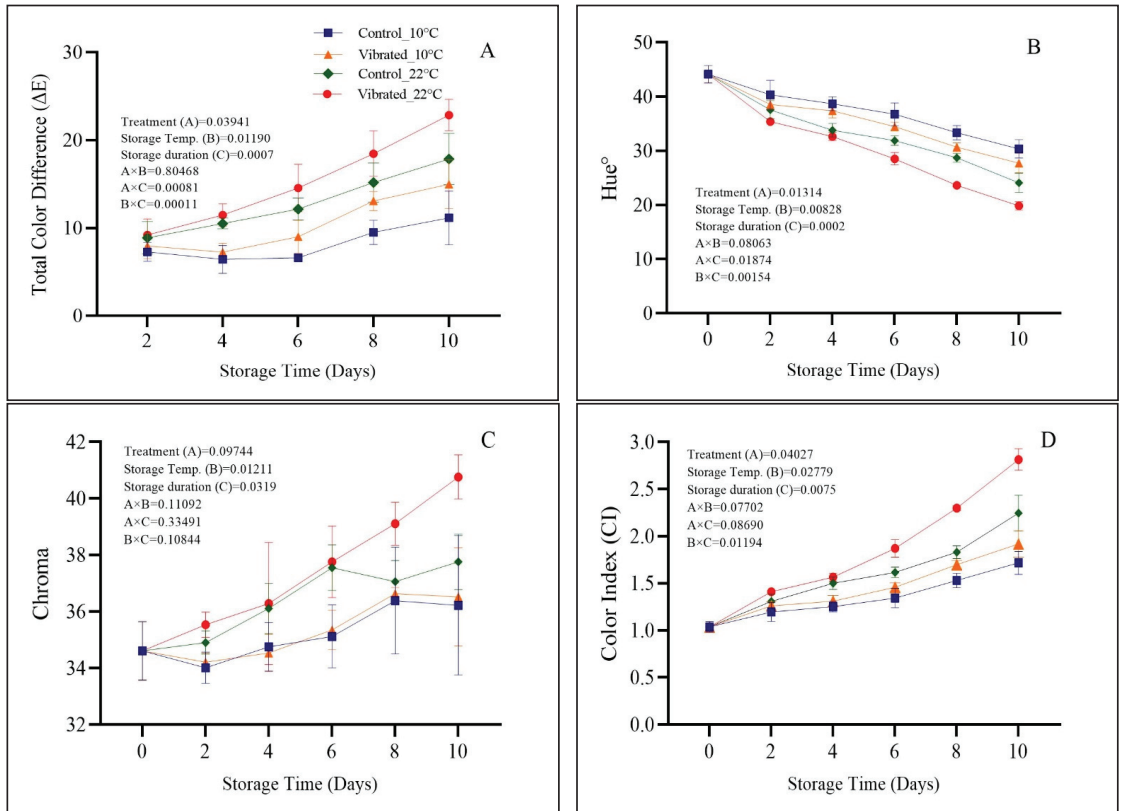
**Figure 9.** (**A**) Total color difference (ΔE), (**B**) hue angle (hue°), (**C**) chroma, and (**D**) tomato color index (CI) value of vibrated and non-vibrated (control) tomatoes stored at 10 °C and 22 °C for 10 days storage. Error bars represent the standard deviation (SD) of the mean values ± S.D 15 readings per 3 replicates.

The zero-order kinetic model was successfully fitted to experimental data of firmness reduction values of both vibrated to control tomato groups stored at 10 °C (Table 2). However, the first-order model gave the highest coefficient of determination (R^2) and low chi-square (X^2), and root mean square error (*RMSE*) of the firmness value of vibrated and non-vibrated tomatoes stored at room condition as shown in Table 2. Figure 11 illustrates the efficiency of the selected models. The straight line was banded by the predicted values of all tomato groups stored at both storage conditions. This can validate the suitability of the model chosen for this parameter.

3.5. Total Soluble Solids (°Brix)

The amount of total soluble solids (TSS) was increased significantly ($p < 0.05$) with storage time and storage conditions. Also, it was varied statistically ($p < 0.05$) between the tomato groups (Figure 12). A higher magnitude of TSS increment was observed in tomatoes exposed to two hours vibration (4.70 °Brix) than in the non-vibrated one (4.48 °Brix) where the increase accelerated by storage at 22 °C. The increase in TSS was also observed in vibrated and control tomatoes stored at 10 °C with 4.51 °Brix and 4.41 °Brix, respectively. Increasing TSS in tomatoes with simulated vibration stress compared to control tomatoes is owing to the rapid ripening of stressed tomatoes under these conditions. During storage, TSS increased more rapidly, suggesting a more ripening resulted in pectin substance

degradation into more simple sugars e.g., Oligosaccharides [29]. More TSS was observed on samples subjected to vibration compared to the control samples by Dagdelen and Aday [32]. Similar results of significance on TSS between control and vibrated samples were also found on apples by Jung and Park [9]. A similar trend was observed by Kabir et al. [21] and Pathare and Al-Dairi [37], where increasing storage time can increase TSS contents. of fresh produce. Besides, Tigist et al. [34] recorded higher TSS content after the 32 days of storage at room temperature.
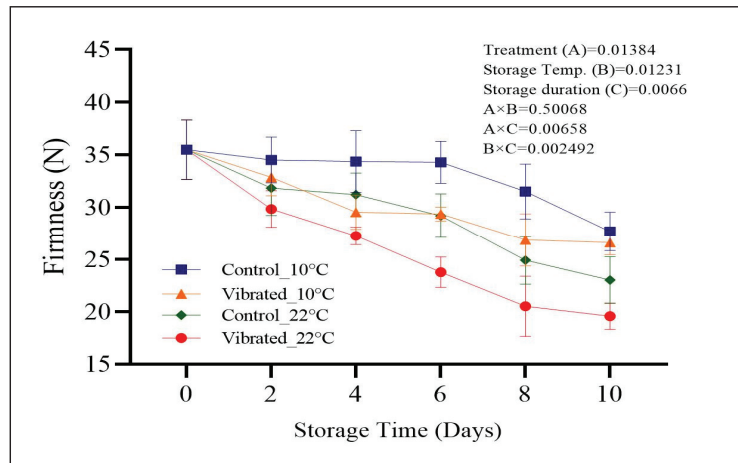
Figure 10. Firmness value (b*) of vibrated and non-vibrated (control) tomatoes stored at 10 °C and 22 °C for 10 days storage. Error bars represent the standard deviation (SD) of the mean values ± S.D of 6 readings per 3 replicates.
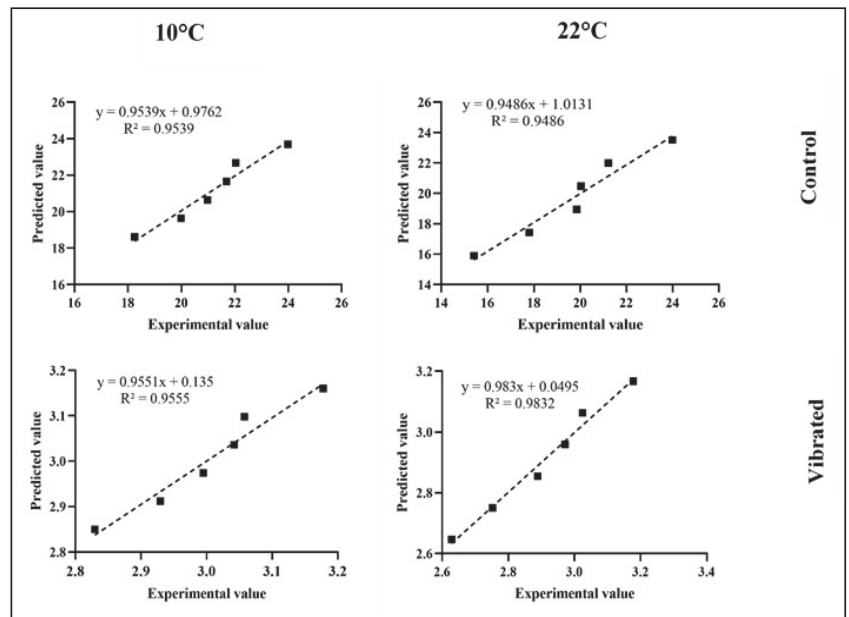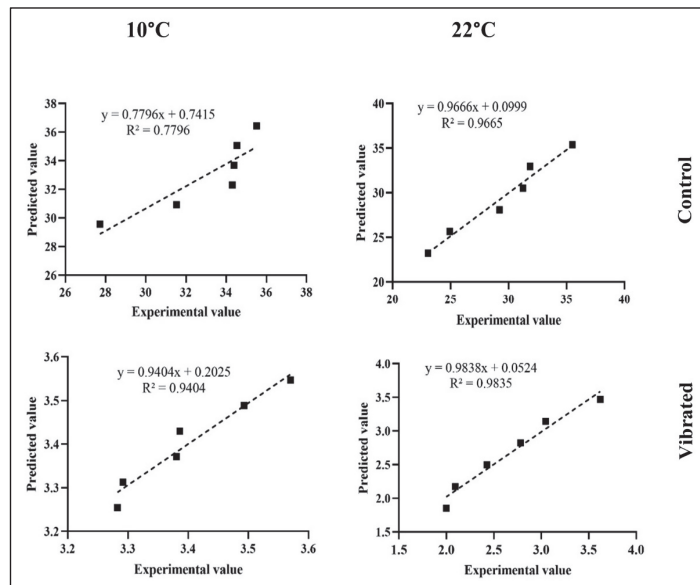

Figure 11. Predicted and experimental results of b* change kinetic of vibrated and non-vibrated (control) tomatoes stored at 10 °C and 22 °C.
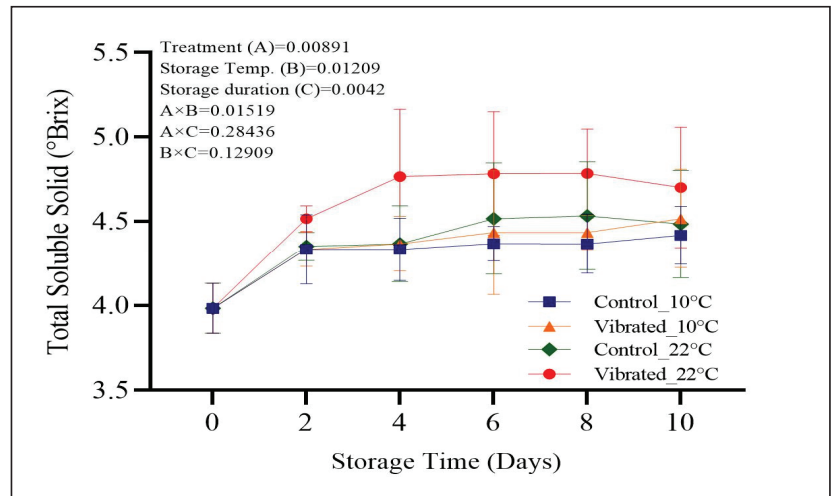
Figure 12. TSS value (Brix°) value of vibrated and non-vibrated (control) tomatoes stored at 10 °C and 22 °C for 10 days storage. Error bars represent the standard deviation(SD) of the mean values ± S.D 6 readings per 3 replicates.

3.6. Headspace Gases

Headspace O_2 and CO_2 concentration significantly ($p < 0.05$) declined over time at both storage temperatures. Headspace O_2 was not varied significantly ($p > 0.05$) between the vibrated and non-vibrated groups Table 3. The average O_2 concentration on day 2 was almost 16.85% and 16% in the control and vibrated stress group which reduced to reach 14.35% and 15.15% at 10 °C on day 8 respectively. More reduction was reported on O_2% in the control and vibrated tomato groups stored at 22 °C. On day 8, the vibrated tomato group showed a reduction in O_2 with 7.80% which later increased by 1% on day 10. Furthermore, more CO_2 increment was observed in tomatoes stored at 22 °C. On day 8, the CO_2 content reached 4.75 and 17.30% on the vibrated and control tomato groups respectively at 10 °C, while it was 4.55 and 17.75% respectively at 22 °C. The study suggested that both O_2 and CO_2 gases are correlated inversely during storage inside the gas collecting containers of tomatoes.

A significant increase was observed in ethylene (C_2H_4) at both storage conditions for 8 days storage period, which reduced on day 10 in all storage temperatures. There was no pronounce significance ($p < 0.05$) in C_2H_4 content between the vibrated group and the control tomato group. However, the vibrated tomatoes stored at room temperature recorded the highest content in C_2H_4 on day 8 with 3.25 ppm followed by the control tomatoes stored with 1.85 ppm compared to the initial value (1.45 and 1.25 ppm) respectively. Ethylene concentrations were 1.26 and 1.55 ppm in the control group and vibration stress group stored at 10 °C on day 8 respectively. All gases reached their equilibrium concentration on day 8 (Table 3). Low O_2 concentration activates anaerobic metabolites. The slow change in O_2 at 10 °C could result from the low rate of respiration at low-temperature storage conditions. Besides, the C_2H_4 production increased due to the continued ripening even after harvest. Therefore, C_2H_4 can accelerate the ripening of fresh produce [9].

3.7. Subjective Quality Analysis/Visual Observation of Mechanical Damage

The visual observation of the physiological damage and bruise incidence was mostly observed on the vibration stress tomato group at 22 °C (Figure 13) compared to the control group stored at both storage conditions. The damage on vibrated tomato at 22 °C reached 38.80%, while it was 5.50% on the control tomato group at the same temperature. No dam-

age was observed on the control tomato stored in both conditions. Overall, the results of this study showed that vibration stress during simulated transport and storage at ambient accelerated the degradation of tomato with storage time.

Table 3. O_2%, CO_2% concentration, and C_2H_4 (ppm) production of control and vibrated tomato groups stored at 10 °C and 22 °C for 10 days storage period. Data are presented in mean values $\pm$ SD.

Headspace Gases	Treatment	Temp. °C	Days of Storage				
			2	4	6	8	10
O_2 (%)	C	10 °C	16.85 ± 0.21	16.35 ± 0.35	14.85 ± 0.07	14.35 ± 0.21	13.80 ± 0.42
		22 °C	12.20 ± 2.26	11.50 ± 2.82	10.80 ± 2.12	8.15 ± 0.91	7.85 ± 1.20
	V	10 °C	16.00 ± 1.41	16.20 ± 1.13	15.25 ± 0.21	15.15 ± 0.21	15.60 ± 0.14
		22 °C	11.80 ± 1.69	10.50 ± 0.70	9.55 ± 0.77	7.80 ± 0.14	8.00 ± 0.00
CO_2 (%)	C	10 °C	3.90 ± 0.00	4.25 ± 0.07	4.45 ± 0.07	4.75 ± 0.35	4.55 ± 0.07
		22 °C	9.15 ± 1.20	9.70 ± 1.83	11.00 ± 1.41	17.30 ± 0.84	15.30 ± 0.28
	V	10 °C	3.85 ± 0.07	3.95 ± 0.07	4.45 ± 0.07	4.55 ± 0.07	4.60 ± 0.00
		22 °C	9.30 ± 0.70	9.80 ± 1.55	11.10 ± 0.14	17.75 ± 1.34	16.15 ± 0.21
C_2H_4 (ppm)	C	10 °C	1.20 ± 0.00	1.20 ± 0.14	1.25 ± 0.07	1.26 ± 0.00	1.15 ± 0.07
		22 °C	1.25 ± 0.07	1.40 ± 0.00	1.65 ± 0.07	1.85 ± 0.07	1.40 ± 0.14
	V	10 °C	1.15 ± 0.21	1.30 ± 0.00	1.35 ± 0.07	1.55 ± 0.49	1.25 ± 0.14
		22 °C	1.45 ± 0.07	1.45 ± 0.07	1.75 ± 0.07	3.25 ± 1.90	1.86 ± 0.35

C indicates the control group; V indicates the vibrated group.
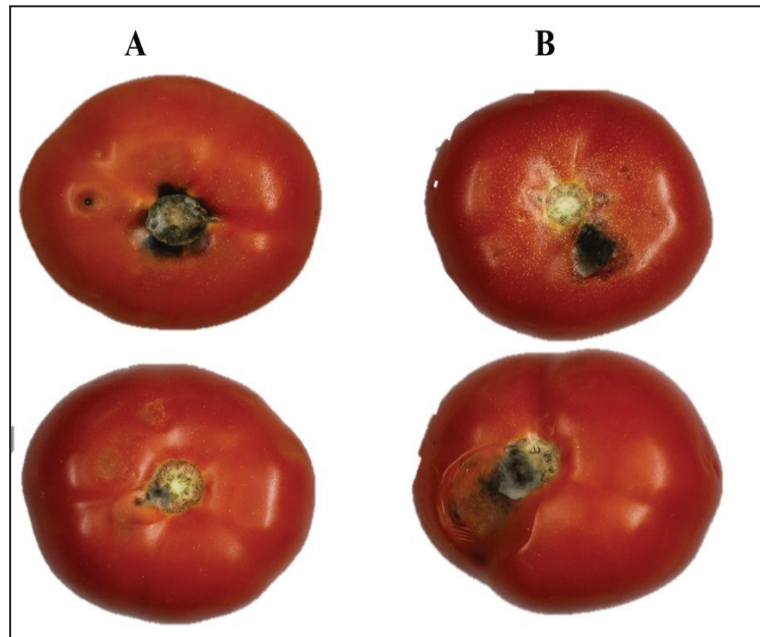
Figure 13. Physiological damages on the vibrated tomatoes stored at (**A**) 10 °C and (**B**) 22 °C after 10 days of storage.

4. Conclusions

The study investigated the effect of vibration stress generated from laboratory simulated transport and storage at two different storage conditions on the quality of tomatoes (weight loss %, color parameters, firmness, total soluble solids (TSS), and headspace

gases) for 10 days. Based on the obtained results, weight loss %, firmness, lightness (L*), redness (a*), yellowness (b*), hue°, and total color changes (ΔE) were highly dependent on all studied factors (storage duration, vibration, and storage temperature conditions). A high reduction in weight, L*, b*, firmness, O_2 and hue angle, and increment in a*, TSS, color index (CI), C_2H_4 content, and CO_2 in the vibrated tomato fruits at room temperature 22 °C. Storage at low temperature (10 °C) reduced the quality changes occurrence of both control and vibrated tomato groups. The experimental data of weight loss, color, and firmness values were highly fitted to zero and first-order kinetic models. It was also found that the first-order kinetic model was the best model applied to represent the quality changes kinetic of both tomato groups at 10 and 22 °C. Proper technologies during transportation and storage are required to minimize the quality changes and degradation of tomatoes in the harvesting-consumption system.

Author Contributions: Conceptualization, P.B.P.; formal analysis, M.A.-D.; data curation, M.A.-D.; writing—original draft preparation, M.A.-D.; writing—review and editing, P.B.P.; supervision, P.B.P.; funding acquisition, P.B.P. All authors have read and agreed to the published version of the manuscript.

Institutional Review Board Statement: Not applicable.

Informed Consent Statement: Not applicable.

Data Availability Statement: Data is contained within the article.

Conflicts of Interest: The authors declare no conflict of interest.

References

1. Famuyini, J.; Sedara, A. Effect of Maturity Stage on Quality and Shelf Life of Tomato (Lycopersicon Esculentum Mill) Using Refrigerator Storage System. *Eurasian J. Agric. Res.* **2020**, *4*, 23–44.
2. Al-Dairi, M.; Pathare, P.B.; Al-Mahdouri, A. Effect of Storage Conditions on Postharvest Quality of Tomatoes: A Case Study at Market-Level. *J. Agric. Mar. Sci.* **2021**, *26*, 13–20.
3. Chero, M.J.S.; Zamora, W.R.M.; Chero, J.A.S.; Villarreyes, S.S.C. Application of the Computer Vision System to the Measurement of the CIE L* a* B* Color Parameters of Fruits. In *Advances in Artificial Intelligence, Software and Systems Engineering*; Ahram, T., Ed.; Advance Intelligent Systems and Computing; Springer: Cham, Switzerland, 2020; Volume 1213.
4. Wu, G.; Wang, C. Investigating the Effects of Simulated Transport Vibration on Tomato Tissue Damage Based on Vis/Nir Spectroscopy. *Postharvest Biol. Technol.* **2014**, *98*, 41–47. [CrossRef]
5. Cherono, K.; Sibomana, M.; Workneh, T.S. Effect of Infield Handling Conditions and Time to Pre-Cooling on the Shelf-Life and Quality of Tomatoes. *Braz. J. Food Technol.* **2018**, *21*, 1–12. [CrossRef]
6. Al-Dairi, M.; Pathare, P.B.; Al-Yahyai, R. Effect of Postharvest Transport and Storage on Color and Firmness Quality of Tomato. *Horticulturae* **2021**, *7*, 163. [CrossRef]
7. Wei, X.; Xie, D.; Mao, L.; Xu, C.; Luo, Z.; Xia, M.; Zhao, X.; Han, X.; Lu, W. Excess Water Loss Induced by Simulated Transport Vibration in Postharvest Kiwifruit. *Sci. Hort.* **2019**, *250*, 113–120. [CrossRef]
8. Alfatni, M.S.M.; Shariff, A.R.M.; Abdullah, M.Z.; Marhaban, M.H.B.; Saaed, O.M.B. The Application of Internal Grading System Technologies for Agricultural Products–Review. *J. Food Eng.* **2013**, *116*, 703–725. [CrossRef]
9. Jung, H.; Park, J.-G. Effects of Vibration Stress on the Quality of Packaged Apples During Simulated Transport. *J. Biosyst. Eng.* **2012**, *37*, 44–50. [CrossRef]
10. Walkowiak-Tomczak, D.; Idaszewska, N.; Łysiak, G.P.; Bieńczak, K. The Effect of Mechanical Vibration During Transport under Model Conditions on the Shelf-Life, Quality and Physico-Chemical Parameters of Four Apple Cultivars. *Agronomy* **2021**, *11*, 81. [CrossRef]
11. Jung, H.M.; Lee, S.; Lee, W.-H.; Cho, B.-K.; Lee, S.H. Effect of Vibration Stress on Quality of Packaged Grapes during Transportation. *Eng. Agric. Environ. Food* **2018**, *11*, 79–83. [CrossRef]
12. Tao, F.; Chen, W.; Jia, Z. Effect of Simulated Transport Vibration on the Quality of Shiitake Mushroom (*Lentinus edodes*) during Storage. *Food Sci. Nutr.* **2020**, *9*, 1152–1159.

13. Xu, F.; Liu, S.; Liu, Y.; Wang, S. Effect of Mechanical Vibration on Postharvest Quality and Volatile Compounds of Blueberry Fruit. *Food Chem.* **2021**, *349*, 129216. [CrossRef] [PubMed]

14. Al-Dairi, M.; Pathare, P.B.; Al-Yahyai, R. Chemical and Nutritional Quality Changes of Tomato during Postharvest Transportation and Storage. *J. Saudi Soci.Agric. Sci.* **2021**, *20*, 401–408.

15. Xu, D.; Zuo, J.; Li, P.; Yan, Z.; Gao, L.; Wang, Q.; Jiang, A. Effect of Methyl Jasmonate on the Quality of Harvested Broccoli after Simulated Transport. *Food Chem.* **2020**, *319*, 126561. [CrossRef] [PubMed]

16. Chaiwong, S.; Bishop, C.F. Effect of Vibration Damage on the Storage Quality Of 'elsanta' strawberry. *Aust. J. Crop Sci.* **2015**, *9*, 859–864.

17. Walkowiak-Tomczak, D.; Idaszewska, N.; Bieńczak, K.; Kómoch, W. The Effect of Mechanical Actions Occurring during Transport on Physicochemical Changes in Agaricus bisporus Mushrooms. *Sustainability* **2020**, *12*, 4993. [CrossRef]

18. Pathare, P.B.; Al-Dairi, M. Bruise Damage and Quality Changes in Impact-Bruised, Stored Tomatoes. *Horticulturae* **2021**, *7*, 113. [CrossRef]

19. Pathare, P.B.; Al-Dairi, M.; Al-Mahdouri, A. Bruise Damage Susceptibility and Fruit Quality Assessment of Pear. *Open Agric. J.* **2021**, *15*, 82–90. [CrossRef]

20. Arah, I.K.; Kumah, E.K.; Anku, E.K.; Amaglo, H. An Overview of Post-Harvest Losses in Tomato Production in Africa: Causes and Possible Prevention Strategies. *J. Bio. Agric. Healthc.* **2015**, *5*, 78–88.

21. Kabir, S.N.; Rasool, K.; Lee, W.-H.; Cho, S.-I.; Chung, S.-O. Influence of Delayed Cooling on the Quality of Tomatoes (*Solanum lycopersicum* L.) Stored in a Controlled Chamber. *AIMS Agric. Food.* **2020**, *5*, 272. [CrossRef]

22. Remini, H.; Mertz, C.; Belbahi, A.; Achir, N.; Dornier, M.; Madani, K. Degradation Kinetic Modelling of Ascorbic Acid and Colour Intensity in Pasteurised Blood Orange Juice During Storage. *Food Chem.* **2015**, *173*, 665–673. [CrossRef]

23. Al-Dairi, M.; Pathare, P.B.; Al-Yahyai, R. Quality Changes Kinetic of Tomato During Postharvest Transportation and Storage. *J. Food Proc. Eng.* **2021**, *44*, e13808. [CrossRef]

24. Al-Dairi, M.; Pathare, P.B. Kinetic Modeling of Quality Changes of Tomato During Storage. *Agric. Eng. Int. CIGR J.* **2021**, *23*, 183–193.

25. Zhang, W.; Luo, Z.; Wang, A.; Gu, X.; Lv, Z. Kinetic Models Applied to Quality Change and Shelf Life Prediction of Kiwifruits. *LWT* **2021**, *138*, 110610. [CrossRef]

26. Pathare, P.B.; Opara, U.L.; Al-Said, F.A. Colour Measurement and Analysis in Fresh and Processed Foods: A Review. *Food Bioproc Technol.* **2013**, *6*, 36–60. [CrossRef]

27. Chayjan, R.A.; Alaei, B. New Model for Colour Kinetics of Plum under Infrared Vacuum Condition and Microwave Drying. *Acta Sci. Pol. Technol. Aliment.* **2016**, *15*, 131–144. [CrossRef]

28. Pinheiro, J.; Alegria, C.; Abreu, M.; Gonçalves, E.M.; Silva, C.L. Kinetics of Changes in the Physical Quality Parameters of Fresh Tomato Fruits (*Solanum lycopersicum*, Cv. 'Zinac') During Storage. *J. Food Eng.* **2013**, *114*, 338–345. [CrossRef]

29. Munhuewyi, K. Postharvest Losses and Changes in Quality of Vegetables from Retail to Consumer: A Case Study of Tomato, Cabbage and Carrot. Master's Thesis, Stellenbosch University, Stellenbosch, WC, South Africa, 2012.

30. Ghazal, A.; El-Masry, G.; El-Sheikh, I.; Radwan, S. Estimation of Some Postharvest Losses in Tomato During Simulated Transport Operation. *Misr J. Agric. Eng.* **2017**, *34*, 291–316. [CrossRef]

31. Endalew, E. Postharvest Loss Assessment of Tomato (*Lycopersicon esculentum* Mill) (Galilea Cultivar) Along the Postharvest Supply Chain, Northwest Ethiopia. Master's Thesis, Bahir Dar University, Amhara, Ethiopia, 2020.

32. Dagdelen, C.; Aday, M.S. The Effect of Simulated Vibration Frequency on the Physico-Mechanical and Physicochemical Properties of Peach During Transportation. *LWT* **2021**, *137*, 110497. [CrossRef]

33. Sun, L.; Liu, S.; Fan, Z.; Li, Y.; Wang, J.; Zhong, Y.; Zhang, Q.; Duan, X. The Impact of Storage Temperature on Fruit Quality and Chilling Injury of 'Okubao' peaches. *Int. J. Food Biosci.* **2018**, *1*, 12–18.

34. Tigist, M.; Workneh, T.S.; Woldetsadik, K. Effects of Variety on the Quality of Tomato Stored under Ambient Conditions. *J. Sci. Technol.* **2013**, *50*, 477–486. [CrossRef] [PubMed]

35. Cherono, K.; Workneh, T. The Efficacy of Postharvest Biocontrol Treatments in Controlling Spoilage of Tomato Fruit in South African Commercial Supply Chains. *J. Eng. Agric. Environ.* **2020**, *5*, 19–25. [CrossRef]

36. Al-Dairi, M.; Pathare, P.B.; Al-Mahdouri, A. Impact of vibration on the quality of tomato produced by stimulated transport. In *IOP Conference Series: Earth and Environmental Science*; IOP Publishing: Bristol, UK; London, UK, 2021; p. 012101.

37. Pathare, P.B.; Al-Dairi, M. Bruise Susceptibility and Impact on Quality Parameters of Pears During Storage. *Front. Sustain. Food Syst.* **2021**, *5*, 658132. [CrossRef]

MDPI

Article

Investigation and Evaluation of Impact Bruising in Guava Using Image Processing and Response Surface Methodology

Than Htike [1,2], Rattapon Saengrayap [1,3], Nattapol Aunsri [3,4], Khemapat Tontiwattanakul [5] and Saowapa Chaiwong [1,3,*]

1   School of Agro-Industry, Mae Fah Luang University, Chiang Rai 57100, Thailand; 6251407007@lamduan.mfu.ac.th (T.H.); rattapon.sae@mfu.ac.th (R.S.)
2   Department of Agriculture, Ministry of Agriculture, Livestock and Irrigation, Nay Pyi Taw 15011, Myanmar
3   Integrated AgriTech Ecosystem Research Group, Mae Fah Luang University, Chiang Rai 57100, Thailand; nattapol.aun@mfu.ac.th
4   School of Information Technology, Mae Fah Luang University, Chiang Rai 57100, Thailand
5   Department of Mechanical and Aerospace Engineering, King Mongkut's University of Technology North Bangkok, Bangkok 10800, Thailand; khemapat.t@eng.kmutnb.ac.th
*   Correspondence: saowapa@mfu.ac.th; Tel.: +66-53-916-766

Abstract: Simulated impact damage testing was investigated by fractal image analysis using response surface methodology (RSM) with a central composite design (CCF) on quality of 'Glom Sali' guava for drop heights (0.2, 0.4, and 0.6 m), number of drops (1, 3, and 5) and storage temperature conditions (10, 20, and 30 °C). After 48 h, impacted fruit were determined and analyzed for bruise area (BA), bruise volume (BV), browning index (BI), total color difference (ΔE), image analysis for bruise area (BAI), and fractal dimension (FD) at the bruising region on peeled guava. Results showed that the correlation coefficient ($r = -0.6055$) between ΔE and FD value was higher than ΔE and either BA ($r = 0.3132$) or BV ($r = 0.2095$). The FD variable was determined as a better indicator than conventional measurement (BA or BV) for pulp browning and impact bruising susceptibility. The FD variable also exhibited highest R^2_{adj} value (81.69%) among the other five variables, as the highest precision model with high determination coefficient value (R^2_{adj}) (>0.8) for impact bruising prediction. Recommended condition of the FD variable to minimize impact bruising was drop height of 0.53 m for five drops under storage at 30 °C. FD variable assessed by image analysis was shown to be a highly capable measurement to determine impact bruising susceptibility in guava fruit.

Keywords: bruise susceptibility; impact bruise; mechanical injury; transportation

1. Introduction

Guava (*Psidium guajava* L.) is one of the most famous and economically important fruits in Thailand, with an export value in 2020 worth 5.50 million USD [1]. Guava is a climacteric fruit with a round shape and thin skin that bruises easily. To maintain fruit quality and shelf life and minimize losses, guava fruit needs proper postharvest handling practices [2]. Thai agriculture and ASEAN standards of guava require slight defects on the skin not exceeding 10% of the total surface area of guava fruit [3,4]. Bruising effects can be distinguished from quality changes in guava such as browning, softening of the fruit peel, cell destruction, and reduction in intercellular air spaces resulting in the bruised tissue losing moisture and becoming desiccated [5]. Impact damage to fruit is more severe than vibration and compression damages. When a fruit falls with sufficient force against a surface, impact damage occurs, while dynamic damage of a single fruit occurs through fruit-to-fruit impact between packaging. Fruit dropping from trees to the ground during harvesting, dynamic impact between single fruit, and between the fruit and packaging or containers are all causes of impact damage [6].

Most previous researchers studied independent factors such as drop height, number of drops, and storage temperature. Drop heights of 0.04 to 0.75 m were investigated in

fruit such as guava [5], apple [7–9], pomegranate [10–12], peach [13], and pear [14,15]. In apple, bruise volume (BV) increased linearly with an increase of drop height level [16], while different storage temperatures were investigated in apple [9], pomegranate [11,17,18], and pear [14,15]. However, few studies have investigated the number of drops on fruit found that the fourth drop of apple resulted in an irreversible change in cell damage that stabilized the bruise energy [19]. Previous studies on impact bruise damage investigated two independent variables as drop height and storage temperature, with a fixed number of drops by using a completely randomized design (CRD) experiment in apple [9], pomegranate [11,18], and pear [14,15]. Impact bruising area of 'Pink Lady' apple was affected by both drop height and storage temperature [9], bruise damage of pomegranate fruit increased at higher drop height with lower storage temperature (5 °C) [18], while in pears bruising was affected by storage temperature with increased susceptibility to bruising at 22 °C [15]. For impact testing of guava, different drop heights and numbers of drop were currently examined in a CRD experiment with a fixed storage temperature of 25 °C [20]. Thus, most studies investigated either individual factors or the combination between drop height and storage temperature as independent variables for impact testing. Few studies have investigated number of drops combined with either drop height or storage temperature.

Response surface methodology (RSM) was used to identify the relationship between independent and response variables to assess the influences of the many factors and their interactions [21]. RSM utilizes a set of mathematical and statistical methods that fit polynomial equations to the experimental data, hence explaining how the data set behaves [22]. Advantages of using RSM were reducing in the number of experimental treatments to evaluate multiple variables and the ability of the statistical tool to identify interaction of independent variable [23,24]. Several researchers used this method for various aspects of experimental design involving extraction process, food preservation, and fruit coating applications [25]. In postharvest research, many studies investigated fruit coating in various fruit such as guava [26], banana [27], pear [28], apple [29], and in postharvest treatment for storage period in lychee [30]. Recently, the number of drops for five times from either 0.3 m or 0.6 m from CRD experiment exhibited the same BA, BV, and bruise susceptibility levels. Also, the number of drops was assumed a major independent variable of impact bruising in 'Gim Ju' guava [20]. Thus, influences of environmental factors such as drop height, number of drops, and storage temperature also remain unclear for impact bruising with a limit of different conditions.

Bruise area (BA) and bruise volume (BV) are most commonly used to measure the amount of impact bruise damage in fruit such as apples [8,31,32], pomegranate [10,33], and peach [13]. Browning index (BI) and total color difference (ΔE) both showed highest values for medium and high drop impact bruise damage after 48 h incubation time in pomegranate fruit [11]. Increase in skin tissue browning appeared to be correlated with higher storage temperature in persimmon [34]. Fractal dimension (FD) is an image analysis technique used to explain the texture features of the image [35]. Previously, most researchers used image textural features as FD to assess color change in pulp, internal browning incidence, and fruit defects in pear [36], apple [37], banana [38], and cucumber [39] to evaluate fruit quality. Recently, FD analysis has exhibited high potential and accuracy for vibration bruising of guava under simulated transportation utilizing RSM design [40]. Only one study of fractal image analysis has been conducted to determine impact bruising in guava [20]. The recent study in impact bruise testing with different drop heights and number of drops was examined. Results showed that FD calculated by image analysis presented higher potential for bruise assessment in guava fruit. The efficiency of FD analysis showed potential when comparing BA with BV (conventional technique) for impact and vibration bruising assessments [20,40].

Interestingly, there has been no previous studies that applied RSM to examine three independent variables as drop height, number of drops, and storage temperature, with three factor levels for free fall drop testing in guava and other fruit. Therefore, this study

(1) examined the optimal impact condition from treatment combinations of drop height, number of drops and storage temperature, and (2) applied fractal image analysis to assess impact bruising in guava fruit utilizing RSM design.

2. Materials and Methods

2.1. Plant Materials and Sample Preparation

Guava fruit cv. 'Glom Sali' were randomly collected from Pangha Homestay Orchard, Mae Sai District, Chiang Rai Province, Thailand (latitude 20°24'22.7" N longitude 100°00'23.9" E). The guava fruit were harvested at the mature green stage (approximately 100 days after fruit set) having a light green skin color and carefully handled to avoid mechanical injuries. The fruit were packed into plastic baskets and covered with two material layers of foam net and polythene bags as cushioning materials to protect against mechanical injuries during transportation to the laboratory S7 building at Mae Fah Luang University within 3 h. The fruit were sorted for uniformity of size (approximately 250 to 300 g), color, and if they were free of distinct signs of bruising and disease with a smooth and clean peduncle cut surface.

The random 'Glom Sali' guava fruit (15 fruits) were selected and examined for fruit properties by checking uniformity, guava maturity, fruit weight, volume, density, diameter, radius of curvature, firmness, total soluble solids (TSS), and dry matter. Average weight of guava and density fruit were 250.26 g and 0.98 g mL^{-1} (Table 1). Fruit density at <1.0 indicates top quality at the mature stage for harvesting and optimal consumer acceptability. The highest bruise susceptibility was occurred in the cheek region of the fruit [17], while the middle and top regions of apple showed higher bruise sensitivity than the bottom region for fruit-to-fruit bruising [41]. In this study, the cheek region was exposed to the highest impact under free fall drop test. The averaged radius of curvature at the cheek region of this guava fruit was 50.94 mm (Table 1).

Table 1. Fruit characteristics of 'Glom Sali' guava subjected to simulated impact testing.

Fruit Characteristics	Mean ± SE
Fruit weight (g)	250.26 ± 1.50
Volume (mL)	235.33 ± 7.81
Density (g mL^{-1})	0.98 ± 0.02
Horizontal diameter (cm)	7.65 ± 0.07
Height (cm)	8.72 ± 0.12
Radius of curvature (mm)	50.94 ± 1.44
Firmness (N)	5.09 ± 0.31
Total Soluble Solids (TSS) (%)	11.51 ± 0.30
Dry matter (%)	13.32 ± 0.30

Results of fifteen random fruit samples before impact testing (n = 15).

2.2. Bruise Susceptibility Testing of Guava Fruit

Simulated impact testing was set up utilizing a 9 cm-diameter pipe, following the method of Hussein et al. [33] for pomegranate impact testing. As shown in Figure 1, each fruit was located over a shallow depression (8 cm diameter) in a foam sheet material with dimensions 20 × 23 × 2 cm. A stainless-steel ball (diameter 8 cm and weight 250 g) of equal size and weight to a guava fruit was dropped on each guava fruit from three different drop heights (0.2, 0.4, and 0.6 m) for 1, 3, and 5 drops at each drop height.

The impact energy (*E*) was calculated using the equation of $E = mgh$, where m is the guava mass, g is the gravitational constant (9.81 m s^{-2}), and h is the drop height (m) [33]. As shown in Table 2, the impact energy of a stainless-steel ball for 1, 3, and 5 drops at each of the three drop heights ranged from 507.05 to 7273.60 J. After impact testing, the fruit were stored at three temperature conditions (10, 20, and 30 °C under 90% RH) and checked for quality measurement after 48 h (see Section 2.3 for more information).
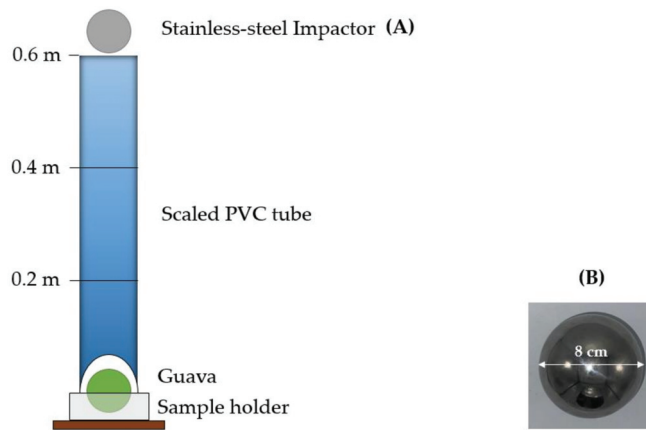
Figure 1. Experimental setup of simulated impact testing in guava (**A**) with stainless-steel ball (250 g, diameter 8 cm) (**B**), adapted following the method of [33].

Table 2. Impact energy for three drop heights (0.2, 0.4, and 0.6 m) and number of drops (1, 3, and 5 times).

Treatment	Impact Energy (J)
0.2 m + 1 drop	507.05
0.2 m + 3 drops	1374.96
0.2 m + 5 drops	2529.00
0.4 m + 1 drop	1141.49
0.4 m + 3 drops	2950.29
0.4 m + 5 drops	4995.25
0.6 m + 1 drop	1590.40
0.6 m + 3 drops	4040.16
0.6 m + 5 drops	7273.60

After simulated impact testing, the bruised guava sample was peeled using a sharp knife with peel thickness of 0.9 mm to reveal browning of the flesh before impact bruising was determined.

2.3. Experimental Design by Response Surface Methodology (RSM)

RSM with central composite face-centered design (CCF) was examined to evaluate the main interaction and quadratic effects of drop height, number of drops, and temperature on impact bruising and color change of the guava fruit (Table 3).

Table 3. Coded independent variables of drop height, number of drops, and storage temperature for RSM with central composite face-centered design (CCF).

Independent Variable	Code	Coded Variable		
		−1	0	+1
Drop height (m)	X_1	0.2	0.4	0.6
Number of drops (times)	X_2	1	3	5
Temperature (°C)	X_3	10	20	30

As shown in Table 4, the three independent variables of CCF design with 20 treatments (runs) were coded as −1 (lowest level), 0 (middle level), and +1 (highest level), and applied with the cube point for 8 times, axial point for 6 times, and the repeated center point (0.0.0) for 6 times. The three independent variables were drop height (X_1) (0.2,

0.4, and 0.6 m), number of drops (X_2) (1, 3, and 5 times), and storage temperature (X_3) (10, 20, and 30 °C). In this study, drop heights (0.2, 0.4, and 0.6 m) were compared with a range of drop heights (0.04 to 0.6 m) onto a rigid impact surface in previous studies on pomegranate [11,12,18], apple [7], and pear [14,15]. Five drops were assumed to be the maximum number throughout the guava supply chain [42]. The optimal storage temperature for guava was recommended at 10 °C [43], while temperature during road transportation in open trucks was estimated to average 30 °C. The response function was determined as bruise area (BA), bruise volume (BV), browning index (BI), total color difference (ΔE), bruise area by image analysis (BAI), and fractal dimension (FD). The response function value (Y) was related to the coded three independent variables (X_i, 1, 2, and 3) following Equation (1).

Table 4. RSM with central composite face-centered design (CCF) to optimize simulated impact conditions of 'Glom Sali' guava.

Run	Code			Treatment Factors		
	X_1	X_2	X_3	Drop Heights (m)	No. of Drops (Times)	Temperature (°C)
1	−1	−1	−1	0.2	1	10
2	−1	−1	+1	0.2	1	20
3	−1	+1	−1	0.2	1	30
4	−1	+1	+1	0.2	5	30
5	+1	−1	−1	0.6	1	10
6	+1	−1	+1	0.6	1	30
7	+1	+1	−1	0.6	5	10
8	+1	+1	+1	0.6	5	30
9	0	0	−1	0.4	3	10
10	0	0	+1	0.4	3	30
11	0	−1	0	0.4	1	20
12	0	+1	0	0.4	5	20
13	−1	0	0	0.2	3	20
14	+1	0	0	0.6	3	20
15	0	0	0	0.4	3	20
16	0	0	0	0.4	3	20
17	0	0	0	0.4	3	20
18	0	0	0	0.4	3	20
19	0	0	0	0.4	3	20
20	0	0	0	0.4	3	20

Response data of the three independent variables to the six dependent variables as BA, BV, BI, ΔE, BAI, and FD were examined, and the quadratic polynomial fitting was accomplished. The equation of the prediction model is shown as polynomial Equation (1).

$$Y = b_0 + b_1X_1 + b_2X_2 + b_3X_3 + b_{11}X_1^2 + b_{22}X_2^2 + b_{33}X_3^2 + b_{12}X_1X_2 + b_{23}X_2X_3 + b_{13}X_1X_3 \tag{1}$$

where, Y is the representation of the predicted response functions (BA, BV, BI, ΔE, BAI, and FD), X_1, X_2, and X_3 are the three independent variables (drop heights, number of drops, and storage temperature), X_1^2, X_2^2 and X_3^2 are the square of each independent variables. The coefficients of the polynomial were denoted by b_0 (constant term), b_1, b_2 and b_3 (linear effects), b_{11}, b_{22} and b_{33} (quadratic effects), and b_{12}, b_{13} and b_{23} (interaction effects).

2.4. Quality Measurements

2.4.1. Bruise Determination of the Guava Fruit

After impact testing, the guava fruit were stored at 10, 20, and 30 °C with 90% RH (Constant climate chamber, HPP750, Memmert GmbH + Co. KG, Schwabach, Germany) and checked for quality measurement after 48 h when the bruised tissues had turned pale [44]. BA and BV, commonly used to measure the amount of fruit bruise damage, were

determined for fruit damage in apple [32]. BA and BV of each fruit were calculated by Equations (2) and (3).

$$BA = \pi/4 \, (ab) \tag{2}$$

$$BV = \pi d/24 \, (3ab + 4d^2) \tag{3}$$

where, *a* and *b* are the major axes of the bruise elliptical and *d* is bruise depth measured by peel thickness [10]. These bruise parameters were measured by a digital caliper (RS PRO 150 mm, RS Components Pte Ltd., Clarke Quay, Singapore) with ±0.01 (mm) accuracy in Figure 2.
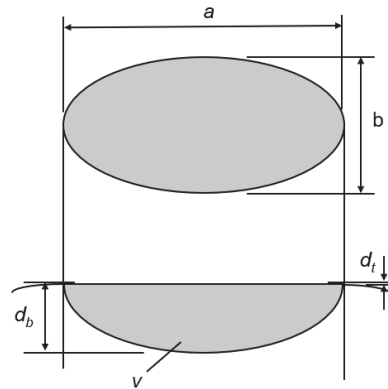
Figure 2. Determining bruise area and volume by using the elliptical method [10].

2.4.2. Pulp Color at Bruise Area

The guava was peeled to reveal either wet bruising (translucent) or browning incidence at four positions with three positions at no bruising region and one position at middle of bruising region that were measured in the equation zone for each fruit by a CIE-Lab color colorimeter (Konica Minolta, Color Reader CR-10, Osaka, Japan) to determine bruise lightness (*L**), redness (*a**), yellowish (*b**). Browning index (BI) was calculated to represent purity of the brown color [45] using Equations (4) and (5). Total color difference (ΔE) was calculated using different color levels on fruit peel (*L**, *a**, and *b** values) between initial (before impact bruise) [46] and after impact damage for 48 h at the bruise area using Equation (6).

$$BI = [100 * (X - 0.31)]/0.172 \tag{4}$$

$$\text{When, } X = (a^* + 1.75L^*)/(5.645L^* + a^* - 3.012b^*) \tag{5}$$

$$\Delta E = ((L_0^* - L^*)^2 + (a_0^* - a^*)^2 + (b_0^* - b^*)^2)^{1/2} \tag{6}$$

where, L_0^*, a_0^*, and b_0^* are the initial color values of the peeled fruit, *L**, *a**, and *b** are the final values at bruised area after storage at 10, 20, and 30 °C with 90% RH for 48 h.

2.4.3. Image Analysis

The bruise region on the fruit surface after impact testing was placed under a square light box (UDIOBIZ 40D, size 40 × 40 × 40 cm, adjustable light, pocket studio with 4 rows of LED as light source intensity 9.6×10^5 lux using a light meter (Tenmars TM-204, Taipei, Taiwan). Guava images were taken at a uniform distance of 40 cm, with camera settings on manual mode, autofocus, lens capture f 7.1, 1/250 shutter speed, and ISO 100 using a digital mirrorless camera (Canon EOS M50, 15–45 mm, Tokyo, Japan). The original image files (6000 × 3368 pixels) were saved in JPEG format with 72-dpi resolution. Guava bruise damage images were analyzed by ImageJ software (version 1.51j8, NIH, Bethesda, MD, USA) following the method of Chaiwong et al. [40]. All original images were pre-processed

and resized. The image analysis procedure is shown in Figure 3. The resized image was cropped around the bruising area, which is the region of interest (ROI). After that, the RGB image was converted into an 8-bit image (grayscale), then the surface plot of bruising image was determined by plotting the grayscale values (z-axis) of each pixel in the image (x- and y-axis). The surface plot showed the roughness of bruise surface texture due to the variation of grayscale level in each pixel of the image. Moreover, the 8-bit image was thresholded to convert to be the binary image. Then, the binary image of bruising was computed as a percentage of the bruise region corresponding to the entire flesh area.
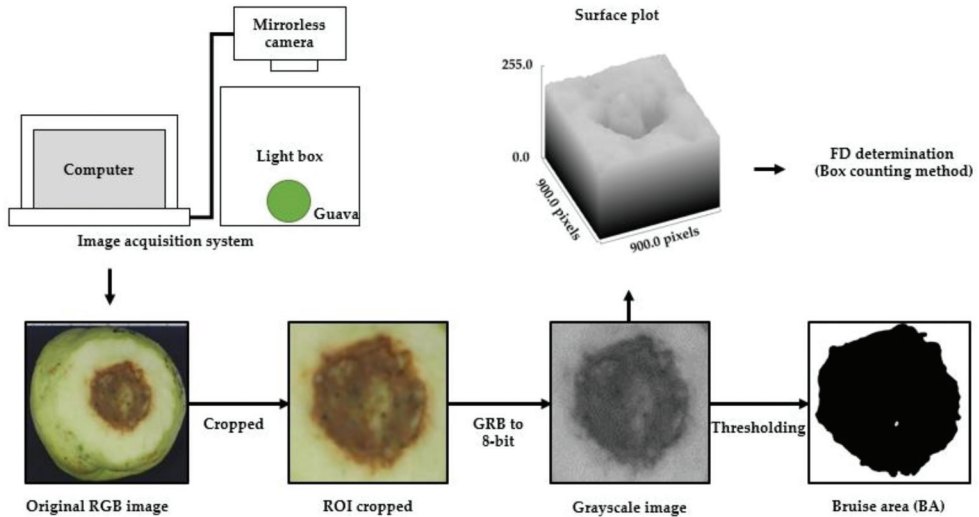
Figure 3. Image acquisition system and image analysis procedure for impact bruise determination.

The intensity of fruit bruise damage was estimated using the binary image. The Fractal dimension (FD) values of the bruise images were then determined using the fractal box counting technique by intercepting N number of various box size r (2–128 pixels) with the binary image. FD value was calculated as FD = log(Nr)/log(1/r) [40].

2.5. Statistical Analysis

The effect of each of the three independent factors, lack-of-fit, and regression coefficients (R^2) in individual linear, quadratic, and interaction terms was determined in analysis of variance (ANOVA) tables and generated to establish the model equation by Minitab version 19 (Minitab, LLC, State college, PA, USA). Three-dimensional response surface plots were created using the overlaid contour plot feature in MATLAB software version R2018a (MathWorks Inc., Natick, MA, USA). Predictive equations for the thirteen treatments within the experimental range conditions were checked for correctness (Table 5). To generate a matrix plot using PAST 4.05 software, all variables were evaluated using Pearson's correlation ($p < 0.05$).

Table 5. Thirteen treatments to verify the predictive model in 'Glom Sali' guava impact bruising by simulated impact testing.

Run	Code			Treatment Factors		
	X_1	X_2	X_3	Drop Heights (m)	No. of Drops	Temperature (°C)
1	−1	−1	−1	0.2	1	10
2	−1	+1	−1	0.2	1	30
3	−1	+1	+1	0.2	5	30
4	+1	+1	+1	0.6	5	30
5	0	0	−1	0.4	3	10
6	0	0	+1	0.4	3	30
7	0	−1	0	0.4	1	20
8	0	+1	0	0.4	5	20
9	−1	0	0	0.2	3	20
10	+1	0	0	0.4	3	30
11	0	0	0	0.4	3	20
12	0	0	0	0.4	3	20
13	0	0	0	0.4	3	20

3. Results and Discussion

3.1. Fractal Image Analysis and Correlation between Bruise Susceptibility and Color

The intensity of fruit bruise damage was analyzed by converting cropped RGB images and calculating the FD values. Using the threshold method, the bruise damage region was cropped and then separated. Before applying a box counting method to determine FD values, the selected BA was transformed into a binary image (Figure 4). Fractal image analysis of guava impact bruising was varied in the drop test under RSM design (Table 4). Image analysis revealed visible damage to the peeled guava surface. A greater impact bruise with lower FD value exhibited as a significantly deeper surface plot image, which related to the low value of grayscale that came from the dark brown color of bruising, relating to increase in drop height, number of drops, and storage temperature. For example, the deepest surface plot image with the lowest FD value (1.900) was a drop height of 0.6 m for five drops (*E* = 7273.60 J) (Table 2) for storage condition at 30 °C (Figure 4H). Lower storage temperature at 10 °C with drop height (0.6 m) and five drops (*E* = 7273.60 J) (Table 2) exhibited the deepest surface with FD value (1.910) (Figure 4G), while the shallowest surface with the highest FD value (1.952) was a drop height of 0.2 m for one drop and storage at 10 °C (Figure 4A). In previous studies, image analysis was used to obtain FD values for lightness and darkness of the surface to assess bruising or browning of banana [38]. Fractal modeling was used to assess the intensity of flesh browning and its color change to acquire improved knowledge of the enzymatic chemical changes and their location within the apple fruit [37]. Recently, it was found that higher impact bruising for both drop heights of 0.3 and 0.6 m repeated five times. Results showed a deeper surface plot with lower FD values of 1.937 and 1.930, respectively, after storage at 25 °C for 48 h [20]. Therefore, fractal image analysis in this study successfully performed impact bruising severity of guava under different drop test conditions utilizing RSM design. Recently, the advanced techniques, i.e., hyperspectral, computerized, and X-ray imaging had successfully achieved assessing bruise severity accurately; however, these techniques required higher invest in the machine and complex computational processes to interpret the data. Although, application of FD was only suitable for characterizing the external bruising such as vibrational bruising damage [40], this technique using simple equipment and data processing technique that may have a change to apply for various commodities.
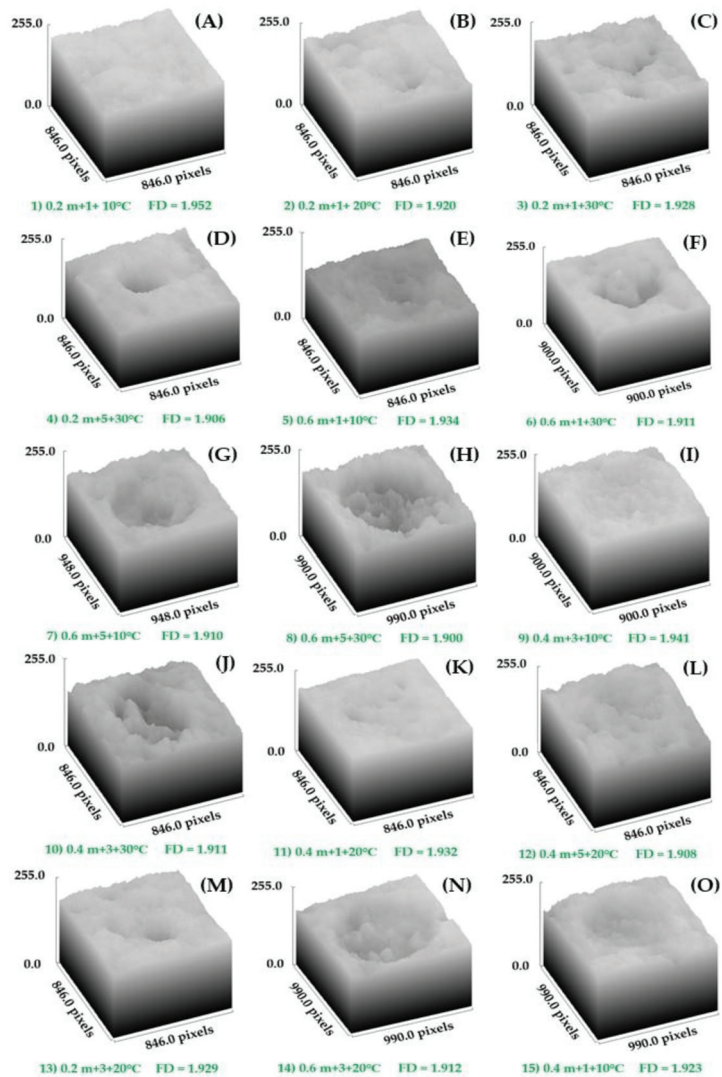
Figure 4. Fifteen pictures of fractal dimension (FD) of surface plots in impact bruising of guava for different drop heights, number of drops, and storage temperature variables under RSM design from fifteen runs (treatments) after storage for 48 h. The fifteen runs were 0.2 m + 1 drop + 10 °C (**A**), 0.2 m + 1 drop + 20 °C (**B**), 0.2 m + 1 drop + 30 °C (**C**), 0.2 m + 5 drops + 30 °C (**D**), 0.6 m + 1 drop + 10 °C (**E**), 0.6 m + 1 drop + 20 °C (**F**), 0.6 m + 5 drops + 10 °C (**G**), 0.6 m + 5 drops + 30 °C (**H**), 0.4 m + 3 drops + 10 °C (**I**), 0.4 m + 3 drops + 30 °C (**J**), 0.4 m + 1 drop + 20 °C (**K**), 0.4 m + 5 drops + 20 °C (**L**), 0.2 m + 3 drops + 20 °C (**M**), 0.6 m + 3 drops + 20 °C (**N**), 0.4 m + 1 drop + 10 °C (**O**).

Guava fruit peel is thin and delicate and easily damaged by rough handling during harvest and postharvest [2]. In this study, Pearson's correlation was performed to establish the relationship between the six measured dependent variables BA, BV, BI, ΔE, BAI, and FD. The FD variable showed good agreement with the ΔE parameter ($r = -0.6055$) when compared with BA, BV, BI, and BAI, while color measurement and analysis of BI and ΔE parameters for impact guava bruising correlated poorly with bruise damages (BA and BV)

as well as FD. Thus, image analysis (FD) was a good indicator to respond to browning incidence of impact guava bruising as the ΔE variable from 20 different impact conditions (Table 6). Heterogeneous changes of fruit and vegetable surfaces such as color intensity and enzymatic browning reaction had a strong correlation with FD value variations [47]. For bruise formation of fresh-cut apple, the higher potential of image analysis detected that ΔE value correlated to color changes [48]. Image analysis by the FD method offers great potential for application where color intensity has a non-homogenous color surface [36]. Increase in the FD value in the selected area indicated major complexity in color distribution during the enzymatic browning kinetic for banana [38]. For vibration bruising of guava, FD analysis exhibited high potential and accuracy under frequency, acceleration, and time duration of vibration testing [40]. For impact bruising of guava, FD analysis showed higher potential than color measurements to evaluate impact bruise damage under testing conditions such as drop height, number of drops, and storage temperature [20]. Thus, the FD variable was a good indicator for impact bruising of guava under varying conditions of drop height, number of drops, and storage temperature. Therefore, high efficacy of the FD technique was suggested to assess mechanical damages in guava, with applications on other sensitive fruit from impact and vibration forces.

Table 6. Bruise assessment parameters of guava fruit stored at 25 °C under 70% RH for four days.

	BA	**BV**	**BI**	**ΔE**	**BAI**	**FD**
BA	1.0000					
BV	0.2363					
BI	−0.1871	0.1332				
ΔE	0.3132	0.2095	0.4332			
BAI	0.9975 *	0.2372	−0.1837	0.3116		
FD	−0.3854	−0.2366	−0.0448	−0.6055 *	−0.3992	1.0000

* Significant at $p < 0.05$: BA = bruise area; BV = bruise volume; BI = browning index; ΔE = total color difference, BAI = bruise area by image analysis; FD = fractal dimension.

In this study, ΔE was a better indicator for impact bruising damage of guava than BI and showed high correlation with the FD variable. Both browning scores and ΔE parameters revealed highest values in pomegranate corresponding to medium and high drop impact bruise damage [11]. At medium and maximum drop levels, a high ΔE value indicated impact bruising of pomegranate [18]. Variations in ΔE value correlated to changes in color of fresh-cut apple over time [48]. Interestingly, the BAI parameter from the image analysis technique showed positive correlation with BA ($r = 0.9975$). Bruise area by image analysis was suggested to apply for BA measurement as a conventional technique, with calculation as Equation (2) to determine the impact bruising area of guava.

3.2. Model Fitting and Statistical Analysis of CCF

RSM values utilizing CCF from 20 treatments (runs) performed the correlation of the response data between three independent variables and six dependent variables (BA, BV, BI, ΔE, BAI, and FD) (Table 4) by quadratic multiple regression equations as follows (Equations (7) to (12)).

$$Y_1 \text{ (BA)} = 219.8 - 2.3X_1 + 57.7X_2 + 117.1X_3 - 7.1X_1{}^2 - 107.6X_2{}^2 + 47.5X_3{}^2 - 2.0X_1X_2 + 4.3X_1X_3 + 29.0X_2X_3 \quad (7)$$

$$Y_2 \text{ (BV)} = 2559 + 1525X_1 + 386X_2 + 862X_3 + 4895X_1{}^2 - 3977X_2{}^2 - 2294X_3{}^2 + 4X_1X_2 + 25X_1X_3 + 372X_2X_3 \quad (8)$$

$$Y_3 \text{ (BI)} = 97.42 + 4.72X_1 - 3.50X_2 + 1.06X_3 + 4.72X_1{}^2 + 5.03X_2{}^2 - 0.35X_3{}^2 - 5.48X_1X_2 - 0.90X_1X_3 - 1.64X_2X_3 \quad (9)$$

$$Y_4 \text{ (ΔE)} = 4.159 + 2.183X_1 + 0.491X_2 + 0.775X_3 + 1.140X_1{}^2 - 0.927X_2{}^2 + 0.567X_3{}^2 - 0.106X_1X_2 + 0.666X_1X_3 + 0.007X_2X_3 \quad (10)$$

$$Y_5 \text{ (BAI)} = 233.5 + 0.3X_1 + 56.6X_2 + 117.1X_3 - 7.3X_1{}^2 - 108.6X_2{}^2 + 48.5X_3{}^2 - 4.1X_1X_2 + 0.3X_1X_3 + 28.1X_2X_3 \quad (11)$$

$$Y_6 \text{ (FD)} = 1.9177 - 0.0117X_1 - 0.0097X_2 - 0.0068X_3 + 0.0049X_1{}^2 - 0.0011X_2{}^2 - 0.0006X_3{}^2 + 0.0029 X_1X_2 + 0.0026X_1X_3 + 0.0004X_2X_3 \quad (12)$$

Table 7 shows the coefficient results of RSM regression equations generated from the ANOVA analysis of BA, BV, BI, ΔE, BAI, and FD models. The predicted six models (BA, BV, BI, ΔE, BAI, and FD) provided the determination coefficient (R^2_{adj}) values of 0.5304, 0.0868, 0.2227, 0.5751, 0.4960, and 0.8169, respectively. These findings indicated that the FD model provided higher response performance than the BA, BV, BI, ΔE, and BAI model predictions. The lack of fit values of the five models (BA, BI, ΔE, BAI, and FD) were not remarkable, except that the BV model showed low levels of reliability and repeatability, with significant lack of fit and R^2_{adj} (8.68%). The FD variable exhibited the highest R^2_{adj} value (81.69%), representing the highest precision model for impact bruising prediction among the other five variables. Also, the ΔE model with R^2_{adj} value (57.51%) exhibited greater liability for impact bruising prediction than BI with R^2_{adj} value (22.27%). In this study, FD exhibited the highest dependent variable for impact damage of guava due to a significant correlation with ΔE (Table 6) as well as the highest levels of reliability and repeatability (Table 7).

Table 7. ANOVA results of each drop height (X_1) (m), number of drops (X_2) (times), and temperature (X_3) (°C) factors as response surface models for BA, BV, BI, ΔE, BAI, and FD values of impact bruise of 'Glom Sali' guava fruit.

Coefficient Terms	Y_1 (BA)		Y_2 (BV)		Y_3 (BI)		Y_4 (ΔE)		Y_5 (BAI)		Y_6 (FD)	
	Regression Coefficient	p-Value	Regression Coefficient	p-Value	Regression Coefficient	p-Value	Regression Coefficient	p-Value	Regression Coefficient	p-Value	Regression Coefficient	p-Value
Constant term	219.8	0.000	2559	0.057	97.42	0.000	4.195	0.000	233.5	0.000	1.9177	0.000
X_1-Drop heights	−2.3	0.934	1525	0.193	4.72	0.101	2.183	0.001 **	0.3	0.993	−0.0117	0.000 **
X_2-Number of drops	57.7	0.057	386	0.731	−3.50	0.209	0.491	0.288	56.6	0.071	−0.0097	0.000 **
X_3-Temperature	117.1	0.001 **	862	0.449	1.06	0.693	0.775	0.107	117.1	0.002 **	−0.0068	0.003 **
$X_1 \times X_2$	−2.0	0.949	4	0.997	−5.84	0.090	−0.106	0.834	−4.1	0.899	0.0049	0.180
$X_1 \times X_3$	4.3	0.888	25	0.984	−0.90	0.764	0.666	0.203	0.3	0.992	0.0011	0.217
$X_2 \times X_3$	29.0	0.355	372	0.767	−1.64	0.588	0.007	0.990	28.1	0.391	0.0006	0.854
X_1^2	−7.1	0.892	4895	0.041 *	4.72	0.365	1.140	0.202	−7.3	0.895	0.0029	0.179
X_2^2	−107.6	0.062	−3977	0.085	5.03	0.337	−0.927	0.293	−108.6	0.070	0.0026	0.755
X_3^2	47.5	0.375	−2294	0.297	−0.35	0.946	0.567	0.513	48.5	0.386	0.0004	0.865
Lack of fit		0.851		0.001 **		0.933		0.403		0.877		0.536
R^2		75.28%		51.93%		59.09%		77.64%		73.47%		90.36%
R^2_{adj}		53.04%		8.68%		22.27%		57.51%		49.60%		81.69%

Significant level: ** significant at p-value < 0.01; * significant at p-value < 0.05.

Until recently, no RSM experiments investigating free fall or impact testing had been conducted for impact bruising susceptibility at various drop heights, number of drops and temperature conditions to simulate the effects on guava and other sensitive fruit. Only two RSM studies on vibration testing for fruit bruising used two independent variables to design vibration conditions of tomato [49] and three independent variables to design vibration conditions of guava [40]. Most studies on simulated impact bruise damage only focused on experimental designs by fixing one or two variables. With their fruit size and spherical shape similar to guava fruit, pomegranate and apple were tested under two variables of three drop heights and two storage temperature conditions with a fixed number of drops [9,11,17], while pear bruises were determined using two variables with three drop heights and two storage temperature conditions with a fixed number of drops [14,15]. Recently, impact bruising using two variables of three drop heights and member of drops (one and five times) on bruise assessment in guava fruit was examined [20]. Thus, no clear factor analysis has demonstrated impact fruit bruising under three independent variables.

In this study, an RSM design for simulated impact testing identified three major independent variables in guava bruising with both individual and combined effects. The ANOVA result showed that all linear coefficients (drop height (X_1), number of drops (X_2), and temperature (X_3)) affected the FD model. The linear coefficients (X_1) and (X_3) also affected color changes (ΔE) and both BA and BAI models, respectively. The quadratic drop height (X_1^2) only had an effect on the BV model (Table 7). Most previous studies focused on two independent variables (drop height and storage temperature) with a fixed number of drop heights using CRD design in pomegranate [11,18], 'Pink Lady' apple [9], and pear [14,15]. For example, in the study of pomegranate fruit, storage temperature factors affected impact bruising with higher refrigerated storage temperature reducing bruise damage [17]. The drop height factor combined with impact materials affected bruise area measurement in apples [9], while the combination of drop height and storage temperature showed the highest increase in bruise area, bruise volume, and color measurements in pear

fruit [14,15]. Recently, the number of drops (five drops) from different heights (0.3 and 0.6 m) affected impact bruising of guava more than the same drop height (0.3 and 0.6 m) with a single drop [20]. Therefore, this is the first study to undertake impact test by RSM experiment for this bruising in guava and other fruit. However, this study of RSM design did not exhibit significant cross-product coefficients among the three independent variables from six dependent variables. Therefore, the linear model was suggested as optimal to predict impact bruising of guava compared with the quadratic model (Table 7). Previous studies investigated impact bruising volume of apple, with impact energy ranging 0 to 2.25 J. Results showed that linear regression fitted the impact energy for apple sizes of 180 and 240 g, with high coefficient of determination (R^2) values at 0.94 and 0.93, respectively [50]. There was also a high linear relationship ($R^2 = 0.94$) between BV and drop height for BV of apple [16]. Recently, a strong linear regression between impact bruise susceptibility and color parameters in pear at different drop heights and storage temperatures was found by Pathare [14].

The FD model was optimized by setting minimum conditions as drop height of 0.53 m for five drops under storage temperature of 30 °C (Equation (12)). To minimize the FD value, postharvest handling of guava must be gentle to avoid impact bruising, coupled with a cool storage temperature. Response surface analysis of CCF (Figure 5) showed that surfaces of the BA, BV, BI, and BAI models for drop height, number of drops, and storage temperature showed no interaction between X_1X_2, X_2X_3, and X_1X_3 (Table 6), while the ΔE model became steeper with increasing number of drops and storage temperature. The 3D graphs of FD model indicated that increasing number of drops and storage temperature in the slope of the curved surface and lower steepness (Figure 5F), giving linear model ($p < 0.05$) (Table 7) when compared with ΔE response surface with a non-significant impact in both number of drops and storage temperature ($p > 0.05$) (Figure 5C) (Table 7).

$$Y_4 (\Delta E) = 4.159 + 2.183X_1 + 0.491X_2 + 0.775X_3 + 1.140X_1^2 - 0.927X_2^2 + 0.567X_3^2 - 0.106X_1X_2 + 0.666X_1X_3 + 0.007X_2X_3$$

$$Y_6 (FD) = 1.9177 - 0.0117X_1 - 0.0097X_2 - 0.0068X_3 + 0.0049X_1^2 - 0.0011X_2^2 - 0.0006X_3^2 + 0.0029\ X_1X_2 + 0.0026X_1X_3 + 0.0004X_2X_3$$
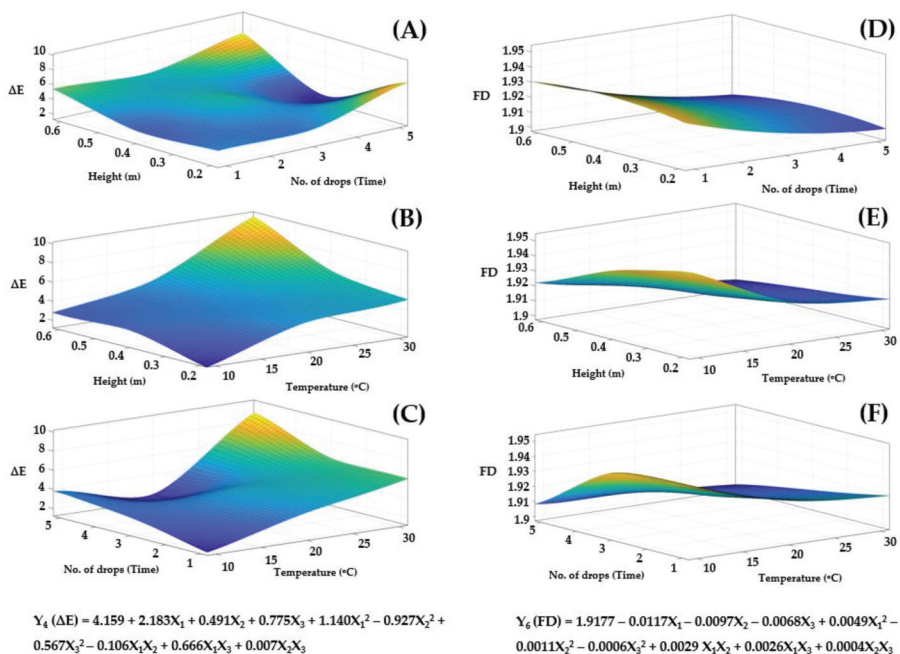
Figure 5. Response surface plot graphs of ΔE and FD variables were created from Equations (10) and (12), respectively. Response surface plots demonstrating effects of drop height, number of drops, and storage temperature on total color difference (ΔE) and fractal dimension (FD) (**D**–**F**) in 'Glom Sali' guava impact bruising at various drop heights and number of drops (**A**,**D**), different drop heights and temperature (**B**,**E**), and different number of drops and storage temperature (**C**,**F**).

3.3. Validation Testing of CCF

Validation of impact bruise damage of guava fruit focused on image analysis by FD (0.82) variables, with higher determination coefficient (R^2_{adj}) value of the predicted model compared to ΔE (0.57), BA (0.53), BAI (0.50), BI (0.2227), and BV (0.09) (Table 7). To evaluate and confirm the predicted FD model value for impact bruising (Equation (12)), the model was verified using thirteen treatments in a range of 20 RSM conditions with three independent variables. As shown in Figure 6, the predicted value of FD exhibited a high linear correlation with the observed value of FD ($R^2 = 0.83$) for impact bruise assessment of guava. Thus, FD by image analysis was proven to predict impact bruising of guava with high determination coefficient value (R^2_{adj}) (>0.8) of the predicted model, with no significant lack of fit compared to the validated model. In a previous study, high values of both R^2 and R^2_{val} were recorded for a polynomial equation (plotting between drop height and storage period) at five drop times, with drop heights of 0.3 (0.95 and 0.88) and 0.6 m (0.99 and 0.92), respectively. The FD value exhibited a higher accuracy for impact bruise prediction with greater bruise susceptibility in guava fruit [20]. Most previous researchers conducted fruit quality evaluation using the FD method to assess internal browning and color change in the flesh [36,38], including fruit bruising [51]. Classification models based on the FD parameter attained a total accuracy rate of 100%, while the support vector machine model based on RGB values only realized 85.29% for bruising detection on red bayberries [51].
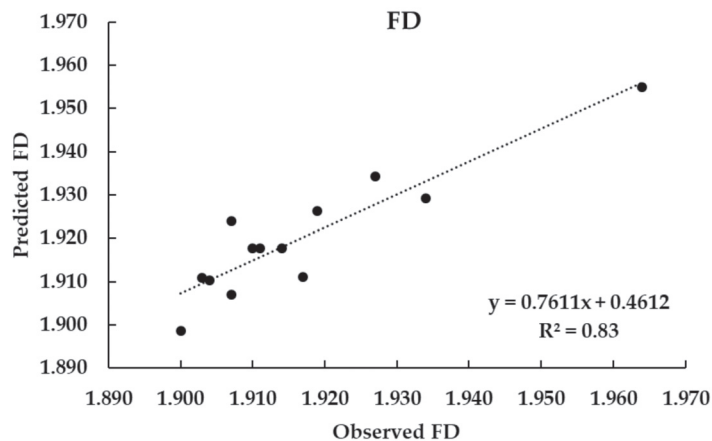
Figure 6. Verification of predictive model equations for fractal dimension (FD) values in 'Glom Sali' bruised guava by impact testing for 48 h.

4. Conclusions

Impact bruising of 'Glom Sali' guava was evaluated using fractal image analysis and RSM design. The FD variable of peeled guava exhibited good agreement with ΔE, indicating that impact bruising browning incidence compared well with BI. Lower FD value correlated with higher impact bruising severity of guava and supported conventional bruise determination. This study represents the first report applying RSM design to assess impact bruising of guava and other fruit. RSM performed for drop height, number of drops, and storage temperature factors showed individual effects on impact bruising of guava. The recommended condition to minimize impact bruising was drop height of 0.53 m for five drops coupled with storage temperature at 30 °C. To reduce impact bruising incidence of guava throughout its supply chain, careful handling to reduce impact energy is suggested, with storage under cool conditions. Impact bruising of guava can be ameliorated by cushioning material to protect fruit areas with high radius of curvature.

Future RSM studies should be performed on spherical or delicate fruit to assess impact bruising related to browning incidence.

References

1. Thai Customs. The Exported Guava from Thailand from 2015–2019. 2021. Available online: http://www.customs.go.th/statistic_report.php?lang=en&ini_content=statistics_report&fbclid=IwAR3fgvhby1iB4O9LUuMedqNtqYNS_ZfyBOOqjPJnBGQlXT6zEWd18v577YQ (accessed on 12 February 2021).
2. Singh, S.P. Guava (*Psidium guajava* L.). In *Postharvest Biology and Technology of Tropical and Subtropical Fruits Volume 3: Cocona to Mango*; Yahia, E.M., Ed.; Woodhead Publishing: Sawston, UK, 2011; pp. 213–245.
3. ASEAN Stan 7:2008. ASEAN Standard for Guava. 2008. Available online: https://asean.org/storage/2012/05/7-ASEAN-STANDARD-FOR-GUAVA-2008.pdf (accessed on 2 February 2021).
4. Thai Agricultural Standard TAS 16-2010. Thai Agricultural Standard for Guava. 2020. Available online: https://www.acfs.go.th/standard/download/eng/guava.pdf (accessed on 2 February 2021).
5. Nila, I.; Harmoko, A.; Imawan, C. The prediction system of bruising depth of guava (*Psidium guajava* L.) based on Vis-NIR imaging. In Proceedings of the 2017 International Conference on Sustainable Information Engineering and Technology (SIET), Malang, Indonesia, 24–25 November 2017; pp. 420–424.
6. Li, Z.; Thomas, C. Quantitative evaluation of mechanical damage to fresh fruits. *Trends Food Sci. Technol.* **2014**, *35*, 138–150. [CrossRef]
7. Lu, L.; Wang, Z.W. Dropping bruise fragility and bruise boundary of apple fruit. *Trans. ASABE* **2007**, *5*, 1323–1329.
8. Lu, F.; Ishikawa, Y.; Kitazawa, H.; Satake, T. Measurement of impact pressure and bruising of apple fruit using pressure-sensitive film technique. *J. Food Eng.* **2010**, *96*, 614–620. [CrossRef]
9. Celik, H.K.; Ustun, H.; Erkan, M.; Rennie, A.E.W.; Akinci, I. Effects of bruising of 'Pink Lady' apple under impact loading in drop test on firmness, colour and gas exchange of fruit during long term storage. *Postharvest Biol. Technol.* **2021**, *179*, 111561. [CrossRef]
10. Shafie, M.; Rajabipour, A.; Mobli, H. Determination of bruise incidence of pomegranate fruit under drop case. *Int. J. Fruit Sci.* **2017**, *17*, 1–14.
11. Hussein, Z.; Fawole, O.; Opara, U. Determination of physical, biochemical and microstructural changes in impact-bruise damaged pomegranate fruit. *J. Food Meas. Charact.* **2019**, *13*, 2177–2189. [CrossRef]
12. Hussein, Z.; Fawole, O.A.; Opara, U.O. Effects of bruising and storage duration on physiological response and quality attributes of pomegranate fruit. *Sci. Hortic.* **2020**, *267*, 109306. [CrossRef]
13. Tabatabaekoloor, R. Engineering properties and bruise susceptibility of peach fruits (*Prunus persica*). *Agric. Eng. Int. CIGR J.* **2013**, *15*, 244–252.
14. Pathare, P. Bruise susceptibility and impact on quality parameters of pears during storage. *Front. Sustain. Food Syst.* **2021**, *5*, 658132. [CrossRef]
15. Pathare, P.B.; Al-Dairi, M.; Al-Mahdouri, A. Bruise damage susceptibility and fruit quality assessment of pear. *Open Agric. J.* **2021**, *15*, 82–90. [CrossRef]
16. Aboud, A.J. Study on factors affecting apple bruises under drop loading. In Proceedings of the 14th. Annual Conference of the Misr Society of Agriculture Engineering, Cairo, Egypt, 22 November 2006; pp. 876–887.
17. Shafie, M.; Rajabipour, A.; Castro-Garcia, S.; Jiménez-Jiménez, F.; Mobli, H. Effect of fruit properties on pomegranate bruising. *Int. J. Food Prop.* **2015**, *18*, 1837–1846. [CrossRef]

18. Hussein, Z.; Fawole, O.A.; Opara, U.L. Bruise damage susceptibility of pomegranates (*Punica granatum*, L.) and impact on fruit physiological response during short term storage. *Sci. Hortic.* **2019**, *246*, 664–674. [CrossRef]
19. Krzysztof, G.; Paweł, R.; Zbigniew, S. The determination of apples bruise resistance by the multiple impact method. *Technol. Sci.* **2009**, *12*, 29–39.
20. Htike, T.; Saengrayap, R.; Kitazawa, H.; Chaiwong, S. Fractal image analysis and bruise susceptibility evaluation of impact damage in guava. 2021; Manuscript submitted for publication.
21. Lin, X.; Wang, L.; Hou, Y.; Zheng, Y.; Jin, P. A combination of melatonin and ethanol treatment improves postharvest quality in bitter melon fruit. *Foods* **2020**, *9*, 1376. [CrossRef]
22. Ranade, S.; Thiagarajan, P. Selection of a design for response surface. *IOP Conf. Ser. Mater. Sci. Eng.* **2017**, *263*, 022043. [CrossRef]
23. Cissé, M.; Montet, D.; Loiseau, G.; Ducamp-Collin, M.-N. Influence of the concentrations of chitosan and glycerol on edible film properties showed by response surface methodology. *J. Environ. Polym. Degrad.* **2012**, *20*, 830–837. [CrossRef]
24. Nandane, A.; Jain, R. Study of mechanical properties of soy protein based edible film as affected by its composition and process parameters by using RSM. *J. Food Sci. Technol.* **2014**, *54*, 1–8. [CrossRef]
25. Said, K.; Afizal, M. Overview on the response surface methodology (RSM) in extraction processes. *J. Appl. Sci. Process Eng.* **2016**, *2*, 8–17.
26. Zahid, M.; Cheow, C.S.; Norizzah, A.R.; Halimahton, M.; Md Sikin, A.; Noorakmar, A.; Ishak, R. Optimization of process conditions for the application of edible coating emulsion on guava (*Psidium guajava*) using response surface methodology. In Proceedings of the International Conference on Biotechnology and Food Science (IPCBEE), Bali Islan, Singapore, 1–3 April 2011; pp. 61–65.
27. Jafarizadeh, H.; Osman, A.; Tan, C.; Abdul Rahman, R. Development of an edible coating based on chitosan-glycerol to delay 'Berangan' banana (*Musa sapientum* cv. Berangan) ripening process. *Int. Food Res. J.* **2011**, *18*, 989–997.
28. Nandane, A.S.; Dave, R.K.; Rao, T.V.R. Optimization of edible coating formulations for improving postharvest quality and shelf life of pear fruit using response surface methodology. *J. Food Sci. Technol.* **2017**, *54*, 1–8. [CrossRef]
29. Rashid, F.; Ahmed, Z.; Ameer, K.; Amir, R.A.I.; Khattak, M. Optimization of polysaccharides-based nanoemulsion using response surface methodology and application to improve postharvest storage of apple (*Malus domestica*). *J. Food Meas. Charact.* **2020**, *14*, 2676–2688. [CrossRef]
30. Tran, D.T.; Hertog, M.; Nicolaï, B.M. Hierarchical response surface methodology for optimization of postharvest treatments to maintain quality of litchi cv. 'Thieu' during cold storage. *Postharvest Biol. Technol.* **2016**, *117*, 94–101. [CrossRef]
31. Lewis, R.; Yoxall, A.; Canty, L.A.; Romo, E.R. Development of engineering design tools to help reduce apple bruising. *J. Food Eng.* **2007**, *83*, 356–365. [CrossRef]
32. Gharaghani, A.; Shahkoomahally, S. Cultivar and fruit size influence bruise susceptibility and some physical properties of apple fruit. *Iran Agric. Res.* **2018**, *37*, 49–56.
33. Hussein, Z.; Fawole, O.; Opara, U. Investigating bruise susceptibility of pomegranate cultivars during postharvest handling. *J. Rural Dev.* **2017**, *2*, 33–39.
34. Lee, H.J.; Kim, T.-C.; Kim, S.J.; Park, S.J. Bruising injury of persimmon (*Diospyros kaki* cv. Fuyu) fruits. *Sci. Hortic.* **2005**, *103*, 179–185. [CrossRef]
35. Zheng, C.; Sun, D.-W.; Zheng, L. Recent developments and applications of image features for food quality evaluation and inspection—A review. *Trends Food Sci. Technol.* **2006**, *17*, 642–655. [CrossRef]
36. Quevedo, R.; Díaz, O.; Caqueo, A.; Ronceros, B.; Aguilera, J.M. Quantification of enzymatic browning kinetics in pear slices using non-homogenous L^* color information from digital images. *LWT* **2009**, *42*, 1367–1373. [CrossRef]
37. Quevedo, R.; Jaramillo, M.; Díaz, O.; Pedreschi, F.; Aguilera, J.M. Quantification of enzymatic browning in apple slices applying the fractal texture Fourier image. *J. Food Eng.* **2009**, *95*, 285–290. [CrossRef]
38. Quevedo, R.; Díaz, O.; Ronceros, B.; Pedreschi, F.; Aguilera, J.M. Description of the kinetic enzymatic browning in banana (*Musa cavendish*) slices using non-uniform color information from digital images. *Food Res. Int.* **2009**, *42*, 1309–1314. [CrossRef]
39. Van Eck, J.W.; van der Heijden, G.W.A.M.; Polder, G. Accurate measurement of size and shape of cucumber fruits with image analysis. *J. Agric. Eng. Res.* **1998**, *70*, 335–343. [CrossRef]
40. Chaiwong, S.; Yoythaisong, P.; Arwatchananukul, S.; Aunsri, N.; Tontiwattanakul, K.; Trongsatitkul, T.; Kitazawa, H.; Saengrayap, R. Vibration damage in guava during simulated transportation assessed by digital image analysis using response surface methodology. *Postharvest Biol. Technol.* **2021**, *181*, 111641. [CrossRef]
41. Fu, H.; Karkee, M.; He, L.; Duan, J.; Li, J.; Zhang, Q. Bruise patterns of fresh market apples caused by fruit-to-fruit impact. *Agronomy* **2020**, *10*, 59. [CrossRef]
42. Kamsiati, E. Postharvest handling practices in maintaining quality and shelf life of guava (*Psidium guajava*). In Proceedings of the International Conference on Agricultural Postharvest Handling, and Processing, Jakarta, Indonesia, 19–20 November 2013; pp. 363–373.
43. Urbano, B.; Ribeiro, R.; Cavalini, F.; Pedro, J.; Trevisan, M. Temperature-related changes in respiration and Q_{10} coefficient of Guava. *Sci. Agric.* **2005**, *62*, 458–463.
44. Komarnicki, P.; Stopa, R.; Kuta, Ł.; Szyjewicz, D. Determination of apple bruise resistance based on the surface pressure and contact area measurements under impact loads. *Comput. Electron. Agric.* **2017**, *142*, 155–164. [CrossRef]

45. Palou, E.; López-Malo, A.; Barbosa-Cánovas, G.; Welti-Chanes, J.; Swanson, B. Polyphenoloxidase activity and color of blanched and high hydrostatic pressure treated banana puree. *J. Food Sci.* **1999**, *64*, 42–45. [CrossRef]
46. Balaban, M.; Aparicio, J.; Zotarelli, M.; Sims, C. Quantifying nonhomogeneous colors in agricultural materials. Part II: Comparison of machine vision and sensory panel evaluations. *J. Food Sci.* **2008**, *73*, S438–S442. [CrossRef] [PubMed]
47. Quevedo, R.; Pedreschi, F.; Bastias, J.M.; Díaz, O. Correlation of the fractal enzymatic browning rate with the temperature in mushroom, pear and apple slices. *LWT* **2016**, *65*, 406–413. [CrossRef]
48. Subhashree, S.N.; Sunoj, S.; Xue, J.; Bora, G.C. Quantification of browning in apples using colour and textural features by image analysis. *Food Qual. Saf.* **2017**, *1*, 221–226. [CrossRef]
49. Widhiantari, I.A.; Sutan, S.M.; Gunomo, D. Optimization of tomato fruit color after simulated transport using response surface methodology (RSM). *Int. J. Food Sci. Nutr. Eng.* **2016**, *6*, 42–47.
50. Jarimopas, B.; Singh, S.; Sayasoonthorn, S.; Singh, J. Comparison of package cushioning materials to protect post-harvest impact damage to apples. *Packag. Technol. Sci.* **2007**, *20*, 315–324. [CrossRef]
51. Lu, H.; Zheng, H.; Hu, Y.; Lou, H.; Kong, X. Bruise detection on red bayberry (*Myrica rubra Sieb*. & Zucc.) using fractal analysis and support vector machine. *J. Food Eng.* **2011**, *104*, 149–153.

Investigating the Molecular Mechanisms of Pepper Fruit Tolerance to Storage via Transcriptomics and Metabolomics

Hao Sun, Qing Li, Lian-Zhen Mao, Qiao-Ling Yuan, Yu Huang, Meng Chen, Can-Fang Fu, Xuan-Hua Zhao, Zi-Yu Li, Yun-Hua Dai, Xue-Xiao Zou and Li-Jun Ou *

Engineering Research Center of Education Ministry for Germplasm Innovation and Breeding New Varieties of Horticultural Crops, College of Horticulture, Hunan Agricultural University, Changsha 410128, China; 314481909@163.com (H.S.); liqinghq@126.com (Q.L.); maolz77@163.com (L.-Z.M.); qiaoling_y1993@163.com (Q.-L.Y.); huangyu153@163.com (Y.H.); chen536@163.com (M.C.); Fucanfang123@163.com (C.-F.F.); zhaoxunhua55@163.com (X.-H.Z.); liziyu753@163.com (Z.-Y.L.); Daiyunhua5@163.com (Y.-H.D.); zouxuexiao428@163.com (X.-X.Z.)
* Correspondence: ou9572@hunau.edu.cn

Abstract: Pepper is one of the most important vegetable crops in China and has high economic value. However, the pepper fruit is easily softened and spoiled after harvest, which seriously affects its flavor, transportation, and economic value. In this study, we used pepper lines with different levels of storage resistance, A144 and A361, and performed physiological examination, transcriptomics, and metabolomics on them at 0 and 3 days after harvest in order to analyze their gene expression patterns and molecular regulatory mechanisms for storage tolerance. A total of 23,477 genes and 985 metabolites were identified. After comparing and analyzing each sample, we identified 7829 differentially expressed genes and 296 differential metabolites. We found that the genes such as ethylene-responsive transcriptional factor (*ERFs*), polygalacturonase (*PG*), cellulose synthase (*CESA*), abscisic acid insensitive (*ABI*), protein kinase 2 (*SnRK2*), and protein phosphatase 2C (*PP2C*) and metabolites such as phenylalanine and glycyl-tyrosine were differentially expressed between different storage times in the two materials. Through GO and KEGG enrichment analysis, we found that the differential genes were mainly enriched in carbohydrate metabolism, small molecule metabolism, and plant hormone signal transduction, and the differential metabolites were mainly enriched in flavonoid biosynthesis, glutathione metabolism, and cysteine and methionine metabolism pathways. This study provides a scientific basis for investigating the molecular mechanisms of storage tolerance and developing new pepper varieties with improved storage resistance.

Keywords: pepper; fruit storage-related genes; gene expression pattern; metabolic pathway; molecular regulation

1. Introduction

Pepper (*Capsicum annuum* L.) is a vegetable crop belonging to the Solanaceae *Capsicum* genus. It is widely cultivated in the world and is the world's largest seasoning crop [1]. China is a major pepper planting country, with an average pepper planting area of 1.33 million hectares and a total economic value of 70 billion yuan, ranking first among all vegetables and accounting for 16.67% of the world's total vegetable production value. Pepper fruit can synthesize and accumulate capsaicin, fragrance, pigments (anthocyanins and carotenoids), and various vitamins such as vitamins C and E; thus, it is considered a good nutrition source with great economic value [2]. Pepper can be eaten fresh or used for food processing. The harvested fruits are not resistant to storage at room temperature or high temperature; under these conditions, the fruits are perishable and deteriorate, and the hardness and nutrient content of the fruits also decrease. Moreover, pepper thrives in a warm climate and is mainly marketed in summer and autumn. Storage at high temperature often causes rapid respiration of pepper fruit, fruit rot, gray mold and black spot,

leading to pepper deterioration, weight loss, and serious economic losses [3]. Therefore, proper storage and transportation of peppers can not only adjust the contradiction between production and market sale, but also extend its supply period, which can greatly increase the variety of vegetables and meet market demand.

The hardness of the fruit is an important indicator of fruit maturity and quality. In general, as the maturity increases, the hardness gradually decreases, which also affects the fruit quality. Studies have shown that the changes in cell wall structure are closely related to the ripening and softening of the fruit. The destruction of the internal structure of the cell wall is the major reason for fruit softening. The dissociation of the intercellular cell wall layer, the degradation of pectin, and the disintegration of fibrous materials lead to successive disintegration and destruction of cell organelles [4–6]. In addition, the differential expression of related genes is also an important factor affecting fruit softening. Montgomery's study found that the expression of tomato PG gene gradually increased with the increase in ethylene production during the fruit ripening [7]. PG-mediated decomposition of pectin was also reported in melon fruits, and three PG cDNAs were obtained: MPG1, MPG2, and MPG3. MPG1 and MPG2 are related to the PG in senescent peach and tomato, and MPG3 is related to tomato fruit PG [8]. The PEL gene in strawberry has a regulatory effect on fruit ripening and softening in the later stage of strawberry development. It has been shown that the PEL gene is a candidate gene for improving strawberry fruit hardness and delaying fruit ripening and softening [9]. There are 6 β-Gal genes in tomato fruits expressed during fruit ripening and softening [10]. In apples, β-Gal gene expression increases as the fruit softens [11].

In recent years, transcriptomics and metabolomics technologies have been widely used in fruit studies, and transcriptome sequencing is the fastest growing technology [12]. Up to now, many studies have used transcriptomics to examine the genetic changes during fruit development and postharvest softening. Guo et al. [13] used transcriptomics to analyze the texture of watermelon fruits at different growth stages and identified a large number of differentially expressed genes that can regulate fruit texture, such as *Cx* and *PME* genes. Dessireé et al. [14] identified four genes related to papaya softening, including *Gal*, endoxylanase gene, *PE*, and *EXP*. Metabolomics has also been widely used in the study of fruit ripening and postharvest storage. Osorio et al. [15] used metabolomics and transcriptional analysis to study the postharvest physiology of tomato fruits; they found that *dfd* gene mutation could delay fruit maturity and softening. Tietel et al. [16] used metabolomics based on gas chromatography–mass spectrometry (GC-MS) to analyze the flavor substances of citrus fruits after anaerobic treatment; they found that the substances that caused the peculiar smell of citrus fruits not only included the well-known ethanol and acetaldehyde, but also included the derivatives of fatty acids and amino acids, such as ethyl esters. However, so far, there are relatively few studies using transcriptomics and metabolomics to investigate the changes in pepper fruit hardness and storage tolerance. Therefore, in order to clarify the molecular mechanisms regulating pepper storage tolerance, this study aimed to perform transcriptomics and metabolomics on two pepper lines with different levels of storage tolerance and investigate the genes and metabolites related to pepper storage tolerance. Our results provide a scientific basis for the improvement of pepper storage tolerance and the cultivation of new storable pepper varieties.

2. Materials and Methods

2.1. Plant Growth and Sampling

Two pepper (*Capsicum annuum* L.) lines with different levels of storage resistance, 'A144' (resistant to storage, named A below) and 'A361' (nonresistant to storage, named B), provided by the pepper department of the College of Horticulture, Hunan Agricultural University, were used as test materials. The test pepper seeds were cultivated in plugs after germinating. During the five-leaf and one-heart period, the seedlings with strong and consistent growth were selected and planted in the greenhouse of the Yun Yuan Base of Hunan Agricultural University. During the plant growth period, regular water and

fertilizer management were applied. At 50 days after the self-pollination of two pepper materials, 6 red ripe fruits were harvested from 6 different plants of each line, and the harvest fruits were evenly divided into two groups. For one group, the hardness of the A144 (A1) and A361 (B1) pepper fruits was measured immediately after harvest (0d), and then the fruits were further cut into three equal parts: two parts were snap-frozen with liquid nitrogen and stored at −80 °C for transcriptomics and metabolomics analysis, and the remaining one was used for physiological index measurement. The other group of A144 (A2) and A361 (B2) pepper fruits was placed in a 30 °C incubator for 3 days after harvest, and the fruit hardness was measured and cut into three equal parts: two were snap-frozen with liquid nitrogen and stored at −80 °C for transcriptomics and metabolomics analysis, and the remaining one was used for physiological index measurement. Three biological replicates were performed in each treatment.

2.2. Determination of Fruit Hardness

Three fruits from each pepper line were selected on the day of harvest (0d) and at 3 days after 30 °C incubation. GY-4 hardness tester (Top Cloud-agriculture, Beijing, China) was used to measure the hardness at the largest fruit diameter, and the averaged value from 3 fruits was calculated.

2.3. Determination of Physiological Indexes Related to Storage

PG activity was assayed spectrophotometrically following derivatization of the reaction product with UV-absorbing 2-cyanoacetamide [17]. For the determination of soluble sugar content, 1 mL distilled water was added to about 0.1 g fruit tissue, which was ground into homogenate. For the determination of the cellulose content, 1 mL of 80% ethanol was added to about 0.3 g of fruit tissue, which was ground into a homogenate. Anthrone colorimetry was used in the follow-up experiment [18]. Before the determination of hemicellulose content, the sample was dried naturally or dried in an oven to constant weight. After the full grinding with a mortar, the appropriate powder was screened with a 30–50 mesh sieve. A sample of about 5 mg sample was taken for the follow-up experiment (Beijing Solarbio & Technology Co., Beijing, China). For the determination of soluble pectin content, 80% ethanol was added to about 0.1 g fruit tissue, which was ground into homogenate. The method of Zhang et al. [19] was used in the follow-up experiment.

2.4. Observation of Fruit Tissue Structure

The conventional paraffin section method [20] was used to make tissue sections. After harvesting, the fruit was fixed with 70% FAA fixative, dehydrated by alcohol gradient, embedded in paraffin, and stained with Safranine O-Fast Green to observe the cell wall structure.

2.5. RNA Extraction, Library Preparation, and Sequencing

Total RNA was extracted from plant tissues using TRI Reagent (Sigma Life Science, St Louis, MO, USA) following the manufacturer's instructions. RNA quality was checked by RNase-free agarose gel electrophoresis to avoid possible degradation and contamination and then verified using Agilent 2100 Bio-analyzer (Agilent Technologies, Santa Clara, CA, USA). Next, poly (A) mRNA was isolated using oligo-dT beads (Qiagen, Germany) and then fragmented into short pieces by adding fragmentation buffer. First-strand cDNA was synthesized using random hexamer-primed reverse transcription, followed by the synthesis of second-strand cDNA using RNase H and DNA polymerase I. The cDNA fragments were purified using a QIA quick PCR extraction kit and then washed with EB buffer for end reparation poly (A) addition and ligated to sequencing adapters. Following agarose gel electrophoresis and extraction of cDNA from gels, the cDNA fragments were purified and enriched by PCR to construct the final cDNA library, which was then sequenced on the Illumina sequencing platform (Illumina-nova6000) using the paired-end technology. Three

biological replicates were performed for each line, and six DGE libraries were generated and sequenced.

2.6. Transcriptome Analysis

Raw reads were filtered through Perl program to remove low-quality sequences (more than 50% bases with quality lower than 20 in one sequence), reads with more than 5% N bases (unknown bases), and reads containing adaptor sequences. Then, the clean reads were mapped to the pepper reference genome using TopHat2, allowing up to one mismatch. The DEGs were identified using the R package edge R. The expression level of each gene was calculated and normalized to FPKM. The FDR was used to determine the threshold of the p-value in multiple tests. In our study, the FDR < 0.05 and fold change > 2 were used as significance cut-offs for differential gene expression. The DEGs were used for GO and KEGG enrichment analyses. GO terms with corrected p-value < 0.05 and KEGG pathways with p-value < 0.05 were considered as significantly enriched terms.

2.7. Metabolite Extraction

Plant tissues (100 mg) were individually grounded with liquid nitrogen, and the homogenate was resuspended with prechilled 80% methanol and 0.1% formic acid by vortexing well. The samples were incubated on ice for 5 min and then centrifuged at $15,000 \times g$ and 4 °C for 20 min. The supernatant was diluted to a final concentration containing 53% methanol by LC-MS-grade water. The samples were subsequently transferred to a fresh Eppendorf tube and centrifuged at $15,000 \times g$ and 4 °C for 20 min. Finally, the supernatant was injected into the LC-MS/MS system for analysis [21].

2.8. HPLC-MS/MS Analysis

LC-MS/MS analyses were performed using an Exion LC AD system (SCIEX) coupled with a QTRAP6500+ mass spectrometer (SCIEX) by Novogene Co., Ltd. (Beijing, China). Samples were injected onto an X select HSS T3 (2.1×150 mm, 2.5 μm) using a 20 min linear gradient at a flow rate of 0.4 mL/min for the positive/negative polarity mode. The eluents were eluent A (0.1% formic acid–water) and eluent B (0.1% formic acid–acetonitrile) [22]. The solvent gradient was set as follows: 2% B, 2 min; 2–100% B, 15.0 min; 100% B, 17.0 min; 100–2% B, 17.1 min; 2% B, 20 min. QTRAP 6500+ mass spectrometer was operated in positive polarity mode with 35 psi curtain gas, medium collision gas, ion spray voltage of 5500 V, temperature of 550 °C, ion source gas 1:60, and ion source gas 2:60. QTRAP 6500+ mass spectrometer was operated in negative polarity mode with 35 psi curtain gas, medium collision gas, ion spray voltage of −4500 V, temperature of 550 °C, ion source gas 1:60, and ion source gas 2:60.

2.9. Data Analysis

2.9.1. Physiological Data Analysis

SPSS 17.0 was used to conduct one-way analysis of variance (ANOVA). LSD and Duncan's method were used for pairwise comparisons. $p < 0.05$ was considered statistically significant.

2.9.2. Metabolite Data Analysis

The metabolites were annotated using the KEGG database (http://www.genome.jp/kegg/, accessed on 30 May 2021), HMDB database (http://www.hmdb.ca/, accessed on 30 May 2021), and LIPID MAPS database (http://www.lipidmaps.org/, accessed on 30 May 2021). Principal components analysis (PCA) and partial least squares discriminant analysis (PLS-DA) were performed by metaX (a flexible and comprehensive software for processing metabolomics data). We applied univariate analysis (*t*-test) to calculate the statistical significance (p-value). The metabolites with VIP > 1, p-value < 0.05, fold change $\geq$ 2, or FC $\leq$ 0.5 were considered to be differential metabolites. ggplot2 in R was used to plot volcano plots and filter the metabolites of interest based on log2(FC)

and −log10(*p*-value) of metabolites. For clustering heatmaps, the data were normalized using z-scores of intensity areas and plotted by *p* heatmap package in R. The correlation between differential metabolites were analyzed by cor () in R (method = Pearson). The statistical significance of the correlation was calculated by cor. Mtest () in R. *p*-value < 0.05 was considered as statistically significant, and correlation plots were plotted by corr plot package in R. The functions of these metabolites and metabolic pathways were analyzed using the KEGG database. The metabolic pathways enriched with differential metabolites were identified with the condition x/n > y/N; when *p*-value < 0.05, the metabolic pathway was considered as a significantly enriched pathway.

2.10. Quantitative Real-Time PCR

qRT-PCR was conducted as described in Osorio et al. [23]. Three replicates were conducted for each sample. Cp actin gene was used as the internal control. Primers used in the study are listed in Table S1. The relative gene expression levels were normalized using the 2 (-Delta Delta C(T)) method [24].

2.11. Registration Number

The RNA-seq data generated in this study can be obtained from SRA archives (http://www.ncbi.nlm.nih.gov/sra, accessed on 30 May 2021). Registration number: PRA-JNA722115.

3. Results

3.1. Hardness- and Storage-Related Physiological Indexes

Through the analysis of the physical and chemical properties of A144 and A361, we found that the fruit hardness and contents of soluble sugar, hemicellulose, cellulose, and polygalacturonase (PG) were significantly different between the two lines and between before and after storage (Figure 1). Specifically, fruit firmness and contents of soluble sugar, cellulose, and hemicellulose were decreased in A2 (A144 at 3 days postharvest) and B2 (A361 at 3 days postharvest) compared with A1 (A144 at 0d) and B1 (A361 at 0d), but the decrease in B2 was greater than that in A2 (Figure 1). The opposite was true for PG and soluble pectin. The contents of PG and soluble pectin in A2 and B2 were significantly higher than those of A1 and B1, and the increase in B2 was greater than that in A2.
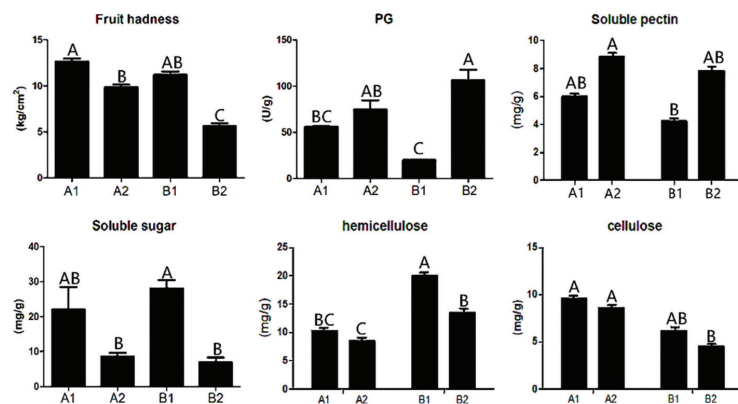
Figure 1. Physiological indexes of pepper before and after storage. Annotation: The abscissa represents different groups; the ordinate represents the content. A1 represents A144 material stored for 0 days; A2 represents A144 material stored for 3 days; B1 represents A361 material stored for 0 days; B2 represents A361 material stored for 3 days. Different letters above the bar chart indicate significant differences (*p* < 0.01).

3.2. Observation of Pulp Structure

For the postharvest fruit structure of A1 and B1, the fruit skin cells were tightly and regularly arranged, with a complete cuticle on the outermost layer, and the degree of compactness of the cuticle and cell arrangement was almost the same (Figure 2). For the postharvest fruit tissue structure of A2 and B2, the cuticle and cells began to rupture to different degrees: the cuticle of the storage-resistant A2 was relatively complete, the degree of cell rupture was smaller, and there was less cell fusion, while the cuticle and cells of the non-storage-resistant B2 were ruptured to a larger extent.
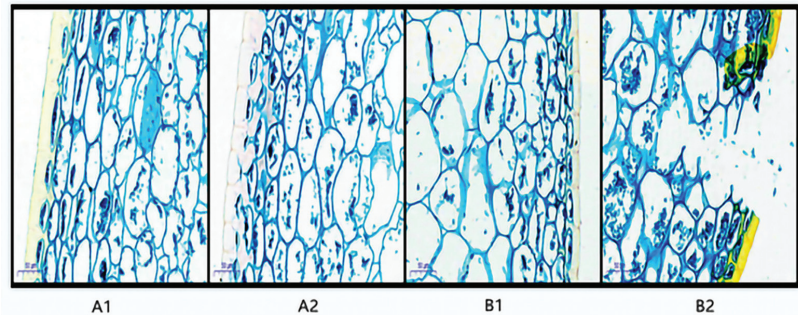
Figure 2. Paraffin section of pepper before and after storage. Annotation: A1 represents A144 material stored for 0 days; A2 represents A144 material stored for 3 days; B1 represents A361 material stored for 0 days; B2 represents A361 material stored for 3 days.

3.3. Transcriptome Sequencing Analysis

From Illumina Nova 6000 sequencing, we obtained more than 5G of sequencing data and a total of 516,522,132 raw reads. After removing the linker sequence, low-quality sequences, and rRNA, 509,298,534 clean reads were obtained. The clean reads were aligned to the reference genome, and more than 87% of all samples were successfully matched to the reference genome. After the alignment, a total of 23,477 genes were identified, from which 18,523 genes were quantified. Among the quantified genes, 15,174 genes were present in all samples, and there were 463, 242, 275, and 125 unique genes in A1, A2, B1, and B2, respectively (Figure 3A).
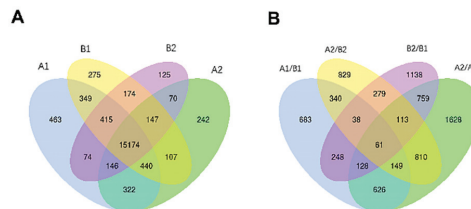
Figure 3. Venn analysis of differentially expressed genes. Annotation: (**A**) A1 represents A144 material stored for 0 days; A2 represents A144 material stored for 3 days; B1 represents A361 material stored for 0 days; B2 represents A361 material stored for 3 days. (**B**) A1/B1 means A1 compared to B1; A2/B2 means A2 compared to B2; B2/B1 means B2 compared to B1; A2/A1 means A2 compared to A1.

3.3.1. Identification and Analysis of Differentially Expressed Genes

In each comparison group, a total of 7829 differentially expressed genes (DEGs) were identified (Figure 3B). Specifically, there were 4274, 2764, 2273, and 2619 DEGs in A2/A1, B2/B1, A1/B1, and A2/B2 comparison groups. Moreover, 61 genes were significantly different in each comparison group, and there were 1628, 1138, 683, and 829 genes that were only significantly different in A2/A1, B2/B1, A1/B1, and A2/B2 groups, respectively.

Through cluster analysis, the gene expression patterns of A1, B1, A2, and B2 were divided into two categories, and the expression patterns in each category were consistent (Figure 4A). In the A and B groups, the gene expression of A1 and B1 showed an upregulation trend, and the gene expression of A2 and B2 showed a downregulation trend; in the D and E groups, the gene expression of A1 and B1 showed a downregulation trend, and the gene expression of A2 and B2 showed an upregulation trend. However, in group C, the gene expression of B1 and B2 were both downregulated, but most of the genes in A1 and A2 were upregulated. Therefore, we hypothesized that these genes might contain key genes for the storage tolerance of pepper. Next, we screened out 14 storage-related genes that exhibited differential expressions after harvesting the two pepper materials, including polygalacturonase (PG), polygalacturonase inhibitor (PGI), cellulose synthase (CESA), abscisic acid insensitive (ABI) and, weakly ethylene-insensitive (WEI) genes (Figure 4B). Among them, the expression level of PG (Capana06g001141) in A2 fruit was significantly lower than that in B2, and its expression level in A2 was significantly lower than that in A1, while B2 was not significantly different from B1. The expression levels of ABI5 (Capana04g000551 and Capana08g002366) and WEI1 (Capana02g002054) in A2 were significantly higher than those in A1, but no significant difference was found between B1 and B2 fruits. The expression levels of PGI (Capana02g003383) and CESA (Capana07g002394), which inhibit pepper fruit softening, were all significantly higher in A2 compared to B2. These results suggest that the differential expression of the above genes might be the important reason for the difference in storage tolerance of the two pepper materials.
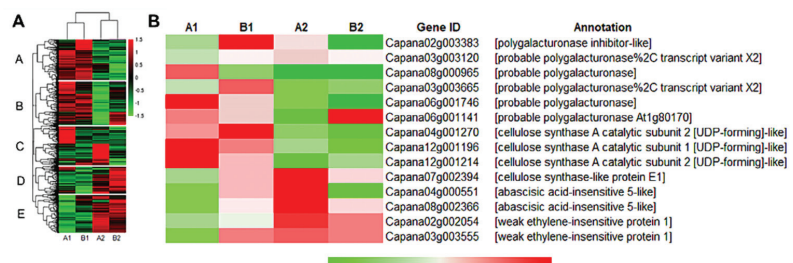
Figure 4. Heat map analysis of storage tolerance genes. Annotation: (**A**) Genes or samples with similar expression patterns in the heat map are gathered together. The color in each grid does not reflect the gene expression value, but the value obtained after homogenizing the rows of expression data (generally between −2 and 2), so the colors in the heat map can only be compared horizontally (the expression of the same gene in different samples); vertical comparison (expression of different genes in the same sample) is not allowed. (**B**): Expression of representative genes among different samples.

3.3.2. GO Enrichment Analysis of Differentially Expressed Genes

We performed further enrichment analysis on the top 40 GO terms containing the largest number of differentially expressed genes. The results show that in the biological processes class, carbohydrate metabolic process (GO:0005975), transmembrane transport (GO:0055085), and small molecule metabolic process (GO:0044281) were significantly enriched in A2/A1, B2/B1, A1/B1, and A2/B2, and each functional item had the highest degree of enrichment in A2/A1 (Figure 5). In the molecular functions class, the transcription regulator activity (GO:0140110), DNA binding transcription factor activity (GO:0003700), and transmembrane transport activity (GO:0022857) were significantly enriched in all the four comparison groups, and the transcription regulator activity (GO:0140110) process was significantly enriched in A2/A1. The cellular components class was divided into 14 categories. The most significantly enriched processes in the comparison groups were the nucleus (GO:0005634) and cytoplasmic parts (GO:0044444). Therefore, the GO enrichment in carbohydrate metabolic process (GO:0005975), transcription regulator activity

(GO:0140110), and DNA binding transcription factor activity (GO:0003700) might be the reason for the difference in storage tolerance between A144 and A361.

GO terms	A2/A1	B2/B1	A1/B1	A2/B2	
carbohydrate metabolic process	111	84	53	59	Biological Process
transmembrane transport	106	58	54	59	
small molecule metabolic process	98	81	48	50	
ion transport	76	47	43	46	
cell communication	75	39	42	56	
cellular response to stimulus	64	48	38	55	
lipid metabolic process	79	33	35	49	
response to stress	58	50	33	45	
proteolysis	55	49	27	47	
organic acid metabolic process	55	51	33	37	
oxoacid metabolic process	55	51	33	36	
carboxylic acid metabolic process	54	50	32	36	
signal transduction	53	34	32	45	
signaling	53	34	32	45	
cation transport	44	33	30	25	
catabolic process	44	33	31	20	
organophosphate metabolic process	49	34	25	19	
transcription regulator activity	123	49	76	59	Molecular Function
DNA binding transcription factor activity	114	42	72	58	
transmembrane transporter activity	93	59	51	55	
transferase activity, transferring glycosyl groups	84	52	58	60	
transferase activity, transferring hexosyl groups	71	47	49	51	
hydrolase activity, acting on glycosyl bonds	72	58	38	36	
coenzyme binding	70	47	40	40	
hydrolase activity, hydrolyzing O-glycosyl compounds	69	54	37	35	
nucleus	98	77	42	56	Cellular Component
cytoplasmic part	77	54	31	32	
organelle part	49	42	28	32	
intracellular organelle part	49	42	28	32	
non-membrane-bounded organelle	43	42	19	27	
intracellular non-membrane-bounded organelle	43	42	19	27	
ribonucleoprotein complex	27	34	7	14	
catalytic complex	22	28	13	18	
cell periphery	28	20	15	15	
ribosome	23	28	6	12	
endomembrane system	18	9	9	14	
mitochondrion	19	13	9	2	
cell wall	15	12	9	6	
chromosome	15	10	4	6	
external encapsulating structure	15	7	9	6	

Figure 5. GO analysis of differentially expressed genes. Annotation: The numbers in the diagram represent the number of genes in the enrichment. The higher the number, the redder the color; the lower the number, the greener the color. A1/B1 means A1 compared to B1; A2/B2 means A2 compared to B2; B2/B1 means B2 compared to B1; A2/A1 means A2 compared to A1.

3.3.3. KEGG Pathway Enrichment Analysis

KEGG pathway enrichment analysis was performed on the differentially expressed genes (DEGs) in each comparison group. The results show that the DEGs in A2/A1 fruits were significantly enriched in photosynthesis-antenna proteins, plant–pathogen interaction, and MAPK signaling pathway-plant pathways (Figure 6A). The DEGs in the B2/B1 fruits were significantly enriched in the protein processing in the endoplasmic reticulum pathway (Figure 6B). The DEGs in A1/B1 were significantly enriched in plant MAPK signaling pathway-plant, alpha-linolenic acid metabolism, and phenylpropanoid biosynthesis pathway (Figure 6C), while the DEGs in A2/B2 were significantly enriched in plant–pathogen interaction pathway (Figure 6D). These results show that these fruits might be regulated by phytohormone signal transduction and protein synthesis-related genes. The enrichment in plant MAPK signal transduction and phytopathogen interaction pathways in A2/A1, A1/B1, and A2/B2 groups indicates that the above enriched pathways might be the cause of the difference in storage tolerance.
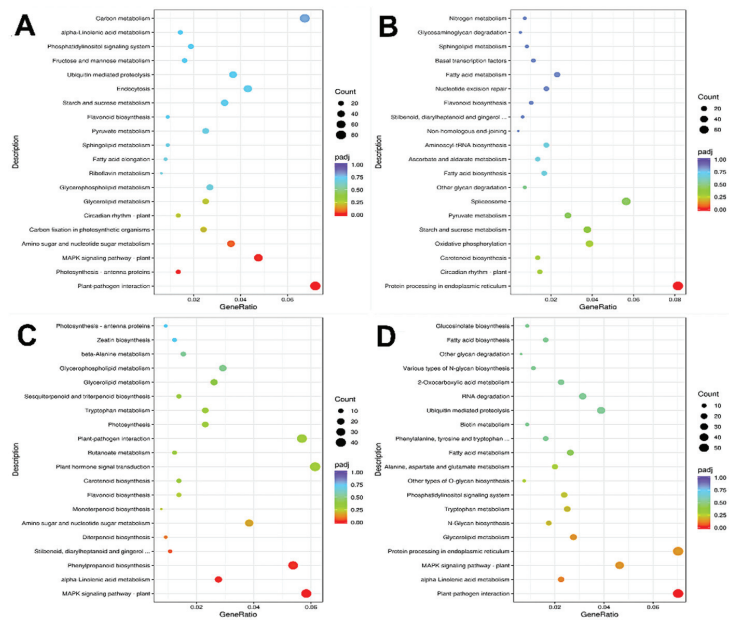
Figure 6. KEGG enrichment analysis of differentially expressed genes. Annotation: (**A**) A2 compared to A1; (**B**) B2 compared to B1; (**C**) A1 compared to B1; (**D**) A2 compared to B2. The horizontal coordinate in the figure is the ratio of the number of different genes and the total number of genes annotated to KEGG pathway. The ordinate is KEGG pathway, the size of the point represents the number of genes annotated to KEGG pathway, red represents the significant enrichment, and purple represents the small enrichment significance.

3.3.4. Expression Analysis of Ethylene-Responsive Transcription Factors (ERFs)

ERFs are important factors regulating plant growth and fruit ripening. In this study, we identified a total of 116 ERFs, of which 77 were quantified (Table S1). We further analyzed 40 ERFs with FPKM value > 5 (Figure 7). Among them, the expression of ERF1B-like (Capana05g001701) was significantly increased by 2.9 times in A2/A1, but there was no significant difference between B2 and B1, and its expression in A2 was significantly higher than that in B2. The expression levels of ERF3-like (Capana10g000161) and ERF096-like (Capana02g001898) in A2 fruits were significantly lower than those in A1 by 2.35 and 3.89 times, while there was no significant difference between B1 and B2; moreover, the expression levels of ERF3-like and ERF096-like in A2 were significantly lower than those in B2. The expression level of ERFRAP2-13-like (Capana04g001107) in A2 and B1 fruits was significantly lower than that in A1, and the expression level of A2 was significantly lower than that of B2. The differential expression of genes such as ERF1B-like, ERF3-like, and ERF096-like might be the reason for the difference in storage tolerance of the two pepper materials.
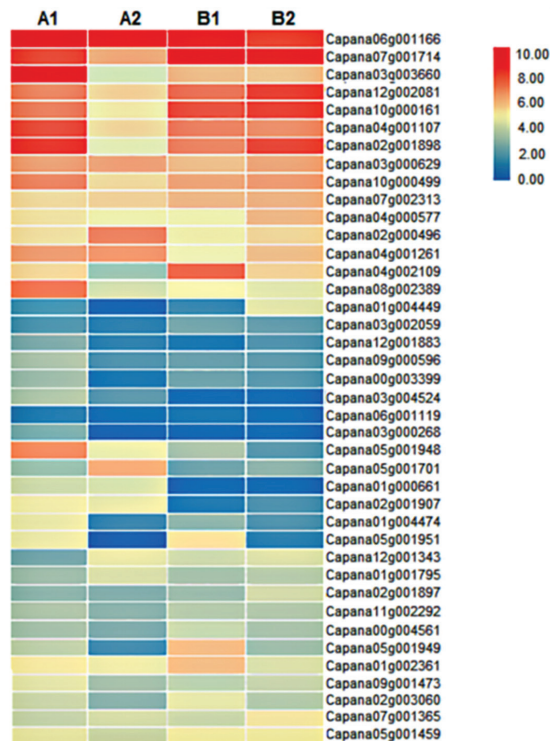
Figure 7. Heat map analysis of ERFs. Annotation: Different colors represent different FPKM values; red represents higher FPKM values, and blue represents lower FPKM values.

3.3.5. The Expression of Abscisic Acid Related Genes

Our study found that a large number of genes in the abscisic acid (ABA) plant hormone signaling pathway were differentially expressed in each comparison group (Figure 8). In the two pepper materials, most genes were upregulated after storage for 3 days, such as abscisic acid receptor PYL (PYL) (Capana00g003406), protein phosphatase 2C (PP2C) (Capana00g003839 and Capana03g002801), and protein kinase 2 (SnRK2) (Capana05g000287), among which PYL had the largest increase, and A2/B2 had significantly higher expression levels of these genes than A1/B1. However, protein kinase 2 (SnRK2) (Capana08g001898 and Capana02g003135) and mitogen-activated protein kinase 7/14 (MPK7/14) (Capana04g000306) showed different trends. The expression of protein kinase 2 (SnRK2) (Capana08g001898 and Capana02g003135) and MPK7/14 (Capana04g000306) in A2 was significantly downregulated compared to A1, while in B2, onlySnRK2 (Capana08g001898) and MPK7/14 (Capana04g000306) were downregulated as compared to B1; moreover, the expression of SnRK2 and MPK7/14 in A2 was significantly lower than that in B2. These results indicate that PP2C, SnRK2, and MPK7/14 might be closely related to the storage tolerance of pepper.
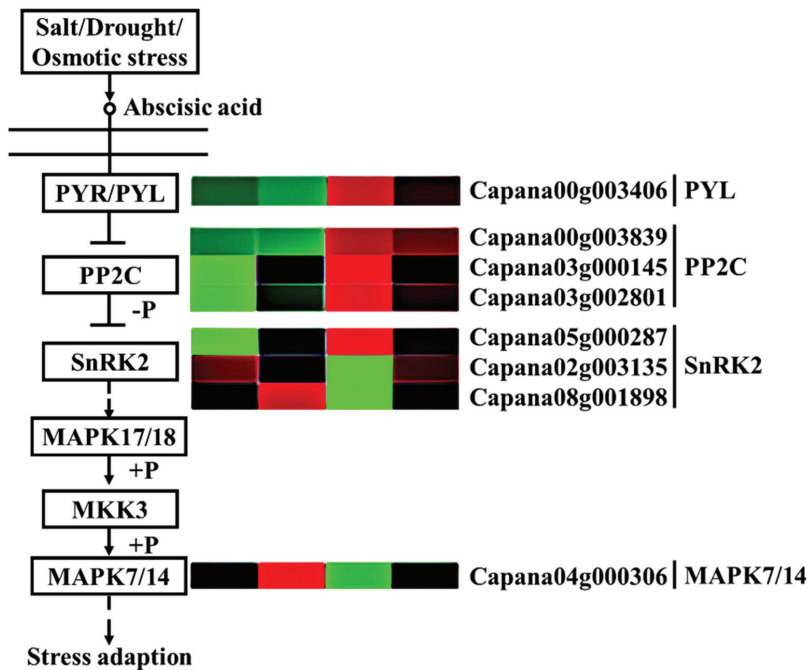
Figure 8. Comparative analysis of ABA signal transduction pathway genes. Annotation: The deeper the green, the lower the gene expression. The deeper the red, the higher the gene expression.

3.4. Metabolome Determination and Differential Metabolite Analysis

The metabolome analysis of the two pepper materials identified a total of 985 metabolites (Table S2). There were 123, 85, 57, and 137 significantly different metabolites in A1/B1, A2/B2, A2/A1, and B2/B1 (Figure 9), respectively. There were four common differential metabolites in the four comparison groups, which were UDP-galactose, cis-4-hydroxy-D-proline, uridine 5′-diphospho-D-glucose, and rotenone. The contents of UDP-galactose and uridine 5′-diphospho-D-glucose in A1 fruit were significantly lower than those in B1, and the contents in both fruits decreased significantly after storage; after storage, the contents in A2 fruit were significantly lower than those in B2 fruit. The content of cis-4-hydroxy-D-proline in A1 fruit was significantly higher than that in B1, and the content in both materials increased after storage; after storage, the content in A2 was significantly higher than that in B2. The content of rotenone in A2 fruit was significantly lower than that in A1, but the content in B2 fruit was significantly higher than that in B1. With |log2FC| > 2 as the cut-off, 30 differential metabolites were identified from each comparison (Table S3). In A2/A1 and B2/B1, 9-KODE and 9-HOTrE showed larger changes, and the contents increased significantly after storage in both materials; the content in B2 was significantly higher than that in B1 by 3.19 times, while the content in A2 was only increased by 2.65 times compared to A1. We also found that Phe-Pro and Gly-Tyr were differentially expressed in A2/A1 and B2/B1. Compared to B1, the contents of Phe-Pro and Gly-Tyr in A1 were higher by 3.9 times and 3.95 times, and the contents in A2 were higher than B2 by 2.75 and 2.3 times. In addition, methyl indole-3-acetate was also different between the two pepper materials. The content of methyl indole-3-acetate in A2 fruit was significantly lower than that in A1 and B2, but there was no significant difference between B1 and B2. The changes of these metabolites might be an important reason for the loss of nutrients in pepper fruit and the difference in fruit's storage tolerance.
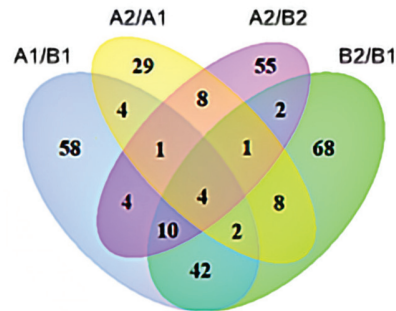
Figure 9. Venn analysis of different metabolites. Annotation: A1/B1 means A1 compared to B1; A2/B2 means A2 compared to B2; B2/B1 means B2 compared to B1; A2/A1 means A2 compared to A1.

3.5. KEGG Pathway Analysis and the Analysis of Correlation between Differential Genes and Differential Metabolites

Pearson correlation analysis was performed between the significantly different genes obtained by transcriptome analysis and the significantly different metabolites obtained by metabolomics analysis in order to measure the degree of correlation between the differential genes and metabolites. The top 50 differential metabolites and the top 100 differential genes based on *p*-value were sorted from small to large (Table S4). Through KEGG enrichment analysis, we identified the metabolic pathways enriched with correlated differential genes and metabolites; we also explored the enrichment degree of these pathways and determined the main biochemical and signaling pathways involving both differential metabolites and genes. In A2/A1, the differential metabolites were mainly enriched in the flavone and flavonol biosynthesis pathway, and the differential genes were mainly enriched in amino sugar and nucleotide sugar metabolism, galactose metabolism, and flavonoid biosynthesis pathways (Figure 10A). In B2/B1, the differential metabolites were mainly enriched in glutathione metabolism, cysteine and methionine metabolism, arginine and proline metabolism, and tyrosine metabolism pathways, and the differential genes were mainly enriched in plant hormone signal transduction, glutathione metabolism, cysteine and methionine metabolism, aminoacyl-tRNA biosynthesis, and fatty acid biosynthesis pathways (Figure 10B). Interestingly, we found that the differential genes and metabolites in A144 were significantly enriched in the flavonoid biosynthesis pathway, which was not observed in A361; on the other hand, the differential genes and metabolites in A361 were significantly enriched in glutathione metabolism and cysteine and methionine metabolism pathways, which was not observed in A144. This result indicated that the reason for the difference in fruit storage tolerance might be related to the changes in metabolites involved in flavonoid biosynthesis, glutathione metabolism, and cysteine and methionine metabolism pathways.
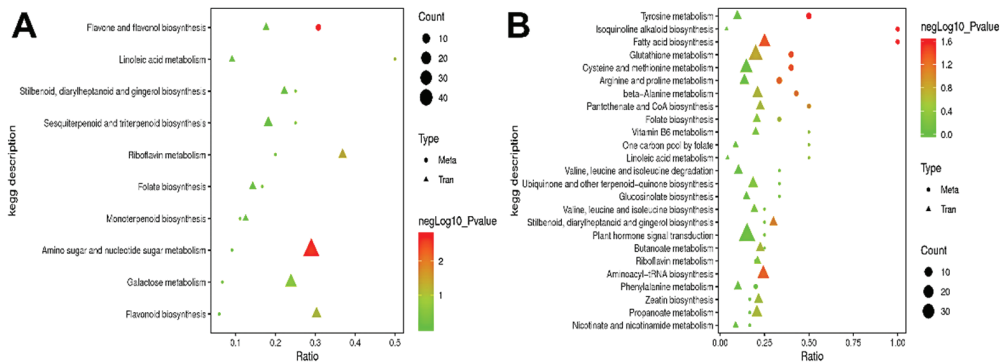
Figure 10. Association analysis of differential genes and KEGG pathways. Annotation: (**A**) A2 compared to A1; (**B**) B2 compared to B1. The abscissa is the ratio of the number of different metabolites or genes enriched in the pathway to the number of metab-olites or genes annotated in the pathway, and the ordinate is the KEGG pathway co-enriched by metabolomics and transcriptomics. Count: the number of metabolites or genes enriched in the pathway.

3.6. Verification of Gene Expression Pattern by qRT-PCR

In order to verify the results of ISO SEQ, eight selected genes (4CLL10, ABI5, BAG6, CESA E1, CIPK6, ERF RAP2-4, ERF1B, and HSP18.2) were analyzed by qRT-PCR with gene-specific primers. The transcriptional abundance patterns of three pepper fruits were calculated. When evaluated by real-time RT-PCR, qRT-PCR analysis showed a similar trend in transcript abundance (Figure 11), thus confirming that the FPKM value of each transcript determined by ISO SEQ was reliable in this study.
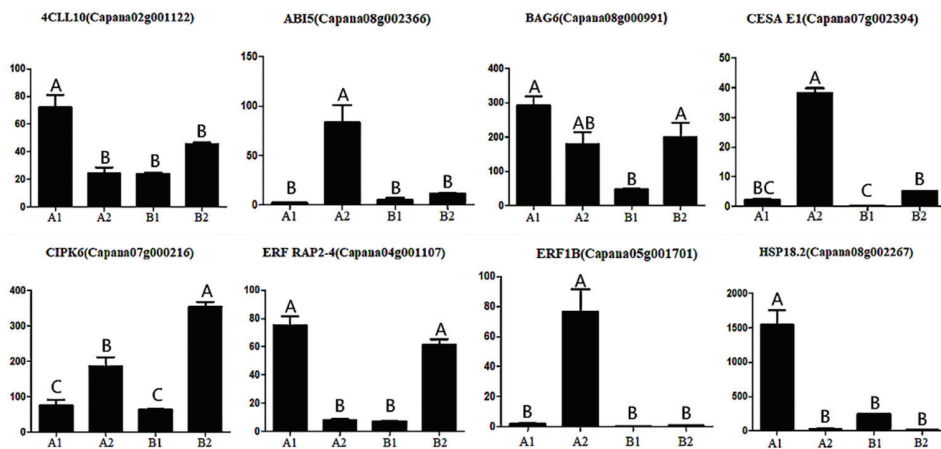
Figure 11. Expression analysis of 8 genes in pepper during different storage periods. Annotation: The horizontal coordinate represents different groups, and the ordinate represents the gene expression. Different letters above the bar chart indicate significant differences ($p < 0.01$).

4. Discussion

Pepper is not a respiratory climacteric fruit, and a series of physiological and biochemical reactions will occur after harvest. During postharvest storage, physiological changes such as fruit softening, dehydration, and wilting are the main factors affecting its economic value. One of the important signs of fruit ripening is softening. Inhibiting or delaying the

decrease in fruit hardness is of great importance for fruit storage and prolonging the sale period. During the ripening and softening of tomatoes, kiwi, strawberry, avocado, and other fruits, the decrease in fruit hardness is closely related to the increase in PG activity [25–30]. The changes in cell wall structure are closely related to fruit ripening and softening. The destruction of the internal structure of the cell wall is the most important reason for fruit softening. The dissociation of intercellular layers of the cell wall, the degradation of the middle lamella, and the disintegration of fibrous material lead to successive disintegration and destruction of cell organelles [31]. Studies have also shown that the degradation of pectin, including water-soluble pectin (WSP), CDTA-soluble pectin (CSP), and ion-bound pectin (SSP), directly leads to the decomposition of cellulose and hemicellulose, which intensifies fruit softening [32,33]. In this study, the PG activity and soluble pectin content of the two pepper lines both showed an increasing trend during postharvest storage, and the contents of cellulose and hemicellulose and fruit hardness showed a decreasing trend. However, the storage-tolerant variety A144 did not show significant change, while the non-storage-tolerant variety A361 showed significantly increased PG activity and soluble pectin content and significantly decreased cellulose content after storage, which is consistent with previous studies. Moreover, the soluble sugar content in pepper fruits decreased to various degrees at 3 days after harvest, suggesting that large amounts of nutrients are lost during the storage process, which seriously affects the fruit quality. However, the relationship between nutrient loss during storage and storage resistance is still unclear and needs further investigation.

Studies have shown that silencing the PG gene in apples can reduce the rate of fruit softening, indicating that the PG gene plays a key role in the ripening and softening of apple fruits [34]. Asif et al. [35] cloned four PG-related genes from banana fruits, of which MAPG3 and MAPG4 were thought to be related to plant maturation and regulated by ethylene, while MAPG2 was more closely related to fruit softening. Studies on a variety of fruits show that the pectin lyase (PEL) gene participates in the ripening and softening of both climacteric and nonclimacteric fruits [36–38], and it can accelerate fruit softening by lysing pectin aggregates. Cellulose is synthesized by CESA protein encoded by the CESA gene [39]. Gerasimo et al. [40] studied the function of the CESA3 gene in Arabidopsis mutants and showed that the accumulation of cellulose required a large amount of CESA. In this study, the expression of PG (Capana06g001141) in A361 was significantly higher than that in A144 after 3 days of storage, while the expression levels of genes that inhibit pepper fruit softening in A144 such as PGI (Capana02g003383), CESA (Capana07g002394), and WEI1 (Capana02g002054) were significantly higher than those in A361. This indicates that the different expression levels of genes such as PG, PGI, CESA, and WEI1 in A144 and A361 may be an important reason for the differences in storage and transportation resistance between the two materials.

Ethylene-responsive transcription factors (ERFs) are important factors for signal transduction, and fruit softening can be regulated by modulating the expression of ethylene-related genes. ERFs can promote the degradation of chlorophyll by regulating the related genes. For example, CitERF6 in sweet orange and ponkan can upregulate the expression of the CitPPH gene involved in chlorophyll degradation in fruits to promote fruit chlorosis, thereby accelerating fruit growth and senescence [41]. BR ERF72 in turnip can be induced by methyl jasmonate and upregulate genes involved in jasmonic acid synthesis to accelerate leaf aging [42]. ERFs can regulate ethylene biosynthesis and signal transduction by regulating the expression of key genes involved in ethylene synthesis. For example, the MdERF3 gene in apple fruits is induced by ethylene and can upregulate the expression of MdACS1, thereby accelerating the synthesis of ethylene and promoting fruit ripening [43]. So far, a number of ERFs have been identified in tomato, some of which can positively regulate fruit ripening and some of which can negatively regulate ripening. In this study, we found that there was no difference in ERF1B-like (Capana05g001701) and ERF3-like (Capana10g000161) expression before and after storage in A361 fruits, but the expression level of ERF1B-like (Capana05g001701) was significantly increased in A144 after storage,

and the expression level of ERF3-like (Capana10g000161) was significantly decreased in A144 fruits after storage and was significantly lower than that in A361. Studies have shown that the overexpression of SlERF4 (Sl-ERF.B3) can inhibit fruit ripening and pigment accumulation [44], which is consistent with our results. SlERF1 (Sl-ERF.H) [45] and SlERF2 (Sl-ERF.E1) [46] can affect fruit softening by responding to ethylene and regulating ethylene synthesis genes. It has also been found that in bananas, MaERF9 and MaERF11 interact with ethylene synthesis genes ACS and ACO to regulate fruit ripening [47], suggesting that ERFs are involved in plant growth, development, and senescence. The differential expression of these ERFs found in this study may be an important reason for the different softening processes in the two pepper lines.

Different from the ripening of respiratory climacteric fruits, ABA plays a positive regulatory role in fruit ripening of both climacteric and nonclimacteric fruits [48–50]. Lara et al. showed that the endogenous ABA in the 'Granny Smith' apple peel might play a role in cold-induced ethylene synthesis by increasing the activity of ACO protein [51]. Exogenous ABA treatment can induce ethylene production by regulating the expression of ACS and ACO genes, thereby promoting the ripening of tomato fruits [52]. Many genes are expressed in the signal transduction of ABA plant hormones, among which genes such as PYR, PYL, PP2C, and SnRK2 play a major role. As a negative regulator of ABA signal transduction, PP2C negatively regulates the SnRK2 protein kinase, which is a positive regulator in ABA response, and they can be rapidly activated by ABA under the action of internal phosphorylation [53]. The Arabidopsis small ubiquitin-related modifier E3 ligase SIZ1 can protect ABI5 from protease degradation by SUMO modification, thereby negatively regulating the effect of ABA on seed germination [54]. In this study, the expression levels of ABI5 and PP2C (Capana03g000145) in A144 after 3 days of storage were significantly higher than those on the day of harvest and significantly higher than those in A361, but there was no significant change after storage in A361. The expression of SnRK2 (capana02g003135) and (capana08g001898) was significantly decreased after 3 days of storage in A144 fruits, but not in A361 fruits, and its expression was significantly lower in A144 than in A361. These results indicate that, after storage, the high expression of PP2C, a negative regulator of ABA signal transduction, and the low expression of SnRK2, a positive regulator in ABA response, can promote the obstruction of ABA synthesis and delay plant senescence in storage-resistant peppers A144, while promoting the synthesis of ABA and accelerating fruit softening and aging in the storage-intolerant pepper A361.

In recent years, due to the development of metabolomics, important progress and breakthroughs have been made in the postharvest research of fruits and vegetables. Metabolomics has become an important research method to reveal the mechanism of fruit and vegetable quality changes [55]. Studies have found that metabolites such as sugars, organic acids, amino acids, lipids, and amines participate in different biological metabolic pathways during fruit development [56]. Vandendriessche et al. [57] used nuclear magnetic resonance (NMR) to study the relationship between metabolic changes of apples during storage and the occurrence of internal browning; they found that there were metabolic differences between apples that were sensitive or not sensitive to browning, such as differences in pyruvate, citric acid, fumaric acid, alanine, acetaldehyde, and 3-hydroxybutanone. Monti et al. [58] performed metabolomics on 15 peach varieties and found that putrescine and pyruvate content decreased and maltose and xylose content increased with fruit ripening and senescence, showing that these metabolites can be useful as markers of postharvest peach maturity and senescence. In this study, we identified quercetin and quercetin 3-D-galactoside in A144 fruits, and their contents were significantly increased after 3 days of storage, while quercetin and quercetin 3-D-galactoside were not identified in A361. The content of indole-3-methyl acetate was significantly reduced after storage in A144 fruits, but not in A361, and its content was significantly lower in A144 fruits than that in A361. Wojdyło and Nowicka [59] analyzed the composition of *Actinidia chinensis* fruit and found that the fruit mainly contained total polyphenols and total flavonoids such as quercetin, quercetin, isoquercitrin, kaempferol, and proanthocyanidin.

Quercetin, as a flavonoid, has antioxidation and antiaging functions [60,61]. Indole-3-acetic acid (IAA) is the main active component of natural plant auxins, and its physiological effects are very extensive, such as regulating the elongation and division of plant cells [62]. These results indicate that, after pepper harvest, the higher quercetin content and the lower indole-3-methyl acetate content were beneficial for delaying the softening of pepper fruit.

5. Conclusions

In this study, we found that the increase in PG activity and soluble pectin content and the decrease in hemicellulose, cellulose, and soluble sugar contents all promoted the softening of pepper fruit. A total of 7829 differentially expressed genes and 296 differential metabolites were identified, of which the number of upregulated genes was less than the number of downregulated genes. Through the KEGG enrichment analysis of these differential genes and metabolites, we found that the storage tolerance of pepper might be affected by the genes related to sugar metabolism, plant hormone signal transduction and protein synthesis and the metabolites related to flavonoid biosynthesis, glutathione metabolism, and cysteine and methionine metabolism, suggesting that the fruit may be positively or negatively regulated by phytohormone-transduction-related genes and flavonoid metabolites. We further identified the genes such as PG, PGI, ABI5, CESA, WEI1, and ERF and as the metabolites such as 13-ketooctadecadienoic acid; 9-hydroxyoctadecadienoic acid; and amino acids and their derivatives phenylalanine, glycyl-tyrosine, and indole-3-methyl acetate that might be important substances in regulating the softening of pepper fruit. Overall, our results provide a scientific reference for a deeper understanding of the complex regulatory mechanisms of pepper storage tolerance.

References

1. Liu, F.; Yu, H.; Deng, Y.; Zheng, J.; Liu, M.; Ou, L. PepperHub, an informatics hub for the chili pepper research community. *Mol. Plant* **2017**, *10*, 1129–1132. [CrossRef] [PubMed]
2. Howard, L.R.; Talcott, S.T.; Brenes, C.H.; Villalon, B. Changes in phytochemical and antioxidant activity of selected pepper cultivars (*Capsicum* species) as influenced by maturity. *J. Agric. Food Chem.* **2000**, *48*, 1713–1720. [CrossRef]
3. Zhou, X.H.; Tao, L.R.; Mei, N.; Liu, L. Research progress on low temperature storage technology of green pepper. *Food Ferment. Technol.* **2017**, *53*, 98–101.
4. Dawson, D.M.; Watkins, C.B. Cell wall changes in nectarines (*Prunuspersica*): Solubilization and depolymerization of pectic and neutral polymers during ripening and in mealy Fruit. *Plant Physiol.* **1992**, *100*, 1203–1210. [CrossRef]
5. Brummell, D.A.; Harpster, M.H.; Dunsmuir, P. Differential expression of expansin gene family members during growth and ripening of tomato fruit. *Plant Mol. Biol.* **1999**, *39*, 161–169. [CrossRef] [PubMed]

6. Rose, J.K.C.; Bennett, A.B. Cooperative disassembly of the cellulose–xyloglucan network of plant cell walls: Parallels between cell expansion and fruit ripening. *Trends Plant Sci.* **1999**, *4*, 176–183. [CrossRef]

7. Montgomery, J.; Pollard, V.; Deikman, J.; Fischer, R.L. Positive and negative regulatory regions control the spatial distribution of polygalacturonase transcription in tomato fruit pericarp. *Plant Cell* **1993**, *5*, 1049–1062. [PubMed]

8. Hadfield, K.A.; Rose, J.K.C.; Yaver, D.S.; Berka, R.M.; Bennett, A.B. Polygalacturonase gene expression in ripe melon fruit supports a role for polygalacturonase in ripening-associated pectin disassembly. *Plant Physiol.* **1998**, *117*, 363–373. [CrossRef]

9. Yonder, M.D.; Keen, N.T.; Jurnak, F. New domain motif: The structure of pectatelyase C, a secreted plant virulence factor. *Science* **1993**, *260*, 1503–1507. [CrossRef]

10. Smith, D.L. A family of at least seven β-galactosidase genes is expressed during tomato fruit development. *Plant Physiol.* **2000**, *123*, 1173–1184. [CrossRef]

11. Ross, G.S.; Wegrzyn, T.; Macrae, E.A.; Redgwell, R.J. Apple β-Galactosidase: Activity against cell wall polysaccharides and characterization of a related cDNA clone. *Plant Physiol.* **1994**, *106*, 521–528. [CrossRef] [PubMed]

12. Lockhart, D.J.; Winzeler, E.A. Genomics, gene expression and DNA arrays. *Nature* **2000**, *405*, 827–836. [CrossRef]

13. Guo, S.; Sun, H.; Zhang, H.; Liu, J.; Ren, Y.; Gong, G. Comparative Transcriptome Analysis of Cultivated and Wild Watermelon during Fruit Development. *PLoS ONE* **2015**, *10*, e0130267. [CrossRef]

14. Dessireé, Z.C.; Patricia, E.; Eric, M.N.; Marco, V.S.; Raúl, H.; Víctor, M. Transcription analysis of softening-related genes during postharvest of papaya fruit (*Carica papaya* L. 'Pococí'hybrid). *Postharvest Biol. Technol.* **2017**, *125*, 42–51.

15. Osorio, S.; Carneiro, R.T.; Lytovchenko, A.; Mcquinn, R.; Srensen, I.; Vallarino, J.G. Genetic and metabolic effects of ripening mutations and vine detachment on tomato fruit quality. *Plant Biotechnol. J.* **2019**, *18*, 106–118. [CrossRef]

16. Tietel, Z.; Lewinsohn, E.; Fallik, E.; Porat, R. Elucidating the Roles of Ethanol Fermentation Metabolism in Causing Off-Flavors in Mandarins. *J. Agric. Food Chem.* **2011**, *59*, 11779–11785. [CrossRef]

17. Andrews, P.K.; Li, S.L. Cell wall hydrolytic enzyme activity during development of nonclimacteric sweet cherry (*Prunus avium* L.) fruit. *J. Hortic. Sci.* **1995**, *70*, 561–567. [CrossRef]

18. Min, L.; Li, Y.; Hu, Q.; Zhu, L.; Gao, W.; Wu, Y. Sugar and auxin signaling pathways respond to high-temperature stress during anther development as revealed by transcript profiling analysis in cotton. *Plant Physiol.* **2014**, *164*, 1293–1308. [CrossRef]

19. Zhang, L.; Chen, F.; Yang, H.; Sun, X.; Liu, H.; Gong, X. Changed in firmness, pectin content and nanostructure of two crisp peach cultivars after storage. *LWT Food Sci. Technol.* **2010**, *43*, 26–32. [CrossRef]

20. Cai, S.; Lashbrook, C.C. Laser capture microdissection of plant cells from tape-trans-ferredparaffin sections promotes recovery of structurallyintact RNA for global gene profiling. *Plant J.* **2006**, *48*, 628–637. [CrossRef]

21. Want, E.J.; Masson, P.; Michopoulos, F.; Wilson, I.D.; Theodoridis, G.; Plumb, R.S. Global metabolic profiling of animal and human tissues via UPLC-MS. *Nat. Protoc.* **2012**, *8*, 17–32. [CrossRef] [PubMed]

22. Ping, L.; Weidong, D.; Peiyuan, Y.; Zhongda, Z.; Hongwei, K.; Lina, Z. Multiple Reaction Monitoring-Ion Pair Finder: A systematic approach to transform non-targeted mode to pseudo-targeted mode for metabolomics study based on liquid chromatography-mass spectrometry. *Anal. Chem.* **2015**, *87*, 5050–5055.

23. Osorio, S.; Alba, R.; Nikoloski, Z.; Kochevenko, A. Integrative Comparative Analyses of Transcript and Metabolite Profiles from Pepper and Tomato Ripening and Development Stages Uncovers Species-Specific Patterns of Network Regulatory Behavior. *Plant Physiol.* **2012**, *159*, 1713–1729. [CrossRef]

24. Livak, K.J.; Schmittgen, T.D. Analysis of Relative Gene Expression Data using Real-Time Quantitative PCR. *Methods* **2002**, *25*, 402–408. [CrossRef]

25. Ali, Z.M.; Chin, L.H.; Lazan, H. A comparative study on wall degrading enzymes, pectin modifications and softening during ripening of selected tropical fruits. *Plant Sci.* **2004**, *167*, 317–327. [CrossRef]

26. Bonghi, C.; Pagni, S.; Vidrih, R.; Ramina, A.; Tonutti, P. Cell wall hydrolases and amylase in kiwifruit softening. *Postharvest Biol. Technol.* **1996**, *9*, 19–29. [CrossRef]

27. Huber, D.J. Strawberry Fruit Softening: The potential roles of polyuronides and hemicelluloses. *J. Food Sci.* **2010**, *49*, 1310–1315. [CrossRef]

28. Villarreal, N.M.; Rosli, H.G.; Martínez, G.A.; Civello, P.M. Polygalacturonase activity and expression of related genes during ripening of strawberry cultivars with contrasting fruit firmness. *Postharvest Biol. Technol.* **2008**, *47*, 141–150. [CrossRef]

29. Huber, D.J.; O'Donoghue, E.M. Polyuronides in avocado (Perseaamericana) and tomato (Lycopersiconesculentum) fruits exhibit markedly different patterns of molecular weight downshifts during ripening. *Plant Physiol.* **1993**, *102*, 473–480. [CrossRef]

30. Kutsunai, S.Y.; Lin, A.C.; Percival, F.W.; Christoffersen, L.R.E. Ripening-related polygalacturonase cDNA from avocado. *Plant Physiol.* **1993**, *103*, 289–290. [CrossRef] [PubMed]

31. Posé, S.; Paniagua, C.; Matas, A.; Gunning, A.P.; Morris, V.J.; Quesada, M.A.; Mercado, J.A. A nanostructural view of the cell wall disassembly process during fruit ripening and postharvest storage by atomic force microscopy. *Trends Food Sci. Technol.* **2018**, *87*, 47–58. [CrossRef]

32. Chen, Y.H.; Hung, Y.C.; Chen, M.Y.; Lin, H.T. Effects of acidic electrolyzed oxidizing water on retarding cell wall degradation and delaying softening of blueberries during postharvest storage. *LWT Food Sci. Technol.* **2017**, *84*, 650–657. [CrossRef]

33. Chen, Y.H.; Sun, J.Z.; Lin, H.T.; Hung, Y.C.; Zhang, Y.F. Paper-based 1-MCP treatment suppresses cell wall metabolism and delays softening of Huanghua pears during storage. *J. Sci. Food Agric.* **2017**, *97*, 2547–2552. [CrossRef]

34. Atkinson, R.G.; Sutherland, P.W.; Johnston, S.L.; Gunaseelan, K.; Hallett, I.C.; Mitra, D. Down-regulation of polygalacturonase 1 alters firmness, tensile strength and water loss in apple (*Malusx domestica*) fruit. *BMC Plant Biol.* **2012**, *12*, 129. [CrossRef]
35. Asif, M.H.; Nath, P. Expression of multiple forms of polygalacturonase gene during ripening in banana fruit. *Plant Physiol. Biochem.* **2005**, *43*, 177–184. [CrossRef]
36. Pua, E.C.; Ong, C.K.; Liu, P.; Liu, J.Z. Isolation and expression of two pectatelyase genes during fruit ripening of banana (Musa acuminata). *Physiol. Plant.* **2010**, *113*, 92–99. [CrossRef]
37. Nieves, S.D.; Silvia, J.B.; Matas, A.J.; Rose, J.K.C.; Juan, M.B.; Mercado, J.A.; Quesada, M.A. Antisense inhibition of a pectatelyase gene supports a role for pectin depolymerization in strawberry fruit softening. *J. Exp. Bot.* **2008**, *59*, 2769–2779.
38. Youssef, S.M.; Silvia, J.B.; Bellido, M.L.; Martín-Pizarro, C.; Barceló, M.; Abdal-Aziz, S.A.; Caballero, J.L. Fruit yield and quality of strawberry plants transformed with a fruit specific strawberry pectatelyase gene. *Sci. Hortic.* **2009**, *119*, 120–125. [CrossRef]
39. Song, L.; Yu, J.; Tian, P.; Hu, X.; Wang, Q.; Pan, Y. Genome-wide characterization of the cellulose synthase gene superfamily in Solanum lycopersicum. *Gene* **2019**, *688*, 71–83. [CrossRef]
40. Daras, G.; Rigas, S.; Penning, B. Thethanatos mutation in Arabidopsis thalianacellulose synthase3 (AtCesA3) has adominant-negative effect on cellulose synthesis and plant growth. *New Phytol.* **2009**, *184*, 114–126. [CrossRef] [PubMed]
41. Li, S.; Xie, X.; Liu, S. Auto-and mutual-regulation between two CitERFs contribute to ethyleneinduced citrus fruit degreening. *Food Chem.* **2019**, *299*, 125163. [CrossRef]
42. Tan, X.L.; Fan, Z.Q.; Shan, W.; Yin, X.R.; Kuang, J.F.; Lu, W.J.; Chen, J.Y. Association of BrERF72 with methyl jasmonate-induced leaf senescence of Chinese flowering cabbage through activating JA biosynthesis-related genes. *Hortic. Res.* **2018**, *5*, 1–11. [CrossRef] [PubMed]
43. Tong, L.; Jiang, Z.; Zhang, L.; Tan, D.; Yun, W.; Hui, Y.; Li, T.; Wang, A. Apple (*Malusdomestica*) MdERF2 negatively affects ethylene biosynthesis during fruit ripening by suppressing MdACS1 transcription. *Plant J.* **2016**, *88*, 735–748.
44. Liu, M.; Diretto, G.; Pirrello, J.; Roustan, J.-P.; Li, Z.; Giuliano, G.; Regad, F.; Bouzayen, M. The chimeric repressor version of an ethylene response factor (ERF) family member, Sl-ERF.B3, shows contrasting effects on tomato fruit ripening. *New Phytol.* **2014**, *203*, 206–218. [CrossRef] [PubMed]
45. Li, Y.; Zhu, B.; Xu, W.; Zhu, H.; Chen, A.; Xie, Y.; Shao, Y.; Luo, Y. LeERF1 positively modulated ethylene triple response on etiolated seedling, plant development and fruit ripening and softening in tomato. *Plant Cell Rep.* **2007**, *26*, 1999–2008. [CrossRef]
46. Zhang, Z.; Zhang, H.; Quan, R.; Wang, X.C.; Huang, R. Transcriptional regulation of the ethylene response factor LeERF2 in the expression of ethylene biosynthesis genes controls ethylene production in tomato and tobacco. *Plant Physiol. Biochem.* **2009**, *150*, 365–377. [CrossRef]
47. Xiao, Y.Y.; Chen, J.Y.; Kuang, J.F.; Shan, W.; Xie, H.; Jiang, Y.M.; Lu, W.J. Banana ethylene response factors are involved in fruit ripening through their interactions with ethylene biosynthesis genes. *J. Exp. Bot.* **2013**, *64*, 2499–2510. [CrossRef]
48. Gupta, M.K.; Lenka, S.K.; Gupta, S.; Rawal, R.K. Agonist, antagonist and signaling modulators of ABA receptor for agronomic and post-harvest management. *Plant Physiol. Biochem.* **2020**, *148*, 10–25. [CrossRef]
49. Jiang, Y.; Joyce, D.C. ABA effects on ethylene production, PAL activity, anthocyanin and phenolic contents of strawberry fruit. *Plant Growth Regul.* **2003**, *39*, 171–174. [CrossRef]
50. Chai, Y.M.; Jia, H.F.; Li, C.L. FaPYR1 is involved in strawberry fruit ripening. *J. Exp. Bot.* **2011**, *62*, 5079–5089. [CrossRef]
51. Lara, I.; Vendrell, M. Cold-induced ethylene biosynthesis is differentially regulated in peel and pulp tissues of 'Granny Smith' apple fruit. *Postharvest Biol. Technol.* **2003**, *29*, 109–119. [CrossRef]
52. Zhang, M.; Yuan, B.; Leng, P. The role of ABA in triggering ethylene biosynthesis and ripening of tomato fruit. *J. Exp. Bot.* **2009**, *60*, 1579–1588. [CrossRef] [PubMed]
53. Ma, Y.; Szostkiewicz, I.; Korte, A.; Moes, D.; Yang, Y.; Christmann, A.; Grill, E. Regulators of PP2C phosphatese activity functions as acid sensors. *Science* **2009**, *324*, 1064–1068.
54. Miura, K.; Lee, J.; Jin, J.B.; Chan, Y.Y.; Miura, T.; Hasegawa, P.M. Sumoylation of ABI5 by the Arabidopsis SUMO E3 ligase SIZ1 negatively regulates abscisic acid signaling. *Proc. Natl. Acad. Sci. USA* **2009**, *106*, 5418–5423. [CrossRef]
55. Picone, G.; Trimigno, A.; Tessarin, P.; Donnini, S.; Rombolà, A.D.; Capozzi, F. ^{1}H NMR foodomics reveals that the biodynamic and the organic cultivation managements produce different grape berries (*Vitisvinifera* L. cv. Sangiovese). *Food Chem.* **2016**, *213*, 187–195. [CrossRef]
56. Lasanajak, Y.; Minocha, R.; Minocha, S.C.; Goyal, R.; Fatima, T.; Handa, A.K.; Mattoo, A.K. Enhanced flux of substrates into polyamine biosynthesis but not ethylene in tomato fruit engineered with yeast S-adenosylmethionine decarboxylase gene. *Amino Acids* **2014**, *46*, 729–742. [CrossRef]
57. Vandendriessche, T.; Schäfer, H.; Verlinden, B.E.; Humpfer, E.; Hertog, M.; Nicolaï, B.M. High-throughput NMR based metabolic profiling of 'Braeburn' apple in relation to internal browning. *Postharvest Biol. Technol.* **2013**, *80*, 18–24. [CrossRef]
58. Monti, L.L.; Bustamante, C.A.; Osorio, S.; Gabilonodo, J.; Borsani, J.; Lauxmann, M.A.; Maulion, E.; Valentini, G.; Budde, C.O.; Fernie, A.R.; et al. Metabolic profiling of a range of peach fruit varieties reveals high metabolic diversity and commonalities and differences during ripening. *Food Chem.* **2016**, *190*, 879–888. [CrossRef]
59. Wojdyło, A.; Nowicka, P. Anticholinergic effects of actinidiaarguta fruits and their polyphenol content determined by liquid chromatography-photodiode array detector-quadrupole/time of flight-mass spectrometry (LC-MS-PDA-Q/TOF). *Food Chem.* **2019**, *271*, 216–223. [CrossRef]

60. Bischoff, S.C. Quercetin: Potentials in the prevention and therapy of disease. *Curr. Opin. Clin. Nutr. Metab. Care* **2008**, *11*, 733–740. [CrossRef]
61. Lesjak, M.; Beara, I.; Simin, N. Antioxidant and anti-inflammatory activities of quercetin and its derivatives. *J. Funct. Foods* **2017**, *40*, 68–75. [CrossRef]
62. Duan, N.; Jia, Y.K.; Xu, J.; Chen, H.L.; Sun, P. Research progress of plant endogenous hormones. *Chin. Agric. Sci. Bull.* **2015**, *31*, 159–165.

Application of Room Cooling and Thermal Insulation Materials to Maintain Quality of Okra during Storage and Transportation

Jutarat Rattanakaran [1], Rattapon Saengrayap [1,2], Chureerat Prahsarn [3], Hiroaki Kitazawa [4] and Saowapa Chaiwong [1,2,*]

[1] School of Agro-Industry, Mae Fah Luang University, Chiang Rai 57100, Thailand; 6151407001@lamduan.mfu.ac.th (J.R.); rattapon.sae@mfu.ac.th (R.S.)

[2] Integrated AgriTech Ecosystem Research Unit, Mae Fah Luang University, Chiang Rai 57100, Thailand

[3] National Metal and Materials Technology Center, National Science and Technology Development Agency, Pathumthani 12120, Thailand; chureerp@mtec.or.th

[4] Institute of Food Research, National Agriculture and Food Research Organization, Tsukuba 305-8642, Japan; ktz@affrc.go.jp

[*] Correspondence: saowapa@mfu.ac.th; Tel.: +66-53-916-766

Abstract: A combination of room cooling and the use of thermal insulation materials to maintain okra quality under simulated storage and transportation was evaluated. Okra pods were packed in plastic baskets and either cooled at 18 °C or not cooled in a room for 2 h. After either room cooling or no cooling, the okra pods were covered with three different materials: (1) perforated linear low-density polyethylene (P-LLDPE), (2) two layers of heat-reflective sheet with thin nonwoven (HRS+TNNW), and (3) metalized foam sheet (MFS). Typical handling (TP) without cooling and covering with P-LLDPE was used as the control. The six treatments were conducted during simulated storage (18 °C for 48 h) and transportation (30 °C for 15 h). Results showed that MFS gave the best insulation properties (Q_x and R-values), followed by HRS and TNNW. After room cooling, both HRS+TNNW and MFS materials delayed the time for pulp temperature to reach 18 °C (10 h), compared to P-LLDPE (2 h). TP presented the highest mass loss (17.8%) throughout simulated conditions, followed by cooling plus P-LLDPE (15.2%) and either of the thermal insulation materials with or without room cooling (3.6% to 5.2%), respectively. TP, cooling plus P-LLDPE, and no cooling plus MFS (44% to 56%) showed the highest percentage of decay, while cooling combined with both HRS+TNNW and MFS gave the lowest decay incidence (11–21%). Findings demonstrated that room cooling combined with HRS+TNNW had the highest efficiency for preserving cool temperature and reducing decay, compared to TP and room cooling plus MFS.

Keywords: decay; covering; nonwoven; mass loss; metalized foam sheet

1. Introduction

Okra (*Abelmoschus esculentus* L.) is an economic vegetable crop widely grown in tropical and sub-tropical global regions. Okra pods are harvested when immature and eaten as vegetables [1]. Okra is an export vegetable crop of Thailand, with the Japanese market accounting for 83.3% of the total exported okra volume. The main growing areas are the central and northern areas of Thailand [2]. A decline in the quality of okra is attributable to various issues, including techniques for determining okra fruit quality, poor harvesting methods, okra harvester training levels, lack of good vehicles, terrible roads, and insufficient pre-cooling facilities [3]. High respiration rate and rapid deterioration causes heat build-up and leads to pod blackening as well as a rapid increase in okra water loss after harvesting [4,5].

Temperature and relative humidity are the most important factors affecting the shelf life of okra [6]. The optimal storage temperature of okra ranged from 7 to 10 °C, and the pods can be stored satisfactorily for 7–10 days [7]. Fresh okra pods exhibited extremely

short shelf life due to high water loss or transpiration rates. Storage of okra at 25 °C resulted in a higher mass loss (14%) compared to a lower temperature of 4 °C after 5 days due to wilting, yellowing, and decay [8]. Storage at low temperatures led to a reduction of respiration rate, transpiration, and ethylene production [9]. At high temperatures, okra is highly susceptible to water loss, color fading, and decay, becoming squashy with a loss of commercial value and not easy to consume when fresh [10].

Heat generation, specifically known as 'Vital heat' in fresh produce, is produced as a by-product, primarily through the respiration process. Okra is classified at a very high respiration level, with a respiration rate of 40–60 mg CO_2 kg^{-1} h^{-1} and vital heat ranging from 427 to 640 J kg^{-1} h^{-1} at 5 °C [9]. Consequently, a cooling process should be taken into consideration when the storage room is designed as well as during transportation [11]. Cooling as quickly as possible after harvesting is critical to remove heat from the fresh produce and is a very important requirement for maintaining optimal product quality, especially for merchandise with naturally high respiration rates [12]. Forced-air cooling has been used for the export of okra received directly from the field [13]. In India, room cooling at 15 °C before storage at 8 °C is used for the export of okra [14]. The procedure of no cooling resulted in decreased fruit quality and increased fruit decay. Post-harvest loss of commercial fruits and vegetables increased by 25–30% when no cooling was employed through the whole storing and transporting chain, while it was only 5–10% when a cooling step at 8 °C was practiced [15]. Wang et al. [16] showed that room cooling at 2 °C reduced changes in the physiological quality of button mushroom (*Agaricus bisporus*). However, scant research has reported on cooling conditions and the efficiency of cooling processes to reduce heat generation in okra to extend storage or shelf life.

Thermal insulation materials are defined as materials or combinations of materials that retard the flow of heat to prevent or minimize temperature changes in the system or space [17]. Thermal insulation materials are normally used as pallet covering, combined with other materials, to protect fresh produce during transportation [18]. Thermal insulation material testing evaluates whether a packaging design succeeds in maintaining a temperature-sensitive product within its appropriate temperature range when exposed to ambient conditions [19]. The main thermal insulation properties are measured as thermal heat transfer and R-value. Heat transfer is the mechanism of energy movement due to temperature differences between two sources [20]. A low rate of heat transfer implies better insulation of the materials via reduction of conductive heat loss [21]. The resistance to heat flow through an insulation material, known as the R-value, is determined by ice-melt processing [22]. A higher R-value presents a better performance of thermal insulation materials [19].

Pallet cover is an alternative method used as packaging technology to reduce waste from food spoilage by minimizing temperature and humidity change during the transportation of fresh produce [18,23,24]. Research on packaging for vegetables revealed that covering the pallet side and bottom with insulated pallet cover (Reflectix™) resulted in a reduction of mass loss and wilting in amaranth and preserved a desirable dark green color. Use of pallet cover for amaranth gave a high score in overall quality, with improvement on no cover [18]. Liu [25] reported the use of an insulated cover to keep pre-chilled lettuce at low temperatures. The insulated cover was also suitable for low-temperature phosphine fumigation to control western flower thrips on harvested lettuce. Chaiwong and Bishop [23] reported on lightweight insulation bags. Results showed that insulated bags provided cool temperature management and reduced the cool chain breakdown of strawberries from the supermarket to domestic refrigerators. The insulated pallet covers also gave better temperature preservation compared to no cover, and temperature changes occurred more slowly in chard, cucumber, and carrot [18,23,24]. However, very few studies exist about the use of thermal insulation cover to prevent post-harvest losses of okra under different temperature conditions.

The main post-harvest problems of okra during domestic transportation are temperature and relative humidity fluctuation. These lead to physiological damages such as

wilting and fruit rot before the freeze-drying process. Cooling treatment could delay the deterioration of okra quality, whereas thermal insulation covering could improve controlling temperature and humidity fluctuations under typical truck transportation. In this study, the efficiency of room cooling and thermal insulation materials in controlling cool temperature and okra quality under simulated storage and transportation were evaluated.

2. Materials and Methods

2.1. Materials Properties

Thermal heat energy was determined according to the procedure of Harvey [21], using an expanded polystyrene box with dimensions ($75 \times 38 \times 38.5$ cm^3) with two sections (Figure 1). The material sample was taped on a hole (C) 10 cm $\times$ 10 cm to allow heat from the heated copper coil (E) at temperature 45 °C in section 1 (A) to pass through the material sample and enter section 2 (B). Temperature data loggers (Tinytag Talk 2: TK-4014-PK, Gemini Data Loggers, West Sussex, UK) were used to monitor the temperature change between the two sections (section 1 (I) and section 2 (J)) of the box for 3 h until a constant temperature was recorded. The rate of transfer of thermal heat energy (Q_x) in J s^{-1} was calculated.

A	An expanded polystyrene box (section 1)
B	An expanded polystyrene box (section 2)
C	Square hole for material cover attachment (10×10 cm²)
D	Rotating fan (section 1)
E	Heating coil
F	Rotating pump
G	Water bath at 45 °C
H	Rotating fan (section 2)
I	Data logger (section 1)
J	Data logger (section 2)
K	Power source
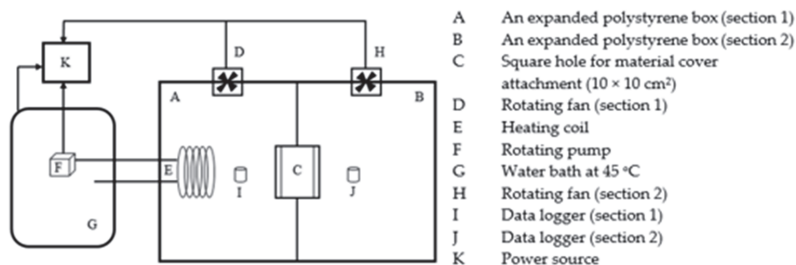
Figure 1. Schematic diagram for heat transfer test through material covers at the laboratory.

The water vapor permeability (WVP) through different materials was determined using the desiccant in cup method. Following ASTM E96 [26], the specimen or cover material was sealed on the open mouth of a test dish containing a desiccant, and the test dish was placed in a constant climate chamber (KBF-115, Binder, Tuttlingen, Germany) at 25 °C and 50% relative humidity (RH). Water vapor permeability was then calculated as rate of water vapor transmission in g h^{-1} m^{-2}.

Air permeability was determined using an air permeability tester (FX 3300 LabAir IV, Textest Instruments, Schwerzenbach, Switzerland) according to ASTM D737-04 [27]. Thermal insulation materials were cut into square pieces of 20×20 cm and measured for air permeability (l m^{-2} s^{-1}). The R-value was determined as resistance to heat flow through the thermal insulation material using the ice-melt test, following Singh et al. [19]. In this method, 2000 g of ice were placed in a non-metallic bucket, which was then positioned in the center of a basket inside thermal insulation bags and wrapped tightly with tape. The package was stored on a shelf at ambient temperature (25 °C) for 12 h. At the end of the test, the thermally insulated containers were opened, and water was collected from the buckets. The weight of water was recorded to calculate the melt rate (m^2 °C W^{-1}). Five samples (replications) in each material were tested.

2.2. Plant Materials

'Lady Finger' okra pods from Green Global Seeds Company Limited, Thailand, were planted with the spacing between plant and row of 50 and 100 cm, respectively, with sprinkler irrigation. The okra pods were harvested 45 days after planting, or 6 days after flowering from an okra plantation (20°13′27.2″ N 99°50′05.2″ E), in Mae Chan district, Chiang Rai Province. The pods were transported from the farm to the Postharvest Laboratory at Mae Fah Luang University within 30 min. After arrival at the laboratory, the okra pods

were graded to uniform size of pod length 7–11 cm (the specific size for okra processing), with minimum requirements being green in color, free of distinct signs of bruising and disease, and a clean-cut peduncle.

2.3. Experimental Treatments and Heat from Respiration Rate (RR)

The research study was divided into two experiments.

2.3.1. Handling Procedures

Six treatments were studied. The control, as typical handling (TP) of the Phayao community enterprise (without room cooling and covered with perforated linear low-density polyethylene (P-LLDPE)) was compared with developing handling (DH), comprising room cooling, covered by two thermal insulation materials (heat-reflective sheet (HRS) + thin nonwoven (TNNW)), which were polypropylene (PP)-based spunbond nonwoven, and metalized foam sheet (MFS)), as shown in Table 1. It is noted that the HRS material was evenly perforated and distributed with a pin of diameter 0.55 mm for a total perforation area of 0.09 cm^2.

Table 1. Six treatments (with or without room cooling) using different material covers.

Treatment	Description
TP (Control)	No room cooling with P-LLDPE covering
DH1	Room cooling with P-LLDPE covering
DH2	No room cooling with HRS+TNNW covering
DH3	No room cooling with MFS covering
DH4	Room cooling with HRS+TNNW covering
DH5	Room cooling with MFS covering

For each treatment, 1500 g of okra pods were packed in a plastic basket (five replications). Initial temperature at the core of the okra pods was approximately 30 °C. Room cooling treatments (DH1, DH4 and DH5) were performed by setting the cooling medium at 0 °C for 2 h, compared with a cool room at 18 °C (no room cooling) (TP, DH2, and DH3) for 2 h as the 7/8 cooling time. Pulp temperature of the okra was monitored by a multichannel data logger (Hioki, LR8431, Nagano, Japan) connected with a type-K thermocouple for 10 channels. Five baskets each room cooling at 0 °C or at 18 °C were allocated for temperature monitor. After room cooling, the okra pods were covered with different thermal insulation materials, except for TP and DH1. Storage and transportation conditions of okra to simulate commercial practice before processing comprised storage at 18 °C for 48 h and transfer at 30 °C for 15 h.

2.3.2. Determination of Respiration Rate

Respiration rate of okra was determined under three storage conditions (10, 20, 30 °C) for 2 and 3 days. Okra pods (150 g) were packed in a plastic food container (8400 mL) (Figure 2). Respiration rate testing was conducted in a closed system for 2 h. A gas sample of 5000 µL was drawn from each container at daily intervals for gas chromatography (GC) analysis. A gas chromatograph (7890A, Agilent Technologies, California, USA) equipped with a thermal conductivity detector (TCD) and HayeSep Q column (80/100 mesh, 3.05-m long) was used to analyze the gas samples. Nitrogen was used as the carrier gas at a flow rate of 52.2 mL min^{-1} with split mode. Injector, oven, and detector temperature conditions were 150, 60, and 275 °C, respectively. The respiration rate (R_{CO2}) was determined on days 2 and 3 for the three storage conditions and calculated by the following Formula (1) [11];

$$R_{CO2} \text{ (mg CO}_2 \text{ kg}^{-1} \text{ h}^{-1}) = \frac{(CO_2 \text{ (\%)} \times \text{volume of container (mL))}}{100 \times \text{(fruit weight (kg))} \times \text{(closing time (h))}} \qquad (1)$$

Figure 2. Okra pods packed in a plastic food container for respiration rate measurement by a closed system.

The respiration rate (R_{CO2}) of okra pods in each closed system storage condition was calculated as the temperature coefficient (Q_{10}) value by Formula (2):

$$Q_{10} = (R_2 R_1)^{10/(T_2 - T_1)} \qquad (2)$$

where R_2 and R_1 are the respiration rate at temperature T_2 and T_1, respectively [28].

The Q_{10} values on day 2 (48 h) and day 3 (72 h) were used to estimate the respiration rate of okra pods (R_C) in different air temperature levels using a temperature data logger (Tinytag Talk 2: TK-4014-PK, Gemini Data Loggers, West Sussex, UK). This depended on the thermal insulation cover treatments under simulated storage (18 °C for 48 h) and transportation (30 °C for 15 h), respectively. The air temperature for estimation of okra respiration rate (R_C) in each cover treatment was determined from the final air temperature level before simulated storage (R_{C1}) and transportation conditions (R_{C2}). Respiration rates of okra pods in each cover material were converted into vital heat by Formula (3) [29]:

$$\text{Vital heat (J kg}^{-1} \text{ h}^{-1}) = R_C \times 10.7 \qquad (3)$$

where R_C = respiration rate of okra pods in each cover treatment.

2.4. Temperature and Relative Humidity Monitoring

Air temperatures inside the covering and pulp temperatures at the core of the okra pods were measured using a temperature data logger for air temperature (Tinytag Talk 2: TK-4014-PK, Gemini Data Loggers, West Sussex, UK) with three replications and pulp temperature (Tinytag Talk 2: TK-4023-PK, Gemini Data Loggers, West Sussex, UK) with four replications. Relative humidity inside the covering was recorded using a temperature and relative humidity data logger (Tinytag Ultra 2: TGU-4500, Gemini Data Loggers, West Sussex, UK) at 30 s intervals. Pulp temperature was analyzed using temperature profile and boxplot at 12 h after simulated storage with stable temperature level. After simulated transportation at 30 °C for 15 h, air and pulp temperature levels were analyzed using a boxplot at 1 h 30 min (air temperature of TP at 25 °C) and 15 h after simulation, and the rate of change during temperature rise after simulated transportation was calculated. Data analysis of both air and pulp temperature focused on the data point at 25 °C and temperature range from 25 °C to 30 °C. Furthermore, heatmap analysis represented pulp temperature levels after simulated storage and transportation for 12 h. Python 3.6.9 was used to create the heatmap chart. The packages Seaborn version 0.11.1, Pandas version 1.1.5, and Matplotlib version 3.2.2 were all required by heatmap. The profile of relative humidity throughout the experiment was also investigated.

2.5. Mass Loss Determination

Mass loss of the okra pods was determined using an electric weighing balance (Pioneer[TM], Ohaus, NJ, USA). Percentage mass loss (%) was calculated on the basis of initial weight (IW) before cooling and final weight (FW) at the end of simulated storage and transportation, using WL (%) = [(IW − FW/IW) × 100 [30].

2.6. Determination of Decay Incidence

The first sign of okra deterioration was observed as a small wet lesion on pod, and then the entire pod coated with a grayish-white mass of mold. The okra pods were evaluated when incidence of decay occurred, calculated based on weight of pods showing symptoms of decay (D), and classified into four categories, including <10% of decay occurrence, 10–25% of decay occurrence, 25–50% of decay occurrence, and >50% of decay occurrence. Percentage decay (%) was calculated on the basis of total weight of pods per plastic basket (TW), using D (%) = [(D/TW) ×100] [30]. Incidence of decay was determined at the end of simulated storage and transportation.

2.7. Statistical Analysis

SPSS for Windows version 20 (SPSS Inc., Chicago, IL, USA) was used for the statistical analysis. Data analysis for the estimated respiration rate with three replicates, averaged pulp temperature in heatmap chart with four replicates as well as material properties, mass loss, and incidence of decay with five replicates compared by mean at a significant level of 0.05 using Tukey's HSD post hoc test.

3. Results and Discussion

3.1. Materials Properties

The properties of the thermal insulation materials, including thickness, thermal heat energy, WVP, air permeability, and R-value, are shown in Table 2. Temperature transfer through the material was studied in terms of the heat transfer processes. Heat transfer is the process of energy movement caused by temperature differences [20]. Lower thermal heat energy (Q_x) value shows a lower heat transfer rate (good insulator) through the substance layer, while higher Q_x shows a higher heat transfer rate (poor insulator) through the layer [21]. In this study, results indicated that MFS with a thickness of 3.1 mm gave the lowest heat transfer property (Q_x = 1.53 J s^{-1}), compared to the other three materials, while P-LLDPE (0.120 mm) had the highest Q_x value (3.85 J s^{-1}). A combination of HRS (1.450 mm) (2.57 J s^{-1}) and TNNW (0.270 mm) (3.23 J s^{-1}) showed improved insulation property and potential for prototype development for covering material in the future. The high insulation properties of MFS and HRS materials may be partly due to greater thickness. Material with lower thermal heat energy (Q_x) also tends to have a higher R-value. MFS had the highest R-value (0.225 m^2 °C W^{-1}), followed by HRS (0.211 m^2 °C W^{-1}), TNNW (0.187 m^2 °C W^{-1}), and P-LLDPE (0.153 m^2 °C W^{-1}), respectively (Table 2). Results showed that MFS and HRS preserved cool temperatures better than the other materials (Figure 3).

Table 2. Covering material properties (thickness, thermal heat energy, WVP, R-value and air permeability).

Material	Thickness (mm)	Thermal Heat Energy ($Q_x \times 10^{-4}$) (J s^{-1})	R-Value (m^2 °C W^{-1})	Water Vapor Permeability (g h^{-1} m^{-2})	Air Permeability (l m^{-2} s^{-1})
P-LLDPE	0.120 ± 0.03 [d]	3.85 ± 0.06 [a]	0.153 ± 0.01 [d]	0.325 ± 0.04 [a]	172.80 ± 12.05 [b]
TNNW	0.270 ± 0.20 [c]	3.23 ± 0.07 [b]	0.187 ± 0.01 [c]	0.450 ± 0.05 [a]	945.60 ± 43.21 [a]
HRS	1.450 ± 0.43 [b]	2.57 ± 0.12 [c]	0.211 ± 0.02 [b]	0.000003 ± 0.00 [b]	0.59 ± 0.01 [d]
MFS	3.100 ± 0.08 [a]	1.53 ± 0.06 [d]	0.225 ± 0.01 [a]	0.000012 ± 0.00 [b]	49.42 ± 0.21 [c]

Note: Different letters for different mean levels in each parameter for Tukey's HSD post hoc test indicate significant differences at *p* < 0.05. Values are mean ± S.E. from five replicates. Four materials were perforated linear low-density polyethylene (P-LLDPE), heat-reflective sheet (HRS), thin nonwoven (TNNW), and metalized foam sheet (MFS).
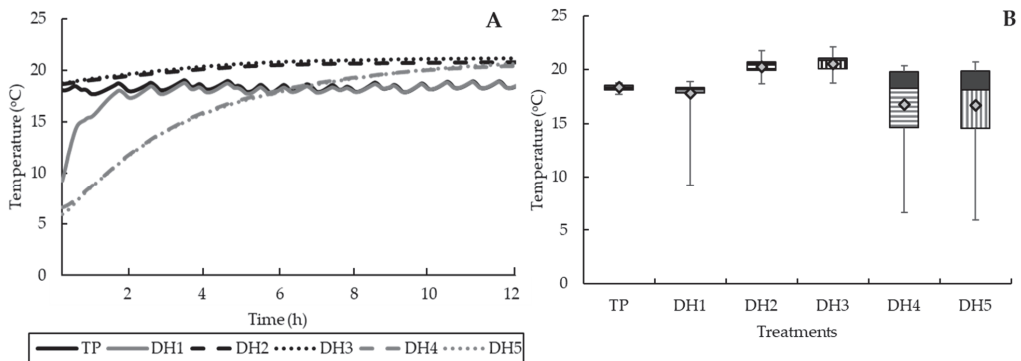
Figure 3. Pulp temperature profiles during simulated storage at 18 °C for 12 h (**A**) and boxplot of pulp temperature profiles during simulated storage at 18 °C for 12 h (**B**). Boxes indicate the lower and upper quartile. The horizontal line in each box represents the median temperature. Mean temperature for each treatment is indicated by ♦. Vertical lines extending above and below each box represent minimum and maximum temperature recorded. Six treatments were no room cooling with P-LLDPE covering (TP as control), room cooling with P-LLDPE covering (DH1), no room cooling with HRS+TNNW covering (DH2), no room cooling with MFS covering (DH3), room cooling with HRS+TNNW covering (DH4), room cooling with MFS covering (DH5).

For water vapor permeability (WVP), a partial pressure difference between the inside and outside of the test material affects the gain or loss of moisture in the product [31]. In this study, TNNW and P-LLDPE showed higher WVP than MFS and HRS, and would be suitable for highly breathable fruits (Table 2). High WVP material had the potential to eliminate vapor condensation, thus inhibiting microbial activity [31]. On the other hand, both MFS and HRS materials had lower WVP values and air permeability, which may cause vapor condensation inside the covering (Table 2). Interestingly, a combination of HRS and TNNW showed good performance in terms of insulation and water and air permeability properties, with the potential to maintain cool temperatures and protect condensation inside the package or cover.

3.2. Respiration Rate, Q_{10} Value, and Heat from Respiration Rate

An increase in storage temperature and time resulted in a rise in okra respiration rate. Respiration rate at three storage conditions (10, 20, 30 °C) for 2 days increased gradually from 186.39 (10 °C) to 355.44 (30 °C) mg CO_2 kg^{-1} h^{-1} as well as on day 3 (Table 3). Similarly, Hardenburg et al. [7] reported that higher storage temperature at 25–27 °C (328–362 mg CO_2 kg^{-1} h^{-1}) increased respiration rate compared to lower temperatures at 5 °C (59 mg CO_2 kg^{-1} h^{-1}) and 10 °C (86 to 95 mg CO_2 kg^{-1} h^{-1}). Furthermore, the widely used Q_{10} value represents an improvement in the rate of a process with a 10 °C increase in temperature [32]. In this study, the Q_{10} value of temperature range (10–20 °C) on days 2 and 3 increased from 1.17 to 1.87, while the Q_{10} value of temperature range (20–30 °C) decreased from 1.50 to 1.37 (Table 3). In lower temperature storage, Q_{10} value is typically less than 2.00 levels, whereas Q_{10} value gradually decreased in higher temperature conditions [33]. However, Q_{10} values of okra during different storage temperatures have never been reported. Yasunaga et al. [34] reported that Q_{10} value of cucumber at 10 to 20 °C was 4.37 and dramatically decreased to 1.89 with higher temperature storage at 20–30 °C. In this study, to estimate okra respiration rate under simulated storage (R_{C1}) and transportation (R_{C2}), the Q_{10} value was calculated for respiration rate in each cover treatment and converted to vital heat as shown in Tables 4 and 5, respectively.

Table 3. Rate of respiration of okra pods at different storage conditions (10, 20, 30 °C) for 2 and 3 days in a closed system.

Temperature (°C)	R_{CO2} (mg CO_2 kg^{-1} h^{-1})		Q_{10}	
	Day 2	Day 3	Day 2	Day 3
10	186.39	207.33		
			1.17	1.87
20	237.70	325.63		
			1.50	1.37
30	355.44	444.61		

Table 4. Estimated respiration rate (R_{C1}) and vital heat among the six treatments under simulated storage at 18 °C for 48 h.

Treatment	Rc_1 (mg CO_2 kg^{-1} h^{-1})	Vital Heat (J kg^{-1} h^{-1})
TP	329 ± 0.0 [a]	3522 ± 0.1 [a]
DH1	329 ± 0.0 [a]	3522 ± 0.1 [a]
DH2	330 ± 0.8 [a]	3529 ± 8.1 [a]
DH3	330 ± 0.9 [a]	3536 ± 9.3 [a]
DH4	214 ± 0.4 [b]	2288 ± 4.7 [b]
DH5	218 ± 1.9 [b]	2329 ± 20.1 [b]

Note: Different letters for different mean levels in each parameter for Tukey's HSD post hoc test indicate significant differences at $p < 0.05$. Values are mean ± S.E. from three replicates. Six treatments were no room cooling with P-LLDPE covering (TP as control), room cooling with P-LLDPE covering (DH1), no room cooling with HRS+TNNW covering (DH2), no room cooling with MFS covering (DH3), room cooling with HRS+TNNW covering (DH4), room cooling with MFS covering (DH5).

Table 5. Estimated respiration rate (R_{C2}) and vital heat among the six treatments under simulated transportation at 30 °C for 1 h (air temperature of TP at 25 °C) and 15 h (the end of simulated transportation).

Treatment	Rc_2 (mg CO_2 kg^{-1} h^{-1}) at 1 h	Vital Heat (J kg^{-1} h^{-1}) at 1 h	Rc_2 (mg CO_2 kg^{-1} h^{-1}) at 15 h	Vital Heat (J kg^{-1} h^{-1}) at 15 h
TP	541 ± 4.7 [a]	5791 ± 49.0 [a]	640 ± 0.3	6853 ± 3.1
DH1	549 ± 2.6 [a]	5873 ± 28.5 [a]	646 ± 0.6	6914 ± 6.3
DH2	486 ± 6.1 [b]	5202 ± 66.3 [bc]	633 ± 4.0	6774 ± 42.5
DH3	483 ± 4.7 [b]	5167 ± 49.7 [bc]	629 ± 8.2	6732 ± 87.4
DH4	506 ± 2.7 [b]	5413 ± 28.0 [b]	632 ± 3.2	6768 ± 34.3
DH5	481 ± 8.4 [b]	5148 ± 88.4 [c]	645 ± 3.8	6900 ± 40.9

Note: Different letters for different mean levels in each parameter for Tukey's HSD post hoc test indicate significant differences at $p < 0.05$. Values are mean ± S.E. from three replicates. Six treatments were no room cooling with P-LLDPE covering (TP as control), room cooling with P-LLDPE covering (DH1), no room cooling with HRS+TNNW covering (DH2), no room cooling with MFS covering (DH3), room cooling with HRS+TNNW covering (DH4), room cooling with MFS covering (DH5).

The efficiency of room cooling and thermal insulation materials under simulated storage and transportation conditions for respiration rate and heat from respiration (vital heat) was studied. Table 4 shows that respiration rates and vital heat levels in DH4 and DH5 were lower than in the other three treatments under simulated storage at 18 °C for 48 h. After room cooling at 0 °C for 2 h, the field heat and vital heat of okra were removed and reduced to around 20% of no room cooling before the cool storage condition. However, no difference was shown between no room cooling plus either P-LLDPE or insulated materials (HRS + TNNW, MFS), as well as room cooling with P-LLDPE. A decrease in vital heat in okra suggested that room cooling combined with insulated material cover should be employed. During simulated transportation at 30 °C for 1 h, the vital heat of DH2, DH3, and DH5 (5148–5202 J kg^{-1} h^{-1}) was lowest compared with TP and DH1, and DH4 treatments (5791–5873 J kg^{-1} h^{-1}). However, at a longer period of simulated transportation

for 15 h, vital heat levels in all DH treatments were similar to TP. The efficiency of thermal insulation materials reduced the vital heat loss for a short period of around an hour. Either room cooling or no room cooling with thermal insulation material covering reduced heat from respiration under heat stress conditions over a short period (Table 5).

3.3. Air and Pulp Temperature Levels of Okra

Room cooling and thermal insulation materials showed efficient cooling under simulated storage and transportation. After simulated storage at 18 °C for 12 h, okra pulp temperature profiles of room cooling treatments (DH1, DH4, and DH5) maintained cool temperature for around 10 h, better than no room cooling treatments (TP, DH2, and DH3). The use of two thermal insulation materials (HRS and MFS) combined with room cooling (DH4 and DH5) maintained cool temperatures, compared to no cover. In addition, the combination of room cooling and thermal insulation as a covering material effectively maintained cool temperature (Figure 3A). Temperature control of cover treatments was presented as a boxplot (Figure 3B) which showed the mean (rhombuses), lowest (lower error bars), and highest temperature (upper error bars) levels. Okra pulp temperature in DH4 and DH5 had the lowest mean temperature (17 °C) compared to the other four treatments (19 °C for TP and DH1; 20 °C for DH2 and DH3). The use of thermal insulation materials without room cooling (DH2 and DH3) gave the significantly highest pulp temperature (highest upper error bars) as well as the warmest level (highest lower error bars) after simulated storage at 18 °C for 48 h. This was presented as a narrow range of cool temperature levels (a smaller boxplot) compared with room cooling (DH4 and DH5) (a larger boxplot).

To simulate actual transportation for 15 h, we designed an experiment to analyze when the air temperature of TP reached a constant level at 25 °C. Thermal insulation materials maintained a cool temperature (average and minimum temperature levels) better, compared to either no covering or covering with P-LLDPE (TP and DH1). However, thermal insulation materials tended to build up pulp temperature (Figure 4C,D). The minimum air and pulp temperatures inside thermal insulation materials were the lowest. (Figure 4A,B). As no published reports were available concerning the effect of room cooling combined with thermal insulation covering under storage and transportation conditions on the quality of okra, the results of this study were compared to published data for other fresh fruits and vegetables. Bollen et al. [35] used low-temperature cooling in combination with pallet covers for asparagus. They found that the use of covering with insulation materials reduced heat generated by fresh produce with high respiratory rates inside the covering. Long-term covering was recognized as a problem due to heat accumulation, leading to a higher temperature than no cover. Other studies reported that thermal insulation covers showed better temperature preservation than no cover, and temperature changes occurred more slowly than with no cover in amaranth [18], strawberries [23], and chard, cucumber, and carrot [24]. However, in this study, both temperature profiles increased to 30 °C within 15 h (Figure 4B,D). Covering with thermal insulation materials maintained cool temperature (<25 °C) under a high-temperature environment for less than 6 h. Additionally, the pulp temperature levels after simulated storage and transportation are presented in the heatmap chart (Figure 5) as a matrix of red–blue color tones with average temperature in each hour for 12 h. At the simulated storage (Figure 5A), DH4 and DH5 had a significantly low average of pulp temperature (blue color tone), while DH2 and DH3 had a significantly high average of pulp temperature (light orange color tone) that related to the highest pulp temperature profiles (Figure 3A) and the smallest boxplot size with the lowest pulp temperature profiles when compared among the five treatments (Figure 3B). Moreover, the heatmap chart during simulated transportation (Figure 5B) showed that the use of thermal insulation materials (DH2, DH3, DH4, and DH5) caused a heat accumulation (light orange color tone) within an hour, then there was no significant difference among all treatments after an hour. The combination of room cooling and thermal insulation materials (DH4 and

DH5) increased the efficiency of maintaining cool temperature more than using thermal insulation materials without room cooling (DH2 and DH3).
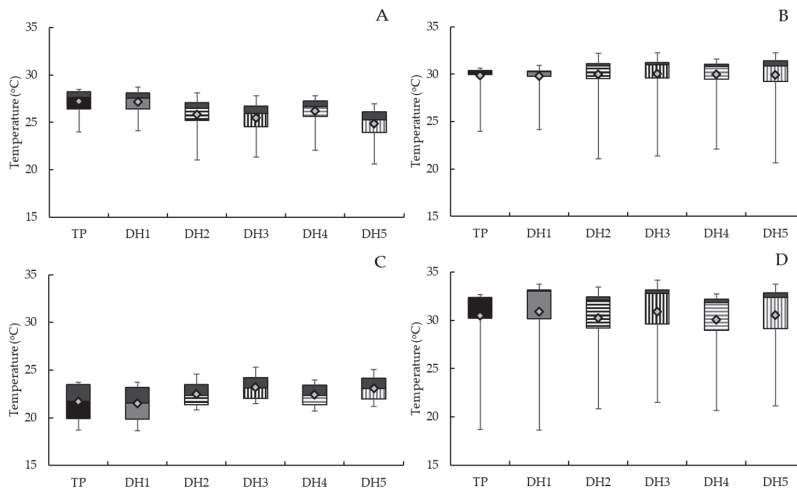

Figure 4. Air temperature profile after 1 h 30 min (**A**) and 15 h (**B**), pulp temperature profile after 1 h 30 min (**C**) and 15 h (**D**) during simulated transportation at 30 °C. An interpretation of the box plot graph is presented as a caption in Figure 3. Six treatments were no room cooling with P-LLDPE covering (TP as control), room cooling with P-LLDPE covering (DH1), no room cooling with HRS+TNNW covering (DH2), no room cooling with MFS covering (DH3), room cooling with HRS+TNNW covering (DH4), room cooling with MFS covering (DH5).

A

Time (h)	TP	DH1	DH2	DH3	DH4	DH5
12	18.5 d	18.5 d	20.8 ab	21.2 a	20.4 c	20.6 bc
11	18.6 c	18.6 c	20.8 a	21.1 a	20.2 b	20.3 b
10	18.3 c	18.2 c	20.8 a	21.1 a	20.0 b	20.0 b
9	18.4 c	18.4 c	20.7 a	21.1 a	19.6 b	19.6 b
8	18.2 c	18.1 c	20.7 a	21.0 a	19.2 b	19.1 b
7	18.2 bc	18.1 c	20.6 a	20.9 a	18.6 b	18.5 bc
6	18.2 b	18.0 bc	20.5 a	20.8 a	17.9 bc	17.7 c
5	18.4 b	18.2 b	20.3 a	20.6 a	16.9 c	16.8 c
4	18.5 b	18.3 b	20.1 a	20.3 a	15.5 c	15.4 c
3	18.4 b	18.0 b	19.8 a	19.9 a	13.6 c	13.6 c
2	18.2 b	17.4 b	19.4 a	19.5 a	11.0 c	10.9 c
1	18.1 a	14.1 b	19.0 a	19.0 a	7.9 c	7.7 c
0	18.1 a	9.3 b	18.7 a	18.8 a	6.6 c	6.0 c

Treatments

B

Time (h)	TP	DH1	DH2	DH3	DH4	DH5
12	32.4 a	33.1 a	32.4 a	33.1 a	32.2 a	32.9 a
11	32.4 a	33.2 a	32.4 a	33.1 a	32.2 a	32.9 a
10	32.5 a	33.2 a	32.4 a	33.1 a	32.2 a	32.8 a
9	32.4 a	33.2 a	32.3 a	33.0 a	32.1 a	32.7 a
8	32.3 a	33.0 a	32.1 a	32.8 a	31.9 a	32.4 a
7	32.2 a	32.9 a	31.8 a	32.5 a	31.6 a	32.0 a
6	31.9 ab	32.4 a	31.2 ab	31.8 ab	31.0 b	31.2 ab
5	31.1 ab	31.4 a	30.3 ab	30.8 ab	30.1 b	30.2 ab
4	30.0 a	29.9 a	29.0 ab	29.4 ab	28.8 b	29.0 ab
3	28.1 a	27.7 ab	27.1 ab	27.6 ab	26.9 b	27.3 ab
2	24.9 a	24.6 a	24.6 a	25.3 a	24.5 a	25.1 a
1	20.5 b	20.4 b	21.7 a	22.4 a	21.7 a	22.4 a
0	18.7 c	18.6 c	20.8 ab	21.5 a	20.7 b	21.1 ab

Treatments

Figure 5. Heatmap chart of pulp temperature profiles during simulated storage at 18 °C for 12 h (**A**) and simulated transportation at 30 °C for 12 h (**B**). Different letters in each row indicate significant differences of mean temperature from four replicates for pulp temperature in each hour at $p < 0.05$. Six treatments were no room cooling with P-LLDPE covering (TP as control), room cooling with P-LLDPE covering (DH1), no room cooling with HRS+TNNW covering (DH2), no room cooling with MFS covering (DH3), room cooling with HRS+TNNW covering (DH4), room cooling with MFS covering (DH5).
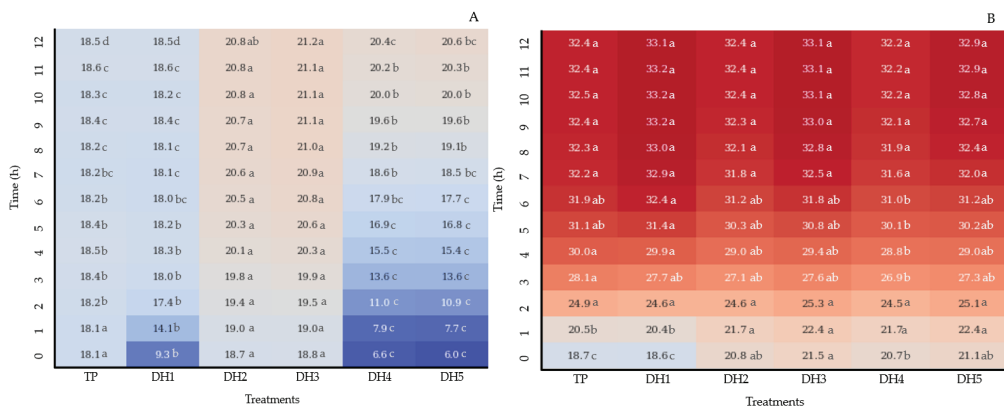
Table 6 compares the air temperature change rate inside the covering under simulated transportation testing. TP and DH1 showed the lowest rates of temperature change, whereas no cover in TP and DH1 treatments showed reduced control of cool temperature due to either high air ventilation through the plastic basket or no thermal insulation covering, respectively, indicating the highest thermal heat energy (Q_x) and lowest R-value of

P-LLPPE (Table 2). P-LLDPE gave poor preservation of cool temperature during simulation compared with the other materials. By contrast, low pulp temperature change rate showed high effectiveness of thermal insulation materials (TNNW, HRS, and MFS) for DH2 to DH5 by maintaining cool pulp temperature (Table 6). In previous studies, cardboard in combination with plastic foil of bottle beer gave control cold temperature than hard plastic crate under air temperature condition at 30 °C due to a reduction of the air movement and transferring contribution of the beer bottle as well as a reduction of vibration damping during transportation [36]. The efficiency of a base material nonwoven fabric on temperature-controlled deliveries was studied by Dieckmann et al. [37]. Nonwoven feather fiber composite isolation gave greater material performance aspects than EPS in terms of thermal insulation, and inexpensive, sustainable, and lightweight material. In this study, HRS and MFS-based aluminum foil material and nonwoven performed good thermal insulation. However, the browning incidence of okra pods also caused vibration damage during handling and transportation. Interestingly, further research should be conducted to investigate the combined effects of thermal insulation materials on cold temperature control and vibration damage reduction during transportation.

Table 6. Rate of changes in air and pulp temperature under simulated transportation at 30 °C for 15 h.

Treatment	Rate of Temperature Changes ($^\circ$Ch^{-1})			
	Air Temperature		Pulp Temperature	
	T_1–25 $^\circ$C	25–30 $^\circ$C	T_1–25 $^\circ$C	25–30 $^\circ$C
TP	7.54 ± 0.17 [b]	1.40 ± 0.02 [a]	4.26 ± 0.20 [a]	2.64 ± 0.15 [a]
DH1	7.34 ± 0.21 [b]	1.40 ± 0.01 [a]	4.00 ± 0.11 [a]	2.58 ± 0.02 [ab]
DH2	9.56 ± 0.47 [ab]	1.13 ± 0.04 [b]	2.55 ± 0.08 [b]	2.02 ± 0.05 [bc]
DH3	10.30 ± 1.41 [ab]	1.32 ± 0.05 [a]	2.50 ± 0.08 [b]	1.88 ± 0.15 [c]
DH4	11.69 ± 0.47 [a]	1.14 ± 0.03 [b]	2.59 ± 0.10 [b]	1.83 ± 0.08 [c]
DH5	9.25 ± 0.45 [ab]	1.08 ± 0.04 [b]	2.75 ± 0.18 [b]	1.75 ± 0.15 [c]

Note: T_1 is the temperature at the end of the simulated storage. Different letters in different mean levels of each parameter for Tukey's HSD post hoc test indicate significant differences at $p < 0.05$. Values are mean ± S.E. from five replicates. Six treatments were no room cooling with P-LLDPE covering (TP as control), room cooling with P-LLDPE covering (DH1), no room cooling with HRS+TNNW covering (DH2), no room cooling with MFS covering (DH3), room cooling with HRS+TNNW covering (DH4), room cooling with MFS covering (DH5).

3.4. Relative Humidity inside Covering Materials

Relative humidity was monitored during simulated storage and transportation. Relative humidity of TP and DH1 as no covering (75%) (Figure 6A) was lower than all the other thermal insulation materials (100% RH) (Figure 6B,C) after storage for 48 h. This showed that the use of thermal insulation materials for covering preserved relative humidity fluctuation inside the covering was better than without covering (Figure 6B,C). Low relative humidity in TP and DH1 increased mass loss (>15%), while thermal insulation covers with 100%RH reduced mass loss (5%) throughout this simulation (Figure 7). The effect of relative humidity (RH) on the quality of 'Niitaka' pears was studied by Lim et al. [38] using two types of pallet covers made of polyethylene film to maintain high RH in commercial low-temperature storage rooms. Use of pallet covers increased RH from 83 to 87% or 93 to 95% for open and closed pallet covers, respectively. Moreover, using insulated material for covering preserved the relative humidity inside the covering and was better than no covering during shipping delays in amaranth [18]. Covering with thermal insulation materials maintained the highest RH level (100% RH) after 12 h, particularly HRS and MFS (Figure 6). This result related to the lowest WVP level of HRS and MFS materials, which preserved the relative humidity inside the covering (Table 2). On the other hand, low WVP of MFS caused condensation inside the covering and accelerated the activity of microorganisms with an increase of decay incidence (Figure 8).
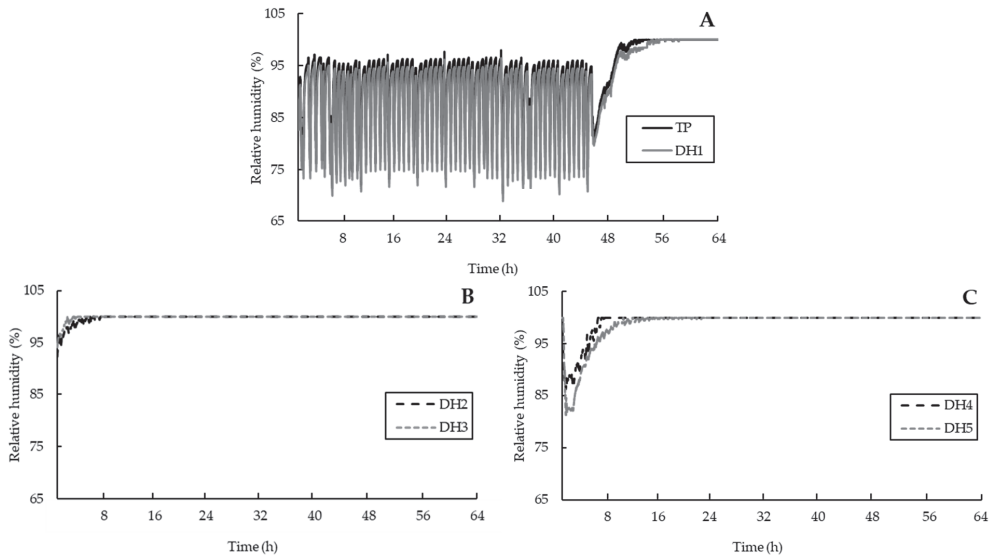
Figure 6. Relative humidity profiles among treatments, including TP and DH1 (**A**), DH2 and DH3 (**B**), DH4 and DH5 (**C**), after simulated storage at 18 °C for 48 h and simulated transportation at 30 °C for 15 h. Six treatments were no room cooling with P-LLDPE covering (TP as control), room cooling with P-LLDPE covering (DH1), no room cooling with HRS+TNNW covering (DH2), no room cooling with MFS covering (DH3), room cooling with HRS+TNNW covering (DH4), room cooling with MFS covering (DH5).

Figure 7. Mass loss (%) among the six treatments after simulated storage at 18 °C for 48 h and simulated transportation at 30 °C for 15 h. Different letters in different mean levels of each parameter for Tukey's HSD post hoc test indicate significant differences at $p < 0.05$. Values are mean ± S.E. from five replicates. Six treatments were no room cooling with P-LLDPE covering (TP as control), room cooling with P-LLDPE covering (DH1), no room cooling with HRS+TNNW covering (DH2), no room cooling with MFS covering (DH3), room cooling with HRS+TNNW covering (DH4), room cooling with MFS covering (DH5).
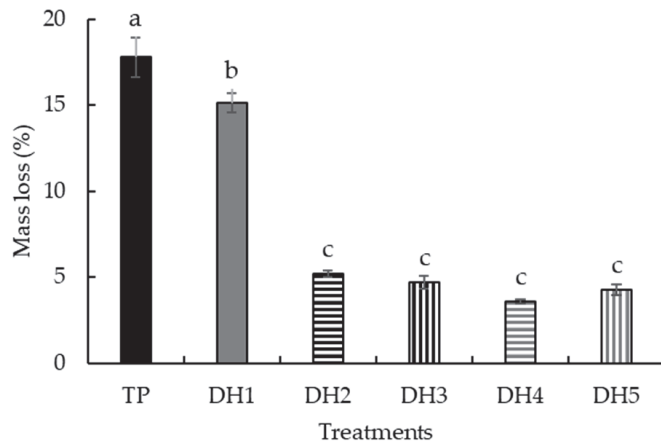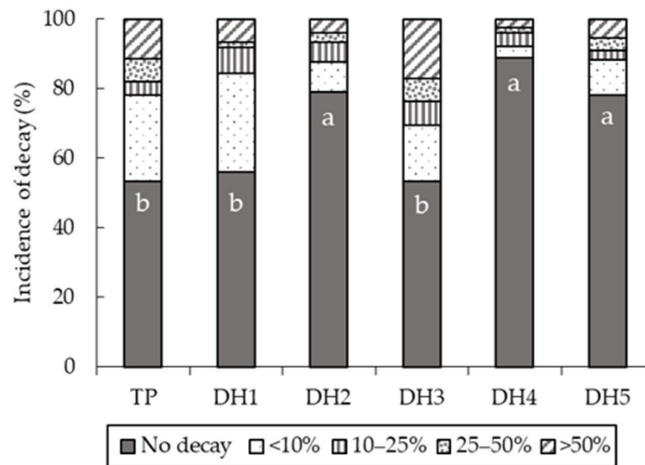
Figure 8. Incidence of decay (%) among the six okra treatments after simulated storage at 18 °C for 48 h and simulated transportation at 30 °C for 15 h. Different letters in different mean levels of each parameter for Tukey's HSD post hoc test indicate significant differences at *p* < 0.05. Values are mean ± S.E. from five replicates. Six treatments were no room cooling with P-LLDPE covering (TP as control), room cooling with P-LLDPE covering (DH1), no room cooling with HRS+TNNW covering (DH2), no room cooling with MFS covering (DH3), room cooling with HRS+TNNW covering (DH4), room cooling with MFS covering (DH5).

3.5. Mass Loss of Okra

Okra pods in TP and DH1 (no cover and P-LLDPE covering) lost a significant amount of fresh weight (around 15%) compared to thermal insulation material treatments (5%) (Figure 7). This corresponded to better performance in maintaining lower temperature and higher relative humidity by thermal insulation materials (Figures 3 and 6). There was no significant difference between room cooling or no cooling combined with thermal insulation materials (Figure 7). However, limited data exist comparing the efficiency of thermal insulation covering on mass loss of fresh produce. Wheeler et al. [18] reported that amaranth contained in uncovered pallets had more weight (11.0%) than in pellets covered with Reflectix[TM] insulation material (2.0%) (bubble pack insulation consisted of reflective aluminum foil and heavy gauge polyethylene) over a 6 h storage cycle. Reflectix[TM] cover effectively minimized the amount of moisture loss during amaranth storage. Macnish et al. [39] compared the performance of four propriety pallet cover systems (CO_2 West, PEAKfresh, PrimePro, and Tectrol) in maintaining the quality of strawberry fruit during transportation with a temperature at 20 °C. Results showed that pallet cover systems significantly reduced transport-related mass loss by less than 0.5%, compared to those with control or no cover material (0.8%). Similarly, Lim et al. [38] found that the use of pallet cover in pear storage for 7 days reduced mass loss compared to no pallet cover. The application of pallet cover is an alternative technique for controlling temperature and humidity fluctuation during transportation [40] as well as reducing the rate of mass loss [41]. In this study, low mass loss of okra in thermal insulation covers after simulation (Figure 7) was related to low levels of WVP (Table 2).

3.6. Incidence of Decay (ID)

Highly significant decay of okra at 50–80% was presented in no room cooling plus covering with either thermal insulation material or P-LLDPE. The okra pods turned black with mold infection. The DH4 and DH5 treatments had the lowest percentage of ID (<20%) compared to the other four treatments (Figures 8 and 9). Thermal insulation materials maintained cool temperature and relative humidity (Figures 3 and 6). This was related

to a lower incidence of decay (Figure 8) and mass loss (Figure 7). Increasing efficiency of thermal insulation covers suggested application with room cooling to maintain a cool temperature under heat stress conditions. However, the application of MFS covering should be considered in case of a high-temperature condition (30 °C) over 15 h, which may lead to heat accumulation (Figure 4). Vapor condensation resulted in an increase of okra decay (Figure 8) due to low WVP (Table 2). Thermal insulation covers may be applied for a short journey (<6 h) for domestic transportation under ambient temperature (no refrigerated vehicle) to maintain cool temperature with less decay. HRS+TNNW covering with cooling technique showed high potential application for fresh produce with high respiration rates, such as asparagus, broccoli, mushroom, and sweet corn [29]. The overall post-harvest loss from mass loss and incidence of decay showed that TP was the highest post-harvest loss (65%), followed by DH1 (59%), DH3 (52%), DH5 (27%), DH2 (26%), and DH4 (15%), respectively (Figures 7 and 8).

Figure 9. Okra pictures from the six treatments including TP (**A**), DH1 (**B**), DH2 (**C**), DH3 (**D**), DH4 (**E**), and DH5 (**F**) after simulated storage at 18 °C for 48 h and simulated transportation at 30 °C for 15 h. Six treatments were no room cooling with P-LLDPE covering (TP as control), room cooling with P-LLDPE covering (DH1), no room cooling with HRS+TNNW covering (DH2), no room cooling with MFS covering (DH3), room cooling with HRS+TNNW covering (DH4), room cooling with MFS covering (DH5).

4. Conclusions

Room cooling with TNNW provided greater efficiency to preserve a cool temperature (2 °C) and reduce the decay of okra (10%), compared to TP (42%) and no room cooling plus MFS (48%) after simulated cool storage and high-temperature transportation conditions. Application of thermal insulation materials for covering reduced mass loss (5%), compared to either no cover or P-LLDPE throughout the simulation test (15–17%). Thus, the room cooling combined with HRS+TNNW (DH4) gave the lowest post-harvest loss (15%) as compared to TP, cooling plus P-LLDPE (DH1), and no cooling plus MFS (DH3) in a range of post-harvest loss (52% to 65%). Results showed that cooling was a very important step to apply in the post-harvest handling of okra before covering to remove both field heat and respiratory heat. Material properties, including low thermal heat energy (Q_x) level and high R-value and WVP value, should be considered for developing thermal insulation material for fresh produce. Future research should be conducted to assess the effect of room cooling and thermal insulation material for other fresh fruits and vegetables, particularly the high respiration rate group.

Author Contributions: J.R. conducted experiments, analyzed data, interpreted results, and assisted manuscript writing. R.S. co-investigated, interpreted results, and assisteddata analysis. C.P. co-investigated, supported cover materials, interpreted results in material analysis, and assisted manuscript writing. H.K. provided comments and suggestions for the final draft of the manuscript. S.C. was the principal investigator of the research, responsible for the overall research management,

interpretation of results, and manuscript writing. All authors have read and agreed to the published version of the manuscript.

References

1. Tripathi, K.K.; Govila, O.P.; Warrier, R.; Ahuja, V. Biology of *Abelmoschus esculentus* L. (Okra). In *Series of Crop Specific Biology Documents*; Department of Biotechnology, Ministry of Science & Technology & Ministry of Environment and Forest, Govt. of India: New Delhi, India, 2011; 26p.
2. Thai Customs. Statistic Report 2020. 2020. Available online: http://www.customs.go.th/statistic_report.php?lang=en&tariff_code=07099990003 (accessed on 14 August 2020).
3. Tsado, E.K. Quality of postharvest handling of marketable okra fruits sold in Minna, Niger State, Nigeria. *Eur. J. Agric. For. Res.* **2015**, *3*, 33–45.
4. Okra: Postharvest Care and Market Preparation; Publications in the Postharvest Handling Technical Bulletin Series No.10. 2003. Available online: http://agriculture.gov.gy/wp-content/uploads/2016/01/Okra.pdf (accessed on 10 November 2020).
5. Perkins-Veazie, P.; Collins, J.K. Cultivar, packing and storage temperature differences in postharvest shelf life of okra. *HortTechnogy* **1992**, *2*, 350–352. [CrossRef]
6. Taain, D.A.; Jasim, A.M.; Al-Hij, M.J.H.H. A study of storage behavior of okra fruits (*Abelmoschus esculuntus* L. Moenth cv. Khnesri). *Int. J. Farming Allied Sci.* **2014**, *3*, 760–766.
7. Okra: The Commercial Storage of Fruits. Vegetables and Florist and Nursery Stocks. USDA-ARS Agriculture Handbook #66 (Revised). 2016. Available online: https://www.ars.usda.gov/arsuserfiles/oc/np/commercialstorage/commercialstorage.pdf (accessed on 10 November 2020).
8. Cheng, Z.; Gong, X.; Jing, W.; Peng, Z.; Li, J. Quality change of postharvest okra at different storage temperatures. *J. Food Eng. Technol.* **2018**, *7*, 43.
9. Kader, A.A. *Postharvest Technology of Horticultural Crops*, 3rd ed.; University of California Agriculture and Natural Resources: Davis, CA, USA, 2002; pp. 39–47.
10. Huang, S.; Li, T.; Jiang, G.; Xie, W.; Chang, S.; Jiang, Y.; Duan, X. 1-Methylcyclopropene reduces chilling injury of harvested okra (*Hibiscus esculentus* L.) pods. *Sci. Hortic.* **2012**, *141*, 42–46. [CrossRef]
11. Saltviet, M.E. Measuring Respiration. 2015. Available online: http://ucce.ucdavis.edu/files/datastore/234-20.pdf (accessed on 10 June 2020).
12. Kienholz, J.; Edeogu, I. *Fresh Fruit and Vegetable Pre-Cooling for Market Gardeners in Alberta*; Alberta Agriculture, Food and Rural Development: Edmonton, AB, Canada, 2002; pp. 1–4.
13. Food and Agriculture Organization of the United Nations (FAO). *Good Practice in the Design Management and Operation of a Fresh Produce Packing-House*; FAO Region Office for Asia and the Pacific: Bangkok, Thailand, 2012; pp. 44–47.
14. Dhall, R.K.; Sharma, S.R.; Mahajan, B.V.C. Development of post-harvest protocol of okra for export marketing. *J. Food Sci. Technol.* **2014**, *51*, 1622–1625. [CrossRef] [PubMed]
15. Yang, Z.; Ma, Z.; Zhao, C.; Chen, Y. Study on forced-air pre-cooling of Longan. In *2007 ASAE Annual Meeting 076267, Minneapolis, MN, 17–20 June 2007*; American Society of Agricultural and Biological Engineers: St. Joseph, MI, USA, 2007.
16. Wang, Z.; Chen, L.; Yang, H.; Wang, A. Effect of exogenous glycine betaine on qualities of button mushrooms (*Agaricus bisporus*) during postharvest storage. *Eur. Food Res. Technol.* **2015**, *240*, 41–48. [CrossRef]
17. Deshmukh, G.; Birwal, P.; Datir, R.; Patel, S. Thermal insulation materials: A tool for energy conservation. *J. Food Process Technol.* **2017**, *8*, 670. [CrossRef]
18. Wheeler, L.; Kitinoja, L.; Barrett, D. Use of insulated covers over product crates to reduce losses in amaranth during shipping delays. *Agriculture* **2015**, *5*, 1204–1223. [CrossRef]
19. Singh, S.P.; Burgess, G.; Singh, J. Performance comparison of thermal insulated packaging boxes, bags and refrigerants for single-parcel shipments. *Packag. Technol. Sci.* **2008**, *21*, 25–35. [CrossRef]
20. Harding, K.G. *Heat Transfer Introduction*; University of the Witwatersrand: Johannesburg, South Africa, 2018; pp. 1–62.

21. Harvey, B.V. Mild Chilling Injury of Banana (Cavendish cv. *Williams*) and Its Control in the Field. Ph.D. Thesis, The University of Adelaide, Adelaide, Australia, September 2005.

22. Desjarlais, A.O.; Zarr, R.R. (Eds.) *Insulation Materials, Testing and Applications, 4th Volume (Vol. 1426)*; ASTM International: West Conshohocken, PA, USA, 2002; 417p.

23. Chaiwong, S.; Bishop, C.F.H. Use of an insulated bag from the supermarket to maintain 'Elsanta' strawberry temperature to households. *Acta Hortic.* **2014**, *1079*, 187–192. [CrossRef]

24. Melis, R.B. New Techniques and Methods for Cold Chain Monitoring and Tracking in Perishable Products. Ph.D. Thesis, Universidad Politécnica de Madrid, Madrid, Spain, 2016; pp. 134–146.

25. Liu, Y.B. Low-temperature phosphine fumigation of chilled lettuce under insulated cover for postharvest control of western flower thrips, *Frankliniella occidentalis* (Pergande) (*Thysanoptera: Thripidae*). *J. Asia Pac. Entomol.* **2011**, *14*, 323–325. [CrossRef]

26. ASTM. *(96). Standard Test Methods for Water Vapor Transmission of Materials*; ASTM International: West Conshohocken, PA, USA, 2005.

27. ASTM. *Standard Test Method for Air Permeability of Textile Fabrics*; D737-96; ASTM International: West Conshohocken, PA, USA, 1996; pp. 230–234.

28. Kader, A.A.; Saltveit, M.E. Respiration and gas exchange. *Post. Physio. Patho. Veg.* **2003**, *2*, 7–29.

29. Patel, B.B.; Roy, F.S.; Saiyad, M.J.S.; Joshi, D.C. Respiration behaviour and heat of respiration of mango (cv. *Langdo*) under different storage conditions. *Int. J. Agric. Environ. Biotechnol.* **2016**, *9*, 855–859. [CrossRef]

30. Ngure, J.W.; Aguyoh, J.N.; Gaoquiong, L. Interactive effects of packaging and storage temperatures on the shelf-life of okra. *ARPN J. Agric. Biol. Sci.* **2009**, *4*, 43–52.

31. Mangaraj, S.; Goswami, T.K.; Panda, D.K. Modeling of gas transmission properties of polymeric films used for MA packaging of fruits. *J. Food Sci. Technol.* **2015**, *52*, 5456–5469. [CrossRef] [PubMed]

32. Tripathi, P.C.; Lawande, K.E. Temperature-related changes in respiration and Q_{10} coefficient in different varieties of onion. *Progress. Hortic.* **2010**, *42*, 88–90.

33. Murata, S.; Miyauchi, K.; Wang, Y. Measurement of respiration of fresh vegetables. *J. Jpn. Soc. Agric. Mach.* **1993**, *55*, 69–75.

34. Yasunaga, E.; Tomita, K.; Hamanaka, D.; Hu, W.; Uchino, T. Effect of temperature on the respiration rate of some vegetables. *IFAC Proc. Vol.* **2001**, *34*, 205–210.

35. Bollen, F.; Bycroft, B.L.; Brash, D.W. Using insulation and cooling to improve the asparagus cool chain. *Acta Hortic.* **1993**, *415*, 323–332.

36. Paternoster, A.; Van Camp, J.; Vanlanduit, S.; Weeren, A.; Springael, J.; Braet, J. The performance of beer packaging: Vibration damping and thermal insulation. *Food Packag. Shelf Life* **2017**, *11*, 91–97. [CrossRef]

37. Dieckmann, E.; Nagy, B.; Yiakoumetti, K.; Sheldrick, L.; Cheeseman, C. Thermal insulation packaging for cold-chain deliveries made from feathers. *Food Packag. Shelf Life* **2019**, *21*, 100360. [CrossRef]

38. Lim, B.S.; Lim, C.I.; Gross, K.C. High relative humidity under pallet coverage maintained 'Niitaka' pear fruit (*Pyruspyrifolia Nakai*) quality during low temperature storage. *Korean J. Hortic. Sci. Technol.* **2005**, *23*, 135–139.

39. Macnish, A.J.; Padda, M.S.; Pupin, F.; Tsouvaltzis, P.I.; Deltsidis, A.I.; Sims, C.A.; Brecht, J.K.; Mitcham, E.J. Comparison of pallet cover systems to maintain strawberry fruit quality during transport. *HortTechnology* **2012**, *22*, 493–501. [CrossRef]

40. Moureh, J.; Laguerre, O.; Flick, D.; Commere, B. Analysis of use of insulating pallet covers for shipping heat-sensitive foodstuffs in ambient conditions. *Comput. Electron. Agric.* **2002**, *34*, 89–109. [CrossRef]

41. Badia-Melis, R.; Mc Carthy, U.; Ruiz-Garcia, L.; Garcia-Hierro, J.; Villalba, J.R. New trends in cold chain monitoring applications-A review. *Food Control* **2018**, *86*, 170–182. [CrossRef]

Article

Enzymatic Browning in Banana Blossoms and Techniques for Its Reduction

Geerada Kaewjumpol [1], Surasak Srisamlee [1], Diane M. Beckles [2] and Kietsuda Luengwilai [1,3,*]

[1] Department of Horticulture, Faculty of Agriculture at Kamphaeng Saen, Kamphaeng Saen Campus, Kasetsart University, Nakhon Pathom 73140, Thailand; geerada20@gmail.com (G.K.); surasak.sri@ku.th (S.S.)

[2] Department of Plant Sciences, Mail Stop 3, University of California, Davis, CA 95616, USA; dmbeckles@ucdavis.edu

[3] Postharvest Technology Innovation Center, Ministry of Higher Education, Science, Research and Innovation, Bangkok 10400, Thailand

[*] Correspondence: kietsuda.l@ku.th

Abstract: Banana blossoms are rich in fiber and nutrients and are a popular plant-based, vegan alternative to fish. However undesirable browning, usually visible at the peduncle cut-end, negatively impacts consumer acceptability of banana blossoms. The aim of this work was to develop safe alternatives to prevent browning in banana blossoms. First, the activities of primary enzymes associated with tissue browning, i.e., polyphenol oxidase (PPO), peroxidase (POD) and phenylalanine ammonia lyase (PAL), were assayed. Our data showed that PPO and POD were the key enzymes responsible for blossom browning as they increased in activity, reaching a maximum at pH 7, as browning developed. In contrast, PAL activity decreased, and total phenolic content did not change as browning progressed, indicating PAL was not induced by cutting and may not be involved in blossom browning. Second, to find antibrowning agents for banana blossoms that can substitute for the use of sodium metabisulfite (SMS), different organic acids of varying concentrations were tested. Among organic acids studied, treatment with 3% (w/v) oxalic acid was the most effective method and thus could be a safe substitution for SMS to prevent browning in banana blossoms.

Keywords: banana buds; antibrowning techniques; PPO; POD; PAL

1. Introduction

Banana blossoms (widely known as flower buds) are purple-skinned bracts that develop at the end of the banana fruit cluster. In Southeast Asia, especially Sri Lanka, Malaysia, Indonesia and the Philippines, banana blossoms are a popular ingredient for cooking, and these tissues are rich in many beneficial nutrients, including fiber; protein; vitamins A, C and E; phosphorus; calcium; iron; magnesium; and antioxidants [1,2]. Banana blossoms are also used as a therapeutic agent to lower the risk of anemia [3], increase milk production of breastfeeding mothers [4] and ameliorate the effects of diabetes [5]. However, there is new interest in banana blossoms because they have a texture similar to cooked fish, and they are set to become widely used in vegan cooking [6]. The current price-point for banana blossoms is 14.00 USD per kilogram as a vegan food [6].

After cutting, an undesirable brown color develops at the cut-end surface of banana blossoms. This reduces the nutritional value of the product and is unacceptable to consumers [7–9]. Three key enzymes, polyphenol oxidase (PPO), peroxidase (POD) and phenylalanine ammonia lyase (PAL), are involved in the browning mechanism in plant tissues [10–13]. PPO (EC 1.10.3.1) is widely distributed in the cytoplasm, while its phenolic substrates are in the vacuoles [10]. When cellular organelles are damaged, e.g., when tissues are cut, PPO mixes with phenolic compounds, catalyzing the oxidation of monophenols into *o*-diphenols. A polymerization reaction then converts *o*-diphenols to quinones, which are the precursors to the visible brown pigment seen at the cut surface of

tissues [10]. POD (EC 1.11.1.7) is a heme-containing enzyme that catalyzes single-electron oxidation of phenolic compounds in the presence of hydrogen peroxide [10]. PAL (EC 4.3.1.5) is the key enzyme in the phenylpropanoid metabolism; it is activated by wounding which leads to the accumulation of phenolic compounds [10]. The relative contribution of these browning enzymes varies according to the species. For example, PAL is the major enzyme responsible for browning in cut lettuce [14], PPO and POD are both important in strawberry [15], and all three enzymes are responsible for browning in peach [16]. In banana, PPO was characterized [17]. However, the relative contribution of PPO, POD and PAL to the browning mechanism in banana blossoms is not known.

Vital factors that limit the rate of the browning reaction include the concentration of related enzymes and phenolic compounds, pH, temperature, and the availability of oxygen to the tissues. Tamarind juice and sodium metabisulfite (SMS) are commonly employed as antibrowning agents to suppress undesirable browning in fresh-cut banana blossoms [18]. However, tamarind juice availability is seasonal and hence unreliable [19] and is thus unsuitable for large-scale production. SMS, while effective, has been restricted for use on most fresh fruit and vegetables in many countries [20]. Therefore, alternative compounds efficient in preventing browning in banana blossoms are required.

Organic acids are considered safe and are widely used as postharvest antibrowning agents. Oxalic acid at 5% (w/v) reduced browning in longan fruit stored at 25 °C [21]. Citric acid at 3% (w/v) suppressed PPO, POD and PAL activities and delayed browning in longkong fruit [22]. Tartaric, citric and ascorbic acids at 3% (w/v) inhibited POD activity and reduced browning in minimally processed yacon tubers after dipping [23]. Malic acid at 1% (v/v) suppressed PPO and POD activities and reduced browning of banana skin [24]. Although it has been demonstrated that organic acid treatment significantly reduces browning in a variety of tissues, there are no reports about the use of organic acid treatment to minimize browning in banana blossoms. Here, mechanisms associated with enzymatic browning and the effects of organic acids as antibrowning agents of banana blossoms after cutting were investigated.

2. Materials and Methods

2.1. Chemicals

L-Ascorbic acid and sodium metabisulfite (SMS) were purchased from Ajax Finechem Pty Ltd. (Taren Point, NSW, Australia). Citric acid monohydrate, sodium dihydrogen phosphate monohydrate and disodium hydrogen phosphate dihydrate were purchased from Merck (Darmstadt, Germany). Oxalic acid, boric acid, sodium carbonate and sodium tetraborate were purchased from KemAus (Cherrybrook, NSW, Australia). Malic acid, tartaric acid, guaiacol, L-phenylalanine catechol, polyvinylpyrrolidone (PVP), gallic acid and 6-hydroxy-2,5,7,8-tetramethylchroman-2-carboxylic acid (Trolox) were purchased from Sigma-Aldrich (Shanghai, China). Bovine serum albumin (BSA) was purchased from Sigma-Aldrich (St. Louis, MO, USA), Folin–Ciocalteu phenol reagent was purchased from Merck (Darmstadt, Germany) and 2,2-diphenyl-l-picrylhydrazyl (DPPH) was purchased from Sigma-Aldrich (Steinheim, Germany). All chemicals were of analytical grade.

2.2. Banana Blossom Sampling and Postharvest Treatments

Banana blossoms (*Musa* ABB 'Kluai Namwa') were collected from the agricultural fields in Kamphaeng Saen district, Nakhon Pathom Province, Thailand. Blossoms were harvested using a fruit picker tool, transported to the laboratory within 5 h and sorted for uniform size (weight ~500 g). The purple-skinned bracts were removed, and only the white-skinned bracts remained. The peduncle of each banana blossom was recut and air-dried before being stored in polyethylene (PE) bags under partial vacuum. To determine the enzymatic browning that occurs in association with wounding and to exclude browning associated with chilling injury, banana blossoms were kept at ambient temperature and humidity (30 ± 5 °C, 72 ± 7% RH) for 0, 12 and 24 h to observe browning at the cut-end surface. All experiments were carried out with six replicates, and the whole

experiments were repeated three times. Similar results were observed; thus, the data from one experiment are presented.

2.3. Browning Score

Browning score evaluation was adapted from Lichanporn et al. [25] with some modification. Degree of browning was expressed as the average of six replicates, scored as a visual determination of the peduncle cut-end surface color, where 0 = completely white (no browning), 1 = light brown, 3 = brown and 5 = dark brown or black.

2.4. Color Assessment

Colors on cut-end surfaces were assessed using a Chroma Meter (CR-400, Konica Minolta, Tokyo, Japan) calibrated with a white porcelain reference plate. Color parameters were quantified using the CIE system where L* corresponds to lightness, a* corresponds to redness (+a*) or green (−a*) and b* corresponds to yellowness (+b*) or blue (−b*). A lower value of L* indicates darker brown color, while a higher value of +a* refers to increased red color [26]. Total color change (ΔE*) was computed by the formula $\Delta E^* = \sqrt{\Delta L^{*2} + \Delta a^{*2} + \Delta b^{*2}}$, where ΔL*, Δa* and Δb* represent differences in lightness, redness and yellowness, respectively, before and after the specified period of storage duration [27]. Differences in perceivable color were analytically classified as very distinct (ΔE > 3), distinct (1.5 < ΔE < 3) and small difference (1.5 < ΔE) [28].

2.5. Total Phenolic Compounds

Crude extracts were extracted from the peduncle cut-end of banana blossom and analyzed for phenolic content and DPPH scavenging activity. Banana blossom peduncles (24 g) were homogenized in 100 mL of 80% methanol (*v/v*) and centrifuged at 19,230× *g* at 4 °C for 10 min. The supernatant was collected and total phenolic content (TPC) was determined by the Folin–Ciocalteu method [29]. A mixture of 0.3 mL of crude extract and 2.25 mL of Folin–Ciocalteu phenol reagent (Folin:DI water; 1:10 *v/v*) was left for 5 min at 25 ± 3 °C. Then, 2.25 mL of 7% sodium carbonate was added to the mixture, which was vortexed and left in the dark at 25 ± 3 °C for 90 min. The reaction was then measured at 725 nm by a spectrophotometer. The standard curve was established by gallic acid equivalent (GAE) and expressed as μg GAE/g FW.

2.6. DPPH Radical Scavenging Assay

Radical scavenging activity of the banana blossom peduncle was determined by DPPH assay following the method of Havananda and Luengwilai [29]. A 0.1 mL aliquot of crude extract was mixed with 1.9 mL of 0.004% DPPH solution in methanol, and the mixture was incubated at 25 ± 3 °C under dark condition for 30 min. Absorbance was read at 515 nm. Percentage DPPH inhibition was calculated by Equation (1) [30].

$$\text{DPPH inhibition (\%)} = A_0 - A_1/A_0 \times 100 \qquad (1)$$

where A_0 is absorbance of the control (using methanol instead of crude extracts) and A_1 is absorbance of the reaction mixture.

2.7. Phenylalanine Ammonia Lyase (PAL) Activity Assay

PAL was extracted from the peduncle of banana blossom. One gram of the cut-end peduncle surface was extracted with 10 mL of 0.1 M borate–boric acid buffer (pH 8.8) solution containing 0.2 g of insoluble PVP and then homogenized for 1 min on ice using a Polytron PT2100 (Kinematica, Luzern, Switzerland). The homogenate was filtered through layers of cheesecloth before centrifugation at 12,000× *g* for 30 min at 4 °C (Model 6500, Kubota Corporation, Tokyo, Japan). The supernatant was collected for PAL activity assay, measured according to Faragher and Chalmers [31] with some modifications. The reaction mixture consisted of 0.1 M borate–boric acid buffer (pH 8.8, 2 mL), 60 mM

L-phenylalanine (0.7 mL) and PAL extract (0.3 mL). The mixture was incubated for 1 h at 30 °C, then the reaction was stopped with 5 N HCl (0.5 mL). During incubation, the reaction of transforming L-phenylalanine into trans-cinnamic acid was catalyzed by PAL activity and assayed by measuring the increase in trans-cinnamic acid at 280 nm using a UV-vis spectrophotometer (Thermo Spectronic, Rochester, NY, USA). The standard curve was created by L-phenylalanine, related to a rise in the amount of trans-cinnamic acid, with PAL activity recorded as mmol trans-cinnamic acid/h/mg protein.

2.8. Polyphenol Oxidase (PPO) and Peroxidase (POD) Activity Assays and Their Optimal pH Condition for Their Activities

A 2.5 g cut-end surface of banana peduncle was homogenized for 1 min at 4 °C in 0.1 M sodium phosphate buffer (pH 7.0, 5 mL) containing 0.2 g of an insoluble PVP. The homogenate was filtered through layers of cheesecloth before centrifugation at $12,000 \times g$ for 10 min at 4 °C. The supernatant was collected for PPO and POD assays following [32,33]. The reaction mixture of PPO activity consisted of 0.1 M sodium phosphate buffer (pH 7.0, 0.4 mL), 0.1 M catechol (0.5 mL) and PPO extract (0.1 mL). Absorbance was measured at 420 nm. The reaction mixture of POD activity contained 0.1 M sodium phosphate buffer (pH 7.0, 0.8 mL), 8 mM guaiacol (0.05 mL), POD extract (0.1 mL) and 24 mM hydrogen peroxide (H_2O_2, 0.05 mL). Absorbance was measured at 470 nm. PPO and POD specific enzyme activities were defined as increase in absorbance per min in 1 mg protein in enzyme of the reaction mixture (A420/min/mg protein for PPO activity and A470/min/mg protein for POD activity). Protein contents in PAL, PPO and POD extract solutions were analyzed using bovine serum albumin (BSA) as a standard [34].

To determine their optimal pH conditions for enzyme activities, PPO and POD activities were monitored at different pH values ranging from 1 to 7. All procedures followed those described above, except that the reaction buffer, i.e., 0.1 M sodium phosphate buffer (pH 7.0) was replaced by 0.1 M citric acid–0.15 M HCl (pH 1 and 2) or 0.3 M citrate–phosphate buffer (pH 3 to 7).

2.9. Inhibition of PPO and POD Activities Using Different Organic Acids as Inhibitors

The inhibitory effects of different organic acids on PPO and POD activities were tested. Tartaric (TA), citric (CA), malic (MA), oxalic (OA) and ascorbic (AA) acids at 1, 3 and 5% (*w/v*) dissolved in 0.1 M phosphate buffer (pH 7.0) were used. Crude enzymes were extracted following the same procedure described in Section 2.7. The PPO activity assay consisted of 0.1 mL crude enzyme extract, 0.1 mL of 0.1 M sodium phosphate buffer (pH 7.0), 0.5 mL of 0.1 M catechol and 0.3 mL of inhibitor (organic acid), while the POD activity assay employed 0.5 mL of 0.1 M sodium phosphate buffer (pH 7.0), 0.05 mL of 8 mM guaiacol, 0.3 mL of inhibitor, 0.05 mL of 24 mM H_2O_2 and 0.1 mL of crude enzyme extract. The positive control was the reaction mixture without inhibitor, while the negative control was the reaction mixture without crude extract. Percentage inhibitions of PPO and POD activities were calculated using Equation (2) [35].

$$\text{Inhibition of enzyme activity (\%)} = A_c - A_i / A_c \times 100 \qquad (2)$$

where A_c is initial PPO or POD activity (without inhibitor) and A_i is PPO or POD activity with inhibitor.

2.10. Antibrowning of Banana Blossoms by Different Organic Acids

The blossoms were harvested and prepared as described in Section 2.2. The peduncle of banana blossom was recut and dipped for 5 min in 5% (*w/v*) TA, 3% (*w/v*) OA or 3% (*w/v*) AA (the optimal concentrations were selected based on preliminary experiments). DI water was used as the negative control, and 1% (*w/v*) SMS and 2.5% (*w/v*) tamarind juice (TJ) were used as positive controls. Samples were dried with a paper towel before being packed into PE bags under partial vacuum and stored at 15 ± 2 °C and 90 ± 5% RH in the dark for 0, 5 and 10 days. These storage conditions, i.e., temperature, humidity, and

duration, were found to be optimal for banana blossom shelf-life based on preliminary testing. Cut-end surfaces of the peduncle were monitored for weight loss and color changes before (0 days) and after storage (5 and 10 days). All experiments were carried out in five replicates and the entire experiment was repeated three times. Similar results were observed; thus, the data from one experiment are presented.

2.11. Determination of Weight Loss Rate

The difference between tissue mass before and after storage, in relation to mass before storage, was calculated and expressed as a percentage of the initial fresh weight.

2.12. Statistical Analysis

All experiments were conducted using a completely randomized design (CRD) with six replicates, unless otherwise stated. Results were analyzed using the SPSS software program version 19 for Windows (SPSS Inc., IBM Company, Chicago, IL, USA). SPSS was used for analysis of variance (ANOVA) and to estimate significant differences between the means, using Tukey's multiple range test. Acceptable significant difference was set at $p < 0.05$. Correlations between enzyme activities, color parameters, phenolic contents and DPPH scavenging activities were also tested by Pearson's correlation coefficient using SPSS software. The principal component analysis (PCA) was analyzed using PAST4.0 software [36].

3. Results

3.1. Browning of Banana Blossom Cut-End Surfaces

Browning scores increased sharply from 1.2, when assayed at harvest, to 4.2, after 12 h storage at 30 °C. Color components (L*, a* and b*) measured by a colorimeter at the cut-end surfaces of the banana blossoms were also determined. At 12 h after harvest, the L* value significantly decreased from 77.5 to 55.7, while the a* value increased from −2.7 to 4.2 giving a total color change of ΔE* ~ 21. In contrast, b* value was not significantly changed during 24 h. In addition, browning and color components of the cut-end surface after 24 h were not significantly different from those at 12 h (Table 1).

3.2. Total Phenolic Content (TPC) and DPPH

At harvest, banana blossoms had a TPC of 46.5 μg GAE/g FW, and this amount did not change after 24 h (Figure 1A). The antioxidant activity of the banana blossoms was evaluated using the DPPH scavenging assay. Similar to TPC, antioxidant activity was not statistically different at 24 h after harvest. DPPH values ranged from 48.3 to 60.9% inhibition (Figure 1A).

3.3. PAL, PPO and POD Activities

The activities of PAL, PPO and POD in the banana blossoms were low after cutting. POD and PPO activities linearly increased from 1.25 to 6.14 and 0.5 to 1.8 unit/min/mg protein, respectively, 12 h after cutting, remaining high after storage for 24 h. In contrast, PAL activity linearly decreased after storage for 24 h from 1.7 to 1.2 mmol trans-cinnamic acid/h/mg protein (Figure 1B).

3.4. TPC, DPPH, PPO, POD and PAL Activities Related to Browning of Banana Blossoms after Cutting

Negative correlations were shown between L* (indicative of lightness) and PPO activity ($r = -0.957$) and between L* and POD activity ($r = -0.752$), while positive correlations were found between browning score and PPO activity ($r = 0.954$) and between browning score and POD activity ($r = 0.782$). In contrast, L* was positively correlated with PAL activity ($r = 0.828$), which was negatively correlated with browning score ($r = -0.840$). Phenolic content and DPPH scavenging activity were stable throughout the 24 h period

after cutting, with a weak relationship found between L* and the browning score, phenolic content and DPPH scavenging activity (*r* < 0.54) (Table 2).

Table 1. Browning of banana blossom cut-end surfaces after cutting. Lightness (L*), redness (a*), yellowness (b*), total color change (ΔE*) and browning score of the cut-end peduncle surface of banana blossoms stored at 30 °C for 0, 12 and 24 h.

Storage Time (h)		L*	a*	b*	ΔE*	Browning Score
0		75.5 ± 0.6 a	−2.7 ± 0.2 b	20.9 ± 1.7 NS	-	1.2 ± 0.4 b
12		55.7 ± 8.6 b	4.2 ± 3.2 a	22.9 ± 1.8 NS	21.2 ± 2.8 NS	4.2 ± 0.8 a
24		55.9 ± 10.1 b	4.8 ± 3.5 a	23.1 ± 1.1 NS	21.6 ± 3.2 NS	4.3 ± 0.6 a

Data are means ± SD (*n* = 6). Means followed by different letters in the same columns indicate significant differences (*p* < 0.05) between storage times. NS indicates nonsignificant differences (*p* ≥ 0.05) between storage times.
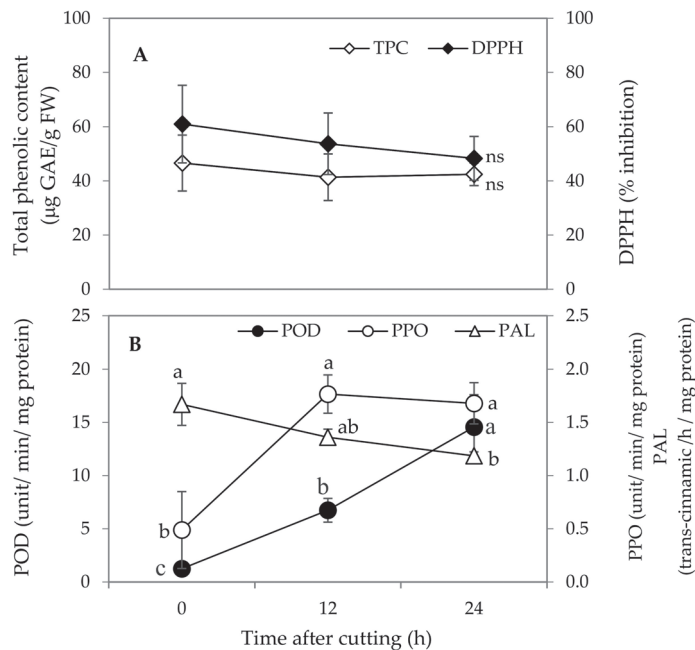
Figure 1. Substrates and enzyme activities associated with browning in cut banana blossom peduncles. Total phenolic content (TPC) and DPPH scavenging activity (**A**); activities of polyphenol oxidase (PPO), peroxidase (POD) and phenylalanine ammonia lyase (PAL) (**B**). Activity and content were assayed in banana blossoms stored at 30 °C for 0, 12 and 24 h. Data are shown as mean ± SD. Different letters (a–c) on the line graph of PPO, POD and PAL activities indicate significant differences (*p* < 0.05) between storage times. ns on the line graph of TPC and DPPH indicates nonsignificant differences (*p* ≥ 0.05) between storage times.

Table 2. Substrates and enzyme activities in relation to browning of banana blossoms after cutting. Pearson's correlation coefficients (*r*) between activities of polyphenol oxidase (PPO), peroxidase (POD) and phenylalanine ammonia lyase (PAL); browning scores; color parameters; phenolic content; and DPPH scavenging activity.

	PAL	**PPO**	**POD**	**L* Value**	**Browning Score**	**Phenolic Content**	**DPPH Assay**
PAL	1.000						
PPO	−0.829 **	1.000					
POD	−0.870 **	0.660	1.000				
L* value	0.826 **	−0.957 **	−0.752 *	1.000			
Browning score	−0.840 **	0.954 **	0.782 *	−0.977	1.000		
Phenolic content	0.430	−0.547	−0.187	0.317	−0.402	1.000	
DPPH assay	0.638	−0.590	−0.481	0.423	−0.532	0.923 **	1.000

* indicates a significant correlation at *p* < 0.05. ** indicates a significant correlation at *p* < 0.01.

3.5. Optimal pH for PPO and POD Activities

One important aim of this study, apart from identifying antibrowning agents, was to identify the pH optima of PPO and POD. The pH within plant cells and of all organic acids is naturally below 7. Therefore, pHs above pH 7 were not included in this study because they would not be physiologically relevant. By monitoring the PPO and POD activities at pH between 1 and 7, it was found that the optimal pH for PPO was 7, whereas a broad optimal pH range of 4–7 was found for POD. Rapid loss of PPO activity occurred below pH 7. PPO activity was relatively stable between pH 6 and pH 4 before decreasing to minimal activity below pH 3. For POD, the activity remained steady at pH 7–4 and then decreased to minimal activity below pH 2 (Figure 2).
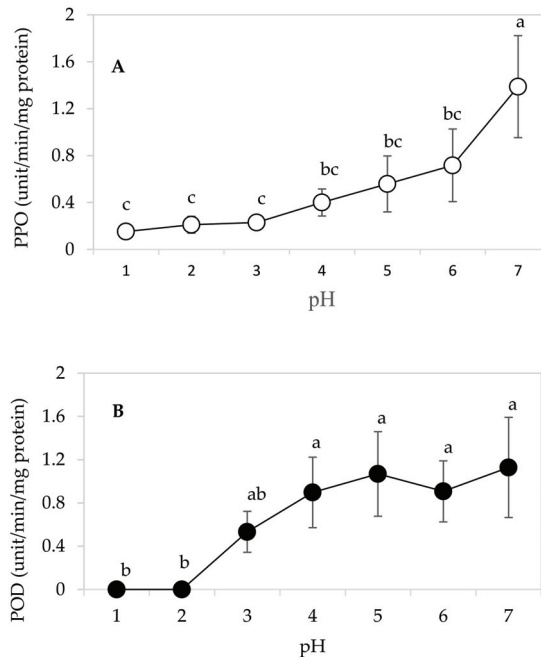
Figure 2. Optimal pH for polyphenol oxidase (PPO) and peroxidase (POD) activities. Activities of PPO (**A**) and POD (**B**) at different pH values. Enzymes were assayed at pH 1 and 2 using 0.1 M citric acid–0.15 M HCL and at pH 3 to 7 using 0.3 M using citrate–phosphate buffer. Data are mean ± SD (*n* = 3). Different letters (a–c) on the line graph of PPO and POD activities indicate significant differences (*p* < 0.05) between different pH conditions.

3.6. Effects of Organic Acids as Inhibitors on PPO and POD Activities of Banana Blossoms

Overall, most of the acid treatments reduced PPO activity by 75–90%, except for 1% citric acid and tartaric acid which led to merely 46% and 68% inhibition, respectively (Table 3). POD activity was 100% inhibited when 5% tartaric acid, 3–5% oxalic acid and ascorbic acid were used. Other acids, i.e., 3% tartaric acid, 5% malic acid and 5% citric acid, also effectively inhibited POD activity by 75–83%. Some acids, i.e., citric, malic, oxalic, and ascorbic acids at the lowest concentrations used, i.e., 1%, did not inhibit POD activity. All organic acids at 3–5% had pH lower than 4, except for 1% ascorbic acid with pH of 6. All organic acids, except for 1% ascorbic acid, inhibited PPO activity. Although control treatment (reaction buffer without organic acid agents) with a pH lower than 3 could inhibit PPO and POD activity by more than 50%, 3% citric acid and malic acid also had pHs lower than 3, but could inhibit POD activity to 0% and 36%, respectively (Table 3).

Table 3. Inhibition of PPO and POD activities using different organic acids as inhibitors. Percentage inhibition of PPO and POD activities by five organic acids of varying concentrations and their natural pH.

Organic Acid Agents	Organic Acid Concentration	pH	Inhibition of Enzyme Activity (%)	
			PPO	POD
Control [1]	0%	7.0 ± 0.0	0 ± 0 d	0 ± 0 d
		5.0 ± 0.0	39 ± 2 c	4 ± 7 d
		3.0 ± 0.0	82 ± 7 a	52 ± 7 bc
		1.0 ± 0.0	88 ± 3 a	100 ± 0 a
TA	1%	3.3 ± 0.4 b	68 ± 8 ab	25 ± 18 c
	3%	2.5 ± 0.3 c	86 ± 4 a	77 ± 9 b
	5%	1.7 ± 0.6 c	83 ± 3 a	99 ± 2 a
CA	1%	4.0 ± 0.0 b	46 ± 11 b	0 ± 0 d
	3%	2.8 ± 0.0 c	76 ± 8 a	0 ± 0 d
	5%	2.5 ± 0.0 c	83 ± 4 a	75 ± 6 b
MA	1%	3.6 ± 0.0 b	79 ± 11 a	0 ± 0 d
	3%	2.8 ± 0.0 c	79 ± 1 a	36 ± 7 c
	5%	2.5 ± 0.0 c	78 ± 3 a	83 ± 2 b
OA	1%	2.6 ± 0.0 c	74 ± 14 a	0 ± 0 d
	3%	0.9 ± 0.3 d	78 ± 10 a	100 ± 0 a
	5%	0.7 ± 0.1 d	90 ± 1 a	100 ± 0 a
AA	1%	5.6 ± 0.1 a	83 ± 2 a	0 ± 0 d
	3%	2.7 ± 0.9 c	86 ± 0 a	100 ± 0 a
	5%	2.6 ± 0.8 c	87 ± 7 a	100 ± 0 a

[1] The control was the reaction mixture without organic acids but with the pH adjusted with HCl. TA = tartaric acid, CA = citric acid, MA = malic acid, OA = oxalic acid and AA = ascorbic acid. Data are shown as mean $\pm$ SD ($n = 6$). Means in columns with different letters indicate significant differences ($p < 0.05$) between different inhibitors at different concentrations.

Three synthetic organic acids at the lowest concentrations of tartaric acid (5%), oxalic acid (3%) and ascorbic acid (3%) provided the greatest inhibition of PPO and POD activity. Therefore, 5% tartaric acid, 3% oxalic acid and 3% ascorbic acid were selected for further study.

3.7. Effect of Antibrowning Agents on Browning and Weight Loss of Banana Blossoms

Among all compounds tested, 3% oxalic acid caused the highest inhibition of browning at the blossom cut-surface after storage at 15 °C for 10 days. The L*, a* and ΔE* values and browning score of the cut-surface of banana blossom treated with 3% oxalic acid were better than that of the control (DI water, 2.5% tamarind juice and 1% SMS). No significant differences in weight loss among inhibitor agents and storage times were observed (Table 4). There was no abnormal odor and no disease incidence in any of the treated banana blossoms after 10 days of storage (data not shown).

Table 4. Browning response of banana blossoms after various organic acid treatments. Color, i.e., lightness (L*), redness (a*) and total color change (ΔE*), was assessed using a colorimeter. Browning score of peduncle cut-end surfaces and weight loss of banana blossoms were calculated as described. All tissues were kept in PE bags at 15 °C for 0, 5 and 10 days.

Inhibitor	L*		
	0 Day	5 Days	10 Days
DI water	68.6 ± 4.6 B,a	60.6 ± 5.8 B,b	61.5 ± 5.5 BC,b
2.5% TJ	71.4 ± 3.0 B,a	60.2 ± 3.3 B,b	60.1 ± 2.5 BC,b
1% SMS	75.5 ± 0.0 A,a	54.3 ± 6.8 C,b	53.4 ± 6.8 C,b
5% TA	76.9 ± 0.5 A,a	55.4 ± 3.2 BC,b	55.9 ± 3.4 BC,b
3% AA	77.7 ± 0.7 A,a	59.6 ± 2.1 B,b	58.5 ± 2.5 B,b
3% OA	77.3 ± 1.4 A,a	66.8 ± 2.8 A,b	66.4 ± 2.4 A,b

Inhibitor	a*		
	0 Day	5 Days	10 Days
DI water	−0.3 ± 1.9 AB,b	4.9 ± 2.5 AB,a	5.2 ± 2.4 AB,a
2.5% TJ	−1.0 ± 1.7 AB,b	5.3 ± 1.8 AB,a	6.3 ± 1.6 AB,a
1% SMS	0.8 ± 0.0 A,b	7.6 ± 1.4 A,a	4.3 ± 1.4 A,a
5% TA	−3.4 ± 0.3 B,b	5.2 ± 1.8 B,a	5.0 ± 1.8 B,a
3% AA	−3.5 ± 0.3 B,b	6.3 ± 1.0 AB,a	7.0 ± 0.5 AB,a
3% OA	−3.4 ± 0.6 B,b	0.0 ± 0.7 C,a	0.0 ± 0.7 C,a

Inhibitor	ΔE*		
	0 Day	5 Days	10 Days
DI water		12.4 ± 4.3 NS	11.8 ± 1.0 NS
2.5% TJ		13.8 ± 2.9 NS	15.5 ± 3.5 NS
1% SMS		23.4 ± 2.5 NS	24.3 ± 5.5 NS
5% TA		23.4 ± 2.6 NS	22.9 ± 2.8 NS
3% AA		22.4 ± 2.0 NS	23.2 ± 2.3 NS
3% OA		11.6 ± 2.2 NS	12.0 ± 1.7 NS

Inhibitor	Browning score		
	0 Day	5 Days	10 Days
DI water	1.0 ± 0.0 A,b	3.6 ± 0.9 B,a	3.6 ± 0.9 B,a
2.5% TJ	1.0 ± 0.0 A,b	3.4 ± 0.5 B,a	3.4 ± 0.5 B,a
1% SMS	1.0 ± 0.5 A,b	2.8 ± 0.8 B,a	3.8 ± 0.8 B,a
5% TA	1.0 ± 0.0 A,b	4.8 ± 0.4 A,a	5.0 ± 0.0 A,a
3% AA	1.0 ± 0.0 A,b	3.8 ± 0.8 B,a	3.8 ± 0.8 B,a
3% OA	1.0 ± 0.0 A,b	2.8 ± 0.8 B,a	3.8 ± 1.3 B,a

Inhibitor	Weight loss (% of initial FW)		
	0 Day	5 Days	10 Days
DI water		0.3 ± 0.4 AB,a	0.8 ± 0.9 A,a
2.5% TJ		0.5 ± 0.3 A,a	0.6 ± 0.3 A,a
1% SMS		0.4 ± 0.2 A,a	0.2 ± 0.0 AB,a
5% TA		0.2 ± 0.1 AB,a	0.3 ± 0.3 AB,a
3% AA		0.3 ± 0.2 AB,a	0.5 ± 0.2 A,a
3% OA		0.2 ± 0.2 AB,a	0.1 ± 0.1 AB,a

Data are shown as mean ± SD (n = 5). Means in columns with different capital letters indicate significant differences ($p < 0.05$) among inhibitors and means in rows with different small letters indicate significant differences ($p < 0.05$) between storage times. NS indicates nonsignificant differences ($p < 0.05$) among inhibitors and storage times. Inhibitors: DI = deionized water, TA = tartaric acid, OA = oxalic acid, AA = ascorbic acid, TJ = tamarind juice and SMS = sodium metabisulfite.

PCA was performed to provide an overview of the differences caused by the four different antibrowning treatments and storage periods on the banana blossoms. The first two principal components together accounted for 73% of the original variance: PC1 explained 44%, and PC2 explained 29%. Tissues clustered into three distinct groups. In group I, all treated tissues assayed before storage (0 d) clustered together; the only tissues treated with acid

and stored that were in this group were those dipped in 3% oxalic acid. The remaining tissues, all stored for 5 or 10 days, separated into either group II or III. Blossoms treated with DI water, or 2.5% tamarind juice clustered together, while blossoms treated with 1% SMS, 3% ascorbic acid and 5% tartaric acid formed the remaining cluster (Figure 3). Loading analysis indicated that the L* and b* values with loading scores of −0.83 and 0.91 on PC1 and PC2, respectively, determined the grouping (data not shown).
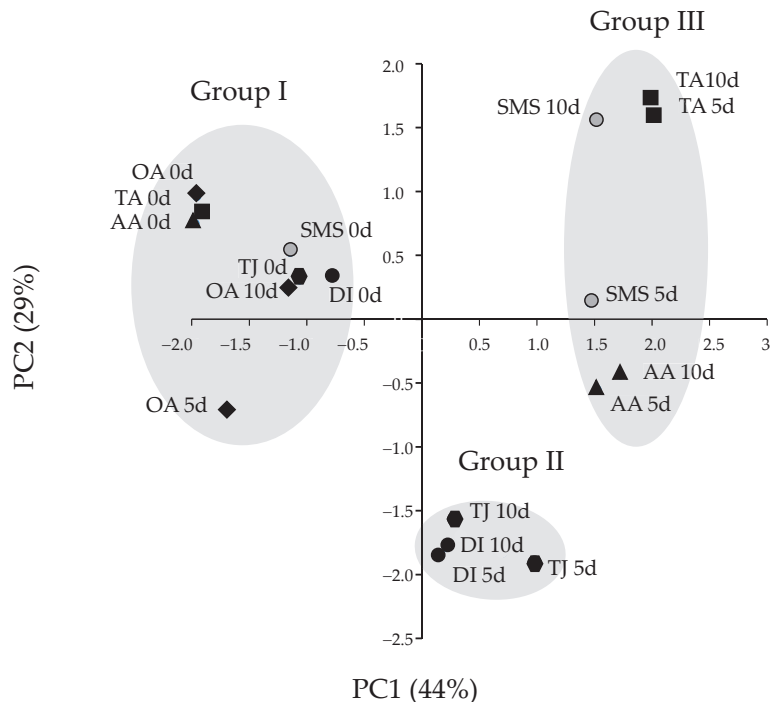

Figure 3. The principal component analysis (PCA) of objective color status and browning of the peduncle cut-end surfaces of banana blossoms after antibrowning treatments. Objective color was assessed by lightness (L*), redness (a*), yellowness (b*) and total color change (ΔE*); the browning score and weight loss of the peduncle cut-end surfaces of banana blossoms were assessed after storage in polyethylene bags at 15 °C for 0, 5 and 10 days. Banana blossoms treated with 3% oxalic acid (OA) and stored for 5 or 10 days were similar to those on the initial day of treatment. Banana blossoms treated with 3% ascorbic acid (AA) and 5% tartaric acid (TA) and stored for 5 or 10 days were similar to those treated with 1% sodium metabisulfite (SMS) and stored for the equivalent period. Banana blossoms treated with 2.5% tamarind juice (TJ) and stored for 5 or 10 days were similar to those treated with DI water.

4. Discussion

Banana blossoms have been traditionally eaten in dishes in SE Asia for hundreds of years, but there is now a growing demand, both locally and globally, for high-quality blossoms with reduced or no browning. This necessitates an investigation of the postharvest browning of fresh-cut banana blossoms. Here, we examined the activity of key browning enzymes and also investigated acid treatments to prevent undesirable browning.

4.1. Browning Mechanism at Cut-End Surface of Banana Blossoms

Browning or blackening from abiotic wounding or cutting occurs by enzymatic oxidation of phenolic compounds [37]. At the site of injury, chemical signals originate

and propagate into adjacent tissue. This induces the de novo synthesis of phenylalanine ammonia lyase (PAL) activity, the first key enzyme that converts L-phenylalanine to trans-cinnamic acid [38,39] resulting in the accumulation of phenolic compounds. In the presence of oxygen, phenolic compounds are oxidized by PPO to quinones that are highly reactive and can combine with other compounds to form brown pigments [40]. POD, on the other hand, acts as an antioxidant enzyme to eliminate excess hydrogen peroxide (H_2O_2) [41] and initiates enzymatic browning of fruit and vegetables [42]. Here, PPO and POD activities increased rapidly 12 h after cutting, in concert with increased browning, while in contrast, PAL activity decreased (Figure 1 and Table 1). Thus, only PPO and POD are induced by wounding, and together they serve as the key enzymes involved in the browning mechanism at the cut-end surface of banana blossoms.

In this study, the phenolic content (TPC) and DPPH scavenging activity of the blossoms were high and did not change as browning progressed (Figure 1). Phenolic compounds contribute to browning by acting as substrates for PPO and POD, and this is true in banana blossoms. The almost constant TPC during browning development indicates that banana blossoms were not limited in the phenolic compounds to supply substrate for PPO and POD.

4.2. Oxalic Acid Treatment as the Most Effective Method to Prevent Browning after Cutting

Different organic acids were tested as effective suppressors of the browning that occurs in the peduncle cut-end surface of banana blossoms. Low pH, the presence of a chelating copper ion and the ability to reduce quinones to their original diphenol are the main properties of organic acids that render them capable of inhibiting PPO and POD activities. Since different types and concentrations of organic acids inhibited the browning of banana blossoms differently, diverse inhibitory mechanisms for PPO and POD by each organic acid were assumed. Both browning scores and browning enzyme activities of banana blossoms were most inhibited by 3% of oxalic acid treatment (Tables 3 and 4). Oxalic acid may have a more effective chelating ability compared to other acids with the same structure [43,44]. Oxalic acid can bind to the PPO copper-containing active sites to form an inactive complex, thus reducing browning [45]. This finding agrees with reports on lettuce where oxalic acid diminished catechol quinone formation and no quinone bleaching was observed [46].

The present study also suggested that pH 2 reduced PPO activity and completely inhibited POD activity in the banana blossoms after tissue wounding by cutting. Similar to our results, Oba et al. [17] found that the activity of PPO from 'Saba' banana blossoms was reduced with decreasing pH from 7.5 to 4. He and Luo [10] reported that environmental pH affected the ionizable groups of the PPO and POD protein structures, which in turn would diminish their ability to catalyze their respective browning reactions. An acidic pH of 3.54 induced the unfolding of the native mushroom PPO with structural changes [47]. Oxalic acid had a low pKa value with a natural pH of 0.9 when 3% concentration was used. Thus, the low pH value of 3% oxalic acid may partially explain why this treatment was the most effective method to prevent banana blossom browning.

In comparison to the commercial antibrowning agent, i.e., 1% SMS, treatment with 3% oxalic acid led to higher browning inhibition at the blossom cut-surface. The 3% oxalic acid treatment is easy to apply, cost-effective and nontoxic. In this study, the organic acid treatments were applied only at the peduncle cut-end surface of the banana blossoms. Possible negative effects on quality attributes that may be caused by the organic acid treatments include unpleasant coloration, browning, weight loss, abnormal odor or disease incidence. However abnormal odor and disease incidence were not detected after organic acid treatment used in this experiment. Hence, this treatment holds great promise for use as a commercial agent for reduced browning of banana blossoms.

5. Conclusions

PPO and POD were identified as the key enzymes involved in browning at the cut-end surface of banana blossoms. Optimal pH values for PPO and POD activity in banana

blossoms were pH 4–6 and pH 7, respectively. A pH value of 2 inhibited PPO and POD activity by as much as 80% and 100%, respectively. Treatment with 3% oxalic acid effectively inhibited browning at the cut-end surface of the banana blossom peduncle for 10 days after 15 °C storage under PE package. It is proposed that 3% oxalic acid should be widely investigated as an effective commercial treatment to reduce browning and enhance the postharvest quality of banana blossoms.

Author Contributions: G.K. and K.L. planned and designed the experiments; G.K. and S.S. performed the experiments; G.K. and K.L. analyzed the data; G.K., K.L. and D.M.B. wrote the manuscript. All authors have read and agreed to the published version of the manuscript.

Conflicts of Interest: The authors confirm that they have no conflicts of interest with respect to the work described in this manuscript.

References

1. Sheng, Z.W.; Ma, W.H.; Jin, Z.Q.; Bi, Y.; Sun, Z.G.; Dou, H.T.; Gao, J.H.; Li, J.Y.; Han, L.N. Investigation of dietary fiber, protein, vitamin E and other nutritional compounds of banana flower of two cultivars grown in China. *Afr. J. Biotechnol.* **2010**, *9*, 3888–3895. [CrossRef]
2. Krishnan, A.; Sinija, V.R. Proximate Composition and Antioxidant Activity of Banana Blossom of Two Cultivars in India. *Int. J. Agric. Food Sci. Technol.* **2016**, *7*, 13–22.
3. Anand, S.; Sharma, M. Product Development from Banana Blossom Powder and Indian Gooseberry Powder for Anaemic Adolescent Girls. *Int. J. Health Sci. Res.* **2019**, *9*, 273–278.
4. Wahyuningsih, D.; Hidayat, S.T.; Khafidhoh, N.; Suwondo, A.; Fatmasari, D.; Susiloretni, K.A. Effect of Musa Balbisiana Colla Extract on Breast Milk Production in Breastfeeding Mothers. *Belitung Nurs. J.* **2017**, *3*, 174–182. [CrossRef]
5. Liyanage, R.; Gunasegaram, S.; Visvanathan, R.; Jayathilake, C.; Weththasinghe, P.; Jayawardana, B.C.; Vidanarachchi, J.K. Banana Blossom (*Musa acuminate* Colla) Incorporated Experimental Diets Modulate Serum Cholesterol and Serum Glucose Level in Wistar Rats Fed with Cholesterol. *Cholesterol* **2016**, *2016*, 9747412. [CrossRef] [PubMed]
6. Berrill, A. Banana blossom: The next vegan food star with the texture of fish. *The Guardian*, 16 March 2019.
7. Jiang, Y.; Duan, X.; Joyce, D.; Zhang, Z.; Li, J. Advances in understanding of enzymatic browning in harvested litchi fruit. *Food Chem.* **2004**, *88*, 443–446. [CrossRef]
8. Vámos-Vigyázó, L.; Haard, N.F. Polyphenol oxidases and peroxidases in fruits and vegetables. *Crit. Rev. Food Sci. Nutr.* **1981**, *15*, 49–127. [CrossRef] [PubMed]
9. Moon, K.M.; Kwon, E.B.; Lee, B.; Kim, C.Y. Recent Trends in Controlling the Enzymatic Browning of Fruit and Vegetable Products. *Molecules* **2020**, *25*, 2754. [CrossRef] [PubMed]
10. He, Q.; Luo, Y. Enzymatic browning and its control in fresh-cut produce. *Stewart Postharvest Rev.* **2007**, *3*, 1–7. [CrossRef]
11. Liu, X.; Wang, T.; Lu, Y.; Yang, Q.; Li, Y.; Deng, X.; Liu, Y.; Du, X.; Qiao, L.; Zheng, J. Effect of high oxygen pretreatment of whole tuber on anti-browning of fresh-cut potato slices during storage. *Food Chem.* **2019**, *301*, 125287. [CrossRef] [PubMed]
12. Degl'Innocenti, E.; Pardossi, A.; Tognoni, F.; Guidi, L. Physiological basis of sensitivity to enzymatic browning in "lettuce", "escarole" and "rocket salad" when stored as fresh-cut products. *Food Chem.* **2007**, *104*, 209–215. [CrossRef]
13. Li-Qin, Z.; Jie, Z.; Shu-Hua, Z.; Lai-Hui, G. Inhibition of browning on the surface of peach slices by short-term exposure to nitric oxide and ascorbic acid. *Food Chem.* **2009**, *114*, 174–179. [CrossRef]
14. Hisaminato, H.; Murata, M.; Homma, S. Relationship between the Enzymatic Browning and Phenylalanine Ammonia-lyase Activity of Cut Lettuce, and the Prevention of Browning by Inhibitors of Polyphenol Biosynthesis. *Biosci. Biotechnol. Biochem.* **2001**, *65*, 1016–1021. [CrossRef] [PubMed]
15. Chisari, M.; Barbagallo, R.N.; Spagna, G. Characterization of Polyphenol Oxidase and Peroxidase and Influence on Browning of Cold Stored Strawberry Fruit. *J. Agric. Food Chem.* **2007**, *55*, 3469–3476. [CrossRef] [PubMed]
16. Jin, P.; Zheng, Y.; Tang, S.; Rui, H.; Wang, C.Y. A combination of hot air and methyl jasmonate vapor treatment alleviates chilling injury of peach fruit. *Postharvest Biol. Technol.* **2009**, *52*, 24–29. [CrossRef]
17. Oba, K.; Uritani, I.; Iwatsuki, N.; Alvarez, A.M.; Garcia, V.V. Partial Purification and Characterization of Polyphenol Oxidase Isozymes in Banana Bud. *Biosci. Biotechnol. Biochem.* **1992**, *56*, 1027–1030. [CrossRef] [PubMed]
18. Chomkitichai, W.; Chaiyakhan, Y.; Petphinit, N.; Pudpang, P.; Chomkitichai, W. Effect of Tamarind Juice on Browning Reduction of Fresh-cut Banana Blossom during Storage. *Agric. Sci. J.* **2018**, *4*, 91–94. (In Thai)
19. Saideswara Rao, Y.; Mary Mathew, K. Tamarind. In *Handbook of Herbs and Spices*, 2nd ed.; Peter, K.V., Ed.; Woodhead Publishing Limited: Cambridge, UK, 2012; Volume 2, pp. 512–533. [CrossRef]
20. Tongdee, S. Postharvest Handling and Technology of Tropical Fruit. *Acta Hortic.* **1992**, 713–717. [CrossRef]

21. Whangchai, K.; Saengnil, K.; Uthaibutra, J. Effect of ozone in combination with some organic acids on the control of postharvest decay and pericarp browning of longan fruit. *Crop Prot.* **2006**, *25*, 821–825. [CrossRef]
22. Venkatachalam, K. The Different Concentrations of Citric Acid on Inhibition of Longkong Pericarp Browning during Low Temperature Storage. *Int. J. Fruit Sci.* **2015**, *15*, 353–368. [CrossRef]
23. Vasconcelos, C.M.; de Oliveira, E.B.; Rossi, S.N.; Arantes, L.F.; Puschmann, R.; Chaves, J.B.P. Evaluating Strategies to Control Enzymatic Browning of Minimally Processed Yacon (*Smallanthus sonchifolius*). *Food Bioprocess Technol.* **2015**, *8*, 1982–1994. [CrossRef]
24. Huang, H.; Jian, Q.; Jiang, Y.; Duan, X.; Qu, H. Enhanced chilling tolerance of banana fruit treated with malic acid prior to low-temperature storage. *Postharvest Biol. Technol.* **2016**, *111*, 209–213. [CrossRef]
25. Lichanporn, I.; Techavuthiporn, C.; Wongs-Aree, C. Effect of Silver Particle-longkong Peel Extract Coating on Postharvest Decay and Browning in Longkong Fruit. *Hortic. J.* **2020**, *89*, 328–336. [CrossRef]
26. Moline, H.E.; Buta, J.G.; Newman, I.M. Prevention of browning of banana slices using natural products and their derivatives. *J. Food Qual.* **1999**, *22*, 499–511. [CrossRef]
27. Nkhata, S.G. Total color change (ΔE∗) is a poor estimator of total carotenoids lost during post-harvest storage of biofortified maize grains. *Heliyon* **2020**, *6*, e05173. [CrossRef] [PubMed]
28. Adekunte, A.O.; Tiwari, B.K.; Cullen, P.J.; Scannell, A.G.M.; O'Donnell, C.P. Effect of sonication on colour, ascorbic acid and yeast inactivation in tomato juice. *Food Chem.* **2010**, *122*, 500–507. [CrossRef]
29. Havananda, T.; Luengwilai, K. Variation in floral antioxidant activities and phytochemical properties among butterfly pea (*Clitoria ternatea* L.) germplasm. *Genet. Resour. Crop. Evol.* **2019**, *66*, 645–658. [CrossRef]
30. Salar, R.K.; Sharma, P.; Purewal, S.S. In Vitro antioxidant and free radical scavenging activities of stem extract of *Euphorbia trigona* Miller. *Tang Humanit. Med.* **2015**, *5*, e14. [CrossRef]
31. Faragher, J.; Chalmers, D. Regulation of Anthocyanin Synthesis in Apple Skin. III. Involvement of Phenylalanine Ammonia-lyase. *Funct. Plant Biol.* **1977**, *4*, 133–141. [CrossRef]
32. Benjamin, N.D.; Montgomery, M.W. Polyphenol Oxidase of Royal Ann Cherries: Purification and Characterization. *J. Food Sci.* **1973**, *38*, 799–806. [CrossRef]
33. Zhang, Z.; Pang, X.; Xuewu, D.; Ji, Z.; Jiang, Y. Role of peroxidase in anthocyanin degradation in litchi fruit pericarp. *Food Chem.* **2005**, *90*, 47–52. [CrossRef]
34. Bradford, M.M. A rapid and sensitive method for the quantitation of microgram quantities of protein utilizing the principle of protein-dye binding. *Anal. Biochem.* **1976**, *72*, 248–254. [CrossRef]
35. Zhang, X.; Shao, X. Characterisation of polyphenol oxidase and peroxidase and the role in browning of loquat fruit. *Czech J. Food Sci.* **2015**, *33*, 109–117. [CrossRef]
36. Hammer, Ø.; Harper, D.A.T.; Ryan, P.D. PAST: Paleontological statistics software package for education and data analysis. *Palaeontol. Electron.* **2001**, *4*, 9.
37. Ahvenainen, R. New approaches in improving the shelf life of minimally processed fruit and vegetables. *Trends Food Sci. Technol.* **1996**, *7*, 179–187. [CrossRef]
38. Ngadze, E.; Icishahayo, D.; Coutinho, T.A.; van der Waals, J.E. Role of Polyphenol Oxidase, Peroxidase, Phenylalanine Ammonia Lyase, Chlorogenic Acid, and Total Soluble Phenols in Resistance of Potatoes to Soft Rot. *Plant Dis.* **2012**, *96*, 186–192. [CrossRef] [PubMed]
39. Saltveit, M.E. Wound induced changes in phenolic metabolism and tissue browning are altered by heat shock. *Postharvest Biol. Technol.* **2000**, *21*, 61–69. [CrossRef]
40. Mayer, A.M. Polyphenol oxidases in plants and fungi: Going places? A review. *Phytochemistry* **2006**, *67*, 2318–2331. [CrossRef] [PubMed]
41. Murata, M.; Nishimura, M.; Murai, N.; Haruta, M.; Homma, S.; Itoh, Y. A Transgenic Apple Callus Showing Reduced Polyphenol Oxidase Activity and Lower Browning Potential. *Biosci. Biotechnol. Biochem.* **2001**, *65*, 383–388. [CrossRef] [PubMed]
42. Richard-Forget, F.C.; Gauillard, F.A. Oxidation of Chlorogenic Acid, Catechins, and 4-Methylcatechol in Model Solutions by Combinations of Pear (*Pyrus communis* Cv. Williams) Polyphenol Oxidase and Peroxidase: A Possible Involvement of Peroxidase in Enzymatic Browning. *J. Agric. Food Chem.* **1997**, *45*, 2472–2476. [CrossRef]
43. Son, S.M.; Moon, K.D.; Lee, C.Y. Kinetic Study of Oxalic Acid Inhibition on Enzymatic Browning. *J. Agric. Food Chem.* **2000**, *48*, 2071–2074. [CrossRef] [PubMed]
44. Yoruk, R.; Marshall, M.R. A Survey on the Potential Mode of Inhibition for Oxalic Acid on Polyphenol Oxidase. *J. Food Sci.* **2003**, *68*, 2479–2485. [CrossRef]
45. Prenen, J.A.; Boer, P.; Dorhout Mees, E.J. Absorption kinetics of oxalate from oxalate-rich food in man. *Am. J. Clin. Nutr.* **1984**, *40*, 1007–1010. [CrossRef] [PubMed]
46. Altunkaya, A.; Gokmen, V. Effect of various inhibitors on enzymatic browning, antioxidant activity and total phenol content of fresh lettuce (*Lactuca sativa*). *Food Chem.* **2008**, *107*, 1173–1179. [CrossRef]
47. Ioniţă, E.; Stănciuc, N.; Aprodu, I.; Râpeanu, G.; Bahrim, G. pH-induced structural changes of tyrosinase from *Agaricus bisporus* using fluorescence and in silico methods. *J. Sci. Food Agric.* **2014**, *94*, 2338–2344. [CrossRef] [PubMed]